



MIT*ei*
MIT Energy Initiative

THE ROLE OF FUSION ENERGY IN A DECARBONIZED ELECTRICITY SYSTEM

A report from the MIT Energy Initiative in collaboration with the
MIT Plasma Science and Fusion Center



Study Participants

Principal Investigator

Robert C. Armstrong

Former Director, MIT Energy Initiative; Chevron Professor of Chemical Engineering, Emeritus, MIT

Co-Principal Investigator

Dennis G. Whyte

Hitachi America Professor of Engineering, Nuclear Science and Engineering, MIT

Executive Director

Randall Field

Executive Director, Future Energy Systems Center, MIT Energy Initiative

Lead Investigators

Ruaridh Macdonald

Research Scientist, MIT Energy Initiative

John Parsons

Deputy Director for Research, Center for Energy and Environmental Policy Research, MIT

Sergey Paltsev

Deputy Director, Joint Program on the Science and Policy of Global Change, MIT
Senior Research Scientist, MIT Energy Initiative

Koroush Shirvan

Atlantic Richfield Career Development Professor in Energy Studies, Nuclear Science and Engineering, MIT

Contributing Authors

Layla Araiinejad

SM ('24), Technology and Policy, MIT Institute for Data, Systems, and Society

Sara Ferry

Research Scientist, Plasma Science and Fusion Center, MIT

Nirmal Bhatt

SM ('24), Technology and Policy, MIT Institute for Data, Systems, and Society

Angelo Gurgel

Research Scientist, Joint Program on the Science and Policy of Global Change and MIT Energy Initiative, MIT

Amanda Farnsworth

PhD, Chemical Engineering ('24), MIT

Theodore Mouratidis

Postdoctoral Associate, Plasma Science and Fusion Center, MIT

Research Advisors

Y.-H. Henry Chen

Research Scientist, Joint Program on the Science and Policy of Global Change and MIT Energy Initiative, MIT

Jeffrey Freidberg

Professor of Nuclear Science and Engineering, Emeritus, MIT

Emre Gençer

Principal Research Scientist, MIT Energy Initiative

Dharik Mallapragada

Principal Research Scientist, MIT Energy Initiative

Samuele Meschini

Postdoctoral Associate, Plasma Science and Fusion Center, MIT

Jennifer Morris

Principal Research Scientist, Joint Program on the Science and Policy of Global Change and MIT Energy Initiative, MIT

Matthew Munderville

Program Director, Plasma Science and Fusion Center, MIT

Elsa Olivetti

Associate Dean of Engineering, Jerry McAfee (1940) Professor in Engineering, Professor of Materials Science and Engineering, MIT

Richard Roth

Director, Materials Systems Laboratory, MIT

Tim Schittekatte

Research Scientist, MIT Energy Initiative

Michael Short

Class of '42 Associate Professor of Nuclear Science and Engineering
Associate Director, Plasma Science and Fusion Center, MIT

Robert Stoner

Interim Director, MIT Energy Initiative

Subject Matter Experts

Zachary Hartwig

Robert N. Noyce Career Development Professor

Stuart Malloy

Senior Nuclear Materials Advisor
Pacific Northwest National Laboratory

Alexander Molodyk

Chief Technology Officer, SuperOx

Daniel Ng

PhD candidate, Materials Science and
Engineering, MIT

Keith Smith

Vice President Nuclear, Science & Government
Affairs, Materion Corporation

Lance Sneed

Senior Advisor to Nuclear Reactor Laboratory
Leader, Irradiation Materials Science Group, MIT

Steve Wukitch

Principal Research Scientist, Plasma Science and
Fusion Center, MIT

Yifei Zhang

Vice President of R&D, SuperPower Inc.

While the subject matter experts provided invaluable knowledge and advice to the study group, the individuals acknowledged here may have different views on the topics addressed in this report. They have not been asked to endorse the findings of this report.

Foreword and acknowledgments

This report is the culmination of a one-and-a-half-year study to examine the potential role of fusion energy in the decarbonization of the electricity system. The study was designed to investigate the factors that will impact the deployment of fusion power plants, such as costs and climate policy. This study is designed to serve as a balanced, fact-based, and analysis-driven guide during a time of great public interest in the prospects for fusion energy. Our study applies a multi-disciplinary approach using economic modeling, electric grid modeling, technology and policy analytics, systems analysis, critical materials and supply chain analysis, and techno-economic analysis to examine important factors that are likely to shape the deployment and utilization of fusion energy.

The MIT Energy Initiative (MITEI) undertook this study in the context of its mission to explore and create solutions that will efficiently meet global energy needs while minimizing environmental impacts and mitigating climate change. MITEI teamed up with the MIT Plasma Science and Fusion Center (PSFC) to provide the fusion energy expertise to this study. MITEI and PSFC gratefully acknowledge Eni for supporting this research and for engaging in discussions with MIT during this research project.

A special thank you to Gail Monahan, MITEI Administrative and Operations Coordinator, for her patience, dedication, and organization in supporting this project. Thanks also to the Kelley Travers, MITEI Communications Manager, and Tom Witkowski, MITEI Communications Director, for their help with the final report from this study. We also thank Kelly McGinity, MITEI Events Planning Manager, for managing the rollout of this report. We thank Elizabeth Hamblin for integrating the final report and solving the publishing software challenges to make this report possible. Finally, we thank Marika Tatsutani for editing the report with great skill and dedication.

This report represents the findings of the study researchers who are solely responsible for its content, including any errors. Eni is not responsible for the findings contained in the report, and Eni has not been asked to endorse the findings of this report.

Table of contents

Executive summary.....	2
Chapter 1. Project overview	13
Chapter 2. Overview of fusion technologies.....	16
Chapter 3. Electricity generation in a decarbonized world.....	27
Chapter 4. Global outlook for fusion energy deployment	38
Chapter 5. Analysis of fusion market penetration in subregions of the United States.....	51
Chapter 6. Critical materials and supply chains for fusion power plants	84
Chapter 7. Techno-economic analysis of fusion power plants.....	109
Appendix A. Global analysis methodology.....	123
Appendix B. Methodology for grid and multi-subregional analysis.....	128
Appendix C. Techno-economic analysis methodology	141
List of figures.....	153
List of tables.....	155
Glossary and acronyms	157

Executive summary

The global supply of energy is under great pressure to transform in response to multiple forces. Global demand for electricity will grow substantially as large numbers of people—more than 100 million each year at the current rate—join the middle class (Kharas 2023), as more households gain access to electricity, and as the electrification of transportation, heating, and industrial processes expands. Electric power systems are also under pressure to decarbonize to achieve net-zero carbon goals. In principle, variable renewable energy (VRE) sources such as wind and solar can deliver low-carbon power at scale—and they are important parts of the solution, but they are non-dispatchable and have low power density. Therefore, an electric power system dominated by VREs will require large-scale energy storage to balance supply and demand.

The system will also require significant new transmission capacity to bring electricity from distributed sources to demand centers. Adding sufficient energy storage to ensure reliable electricity supply for a zero-emissions grid dominated by VREs is technically feasible, but the scale and cost of energy storage and the need to curtail generation during periods of excess supply increase nonlinearly with VRE penetration. It has been estimated that the total system cost to build and operate a 100% VRE grid in the United States could exceed \$1 trillion per year (Jenkins et al. 2018). Given these cost and deployment challenges, the world requires a build-out of firm, carbon-free power generation with high power density as a complement to other low-carbon options and to provide zero-carbon solutions for locations that do not have the space, local climate, and natural resources for VREs (Sepulveda et al. 2018).

Fusion energy has the potential to help fill this need. This study examines the potential role fusion could play as a major contributor to future electric power systems and identifies requirements for achieving that mission. Fusion energy combines several advantages that are especially important in a decarbonized world: high power density, good siting flexibility, the ability to deliver “firm” power (i.e., power that can be counted on to meet demand when needed in all seasons), and, of course, no greenhouse gas emissions. As such, fusion energy is complementary to other low-carbon technologies and does not need to compete with solar, wind, or fossil fuels on the simple metric of levelized cost of electricity. To understand the role of fusion in the future, we must understand how fusion will contribute to the overall energy system and assess the value of its dispatchability and firm delivery capabilities.

At the time of this writing, more than 40 companies worldwide are working to develop fusion energy technology, and governments are supporting more than 111 fusion projects, with different strategies, designs, and timelines. This study is not specific to any particular fusion technology. Common goals for fusion power research efforts are zero-carbon emissions, high power density, and delivery of dispatchable, firm power. Technologies that can achieve these

goals are approximately ten or more years away from commercial deployment, so the detailed characteristics and costs of future commercial fusion power plants are not known at this stage. This study examines the cost threshold that fusion plants must reach by 2050 to achieve strong market penetration and make a significant contribution to the decarbonization of global electricity supply in the latter half of the century.

A major motivation for this study arises from recent science and technology advances that provide multiple potential pathways to commercialize fusion. For example, in magnetic confinement fusion, where fusion power density is proportional to the magnetic field to the fourth power (if stability physics is kept constant), the arrival of high field superconductors appears to have significantly decreased size and cost requirements. Two burning plasma experiments under construction now—ITER (International Atomic Energy Agency 2002) and SPARC (Creely et al. 2023)—aim to achieve power-plant-relevant scientific energy gain ($Q>10$) with the tokamak magnetic confinement configuration. Although neither experiment seeks to deliver electricity to the grid, both are expected to provide important insights relevant to that ultimate goal. Using prior-generation, lower-field superconductors, ITER requires a plasma volume of 840 cubic meters (m^3) to generate 500 megawatts (MW) of fusion power, whereas SPARC (Creely et al. 2023), at 1/40th of that volume, is designed to generate 140 MW of fusion power—in other words, SPARC requires less than one-tenth the plasma volume per unit of fusion power compared to ITER. This simple volumetric comparison shows the potential order-of-magnitude impact that breakthrough technologies like high-magnetic-field magnets can have on cost projections for fusion energy systems.

Furthermore, significant cost reductions are expected in adjacent magnetic fusion concepts like stellarators (Hegna et al. 2022; Kumar et al. 2023) and mirrors (Endrizzi et al. 2023), since high-magnetic-field superconductors reduce the required size of these systems as well. Cost improvements can also be expected from other fusion breakthroughs. One example is the promising development of energy-efficient, high-average-power lasers, which is being motivated by the recent $Q>1$ results for inertial confinement fusion at the National Ignition Facility. Vast gains in computational power and the advent of new tools like AI and machine learning (Wang et al. 2024) are also improving economic prospects for fusion systems through better design (e.g., stellarator coil fabrication (Lonigro et al. 2024)) and operational optimization in a manner that was inaccessible even a decade ago. Synergies between these technology and design tools and recent science advances are enabling the resurgence of previously abandoned fusion concepts. The achievements of hot confined electrons in both mirrors (Endrizzi et al. 2023) and pinches (Levitt et al. 2023) are outstanding examples that have potentially compelling advantages in energy systems. In summary, the last decade has seen a swath of advances in fusion science and technology that have increased the promise of achieving economically competitive fusion.

The first deployments of fusion energy are expected to be for electric power generation, but in a deeply decarbonized world, the expectation is that fusion energy will have a vital role in tough-to-decarbonize sectors of the economy as well. To achieve maximum impact, fusion could be instrumental for producing hydrogen and low-carbon fuels, supplying high-temperature process heat, and powering negative emissions processes. This study focuses solely on fusion power plants (FPPs). A separate, future study will address the broader range of applications for fusion energy, including for transportation fuels, heat, and negative emissions.

Several key findings emerge from this study:

Fusion has a potential societal value in the trillions of dollars in a decarbonized world. Over the period from 2035 to 2100 in a deep decarbonization scenario, fusion power plants can increase overall societal value today by \$3.6 trillion¹ if FPP overnight costs in 2050 in the United States are \$8,000/kW and fall to \$4,300/kW in 2100. The societal value of fusion today would be \$8.7 trillion if FPP overnight costs reach \$5,600/kW in the United States in 2050 and \$3,000/kW in 2100. These benefits provide economic and social justification to invest in developing cost-effective fusion energy.

The scale of fusion deployment in the electricity system will depend on FPP costs. As shown in [Figure ES.1](#), for a deep decarbonization scenario, the total global share of electricity generation from fusion in 2100 ranges from less than 10% to about 50% depending on the assumed cost for fusion.

The scale and timing of fusion deployment in different regions of the world will be driven by economic growth, population density, electrification needs, regional costs, decarbonization targets, relative prices of electricity, limitations of fission-based nuclear generation,² and resource availability for other low-carbon technologies (wind, solar, and biomass). [Figure ES.2](#) shows that while initial deployment is strongest in the United States and Europe, the largest increase in fusion takes place in India during the last three decades of the century. Africa is a late adopter of fusion but likewise sees strong growth late in the century. These fusion growth patterns are strongly related to electrification. Economies in all regions undergo substantial electrification and experience a corresponding increase in demand for electricity. While electricity consumption in the United States, Europe, and China grows between 1.9- and 2.4-

¹ The net present value (NPV) of the societal value of fusion is calculated as the difference in global gross domestic product in scenarios where fusion is available compared to scenarios where it is not available, over the period from 2035 to 2100 for a deep decarbonization scenario. The discount rate used is 6%. The undiscounted value is about 20 times larger.

² Fission-based nuclear generation is assumed to be constrained by social acceptance and non-proliferation issues. See [Chapter 4](#) for details.

fold from 2020 to 2100, in India, it grows 8.2-fold, and in Africa, it grows 9.3-fold over the same period of time.

Figure ES.1 Projected fusion penetration in the global electricity system under different FPP cost assumptions for a 1.5°C stabilization pathway scenario



Fusion costs shown are for the overnight cost³ of constructing a fusion power plant in the United States in the year 2050. At the end of the century, costs are 46% lower. Fusion costs in other regions will differ based on capital and labor costs in those other regions. See Chapter 4 for details.

The scale of fusion deployment in the electricity system will highly depend on the availability and cost of other low-carbon technologies and on how tightly carbon emissions are constrained in the future. As shown in Figure ES.3, the penetration of fusion in different subregions of the United States⁴ is highly dependent on the availability of other low-carbon resources such as wind, solar, and hydro. Furthermore, as shown in Figure ES.3, the penetration of fusion depends on the emissions intensity cap. For example, the Central U.S. subregion has excellent renewable resources led by wind. Thus, fusion competes in the Central subregion only when emissions are capped at less than 4 gCO₂/kWh (assuming a 2050 fusion price point of \$6,000/kW). By contrast, the Southeast subregion has low renewable resources—thus, that

³ All dollar values are reported in 2021 U.S. dollars throughout this report, unless indicated otherwise. Overnight cost is the cost of a construction project if we assume there are no financing costs to cover the duration of the construction.

⁴ A map of the U.S. subregions is provided in Figure 5.1.

region needs fusion to serve its electricity demand over a wider range of emissions intensity constraints. In sum, our analysis of fusion penetration across the nine subregions of the United States indicates that, in a decarbonized world, fusion power plants will have the highest penetration in locations with poor diversity, capacity, and quality of renewable resources, as shown in [Table ES.1](#).

Figure ES.2 Fusion electricity generation in major world regions under different \$/kW capital cost assumptions and under a 1.5°C climate stabilization pathway

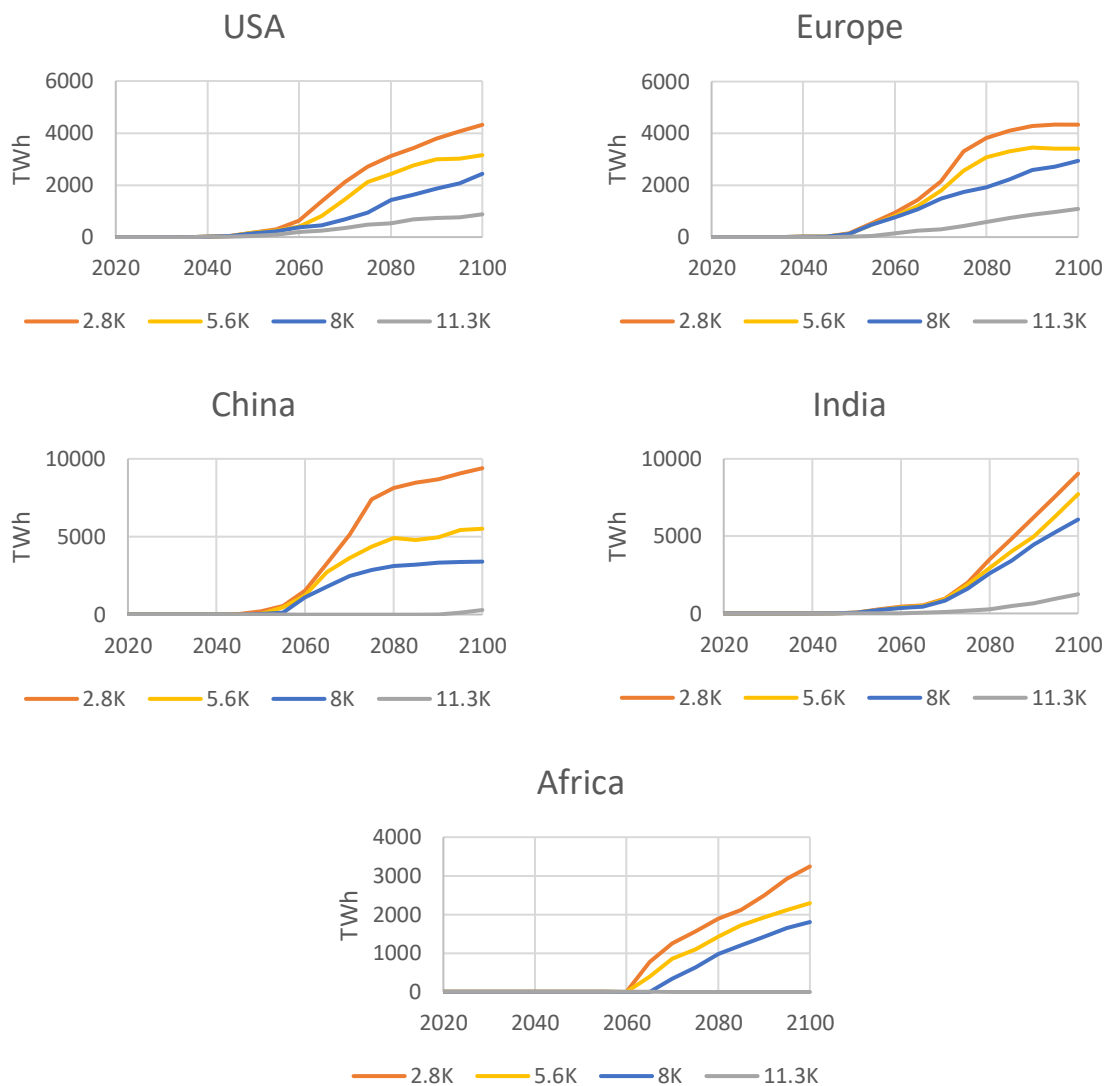
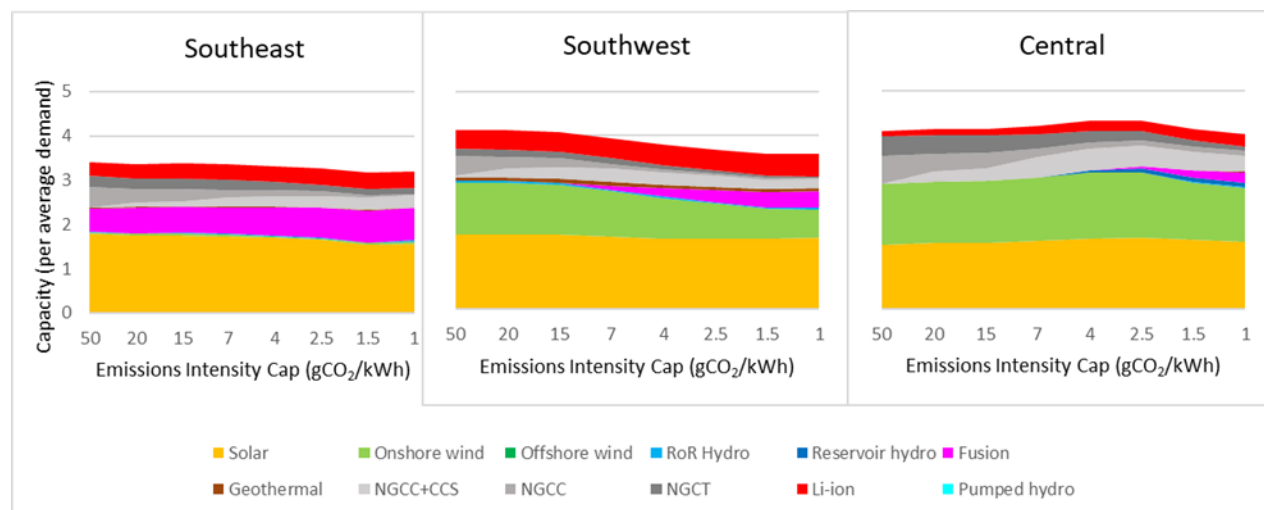


Figure ES.3 Fusion penetration⁵ in U.S. subregions with different endowments of other low-carbon electricity resources for a range of emission intensity caps in a scenario with FPP capital costs of \$6,000/kW in 2050



The role of FPPs in the electric power system is also highly sensitive to costs. Based on our analysis of the New England subregion of the United States, which has lower-than-average insolation and limited siting options for onshore wind, Figure ES.4 shows that FPPs serve as low-capacity-factor, dispatchable electric generation when fusion costs are high, but tend to serve mostly as a baseload resource when FPP costs are moderate and as dispatchable generation with a moderate capacity factor when FPP costs are low. This trend is directly related to the penetration and relative mix of FPPs with non-dispatchable and dispatchable resources, including energy storage.

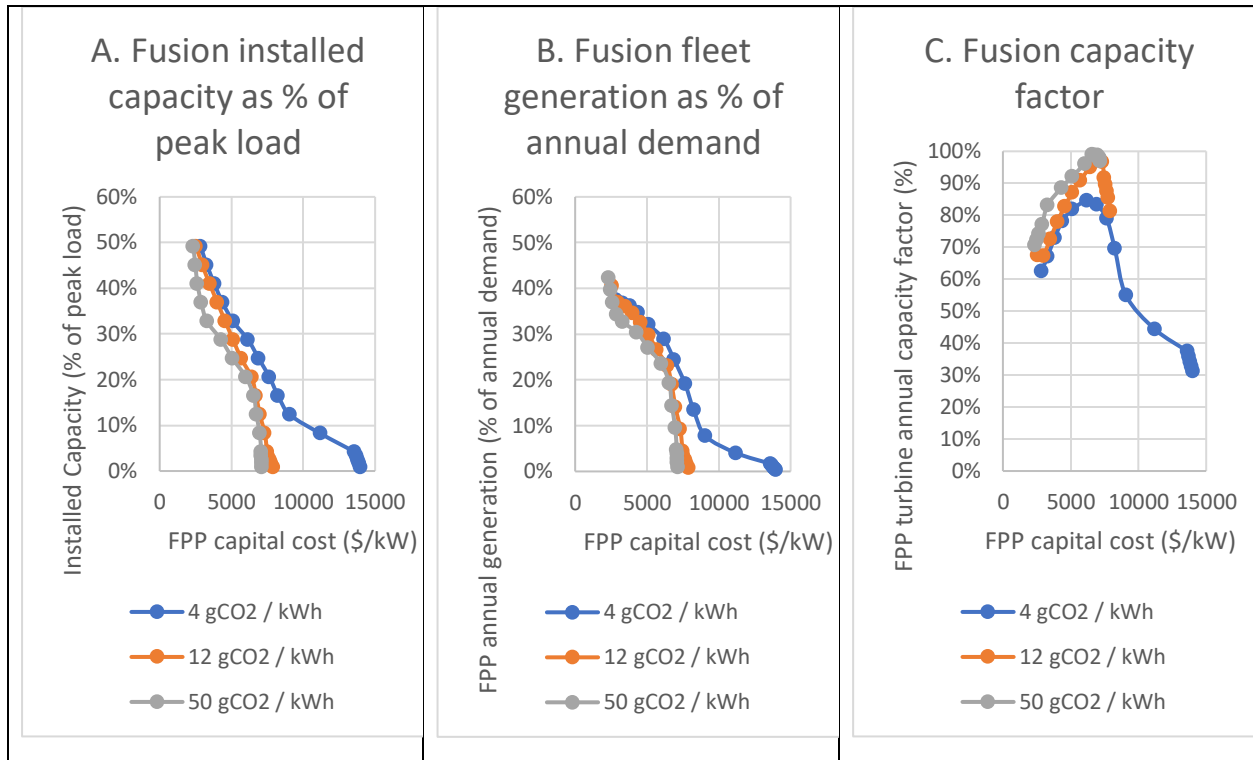
⁵ The capacity values in this figure represent installed generating capacity divided by the average annual demand for electricity. This scaling of capacity by subregional demand enables comparison of the generator mix across the subregions. In these scenarios, installed capacity is more than three times average demand because there must be enough capacity to meet peak annual demand and because some generators have low capacity factors.

Table ES.1 Renewable resource attributes of different U.S. subregions

	High penetration, low sensitivity	Medium penetration, medium sensitivity	Low penetration, low sensitivity	Low penetration, high sensitivity
Subregions	Atlantic and Southeast	California, Northeast, Southwest	Northwest	Central, North Central, Texas
Renewable attributes	Poor onshore wind, hydro, and geothermal resources	Northeast has best offshore wind; California has best geothermal; Southwest has best solar; all three have modest onshore wind capacity or quality	Below average solar and wind resources, but excellent diversity of renewable resources, including good hydro and moderate geothermal	Abundant, high-quality, and low-cost onshore wind; limited renewables beyond onshore wind and solar
Fusion penetration at \$6,000/kW	Required at all emission caps from 1 to 50 gCO ₂ /kWh	No penetration at 50 gCO ₂ /kWh, but capacity reaches 33%–55% of demand at 1 gCO ₂ /kWh	Required at all emission caps 1–20 gCO ₂ /kWh, but capacity is never more than 26% of demand	Required only at 4 gCO ₂ /kWh and below, but capacity reaches 25%–45% of demand at 1 gCO ₂ /kWh

Levels of fusion penetration are based on overnight FPP capital cost of \$6,000/kW. We assume constraints on renewable energy capacity are driven by technical criteria, not social and environmental factors.

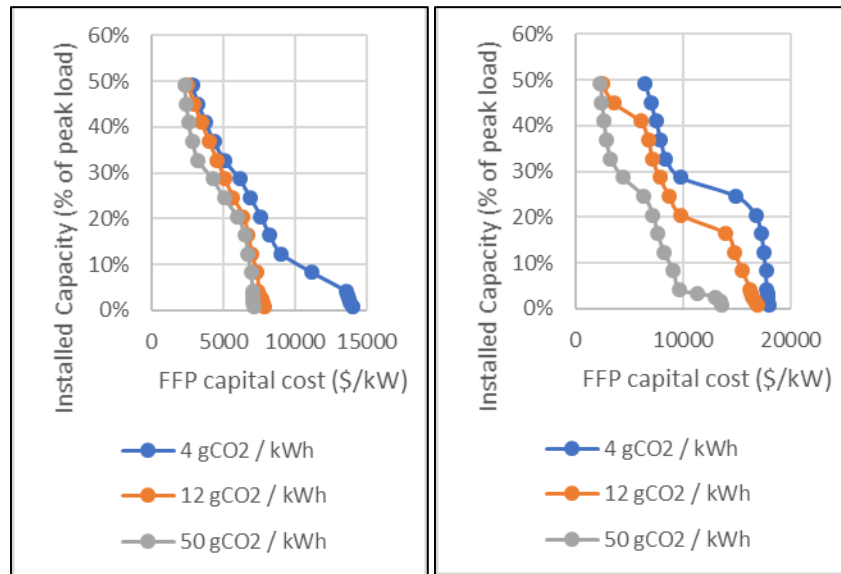
Figure ES.4 FPP installed capacity (A), generation (B), and capacity factor (C) in the New England grid, assuming that VRE installed capacity is constrained by land use



The availability of firm, low-carbon natural gas power plants can have a large impact on the deployment of FPPs. Based on our analysis of the New England subregion, which does not have a local supply of natural gas or geological storage sites for carbon dioxide, we see that fusion deployment is strongly influenced by the availability of natural gas combined cycle (NGCC) generation with 95% carbon capture and low upstream methane emissions. As shown in [Figure ES.5](#), the threshold price point at which fusion becomes competitive is \$4,000/kW lower when NGCC with 95% carbon capture is available than when NGCC with 95% carbon capture is not available.

Figure ES.5 Installed fusion capacity (as a % of peak load) in the U.S. subregion of New England in 2050

(A) With NGCC w/95% capture (B) Without NGCC w/95% capture



The curves show the influence of FPP cost on installed capacity with (A) and without (B) the option for NGCC with 95% carbon capture. If NGCC plants with 95% carbon capture are not available, the threshold cost for initial FPP penetration is higher by \$4,000/kW or more.

Key cost drivers for fusion power plants include reactor equipment cost, regulatory considerations, and operations and maintenance costs. Regardless of the confinement method used, reactor equipment is the leading cost contributor, ranging from 30% to 65% of the total capital cost for a fusion power plant. Regulation can be a potentially large cost driver, which should motivate fusion companies to minimize their regulatory and environmental footprint with respect to fuels and activated materials, while also motivating governments to adopt appropriate and effective regulatory policies to maximize their ability to use fusion energy in achieving decarbonization goals. Operating and maintenance (O&M) costs can be significant for a fusion power plant. FPP design concepts with reduced O&M costs and reasonable capacity factors will have a significant edge in providing a commercially viable product.

Supply chains for the processed materials and manufactured parts needed to build fusion power plants vary widely in maturity. Understanding the potential growth rate of fusion power requires an examination of possible roadblocks in the crucial supply chains needed to enable large-scale deployment of fusion power plants. There are no showstopper requirements for raw materials: The elements used in fusion power plants are generally abundant on Earth. Beryllium is potentially the most problematic in the near term, but it poses no immediate supply concerns. Fusion components can be separated into two categories: (1) niche components that have only small market opportunities outside of fusion, such as tungsten heavy and other

plasma-facing materials, and (2) multiple-use components that have large potential markets outside of fusion, such as high-temperature superconductors and radio-frequency devices, which have potential commercial uses in other fields. Ensuring the availability of niche components may require significant investment by governments and the fusion industry.

In summary, the technology demands of fusion energy are formidable but so are the potential economic and environmental payoffs of adding a firm low-carbon technology with critical advantages for decarbonized power systems to the world's portfolio of energy options. If the cost and performance targets identified in this report can be achieved, our analysis shows that fusion energy can play a major role in meeting future electricity needs and achieving global net-zero carbon goals.

Box ES.1 Two important candidates for firm power: Fusion and fission

Power system operators typically deploy a portfolio of generation technologies to supply the varying demand for electricity throughout the calendar year. Different technologies complement one another along a number of dimensions. The increasing penetration of low-cost variable renewable energy (VRE) technologies creates a complementary need for technologies that provide “firm” or dispatchable, low-carbon electricity to assure sufficient generation in hours when VRE generation is low. Nuclear fusion and nuclear fission are both firm, low-carbon-electricity-generating technologies. Both are also energy-dense technologies. In these respects, they are candidates for the same competitive space in a country's or region's portfolio of generating capacity. A few other developing technologies, such as enhanced geothermal or bioenergy with carbon capture and storage, may also vie for that competitive space.

Of course, nuclear fusion and fission differ in other respects. For example, their safety profiles are unique, and the two technologies may therefore face different regulatory requirements. They also rely on different sets of materials and different evolving areas of technological development. Social acceptance of fission technology is highly variable across countries. Fusion's social acceptance is almost entirely untested.

This research project focused on the economic opportunity for fusion technology as a firm, low-carbon generation option, and on assessing global and regional variation in the magnitude of that economic opportunity. The competition between fusion and fission for a share of the power generation market will depend on many complicated developments across both technologies—scientific, economic, political, and social. We have not attempted to characterize how these developments might favor fusion relative to fission or fusion relative to other firm, low-carbon, energy-dense technologies.

References

- Creely, A. J., D. Brunner, R. T. Mumgaard, M. L. Reinke, M. Segal, B. N. Sorbom, and M. J. Greenwald. 2023. "SPARC as a Platform to Advance Tokamak Science." *Physics of Plasmas* 30 (9): 90601. <https://doi.org/10.1063/5.0162457/2909870/SPARC-AS-A-PLATFORM-TO-ADVANCE-TOKAMAK-SCIENCE>.
- Endrizzi, D., J. K. Anderson, M. Brown, J. Egedal, B. Geiger, R. W. Harvey, M. Ialovega, et al. 2023. "Physics Basis for the Wisconsin HTS Axisymmetric Mirror (WHAM)." *Journal of Plasma Physics* 89 (5): 975890501. <https://doi.org/10.1017/S0022377823000806>.
- Hegna, C. C., D. T. Anderson, A. Bader, T. A. Bechtel, A. Bhattacharjee, M. Cole, M. Drevlak, et al. 2022. "Improving the Stellarator through Advances in Plasma Theory." *Nuclear Fusion* 62 (4): 042012. <https://doi.org/10.1088/1741-4326/AC29D0>.
- International Atomic Energy Agency. 2002. "ITER Technical Basis." Vienna, Austria. <https://www.iaea.org/publications/6492/iter-technical-basis>.
- Jenkins, Jesse D, Max Luke, and Samuel Thernstrom. 2018. "Getting to Zero Carbon Emissions in the Electric Power Sector." *Joule*. <https://doi.org/10.1038/nenergy>.
- Kharas, Homi. 2023. *The Rise of the Global Middle Class* | Brookings. Brookings Institute Press. <https://www.brookings.edu/books/the-rise-of-the-global-middle-class/>.
- Kumar, S.T.A., S. Aslam, B. Chen, A. Cote, D.H. Fort, D. Gates, P.S. Swanson, K. Tang, and J. Wasserman. 2023. "Prototyping HTS Stellarator Magnet System." 65th APS-DPP. November 2023. https://thea.energy/wp-content/uploads/2024/02/Prototyping-HTS-Stellarator-Magnet-System_APS-DPP-23-Updated-1.pdf.
- Levitt, B., E. T. Meier, R. Umstattd, J. R. Barhydt, I. A.M. Datta, C. Liekhus-Schmaltz, D. A. Sutherland, and B. A. Nelson. 2023. "The Zap Energy Approach to Commercial Fusion." *Physics of Plasmas* 30 (9): 90603. <https://doi.org/10.1063/5.0163361/2911595>.
- Lonigro, Nicola, Caoxiang Zhu -, John Kappel, Matt Landreman, and Dhairya Malhotra. 2024. "The Magnetic Gradient Scale Length Explains Why Certain Plasmas Require Close External Magnetic Coils." *Plasma Physics and Controlled Fusion* 66 (2): 025018. <https://doi.org/10.1088/1361-6587/AD1A3E>.
- Sepulveda, Nestor A., Jesse D. Jenkins, Fernando J. de Sisternes, and Richard K. Lester. 2018. "The Role of Firm Low-Carbon Electricity Resources in Deep Decarbonization of Power Generation." *Joule* 2 (11): 2403–20. <https://doi.org/10.1016/J.JOULE.2018.08.006>.
- Wang, Allen M., Oswin So, Charles Dawson, Darren T. Garnier, Cristina Rea, and Chuchu Fan. 2024. "Active Disruption Avoidance and Trajectory Design for Tokamak Ramp-Downs with Neural Differential Equations and Reinforcement Learning," February. <http://arxiv.org/abs/2402.09387>.

1. Project overview

1.1. Introduction and background

Electric power systems are under great pressure to transform in response to multiple forces. Global demand for electricity will grow substantially as more than 100 million people are added to the middle class each year, more people gain access to electricity, and the electrification of transportation, heating, and industrial processes expands. Electric power systems are also under pressure to decarbonize to achieve net-zero carbon goals.

Fusion energy has the potential to help fill this need. The purpose of this study is to examine fusion energy's potential role as a major contributor in the future energy system and the requirements for achieving that role. In a decarbonized world, fusion energy combines the advantages of high power density, good siting flexibility, and the ability to deliver firm power. As such, fusion energy is complementary to other low-carbon technologies and does not need to compete with solar, wind, or fossil fuels on the simple metric of levelized cost of electricity. To understand the role of fusion in the future, we must understand how it will contribute to the overall energy system and assess the value of its dispatchability and firm delivery capabilities.

Fusion energy technology is being developed by dozens of companies, each with different strategies, designs, and timelines. This study is not specific to any particular fusion technology. Common goals for all fusion technologies are zero-carbon emissions, high power density, and delivery of dispatchable firm power. These technologies are more than ten years away from commercial deployment in fusion power plants, and the final characteristics of commercial fusion power plants are not known at this stage. Therefore, this study examines the threshold cost and performance characteristics that must be reached for fusion to achieve strong market penetration and have a significant impact on decarbonization.

The first deployments of fusion energy are expected to be for electric power generation; but in a deeply decarbonized world, the expectation is that fusion energy will play a vital role in tough-to-decarbonize sectors of the economy as well. To achieve maximum impact, fusion will likely be deployed for the production of hydrogen, low-carbon fuels, high-temperature process heat, and negative emissions. This study focuses solely on fusion power plants (). A separate future study will address a broader range of potential applications, including for transportation fuels, heat, and negative emissions.

The timing of this study is driven by the multiple forces currently shaping the decarbonization of the electric power sector. With aggressive grid decarbonization and electrification goals, the scale and type of electricity generation are expected to undergo massive changes in the coming decades. There is a role for variable renewable energy (wind and solar) and low-carbon firm power. How the mix evolves will depend on many factors. This study examines those factors and their impact on the electricity systems of the future.

1.2. Study objectives

This study aims to understand how fusion energy will contribute to the expansion, decarbonization, reliability, and economics of the electric power system. It addresses several important questions:

- How much FPP deployment could happen this century and where?
- How sensitive is FPP deployment to FPP cost?
- How sensitive is FPP deployment to climate policy?
- How sensitive is FPP deployment to other power generation resources?
- Under what scenarios will FPPs be operated as baseload versus peaker plants?
- How will thermal energy storage impact the FPP operating strategy?
- What are the dominant drivers of FPP cost?
- What is the potential for cost reductions?
- How can electricity markets be improved to enhance the deployment of FPPs and other firm power technologies?
- Are there critical material constraints that may impact the deployment of FPPs?
- What are potential bottlenecks in component manufacturing supply chains for FPPs?
- What other factors may impact FPP deployment?

This study does not predict when fusion technology will be commercialized, which fusion company will be first to market, or what fusion power will cost. Rather, we describe the various fusion confinement concepts and fuels, and we identify major cost and risk considerations for various fusion alternatives. Many of the analyses in this report center on the combination of magnetic confinement and deuterium-tritium fuel, because this combination is the most mature and defined FPP approach.

1.3. Overview of modeling and analysis methods

Our analysis applies three technology deployment models to evaluate optimal investments in fusion as a function of key inputs such as investment costs, energy demand, and carbon constraints, among others. The three models are applied at increasing levels of granularity in renewable resource availability and fusion technology detail, trading off decreasing breadth of geographical coverage and model horizons.

The **global model** provides worldwide coverage (explicitly representing 18 world regions) and extends out to the end of this century. It uses regional solar, wind, and hydro information for large geographical entities such as the United States, Europe, China, India, and Africa to assess renewable economics, model fusion technology as a firm power option, and represent the impact of electricity costs on consumption and on other parts of the economy. This global analysis is conducted under a deep decarbonization 1.5°C stabilization pathway. Details

regarding the global outlook are provided in [Chapter 4](#). The global model and the decarbonization scenario are described in [Appendix A](#).

The **multi-subregional model** covers subregions within the United States and models renewables and firm power within each U.S. subregion at an hourly resolution with a projected demand profile for 2050. This model is used to assess how local renewable resource attributes (solar, onshore wind, offshore wind, geothermal, run-of-river hydro, and reservoir hydro) impact the deployment of fusion power plants in each subregion and to test sensitivity to carbon emission caps and fusion costs. Details regarding the multi-subregion model and results are provided in [Chapter 5](#) and [Appendix B](#).

The **grid model** focuses on a single subregion constructed from more granular information on renewable resource availability at locations within the region, spatially resolved hourly demand loads across the region, transmission costs, and additional detail on generator flexibility. This model is used to examine important questions such as how land-use constraints for renewables, availability of carbon capture technology, and lower-cost renewables and batteries may impact the deployment of fusion energy. The grid model is also used to assess how fusion power plants will be operated at different price points for fusion. Details regarding the grid model and results are provided in [Chapter 5](#) and [Appendix B](#).

Fusion deployment also depends on access to the components needed to construct and operate these complex systems, which in turn requires raw materials, processing capacity for material refinement, and specialized manufacturing capacity. [Chapter 6](#) examines four component **supply chains**: high-temperature superconductors (HTS) and magnet assembly, plasma heating, blanket materials, and alloys and composites. We also assess the **critical materials** required for these fusion power plant subsystems, examining the quantities needed per power plant and how those quantities compare with annual production and reserves of key minerals.

[Chapter 7](#) discusses the results of a **techno-economic analysis** (TEA) designed to provide insights into fusion energy cost drivers and the potential impact of regulation on fusion costs. Given the current maturity of fusion concepts, we outline relative costs. The TEA considers the three broad categories of fusion confinement currently being pursued by more than 40 fusion companies, comparing their relative costs and maturity. We apply a bottom-up methodology that leverages data and cost estimation tools developed for fission power plants to develop cost estimates for fusion power plants, while still accounting for the inherent differences between fusion and fission technology. The techno-economic analysis methodology is described in [Appendix C](#).

2. Overview of fusion technologies

2.1. Introduction

More than 40 companies are currently pursuing the development of fusion energy (Fusion Industry Association 2023). Most of these companies are relatively new (30 of them were formed after 2016) and most are seeking to harness fusion energy for the generation of electricity. Across the nascent fusion industry, different approaches to achieve net-positive energy and, eventually, net electricity are being explored. These approaches can be distinguished by different choices of fuel and confinement method. Also important is the current status of technology development for each of the proposed concepts.

2.2. Fusion fuels

Fundamental laws of physics limit manmade fusion to a few fuel options. The nuclei of any pair of atoms can be fused if they can be brought together with sufficient energy. However, only a few fuels have the potential to serve as fusion fuels based on their required collision energy, the energy released per fusion reaction, and the relative probability of producing fusion reactions.

Deuterium-tritium (DT) is the leading fuel choice among 43 fusion companies surveyed recently by the Fusion Industry Association (Fusion Industry Association 2023). The main merits of DT fuel are that it requires the lowest plasma temperature and has by far the highest fusion reaction probability. The engineering challenge for DT-based designs is building a device that can withstand high-energy neutron fluence over a sufficient period of time, since 80% of the energy released by fusing deuterium and tritium is carried by high-energy neutrons that cause material damage and activation. Simultaneously, this fuel choice confers the advantage that neutrons cause volumetric heating due to their deep penetration in solids and liquids. Although there is no natural source for tritium, tritium can be produced from lithium by exposing lithium to the high-energy neutrons generated by DT fusion. Thus, lithium is included in the blanket material which surrounds the fusion reactor. To be self-sufficient in tritium, a DT device must be designed to generate at least as many tritium atoms as it consumes. Also, the existing fleet of heavy-water-moderated fission reactors in Canada and South Korea generate 1–2 kilograms (kg) of tritium per year; globally, the tritium inventory exceeds 30 kg (Pearson et al. 2018), which is enough to start a number of commercial fusion plants that could then be used to generate electricity and additional tritium.

A disadvantage of DT fusion is that tritium is radioactive and highly mobile, which means that various systems are needed for containment, extraction, and recycling. Nevertheless, experience with handling tritium and performing DT fusion experiments already exists, as a result of the Joint European Torus (JET) project in the United Kingdom, and the Tokamak Fusion Test Reactor (TFTR) and the National Ignition Facility (NIF) in the United States.

Deuterium-deuterium (DD) is the easiest fusion fuel to supply because deuterium is present in all water on Earth. However, achieving energy gain using DD fuel is more difficult than with DT fuel because the reaction probability of DD fusion is roughly 100 times lower than for DT fuel at the plasma temperatures that have been achieved in laboratory settings. Thus, DD fusion has lower power density than DT fusion at fixed physics conditions. DD fusion produces half as many neutrons per fusion reaction as DT fusion. DD fusion produces tritium, which is likely to fuse with deuterium and contributes to energy output. Simultaneously, DD fusion still produces high-energy neutrons that cause material damage and activation, but at a lesser rate than DT neutrons per unit of output energy. These disadvantages explain why more fusion startups developing magnetic-confinement-based designs are pursuing DT fuel, despite the challenges of producing and handling tritium.

Deuterium-helium-3 (DHe3) is another fuel option. Compared to DT fusion, it requires a four-times-higher temperature, and its reaction probability is about 50 times less. However, the DHe3 fusion reaction has the major potential advantage of producing helium-4 and a high-energy proton, which enables highly effective self-heating of the plasma through charged particle collisions of these products with the background fuel. This creates both a challenge and an opportunity since nearly all the fusion power is released as charged particles, which have low penetration depth through material surfaces (on the order of 1 micron in steel). Thus, DHe3 designs can potentially employ direct energy conversion of charged particles and photons emitted by the plasma rather than the volumetric heating method used for DT and DD fusion. This technology is challenging but skips over the step of first converting fusion kinetic energy to heat before converting the heat to electricity. The production of neutrons is not avoided, since DD fusion will still occur in a DHe3-fueled reactor and produce high-energy neutrons, though in smaller numbers per fusion power output. In addition to high temperature requirements and low reaction probability, the other major challenge for DHe3 fusion is the very limited availability of helium-3 (He3) on Earth. He3 can be supplied in sufficient quantities by deuterium-deuterium fusion which produces helium3 and tritium. Therefore, the DHe3 fuel cycle still involves tritium production and handling.

Proton-Boron (pB11) is the last potential fuel option currently under consideration for fusion. The major advantage of pB11 is that only charged particles (three alpha particles) are produced by the primary reaction—the reaction produces no neutrons. In addition, this fuel is highly abundant on Earth. However, the maximum reaction probability of pB11 fuel occurs at 10 times the target temperature for DT fusion. At this temperature, the pB11 reaction probability is 300 times less than the maximum reaction probability for DT fuel. Because of the extremely high collision energies required for proton-boron fusion, achieving net energy is more challenging than for the other fuel options. If the plasma particles are in thermodynamic equilibrium (i.e., Maxwellian velocity distribution), plasma radiative cooling losses will exceed the energy from p-

boron fusion by a multiple of 1.74. This problem could be overcome if a method were found to allow non-thermal ion velocity distributions (Rider 1995). Another potential option is to recover the radiative cooling energy with high efficiency. The pB11 fuel cycle features the smallest relative amount of energy released in neutrons—approximately 1%—due to neutron-producing side reactions.

2.3. Confinement methods

Confining fuels is essential to enable fusion to occur because the nuclei in the fuels have to have enough high-energy collisions to overcome the low probability of fusing. The high-temperature plasma conditions necessary for fusion require special confinement strategies. Several confinement methods are currently being investigated by the various fusion companies.

Magnetic confinement is the most widely pursued confinement method at present, but many different varieties of magnetic confinement devices are being developed by fusion startups. The basic approach is to use a magnetic field to contain and compress the plasma, using the magnetic force to provide adequate density and confinement time. Current design variations relate to the shape of the device and of the magnetic field, which is generally produced by energy-efficient superconducting electromagnets. Candidate designs include tokamak, spherical tokamak, mirror, and stellarator. Over 100 magnetic confinement devices have been built and operated worldwide, providing a large and robust science basis, particularly for tokamaks and stellarators. Two projects currently under construction, ITER in France and SPARC in the United States, are prominent examples of DT magnetic confinement research devices that aim to produce net-fusion energy.

Inertial confinement is the next most widely pursued confinement method. In these systems, the fuel is contained in a small, solid target that is bombarded with high-energy beams or a high-velocity projectile. The idea is to implode the target so that it rapidly compresses and heats the fuel, thereby enabling fusion to take place. The process is repeated in a rapid-fire manner using many targets to provide a steady supply of time-averaged fusion energy. The National Ignition Facility (NIF) in the United States is the most widely known research inertial confinement device.

Magneto-inertial confinement combines elements of magnetic confinement and inertial confinement and occurs at densities that are intermediate between magnetic confinement and inertia confinement. Although the methods vary substantially, the general concept is to exploit magnetic fields for containment, while also increasing fuel density and heating by compression. As with inertial confinement, this leads to pulsed designs.

2.4. Technology overview by company

This section outlines the confinement methods being pursued by 11 of the 43 companies currently seeking to develop fusion energy. [Table 2.1](#) groups companies by the fuel type and

confinement method they are targeting (all of the companies in this subset are focused on electricity generation) and gives a flavor of the wide range of different approaches being taken by the private sector.

Table 2.1 Categorization of fusion companies by fuel and confinement method

Fuel type	Confinement		
	Magnetic	Inertial	Magneto-inertial
Deuterium-tritium	Commonwealth Fusion Systems, Realta Fusion, Tokamak Energy, Type One Energy	First Light Fusion, Xcimer	General Fusion, Zap Energy
Deuterium-deuterium			
Deuterium-helium3			Helion Energy
Proton-boron11	TAE Technologies	Marvel Energy	

2.4.1. DT-magnetic confinement

Commonwealth Fusion Systems (CFS) is developing a DT-fueled, high-field compact tokamak that uses a molten lithium tetrafluoroberyllate salt (FLiBe) blanket for energy capture and breeding of tritium. Distinguishing features of CFS's technical approach are high-field magnetic containment using rare-earth barium copper oxide (REBCO) high-temperature superconducting (HTS) magnets designed to enable periodic replacement of the vacuum vessel, use of a FLiBe liquid immersion blanket, and modest requirements on plasma performance. The company has demonstrated a large-bore HTS magnet above 20 tesla.

Realta Fusion is developing a high-field, DT-fueled linear fusion reactor with two end plugs. Mirror coils will be built with REBCO HTS magnets. The company's initial target application is to provide process heat, but the ultimate objective is power generation at 100-MW_e scale. The distinguishing feature of this technology is high-field, mirror configuration.

Tokamak Energy is developing a DT-fueled spherical tokamak that uses a liquid lithium blanket for energy capture and tritium breeding. The company has focused on developing HTS magnets needed for compact tokamak designs and has demonstrated a small-scale HTS magnet producing a 26-tesla magnetic field. The distinguishing feature of this technology is high field in a spherical tokamak configuration with more demanding requirements on plasma performance.

Type One Energy is developing a stellarator technology to confine plasma along a twisted circular path. A stellarator offers plasma stability and can be operated continuously without

pulsing, an important intrinsic advantage over the tokamak. Type One Energy is using REBCO HTS magnets for confinement, with DT as the fuel and a lithium blanket for energy capture and tritium breeding. The distinguishing features of this approach are steady-state operation and reliance on additive manufacturing for economically manufacturing the device.

2.4.2. pB11-magnetic confinement

TAE Technologies, founded in 1998, is one of the oldest fusion companies and is developing a field-reversed-configuration fusion technology. Its target fusion fuel is pB11, but its confinement method can also work with other fusion fuels. The company's initial choice for energy conversion method will be thermal energy conversion to electricity, but its ultimate goal is direct energy conversion. TAE has developed multiple spinoff applications, including in the life sciences and for energy storage. Distinguishing features of its approach include pB11 fuel and multiple generations of field-reversed-configuration devices.

2.4.3. DT-inertial confinement

First Light Fusion is developing a projectile fusion technology. The purpose of the projectile is to create a shockwave that implodes the fuel target such that the fuel compresses and heats to achieve the required density and temperature for fusion. Each target includes the DT-fuel capsule surrounded by an amplifier solid material. The purpose of the amplifier is to boost the shockwave and direct it to converge on all sides of the fuel capsule. Heat and neutrons from the fusion reaction are captured by a first wall of liquid lithium. Distinguishing features of this technology include the liquid first wall and the use of projectile and amplifier to achieve compression.

Xcimer Energy is developing high-energy excimer laser technology by building on technology developed through the Strategic Defense Initiative. The company's laser development goals include longer-pulse, larger amplifiers and a lower repetition rate. Its chamber design uses a thick liquid waterfall wall of FLiBe to minimize activation and maximize the lifetime of the structure wall. Distinguishing features include the development of high-efficiency, high-energy, low-cost laser technology and the elimination of laser windows (Galloway 2023).

2.4.4. pB11-inertial confinement

Marvel Fusion is developing a proton-boron-fueled inertial confinement fusion system. This company's key focus is on ultra-short-pulsed, high-energy laser technology, which is used to rapidly heat nanostructured fuel targets. Each fusion of proton and boron generates three high-energy helium ions, which Marvel plans to directly convert to electricity via induction. Distinguishing features of Marvel's approach include ultra-short-pulsed lasers and the choice of pB11 fuel.

2.4.5. DT-magneto-inertial confinement

General Fusion is developing magneto-inertial fusion technology that injects the fuel plasma (DT fuel) into a spinning sphere of liquid-metal first wall/blanket, which is then compressed with hundreds of high-pressure pneumatic pistons. The resulting rapid compression of the plasma increases the plasma density and temperature to enable fusion. The molten lead-lithium metal captures the heat and neutrons and also breeds tritium. This design's distinguishing feature is the mechanically driven compression of the plasma within a molten metal envelope.

Zap Energy is developing a Z-pinch technology for magnetic confinement. The Z-pinch device does not require electromagnets. A strong magnetic field is created by running an electric current through the plasma. The magnetic field compresses the plasma, and the high current heats the plasma. Zap will use DT fuel and plans to use liquid lithium-lead for energy capture and tritium breeding. Compared with other magnetic confinement strategies, this design will support power-generation modules of 50 MW_e. Distinguishing features include magnetic confinement without magnets and modular 50-MW_e scale.

2.4.6. DHe3-magneto-inertial confinement

Helion Energy is developing a field-reversed-configuration fusion technology to be fueled with DHe3. The company uses a field-reversed configuration to hold two plasmas and then uses magnets to accelerate the two plasmas together at about 500 km per second. Upon collision, the plasma is further compressed by magnetic fields to reach fusion temperatures. The resulting fusion products are high-velocity ions, which are used to generate electricity directly by induction. Distinguishing features are the choice of DHe3 fuel and direct electromagnetic energy conversion.

2.5. Regulatory considerations and public perceptions

How fusion power plants (FPPs) are regulated and how they are perceived by the public can have a major impact on the future rate of fusion energy deployment around the world. Fusion is scientifically and technically distinct from fission, but much of the public is unaware of what fusion is and how it differs from fission. An FPP has never been built—thus, public opinion is still largely unformed and regulatory frameworks for this new type of power plant have not been developed in most countries. See [Section 7.1](#) regarding regulatory oversight in the United Kingdom and the United States.

This situation gives rise to several compelling questions:

- Will FPPs be welcomed in general?
- Will FPPs be accepted at the local level?
- Will a regulatory framework be developed soon enough to enable commercial FPP construction and operations in the 2030s?
- Will there be regulatory certainty, and will the regulatory process be time-efficient and cost-efficient?

This report does not make predictions about how public opinions of fusion might develop over the next decade, but it is worth noting that fusion advocates have been successful so far in differentiating fusion from fission. At present, regulators agree on several key points:

- Fusion energy systems cannot create self-sustaining neutron chain reactions. This has important safety implications for the operation of fusion systems relative to fission systems.
- The fuel cycle for fusion energy systems does not use fissile materials nor does it generate significant amounts of fission products with long radioactive lifetimes. This has implications for the fusion fuel cycle as it avoids the spent fuel and waste management issues associated with the fission fuel cycle.⁶

The potential for accidental radiological releases due to overheating and the challenges of safely managing long-lived nuclear fuel waste are the primary concerns of the public when considering fission power plants today. With adequate communications and public education regarding fusion, those two fears should not transfer from fission to fusion. However, fusion energy has health and safety issues of its own. The most widely pursued fuel for fusion is deuterium-tritium. While the amount of tritium within the reactor chamber is very small (typically < 1 gram), the total inventory of tritium fuel at a FPP would present a health hazard if released into the environment (White 2019).

The inventory of tritium needed at each DT-fueled fusion reactor is highly sensitive to the FPP design. One of the design goals is to minimize tritium inventories in order to minimize risk, cost, and regulatory burdens. Research efforts to date involving tritium, including the upcoming DT-fueled ITER and SPARC devices as well as the previously noted TFTR, JET, and NIF projects, have provided relatively positive experiences with tritium licensing and public acceptance, but FPPs may require significantly larger tritium inventories and processing rates. Therefore, effective designs are required to ensure that there are no uncontrolled releases into the environment. In

⁶ Fissile impurities may be present in blanket materials in low concentrations. Those impurities as well as other materials in the blanket, first wall, and structural materials will be activated by fusion-generated neutrons.

all forms of fusion, the solid, liquid, and gas atoms in engineered systems near the fusion plasma will become activated for a period of time depending on materials of construction. The details of these designs are highly sensitive to fuel cycle choice (described in previous sections), engineering design, and materials choices. Decisions about fuel, design, and materials will therefore be extremely important to the regulatory and environmental profile for FPPs.

2.6. Current status

While each of the concepts for fusion energy under consideration today promises a viable strategy for generating fusion electricity, significant differences exist in their present level of scientific and engineering development. Concepts that are at an earlier stage of development may indeed lead to more desirable reactors in the future. However, such configurations may need one or more intermediate facilities to demonstrate scientific or technical performance before extrapolation to large-scale power reactors is credible. In other words, the timeline for actual energy production will likely be longer for less mature fusion technologies.

An approximate way to compare the current status of each concept is to compare key performance ratios. The first metric focuses on the science status achieved in actual experiments for each concept. Scientific energy gain ($Q = P_{\text{fus}}/P_{\text{abs}}$) is the ratio of (equivalent) fusion power produced to power absorbed by the plasma to sustain plasma conditions. Equivalent refers to experiments using only D as the fuel rather than DT. Typically, reactors have to achieve Q greater than 20–50 to serve as the energy source for an electricity generator and, to date, none of the fusion concepts has achieved the level of gain required for power production.

Nevertheless, scientific energy gain is a valuable metric for measuring progress toward the eventual production of net electricity in a power plant. For the three broad confinement methods that have been most investigated to date, the reported maximum scientific gain for each is 0.62 for magnetic confinement (based on results from the Joint European Torus (JET)), 0.02 for magneto-inertial confinement (based on Magnetic Liner Inertial Fusion (MagLIF) experiments at the Sandia National Laboratory), and 1.54 for inertial confinement (based on 2022 results from the U.S. National Ignition Facility at the Lawrence Livermore National Laboratory; Keilhacker et al. 2001; Wurzel and Hsu 2022; Messinger 2022). Another important metric is the ratio of achieved temperature divided by the target temperature. The target temperature is defined as the temperature at which the product of required *plasma density and confinement time product* is minimized. For DT fusion, this target temperature is 200 million Kelvin (K). [Table 2.2](#) summarizes these performance metrics for the three broad confinement methods, while [Box 2.1](#) provides an overview of DT magnetic confinement and the corresponding challenges.

Table 2.2 Performance metrics achieved to date by fusion confinement method

Confinement method	Scientific gain (Q)	Temperature achieved/DT target temperature
Magnetic	0.62	1.07
Magneto-inertial	0.02	0.11
Inertial	1.54	0.5

Magnetic confinement values are based on the Joint European Torus (JET) in 1997; magneto-inertial confinement values are based on Magnetic Liner Inertial Fusion (MagLIF) in 2015; Inertial confinement values are based on the U.S. National Ignition Facility (NIF) in 2022 (Keilhacker et al. 2001; Wurzel and Hsu 2022; Messinger 2022).

Box 2.1 Overview of deuterium-tritium magnetic-confinement fusion technology and challenges

The key to harnessing fusion energy is what is referred to as containment. Successful containment requires that the fusion fuels be brought together with sufficient duration and sufficient energy such that the fuels collide enough times and with enough force to overcome the relatively low probability of the fusion reaction. Magnetic confinement makes use of strong magnetic fields to confine the positively charged fuel nuclei. Several techniques have been developed to heat plasmas to more than 100 million degrees Kelvin. These heating methods include using electromagnetic waves with high frequencies such that they are resonant with the fuel nuclei.

Scientific knowledge of magnetic confinement and plasma science has been built up over more than 60 years with extensive research programs conducted in more than 100 magnetic-confinement devices. The science of fusion is well established and the ability to produce fusion reactions is straightforward. The remaining challenge is to create a system in which fusion energy can be harnessed to economically generate electricity.

As indicated in [Table 2.2](#), magnetic confinement has achieved scientific energy gain of 0.62. This means that the fusion energy released is 62% of the energy used to heat up the plasma. Of course, a power plant must produce more energy than it consumes, but simply pushing scientific gain to exceed 1 is not adequate. We must have a net gain from the overall power plant. Therefore, we must account for all the efficiencies throughout the power plant, including the conversion of electricity to radio-frequency energy required to heat the plasma, the efficiency for converting thermal energy to electricity, the energy required for cryogenic cooling of the magnetics, and the energy required for extracting tritium from the blanket.

The current phase of fusion energy development goes beyond plasma science and short duration experiments. Fusion power plants require solutions to the engineering, material, and technological challenges to enable plants to operate 24/7 with good annual availability and competitive costs. Major breakthroughs such as high-temperature superconductors are consequential, but not sufficient on their own. Key engineering, material, and technological challenges include:

- Fabrication of magnet assemblies that can withstand forces from their own magnetic field
- Control of the plasma with advanced techniques and machine learning to detect and mitigate plasma disruptions
- Development of supply chains for manufacturing high-efficiency plasma-heating technologies
- Production at scale of materials with the following required characteristics
 - Strength at elevated temperatures
 - Ductility
 - High thermal conductivity
 - Radiation resistance
 - Low activation
 - High melting temperature
 - Corrosion resistance
 - Manufacturability

References

- Galloway, Conner. 2023. "Excimer Lasers for IFE with Raman and Brillouin Staged Boosting ARPA-E Workshop." March 7, 2023. https://arpa-e.energy.gov/sites/default/files/A06-Galloway-FusionWorkshop_03-07-23.pdf
- Holland, Andrew. 2022. "The Global Fusion Industry in 2022." <https://www.fusionindustryassociation.org/wp-content/uploads/2023/05/globalFusionEnergyReport.pdf>
- Keilhacker, M., A. Gibson, C. Gormezano, and P. H. Rebut. 2001. "The Scientific Success of JET." *Nuclear Fusion* 41 (12): 1925.
- Messinger, Jonah. 2022. "Fusion Breakeven Is a Science Breakthrough." The Breakthrough Institute. December 13, 2022. <https://thebreakthrough.org/issues/energy/fusion-breakeven-is-a-science-breakthrough>.
- Pearson, Richard J., Armando B. Antoniazzi, and William J. Nuttall. 2018. "Tritium Supply and Use: A Key Issue for the Development of Nuclear Fusion Energy." *Fusion Engineering and Design* 136 (November): 1140–48. <https://doi.org/10.1016/J.FUSENGDES.2018.04.090>.
- Rider, Todd H. 1995. "Fundamental Limitations of Plasma Fusion Systems Not in Thermodynamic Equilibrium." Doctoral Thesis, Department of Electrical Engineering and Computer Science, MIT. Cambridge, Massachusetts: Massachusetts Institute of Technology.
- White, Robert Patrick. 2019. "Pathways and Frameworks for the Licensing and Regulation of Advanced Nuclear Reactors in the United States." Master's Thesis, Department of Mechanical Engineering, MIT. Cambridge, Massachusetts: Massachusetts Institute of Technology. <https://dspace.mit.edu/handle/1721.1/121714>.
- Wurzel, Samuel E., and Scott C. Hsu. 2022. "Progress toward Fusion Energy Breakeven and Gain as Measured against the Lawson Criterion." *Physics of Plasmas* 29 (6): 66. https://doi.org/10.1063/5.0083990/16620691/062103_1_ACCEPTED_MANUSCRIPT.PDF.

3. Electricity generation in a decarbonized world

3.1. Overview of low-carbon power generation and energy storage

Power systems across the globe confront the dual challenge of meeting increased demand for electricity while also reducing greenhouse gas emissions. Primarily this involves replacing fossil fuel-fired generation with low-carbon generation, building new low-carbon capacity, and enhancing infrastructure. A range of established low-carbon technologies is available today, including on- and off-shore wind, solar photovoltaic (PV), hydroelectric, and nuclear fission. Many additional low-carbon technologies are at various stages of research, development, and demonstration. These include fusion, but also enhanced geothermal and bioenergy with carbon capture and storage (CCS), as well as thermal generation from low-carbon fuels. Alongside these generation technologies is a set of established energy storage technologies, such as pumped hydro and various batteries, as well as new forms of storage that are currently in the development and demonstration stages.

These technologies differ from one another along many dimensions. They have different capital and operating costs, require different materials and resources (including different amounts of land for siting), and have different ecological impacts (including different lifecycle greenhouse gas emissions). They each require differently trained workforces, have different safety profiles, and will enjoy different levels of social acceptance. The exact nature of these differences as well as their saliency varies across regions of the globe. Consequently, we can expect regional diversity in the portfolio of low-carbon-generating technologies selected to meet future power system needs.

The advantages and disadvantages of different technologies will also evolve over time as the technologies themselves develop, and as the societies within which they operate change. So, we can also expect the preferred mix of options for different regions to shift over time.

Keeping this diversity of contexts and trade-offs in mind, we focus in this chapter on one key dynamic shaping the role of fusion as a power technology: its value as a zero-carbon source of firm power.

3.2. Role of zero-carbon firm power

Recent decades have seen impressive reductions in the cost of both wind and solar PV. These cost declines, together with the need to reduce carbon emissions, have led to increased investment in both technologies. Accordingly, almost all pathways to net-zero grids involve dramatically expanded penetration of wind and solar power generation.

A key feature of these resources is their variable nature. A major buildout of variable renewable energy (VRE) technologies saturates the supply in certain hours of the year while leaving demand unmet in other hours. It is possible to serve some of this unmet demand with further

investments in VRE capacity, but at the expense of greater curtailment in hours of plentiful supply. As a result, the cost per unit of useful generation gradually increases with the level of penetration of VREs. Total system cost can be minimized by identifying complementary technologies and investments. These include storage, interregional transmission, and expanded demand response. They also include zero-carbon firm power technologies. Firm power technologies “can be counted on to meet demand when needed in all seasons and over long durations (e.g., weeks or longer) and include nuclear power plants capable of flexible operations, hydro plants with high-capacity reservoirs, coal and natural gas plants with CCS and capable of flexible operations, geothermal power, and biomass- and biogas-fueled power plants” (Jenkins et al. 2018; Sepulveda et al. 2018). Fusion is another zero-carbon firm power technology.

To illustrate the value of incorporating zero-carbon firm power as an option, we constructed an experiment using the GenX capacity expansion model featured in [Chapter 5](#). There the model is used to understand the competitive landscape for fusion power plants on the electric grid of the six-state U.S. region of New England. For the illustrative experiment here, we calculate the total system cost for two alternative scenarios. In one scenario, we assume that no zero-carbon firm technology is available. In the second scenario, we make fusion power plants available using the base case assumptions detailed in [Chapter 5](#). Adding the option of fusion power plants reduces total generation costs from \$508 billion per year to \$471 billion per year, a savings of \$36 billion or 7% of annual system cost in 2050 in New England.

A full appreciation of the value of fusion and other zero-carbon firm technologies requires an expanded understanding of uncertainty and improved capacity planning models to account for uncertainty. This is because the increasing penetration of VREs such as wind and solar, and the accompanying increase in utilization of storage resources and demand response programs complicate the assessment of resource adequacy (Stenclik et al. 2021). It is no longer sufficient to focus on a single peak load hour—rather, it becomes necessary to assess chronological grid operations. Sequential hours with low renewables output can produce a deficit of energy even when there is no peak in demand. Likewise, sequential hours with relatively high demand can exhaust stored energy even when there is no demand peak. A study by Ruhnau and Qvist (2022) illustrates these issues. The authors use a weather reanalysis dataset covering the 35 years from 1982 to 2016 to optimize a German power system using only renewables and various types of storage. They find that multiple periods of energy scarcity can closely follow one another, so that the maximum period of energy deficit is 9 weeks, as opposed to the 2 weeks calculated by focusing on discrete deficit events. Incorporating storage losses and charging limits in the analysis results in storage requirements that are three times larger than those required to cover the most extreme 2-week scarcity event. Required storage capacity

calculated based on the full 35-year dataset is double the average calculated from single-year optimization.

Similar reassessments can be used to evaluate the optimal amount of zero-carbon firm power capacity in a high-VRE system. The GenX modeling discussed in [Chapter 5](#) employed 20 years of weather data to represent weather and load uncertainty in New England. Until recently, it has been standard practice in the capacity modeling literature to focus on a single year of variable weather data. Even this simple increase in the representation of uncertainty—moving from a single year to 20 scenario-years—caused the model to recommend double the amount of fusion capacity compared to the average of 20 single-year optimizations.

This section previews one select grid modeling result out of the many that are discussed extensively in [Chapters 4](#) and [5](#). It demonstrates that fusion power plants can be an element of the least-cost portfolio of capacity investments depending on the realized capital cost of a plant and other factors. This modeling result addresses the question of whether fusion power plants *should* be built, and in what quantity. A slightly different question is whether fusion power plants *will* be built, and in sufficient quantity. Are electricity markets designed such that developers of fusion plants can recoup their up-front investment plus a reasonable rate of return? What features of current market designs disincentivize investments in socially valuable fusion power plants? Conversely, what market designs would enable investments in socially valuable fusion power plants?

3.3. Wholesale power markets and financing investments in fusion power plants

The early-stage research, development, and demonstration of fusion power plants is being financed through a combination of government funding and venture capital investments. Down the road, once one or more designs have been demonstrated and the focus shifts to deployment, the structure of financing must also shift. The case for investing in a fusion power plant will be based on the value of the electricity produced by that plant. Investors will have to be convinced the plant will produce a reliable cash flow sufficient to cover principal and interest on the project's debt, while also providing a satisfactory profit to equity shareholders. What electricity market structure can facilitate the profitable deployment of fusion power plants?

The institutional structure of the electricity industry varies widely across countries, and almost as widely within some countries. Generation assets can be owned by state-owned corporations, cooperatives, investor-owned utilities granted a monopoly franchise under state regulation, and privately owned corporations competing in relatively free market structures. They can also be owned by non-profit companies and a variety of government agencies. In many countries, different structures operate side by side. For example, competitive markets and private investment can coexist with state ownership of some assets.

Many of these seemingly diverse institutional structures evaluate investments in individual plants in the context of an assessment of the full portfolio of system assets and by considering the many alternatives and combinations of options available to them. In the United States, this approach goes by the name of integrated resource planning (IRP). Investor-owned utilities are often mandated by law or regulation to prepare integrated resource plans; this practice is common among publicly owned power corporations and cooperatives as well. An IRP involves assessing future load, the future in-service capability of existing assets, and the set of available new generation options. All aspects of the electric system are looked at comprehensively, including wires, generation, storage, and demand management opportunities, among others. In addition, alternative rate structures for financing needed investments are evaluated. The aim of the process is to identify the set of new generation assets that will be targeted for procurement in coming years, together with anticipated financing needs and planned rates to service the financing. Similarly comprehensive power system planning processes occur in regions around the globe, although the institutions involved and the process details vary.

Individual power plant investment decisions occur downstream from an IRP. At investor-owned utilities in the United States, a proposal for a specific investment must be brought to a state utility commission for review and approval. The proposal typically includes full details on the technology, vendor, timeline, financing, and rate increases needed to service any additional debt and provide a return on capital to the equity shareholders. The utility makes a case that the specific plant is a cost-efficient contribution to its overall long-term plan and that the financing and proposed rates are good for utility customers. Once the state commission approves the plan—perhaps with amendments—the investment can be made, the financing can be arranged, and rates will be adjusted to cover the financing. Publicly owned power corporations approve specific investments in a similar fashion, although instead of seeking approval from a state commission, they may have to get permission from a board or other supervisory authority. Especially large investments often involve joint ownership by multiple power authorities.

From the point of view of investors, the key benefit of obtaining regulatory approval via a planning process is the revenue certainty it provides. Public authorities make an up-front commitment to levy future customer charges sufficient to fund the amortization of the original investment plus a return on capital. In each case, the customers take part in approving the investment decision—whether directly, in the case of an industrial customer or cooperative member, or indirectly, through their political representatives, in the case of a state-owned corporation or public utility commission. Once investments are approved, customers are obligated to pay for them. This commitment makes it possible to finance new plant construction, since the utility can count on a reliable stream of future revenue to support low-cost borrowing alongside equity capital.

It is important to appreciate that this “forward contracting” model for financing power plant investment puts significant risk on customers. Uncertainty applies to all investments. The best-laid plans are based on forecasts of future variables, and the actual future may look very different from the forecast. For example, an investment in a natural gas-fired power plant may look cost-efficient because the price of natural gas is expected to be very low. Once the plant is built, the price of gas could escalate beyond what was forecasted. In that case, customers’ rates will have to be increased to cover the higher price of gas. Even if the plant owner runs the plant less often and purchases less expensive electricity from others, costs (and hence rates) will likely be higher than if planners had anticipated higher gas prices and made a different investment.

To take another example, consider that investments in capacity are made to serve expected demand. If demand does not grow as forecasted, customer rates must still be set to repay investors for the excess capacity. Because customers largely bear these risks, however, the rate of return required to finance a power plant investment is relatively low, which benefits customers.

Many regions around the globe, including the European Union, the United Kingdom, several countries in South America, and several subregions of the United States, have developed competitive wholesale markets for electricity. The primary focus for introducing competition has been the short-term or spot market for energy. Generators bid into a rolling series of daily and intraday markets to supply electricity across the hours of the day. These markets serve to optimize the short-run operation of the power system. A short-term wholesale market can be consistent with the variety of institutional ownership models described above. The generators bidding to supply electricity can be privately or publicly owned. They can be owned by regulated utilities or unregulated companies.

Some regions with competitive wholesale markets also restructured their utilities to encourage private investment in generation. In many cases, regulated, investor-owned utilities were required to divest themselves of generation assets, such that they became wires companies. This “merchant model” relies on private companies to make new investments in generation capacity based on private companies’ individual assessments of future demand, available technologies, and costs. In this model, merchant generators make speculative investment decisions based on the uncertain future wholesale market price of electricity. They will make investments only where their expectations about future prices yield sufficient profit. However, the future price may turn out to be much higher or lower than originally expected, and the investment may return an outsized profit, or it could return a loss. The merchant generator bears that risk. Customers have made no forward commitment, and they avoid the investment risk.

How hard or easy it may be to finance investments in new power plants under this merchant model will depend on the structure of the electricity market and the ability to forecast prices and sales for a power plant's output. Under idealized assumptions about competition and pricing in spot markets, the revenue earned in the spot market ought to incentivize efficient investment in a portfolio of generation assets (see Boiteux 1960; 1964; Turvey 1968; Joskow and Tirole 2007). This ideal is known as an “energy-only” market.

Many regions developed their competitive wholesale markets in an era of excess generating capacity, so the problems of this ideal were not initially obvious. However, there are a number of practical impediments to translating short-run efficient pricing into long-run incentives for capacity investment. Together, those impediments produce what is known as the “missing money” problem—i.e., the persistently observed failure of the energy-only market to provide revenues sufficient to justify needed investment in capacity (Joskow 2007; 2008).⁷ Attention focuses on “scarcity events”—when demand exhausts available supply and the system operator finds it difficult to maintain the power balance. At such times, the marginal value of an increment of supply is very, very high. The prices set during these events are called “scarcity prices.”

During scarcity events, obstacles arise on both the demand and supply side that limit the ability of price to be an efficient signal of value. Cases of load shedding happen within scarcity events, but the costs of load shedding are socialized across all buyers. Individual buyers cannot signal their willingness to pay for reliable power and cannot lay claim to power based on prudent contracting ahead of time (Wolak 2013; 2022). Prices also cannot be set by seller offers because scarcity events enable the extreme exercise of market power. Consequently, scarcity prices are set administratively. While they are quite high—hundreds of times higher than the average wholesale price in non-scarcity events—they nevertheless have not been high enough to adequately incentivize sufficient investment in capacity.

Where the merchant model is operative, supplementary sources of revenue have been developed to incentivize needed investments in generation capacity. For example, across North America, South America, and Europe, authorities have shifted away from an energy-only market paradigm and have added capacity markets or other remuneration mechanisms to provide a supplementary source of revenue on top of the energy market to assure adequate incentives for capacity investments. There is a great diversity in the designs of these

⁷ Some investments in generation capacity have been made under this merchant model in various countries, in various eras, and for particular types of technologies. However, those investments can also be seen as the exception that proves the rule.

mechanisms, and the rules for defining and accrediting capacity and setting prices have evolved over time.

In parallel with the development of within-market capacity mechanisms, the pressing need to reduce greenhouse gas emissions has also spurred many regions to provide a separate channel of out-of-market subsidies to support investment in various low-carbon generation technologies. Initially, these subsidies were primarily restricted to investments in wind and solar PV and took the form of feed-in tariffs, renewable portfolio standards, contracts-for-differences, and/or tax credits. Most have been structured like the forward commitments mentioned earlier, in that they provide a reliable cash flow over a sufficiently long number of years to enable developers to finance the up-front capacity investment. Recently, some regions have broadened the set of technologies that are eligible for subsidies to include, for example, life extensions and uprates at existing nuclear fission plants or for nuclear new builds. More recently, the U.S. Inflation Reduction Act (118th Congress 2022) greatly expanded the scale of production tax credits available for new investments in a wide array of designated low-carbon generation technologies.

Regions employing the merchant model face two related challenges. The first challenge is to plan and structure the overall set of capacity payments so that, taken together, they produce a cost-efficient portfolio of capacity. The second is to structure the terms of the various streams of payments so that they are aligned with the efficient operation of the short-run competitive wholesale energy market—for example, to avoid creating windows of negative energy prices. To this end, the European Union has been coalescing around the use of subsidies integrated with the wholesale market via contracts for difference (CfDs)⁸, and enhanced designs for CfD structures—most recently, see ENTSO-E (2024).

The missing money problem is likely to become more severe as electricity systems shift to low-carbon generation technologies, and especially as the penetration of VREs expands (Mallapragada et al. 2023). Most low-carbon generation technologies are capital-intensive. Many, especially wind and solar PV, have zero marginal operating cost. Therefore, in periods of high wind and solar availability, the marginal value of energy is zero. Since the marginal value of

⁸ A CfD is based on the difference between the market price and an agreed “strike price.” If the “strike price” is higher than the market price, the CfD counterparty must pay the renewable generator the difference between the “strike price” and the market price. If the market price is higher than the agreed “strike price,” the renewable generator must reimburse the CfD counterparty for the difference between the market price and the “strike price.” (“Contract for Difference (CfD) – Policies - IEA,” n.d.)

energy is what sets the wholesale electricity price, the price should fall to zero in these hours.⁹ As penetration of VREs expands, these zero-price hours will happen with increasing frequency. Conversely, the total revenues needed to justify investment must be earned in fewer and fewer hours of the year, and in what are increasingly likely to be scarcity hours.

These dynamics have dramatic implications for the pattern of energy market revenues that a fusion power plant can expect to earn in a competitive wholesale market supplied by low-carbon generation. To illustrate this point, [Figure 3.1](#) shows two distributions of total energy market revenues earned by a fusion power plant. These distributions were calculated using the GenX capacity expansion model of the six-state New England region featured in [Chapter 5](#).¹⁰ One distribution is calculated under the assumption that the average capital cost of a fusion power plant in the United States in 2050 is \$8,500/kW, while the other is calculated assuming a lower capital cost of \$6,000/kW.¹¹

The distribution is displayed as a Lorenz curve. On the horizontal axis, the hours in the simulation are ordered from the hour with the lowest energy market revenue on the left, to the hour with the highest energy market revenue on the right. The vertical axis is the cumulative share of total annual energy market revenue. Each line reports the share of revenue accounted for by the hours to the left of the curve—it starts at 0% for the lowest-revenue hour and rises to 100% for the highest, by definition, but the shape of the path between those two points varies with the distribution across hours.

A Lorenz curve is designed to measure inequality. If all hours of the year had the same price of energy and the same load, then the line would track along a 45-degree slope. When the line is bowed down, there are more hours with less-than-average energy market revenue, and fewer remaining hours with above-average energy market revenue.

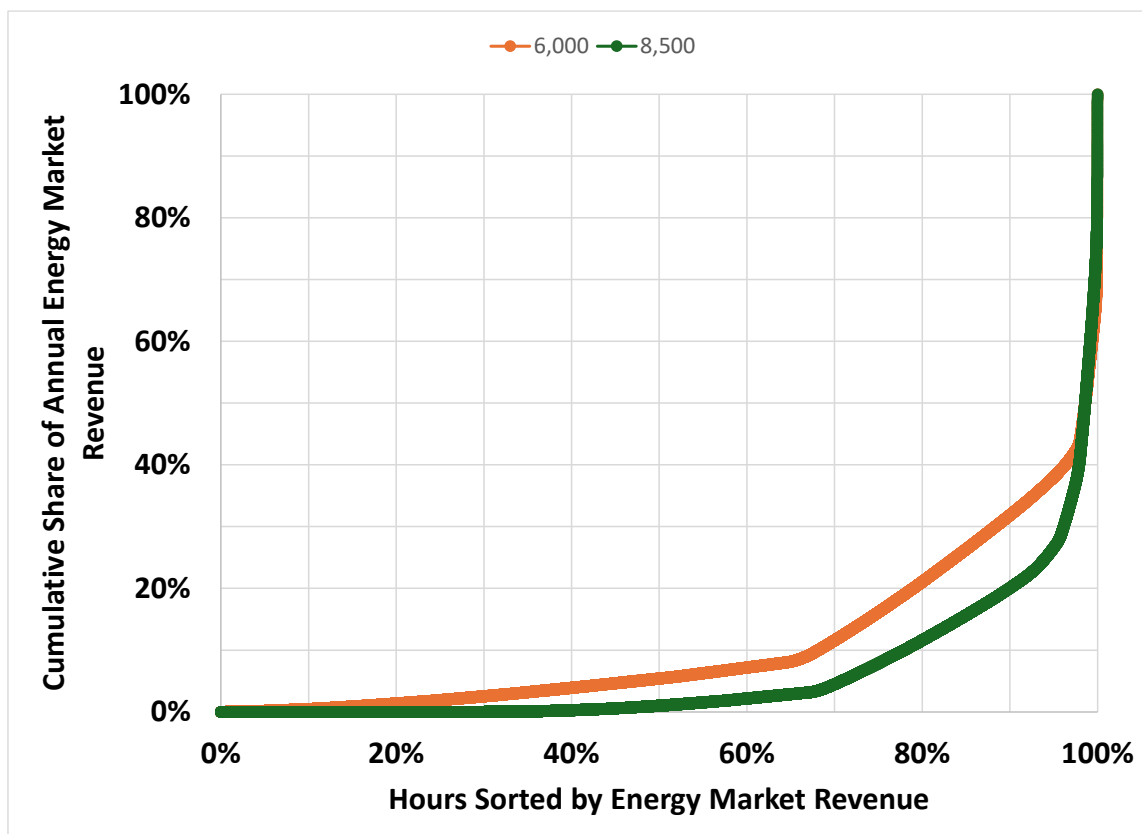
⁹ In fact, high wind availability has sometimes driven the wholesale market price in some regions to be negative (Seel et al. 2018). This is an artifact of the structure of the out-of-market subsidies used to incentivize investments in wind capacity. When the marginal value of electricity is zero, there should be no incentive for a wind farm to produce. However, the owner of the wind farm receives a production tax credit based on the wind farm's output regardless of the market into which the electricity is fed. Therefore, the owner is willing to produce even when doing so causes a negative price. It would be better for the subsidy to be designed to harmonize with short-run dispatch optimization.

¹⁰ Hourly energy market revenue is calculated by multiplying hourly generation from the fusion power plant by the hourly marginal value of energy. Total energy market revenue is the sum of hourly energy market revenue across all hours of the year. Since the GenX model in [Chapter 5](#) simulates operation across 20 different scenario-years, the total is taken across all scenarios and then divided by 20 to reflect the average expectation for a single year.

¹¹ Both distributions were calculated for the base case detailed in [Chapter 5](#), and for the tightest CO₂ emissions cap considered: 4 g-CO₂/kWh.

Looking at the line for the \$8,500/kW fusion power plant in [Figure 3.1](#), we can see that revenue is approximately zero in the lowest-revenue 40% of hours. The lowest 76% of hours bring in less than 10% of annual energy market revenue. That leaves the remaining 24% of hours to bring in more than 90% of annual revenue. Indeed, 1% of hours are expected to bring in 57% of annual energy market revenue. The revenue distribution graphed by the second line, for the \$6,500/kW fusion power plant, is still markedly skewed, although slightly less so.

Figure 3.1 Lorenz curve of hourly energy market revenue earned by a fusion power plant



These results were obtained using the GenX model for two cost cases.

Although [Figure 3.1](#) is very striking, it fails to fully reflect the extreme skewness of the distribution of energy revenue. That is because it shows the average distribution across many scenario-years. There will be years when higher-than-average availability of renewable energy keeps prices low throughout the year. There may be no scarcity hours at all in some years, and a concentration of scarcity hours in a few years out of the 20 scenario-years considered. In 16 of the 20 scenario-years input to the GenX base case, the \$8,500/kW fusion power plant earns less than its required average annual revenue. In the other four scenario-years, it makes much, much more than its required average annual revenue—in fact, ten times more in one scenario-year. That is not a bankable revenue stream.

This extremely skewed distribution of energy market revenue may be expected in a competitive wholesale energy market characterized by low-carbon generation and high penetration of VREs. Increased reliance on scarcity hours for revenue exacerbates the missing money problem. Therefore, some sort of capacity mechanism or out-of-market subsidy is necessary to incentivize investments in generation capacity.

3.4. Conclusions

Fusion power plants are a potentially valuable source of zero-carbon firm power and an important part of the portfolio of generating capacity and other grid assets needed to achieve cost-effective decarbonization. The increasing penetration of inexpensive VREs is an important feature of a net-zero grid. As a result, system planners will need to focus more attention on uncertainty, especially surrounding the availability of wind and solar resources. Fusion power plants can be a valuable complement to VREs, and uncertainty about VRE availability increases the value of these plants to the grid.

A reliable source of revenue to cover debt repayment and a return to equity shareholders is key to financing capital-intensive generation technologies, including fusion power plants. In most regions, this reliable source of revenue comes from a forward commitment made by customers or by their political representatives. The forward commitment takes widely varied forms across regions with diverse institutional and ownership structures.

Other regions use a merchant model that relies on investors making speculative investments based on expectations about future wholesale market revenues. Due to the missing money problem, the energy-only market version of the merchant model does not provide sufficient incentives for investment. Regions have been forced to supplement energy market revenues with capacity market revenues or with revenues from other mechanisms to incentivize merchant investments in new capacity. In some regions, targeted subsidies for low-carbon generation technologies have been structured to provide the reliable revenue stream necessary to finance investments. Efforts to decarbonize the grid, including through increased deployment of VREs, will exacerbate the missing money problem. Regions that are using the merchant model must develop one or more capacity mechanisms to provide the steady source of revenue required to finance investments in fusion power plants.

References

- 118th Congress. 2022. Inflation Reduction Act of 2022. United States.
- Boiteux, Marcel. 1960. "Peak-Load Pricing." *The Journal of Business* 33 (2): 157–79.
- . 1964. "The Choice of Plant and Equipment for the Production of Electric Energy." In *Marginal Cost Pricing in Practice*. Englewood Cliffs, NJ: Prentice-Hall.
- "Contract for Difference (CfD) – Policies - IEA." n.d. Accessed March 8, 2024. <https://www.iea.org/policies/5731-contract-for-difference-cfd>.

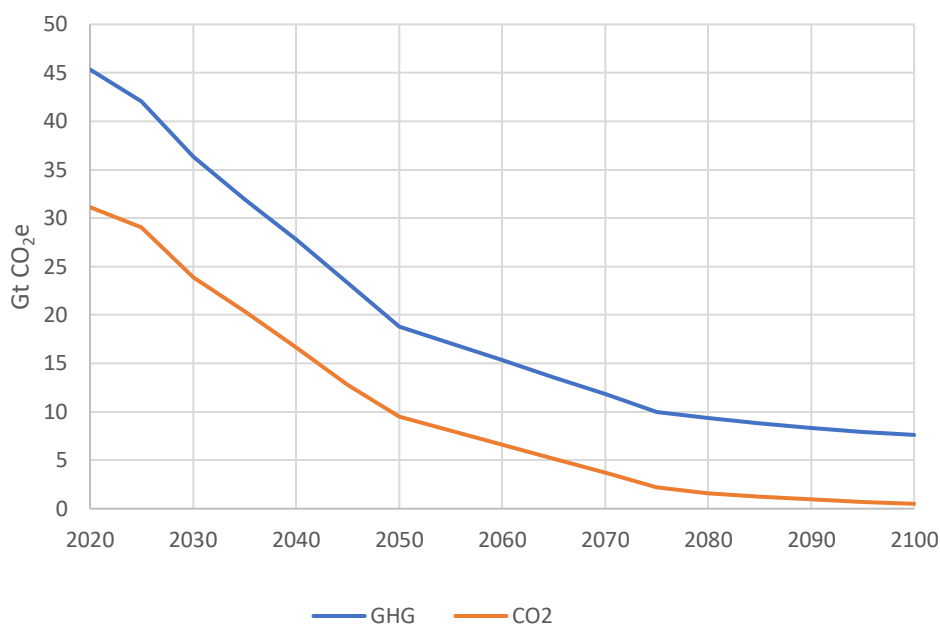
- ENTSO-E Working Group Market Design & Renewable Energy Sources. 2024. "Position Paper: Sustainable Contracts for Difference (CfDs) Design." <https://www.entsoe.eu/2024/02/20/position-paper-on-sustainable-contracts-for-difference-design/>. Brussels, Belgium: ENTSO-E AISBL.
- Jenkins, Jesse D., Max Luke, and Samuel Thernstrom. 2018. "Getting to Zero Carbon Emissions in the Electric Power Sector." *Joule* 2 (12): 2487–510. <https://doi.org/10.1016/j.joule.2018.11.013>
- Joskow, Paul. 2007. "Competitive Electricity Markets and Investment in New Generating Capacity ." In *The New Energy Paradigm*, edited by Dieter Helm. Oxford University Press.
- . 2008. "Capacity Payments in Imperfect Electricity Markets: Need and Design." *Utilities Policy* 16 (3): 159–70.
- Joskow, Paul, and Jean Tirole. 2007. "Reliability and Competitive Electricity Markets." *The RAND Journal of Economics* 38 (1): 60–84.
- Mallapragada, Dharik S., Cristian Junge, Cathy Wang, Hannes Pfeifenberger, Paul L. Joskow, and Richard Schmalensee. 2023. "Electricity Pricing Challenges in Future Renewables-Dominant Power Systems." *Energy Economics* 126 (October): 106981. <https://doi.org/10.1016/j.eneco.2023.106981>.
- Ruhnau, Oliver, and Staffan Qvist. 2022. "Storage Requirements in a 100% Renewable Electricity System: Extreme Events and Inter-Annual Variability." *Environmental Research Letters* 17 (4): 044018. <https://doi.org/10.1088/1748-9326/AC4DC8>.
- Seel, Joachim, Andrew D. Mills, Ryan H. Wiser, Sidart Deb, Aarthi Asokkumar, Mohammad Hassanzadeh, and Amirsaman Aarabali. 2018. "Impacts of High Variable Renewable Energy Futures on Wholesale Electricity Prices, and on Electric-Sector Decision Making." E-Scholarship Repository, Berkeley, CA (United States). <https://doi.org/10.2172/1437006>.
- Sepulveda, Nestor A., Jesse D. Jenkins, Fernando J. de Sisternes, and Richard K. Lester. 2018. "The Role of Firm Low-Carbon Electricity Resources in Deep Decarbonization of Power Generation." *Joule* 2 (11): 2403–20. <https://doi.org/10.1016/j.joule.2018.08.006>.
- Stenlik, Derek, Aaron Bloom, Wesley Cole, Gord Stephen, Armand Figueroa Acevedo, Rob Gramlich, Chris Dent, Nick Schlag, and Michael Milligan. 2021. "Quantifying Risk in an Uncertain Future: The Evolution of Resource Adequacy." *IEEE Power and Energy Magazine* 19 (6): 29–36. <https://doi.org/10.1109/MPE.2021.3104076>.
- Turvey, Ralph. 1968. *Optimal Pricing and Investment in Electricity Supply: An Essay in Applied Welfare Economics*. Cambridge, MA: MIT Press.
- Wolak, Frank A. 2013. "Economic and Political Constraints on the Demand-Side of Electricity Industry Restructuring Processes." *Review of Economics and Institutions* 4 (2): 42.
- . 2022. "Long-Term Resource Adequacy in Wholesale Electricity Markets with Significant Intermittent Renewables." *Environmental and Energy Policy and the Economy* 3 (1): 155–220.

4. Global outlook for fusion energy deployment

4.1. Introduction

To assess the cost parameters that fusion technology must deliver to become a substantial contributor to decarbonization at the global scale, we evaluate its cost competitiveness as part of a portfolio of low-carbon power generation options by applying our global model, an enhanced version of the MIT Economic Projection and Policy Analysis (EPPA) model ([Appendix A.1](#) provides a description of the EPPA model). For profiles of annual global greenhouse gas (GHG) emissions from 2020 to 2100, we use the Accelerated Actions scenario, a 1.5°C stabilization pathway based on the MIT Global Change Outlook (MIT Joint Program 2023). Global annual CO₂ and GHG emissions for this scenario are shown in [Figure 4.1](#) ([Appendix A.2](#) provides further information about the Accelerated Actions scenario).

Figure 4.1 Global annual emissions of greenhouse gases (GHG) and carbon dioxide (CO₂) in the Accelerated Actions scenario



4.2. Global power demand and resources

Key drivers of future increases in global energy consumption are population and economic growth. While efficiency improvements will offset some of the impact of these drivers, we project a substantial electrification of the global economy and a large expansion of renewable sources for electricity production. This is because expanded deployment of low-carbon electricity generation and accelerated electrification of transport, buildings, and industry are widely viewed as necessary to substantially decarbonize national economies. From 2020 to 2100, global electricity consumption is projected to grow by 340%, from about 25,000 TWh in

2020 to more than 85,000 TWh by the end of the century. In the Accelerated Actions scenario, much of this increase is supplied by renewable sources, such as wind, solar, and biomass. Generation from these sources is projected to grow 20-fold, from about 2,000 TWh in 2020 to more than 40,000 TWh in 2100. To realize a renewables scale-up of this magnitude, challenges related to energy storage (to address the intermittency of variable renewables), land-use implications for biomass, permitting reforms for generation and transmission lines, as well as materials and critical minerals availability, should be addressed. For this analysis, we apply resource availability assessments from previous studies related to variable renewables (Gurgel et al. 2023), biomass (Fajardy et al. 2021), and negative emission technologies (Desport et al. 2024), but it is important to recognize that many potential bottlenecks or unexpected technological advances may affect the pace of technology development and the resulting power generation mix. Our exploration here does not intend to provide a comprehensive evaluation of all technology and policy dimensions—rather we focus on exploring the role of fusion power generation in a decarbonized future.

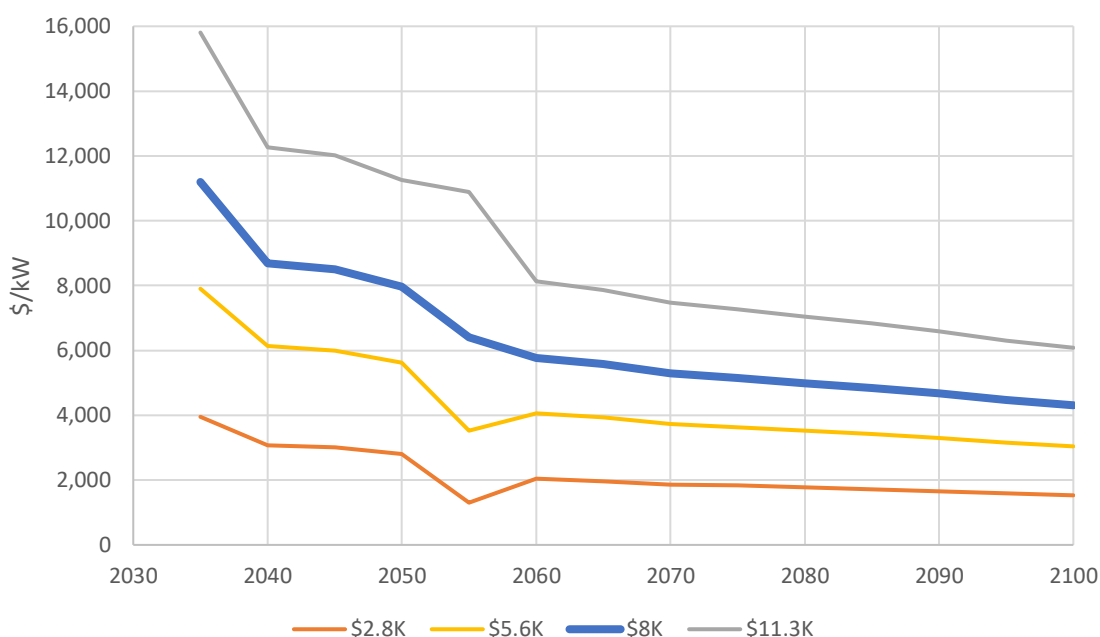
4.3. Key assumptions regarding fusion power generation

Costs for future fusion power generation are uncertain, but the impact of different potential cost ranges can be explored. For our base case, we assume that fusion technology is commercially available in 2035 at an overnight capital cost of about \$11,000/kW (all monetary values are given in 2021 U.S. dollars; for a discussion of the levelized cost of electricity, see [Appendix A.3](#)). Future technology costs decline endogenously in the EPPA model via learning and other factors (Morris et al. 2019a). As shown in [Figure 4.2](#), the resulting overnight cost of fusion generation as projected by the EPPA model in our base case falls to about \$8,000/kW by 2050 and about \$4,300/kW by 2100.

We assume that fusion-based power generation is fully dispatchable, but that early fusion power plants operate at a capacity factor of just 40% due to anticipated downtime for this new technology. Starting in 2035, we assume that capacity factor increases linearly to 85% over the first 25 years of commercial deployment (and stays at 85% thereafter). This assumption is consistent with performance data from the existing U.S. fleet of nuclear fission power plants (U.S. Energy Information Administration (EIA) 2023). Although we assume some deployment constraints analogous to those encountered in the initial scale-up of nuclear fission technology (Morris et al. 2019a), we do not impose any additional constraints on the future expansion of fusion power (for example, due to critical materials availability, regulatory obstacles, etc.).

As part of a sensitivity analysis, we also looked at initial overnight capital costs of \$4,000/kW, \$8,000/kW, and \$16,000/kW in 2035 (see Figure 4.2). We assume these costs decline by 2050 to \$2,800/kW, \$5,600/kW, and \$11,300/kW, respectively, and to \$1,500/kW, \$4,300/kW, and \$6,000/kW by 2100, respectively. Because the subregional grid models used in this study focus on 2050, we label our cases by their corresponding overnight costs in 2050 (i.e., \$2.8K, \$5.6K, \$8K, \$11.3K). These numbers reflect the cost of fusion power plants in the United States. Fusion costs in other parts of the world would be expected to differ based on the evolution of regional capital, labor, and energy costs.

Figure 4.2 Evolution of overnight capital costs of fusion power generation (2021\$/kW)



4.4. Key assumptions regarding other power generation technologies

To estimate costs for other generation technologies, we use an approach described by Morris et al. (2019b), updated with 2021 cost data from the U.S. Energy Information Administration (EIA 2023). Table 4.1 shows estimated overnight capital costs for non-fusion generation technologies, including coal and natural gas with carbon capture and storage (CCS), in 2021. As already noted, the EPPA model assumes the future costs of these technologies decline endogenously (Morris et al. 2019a).

For variable renewable energy technologies, namely wind and solar, the value of new capacity additions is affected by these technologies' deployed market shares over time (Gurgel et al. 2023). In addition to facing greater resource constraints, the relative value of variable renewables declines as their share increases, because their presence in the energy mix suppresses energy prices at the locations and during the time periods when they operate (and

receives declining capacity credit as well). To account for these dynamics, we introduce additive value adjustments for wind and solar that increase the costs of these technologies in the EPPA model based on their shares of total electricity generation. For example, the value adjustment for wind is \$27/MWh if the share of wind generation is 25%. It grows to \$66/MWh if the share is 45%. The corresponding values for solar are \$32/MWh and \$97/MWh.

Table 4.1 Overnight capital costs in 2021 for non-fusion power-generating technologies (2021\$/kW)

Electricity generation type	Overnight cost in 2021\$
Coal	\$4,074/kW
Coal with CCS	\$6,625/kW
Natural gas combined cycle	\$1,201/kW
Natural gas combined cycle with CCS	\$2,845/kW
Nuclear fission	\$7,030/kW
Biomass	\$4,525/kW
Wind	\$1,718/kW
Solar	\$1,327/kW

Using information for resource value at all shares of deployment, we implement these value adjustments in the EPPA model as explicit increases in the cost of the technology, which are endogenously determined in each time period given the shares of wind and solar deployed. Additional information about this approach to modeling variable renewable electricity sources by explicitly considering their changing value at larger shares of deployment is provided in Gurgel et al. (2023). We also assume that fission electricity generation remains limited in countries where it is limited today (and that fusion electricity generation is not constrained in any country). Although growth in fission-based nuclear generation is constrained by social acceptance and non-proliferation issues, our analysis projects that global fission electricity generation in 2050 will be almost 250% of actual generation in 2020. This total is within reach of the COP28 pledge by 22 countries to triple global nuclear generation capacity by 2050 (United Nations Framework Convention on Climate Change 2023). Our projections assume that growth in nuclear fission is located in China, India, and other emerging Southeast Asian countries. In the United States and Europe, where nuclear fission is more constrained by public acceptance, regulatory burdens, and corresponding risks, delays, and costs, the EPPA model assumes that nuclear fission generation is virtually flat.

4.5. Results for global analysis

Figure 4.3 shows results for the global electricity generation mix in the base case (\$8K), where fusion generation grows from 2 TWh in 2035 to 375 TWh in 2050. Fusion generation expands much more dramatically in the second half of the century, reaching almost 25,000 TWh by 2100 in this case. While renewables (wind, solar, biomass) experience dramatic growth from 2030 to 2050, resource constraints and issues related to the integration of variable energy sources into the electricity system (Gurgel et al. 2023) bound the expansion of these technologies after 2050. After 2085, bioenergy with carbon capture drives a further (more modest) expansion of the renewables contribution because the model assumes that this technology benefits from additional revenue from carbon credits for CO₂ removals from the atmosphere. Even so, the sizeable increase of fusion in EPPA’s results for the second half of the century illustrates the world’s need for a zero-carbon, dispatchable electricity generation technology in light of anticipated demand growth and electrification. Overall, the share of fusion in global electricity generation reaches 15% by 2075 and 27% by 2100 in the base case.

Figure 4.3 Evolution of the global electricity generation mix in the base case where overnight costs for a fusion power plant in the U.S. reach about \$8,000/kW in 2050 and about \$4,300/kW in 2100

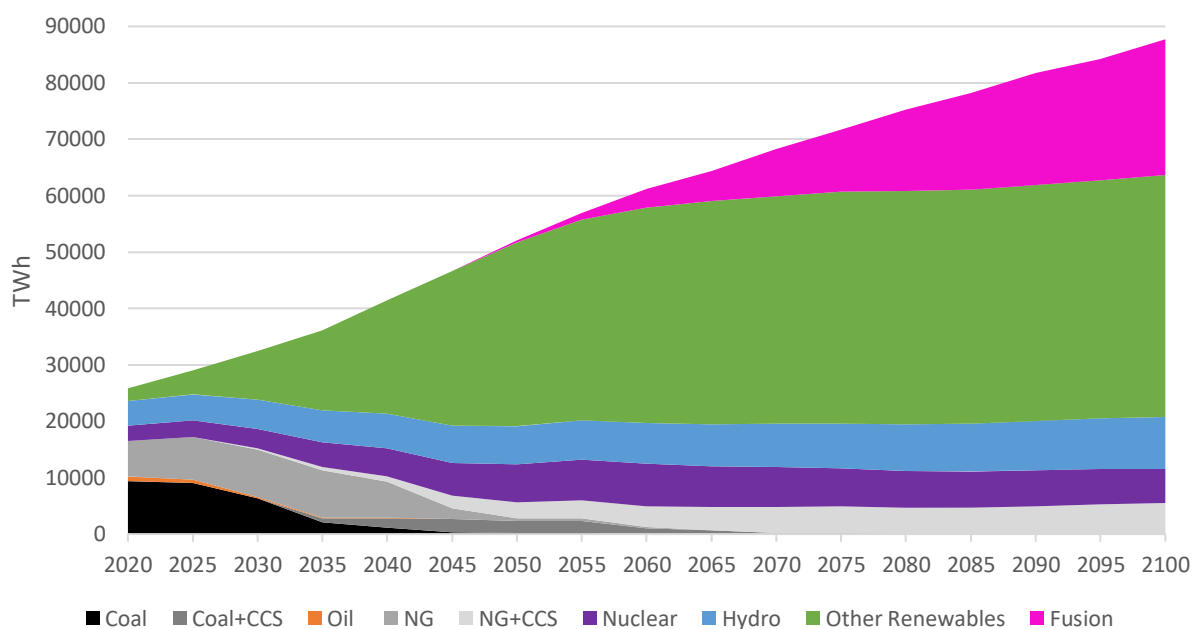
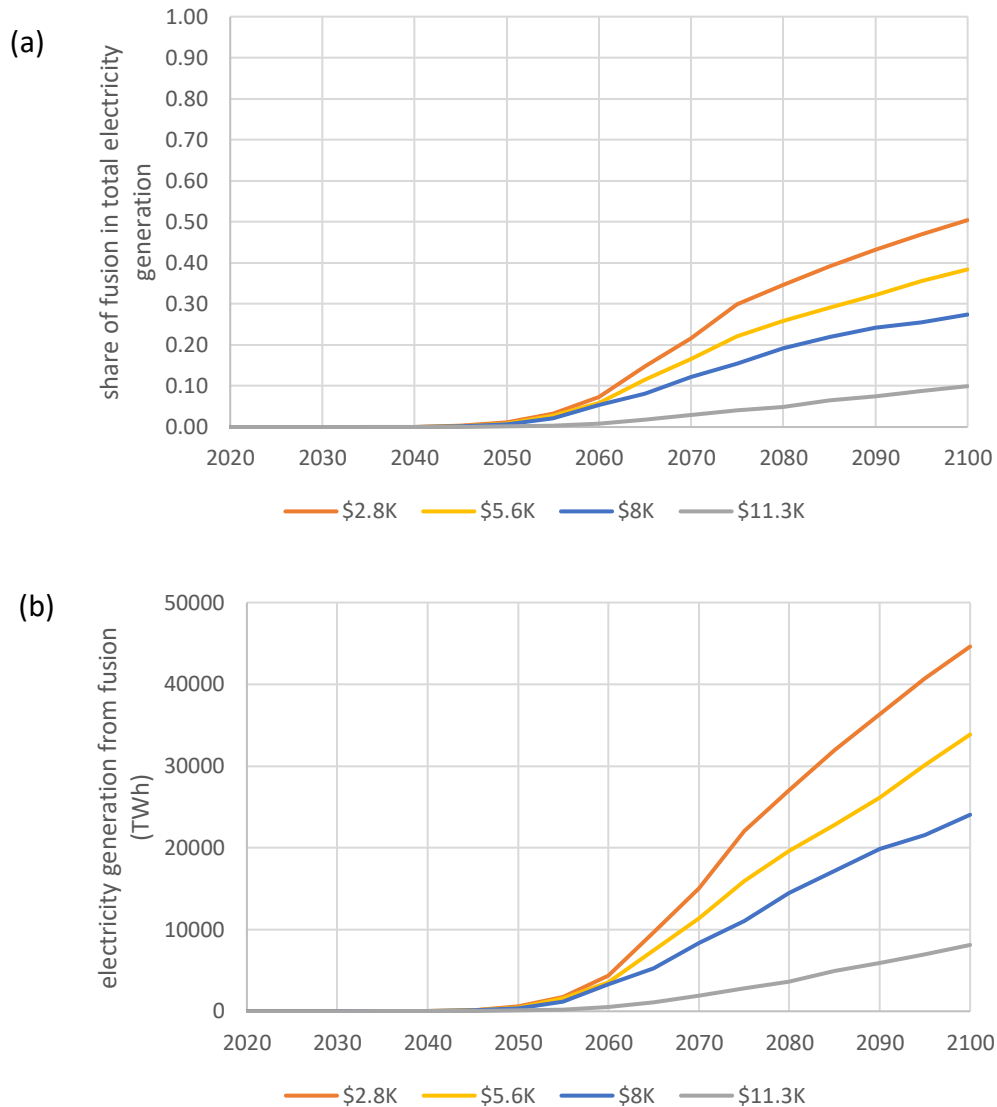


Figure 4.4a shows fusion as a share of total electricity generation for the cost cases we considered. Lower capital cost (i.e., the \$5.6K case) results in higher shares of global electricity generation, at 22% in 2075 and 38% by 2100. Assuming even lower capital cost (i.e., the \$2.8K case) leads to even higher projected fusion shares, at 30% of global electricity generation in 2075 and 50% by 2100. Conversely, higher capital cost corresponds to a lower projected future

contribution. In the \$11.3K case, the fusion share in 2075 is 4%; it reaches only 10% by 2100. [Figure 4.4b](#) shows corresponding results for fusion generation in energy units (TWh).

Figure 4.4 (a) Fusion share of global electricity generation for different cost cases; (b) global electricity generation from fusion technology for different cost cases



[Figure 4.5](#) shows results for the global electricity generation mix in all cost cases. It offers another illustration of how projected fusion penetration depends on cost. Lower costs allow fusion electricity generation to be more competitive with other low-carbon electricity options. It bears emphasizing, however, that all scenarios show future global electricity generation dominated by a mix of renewables, nuclear fission, and fusion.

Figure 4.5 Evolution of the global electricity generation mix in different cost cases

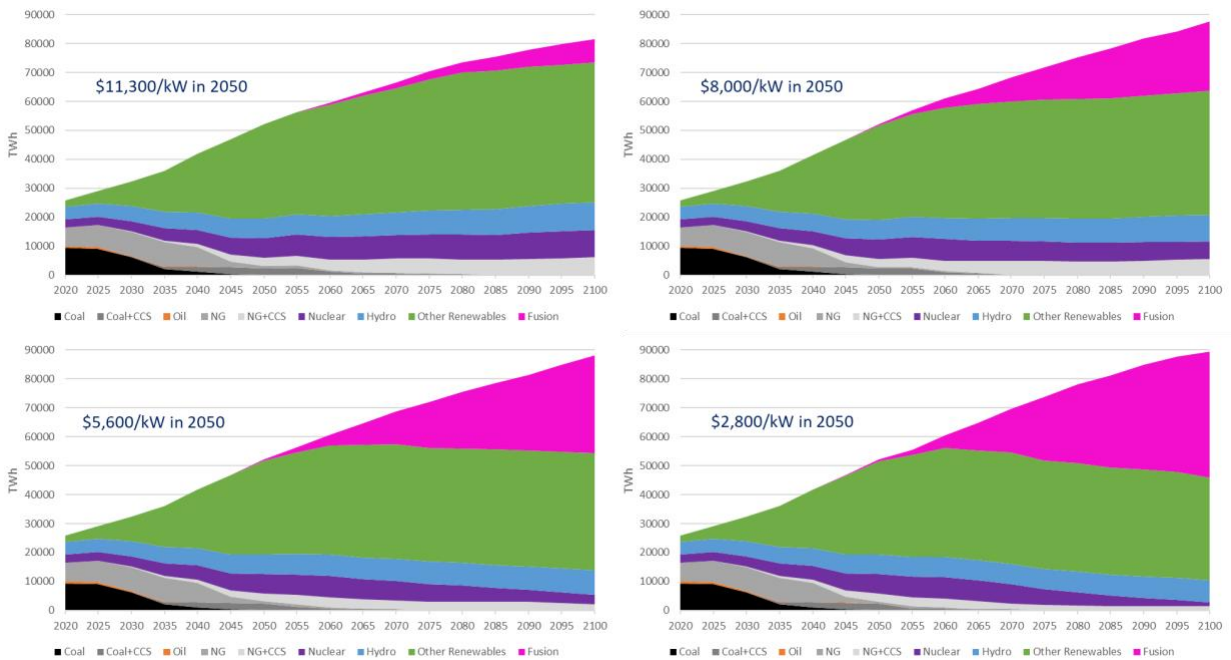
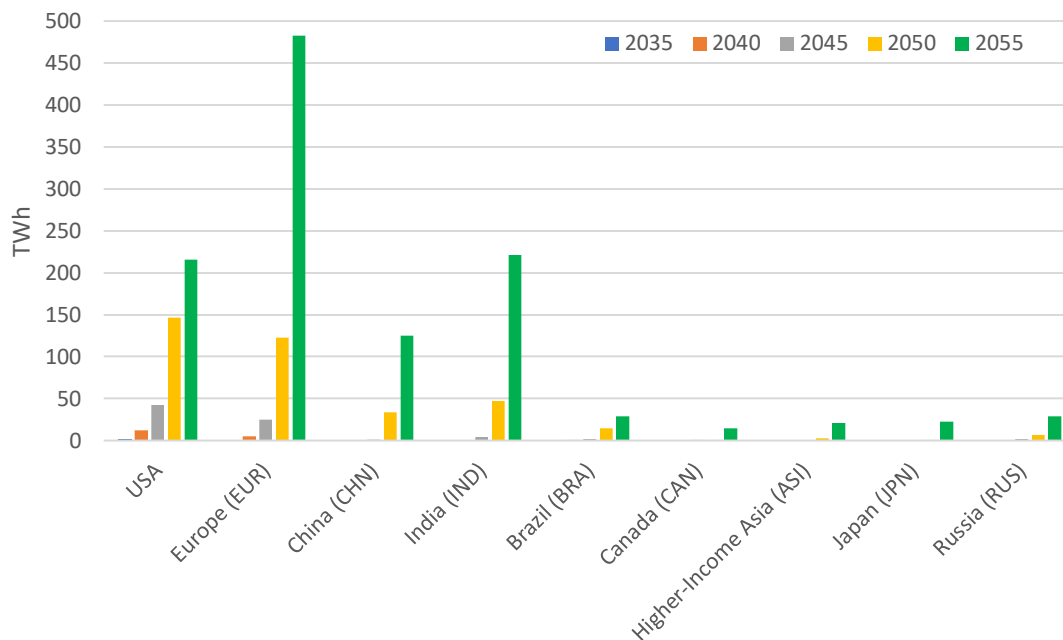


Figure 4.6 shows estimated base case fusion deployment over the next three decades by region. Although the United States and Europe start deploying fusion earlier than other regions, India and China catch up fast because of the magnitude of their growing power generation needs. By 2055, India overtakes the United States in terms of electricity generation from fusion power. Brazil, Japan, higher-income Asian countries¹², Russia, and Canada also start deploying fusion power around mid-century.

¹² See Appendix A.1 for a regional composition.

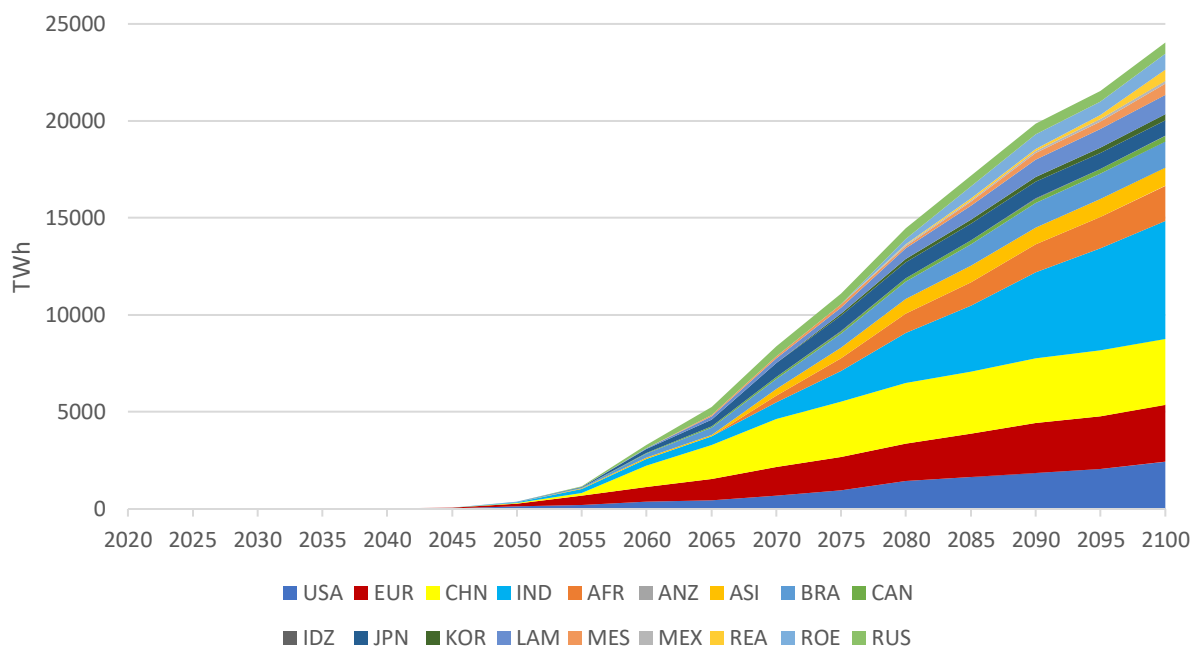
Figure 4.6 Electricity generation from fusion technology in major world regions (United States, Europe, China, India, Brazil, Canada, Higher-Income Asia, Japan, Russia) over the 2035–2055 period



The base case assumes U.S. overnight costs for a fusion power plant at \$8,000/kW in 2050 and about \$4,300/kW in 2100. In 2035, fusion generation is deployed in the United States only, at the level of 2 TWh, which is barely visible on the figure.

Figure 4.7 shows results for all EPPA regions (defined in Appendix A.1) for the 21st century in the base case. While about 60% of total fusion generation by 2100 is located in four regions (United States, Europe, India, and China), we also project substantial deployment in other regions (i.e., Brazil and other Latin American countries, Africa, higher-income Asian countries, and Canada). These regional results are driven by economic growth, population density, and electrification needs, which together determine future electricity demand, as well as by regional costs, decarbonization targets, relative prices of electricity, and the availability of other low-carbon resources (wind, solar, and biomass). In Africa, fusion begins to be deployed in 2065, with fusion generation growing to about 1,800 TWh, or about 25% of total electricity generation on the continent, by 2100. Fusion grows even more rapidly in Southeast Asia, reaching more than 2,600 TWh (excluding China and India) by the end of the century.

Figure 4.7 Electricity generation from fusion technology in EPPA regions in the 21st century



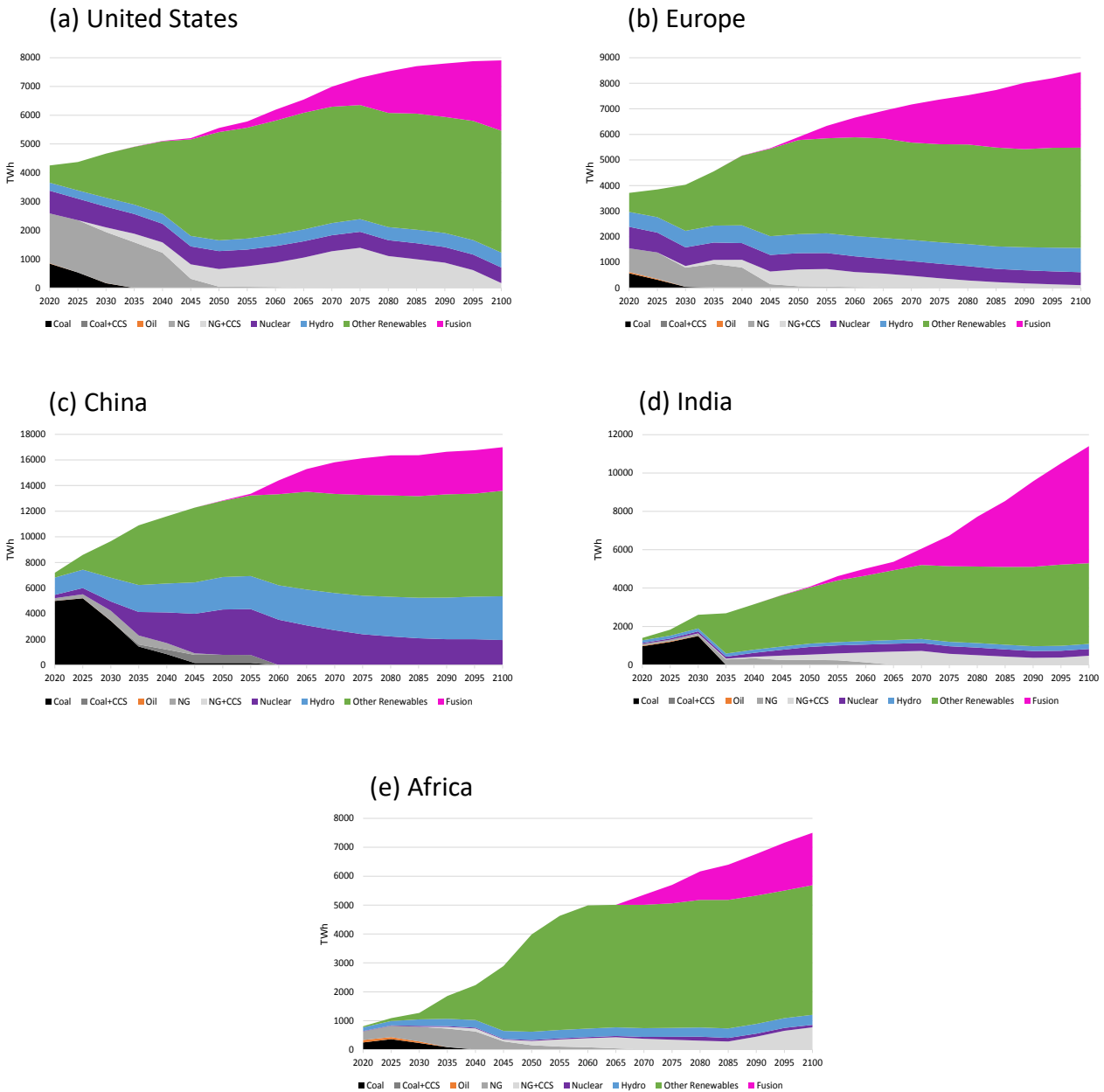
The base case assumes overnight costs in the U.S. at about \$8,000/kW in 2050 and about \$4,300/kW in 2100. Regions: USA: United States, EUR: Europe, CHN: China, IND: India, LAM: Other Latin America, JPN: Japan, AFR: Africa, ANZ: Australia and New Zealand, ASI: Dynamic Asia, BRA: Brazil, CAN: Canada, IDZ: Indonesia, KOR: Korea, MES: Middle East, MEX: Mexico, REA: Other East Asia, ROE: Other Eurasia, RUS: Russia.

Figure 4.8 shows model results for the projected electricity generation mix in five major regions: the United States, Europe, China, India, and Africa. All regions experience substantial electrification of their economies and see a corresponding rise in demand for electricity. While electricity consumption grows between 1.9- and 2.4-fold from 2020 to 2100 in the United States, Europe, and China, in India it grows 8.2-fold and in Africa it grows 9.3-fold over the same period. Because electricity consumption per capita in Africa and India is currently substantially lower than in advanced economies (about 0.6–1 MWh/person compared to 6–7 MWh/person in Europe, about 6 MWh/person in China, and about 13 MWh/person in the United States), Africa and India are projected to see faster growth in electricity consumption.

In all regions, renewables grow rapidly by mid-century, while coal disappears and natural gas without carbon capture and storage is substantially reduced and replaced with natural gas with carbon capture and storage. Conventional (fission) nuclear power is constrained for reasons having to do with political and public acceptance. In the second half of the century, the contribution from conventional fission generation declines after peaking in about 2050 because of falling costs for competing fusion technology (see Figure 4.2). China continues to slightly expand hydropower generation. As mentioned before, an increase in electricity demand

coupled with limiting factors related to integrating renewable energy into a net-zero emissions scenario provides fusion energy with a pathway for expansion in the second part of the century.

Figure 4.8 Electricity generation mix in major world regions: (a) United States, (b) Europe, (c) China, (d) India, and (e) Africa



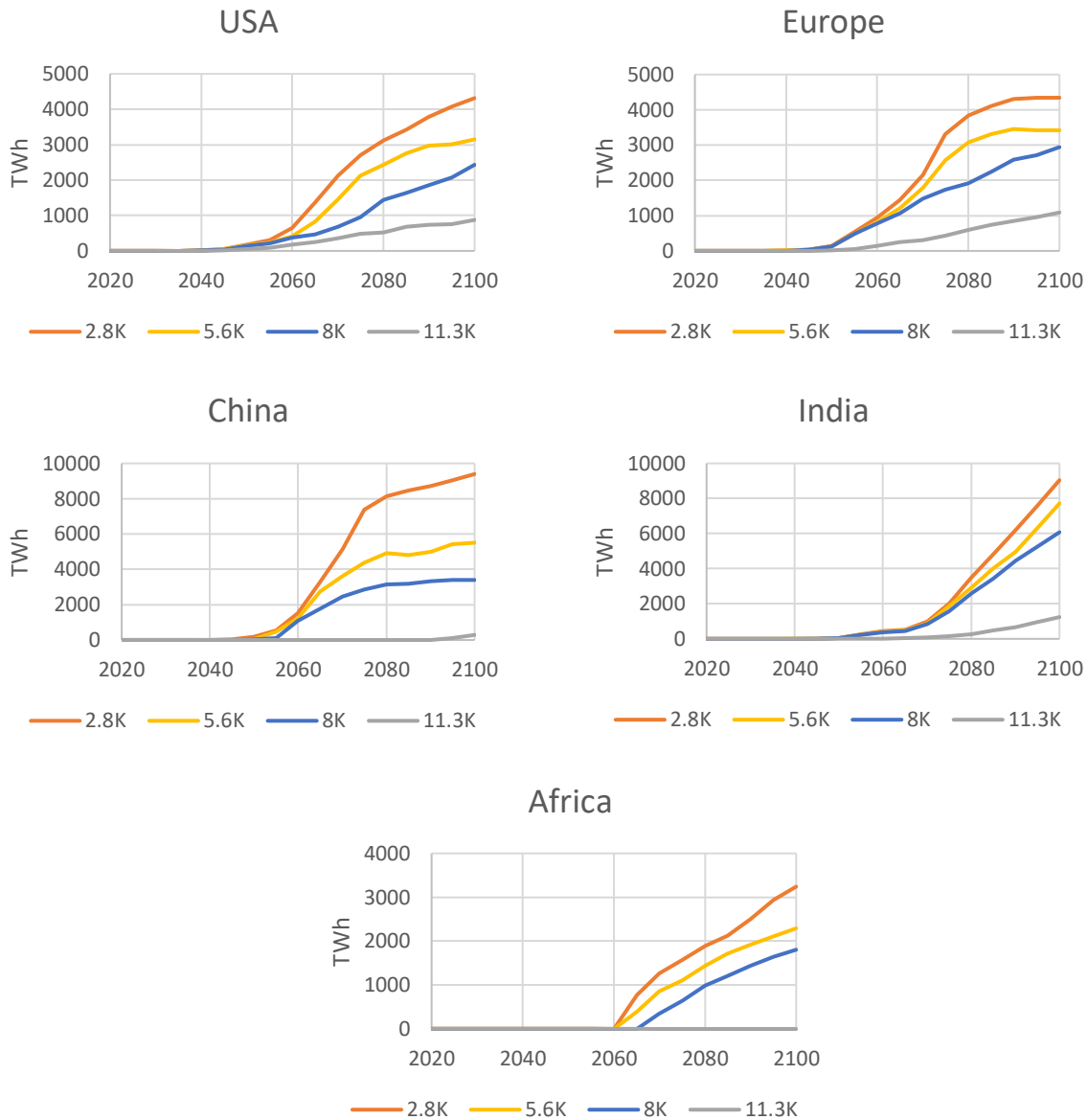
In the base case, U.S. overnight costs for fusion power reach about \$8,000/kW in 2050 and about \$4,300/kW in 2100.

As one would expect, these results are sensitive to assumptions about the future cost of fusion.

Figure 4.9 shows modeled fusion generation in different cost cases. While fusion still plays a

role in the United States and Europe in the high-cost (\$11.3K) case, deployment in China and India is quite limited because of lower relative prices for capital, labor, and other technologies in these regions. In Africa, fusion does not enter the electricity mix in the \$11.3K case for the same reasons. At lower assumed fusion costs, the model projects a substantial increase in fusion electricity generation in all major regions.

Figure 4.9 Fusion electricity generation in major world regions under different cost assumptions



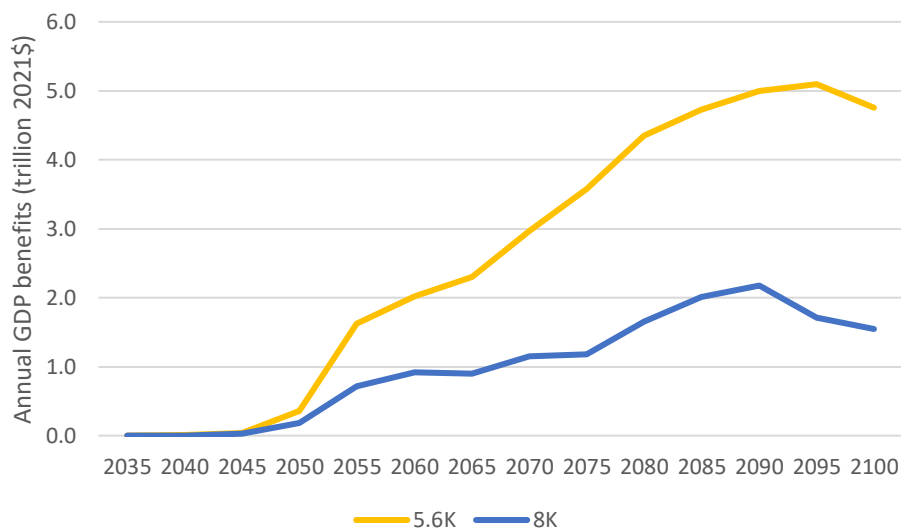
4.6. Global economic impact of fusion

As a firm generation resource that could reduce the total cost of decarbonization, fusion's potential value to society in a decarbonized world could be in the trillions of dollars. To assess

this value, we compared global gross domestic product (GDP) in scenarios where fusion is available to global GDP in scenarios where it is not. In a deep decarbonization scenario, such as we explored in this study, the undiscounted societal value of fusion power plants is \$68 trillion in the base case (where overnight costs for a U.S. fusion plant are \$8,000/kW in 2050 and fall to \$4,300/kW in 2100). At a lower cost for fusion, its social value increases to \$175 trillion in the case where overnight costs for a U.S. plant reach \$5,600/kW in 2050 and \$3,000/kW in 2100. The corresponding net present value (NPV) of these benefits (discounted to 2024 at 6%) is \$3.6 trillion in the base case and \$8.7 trillion in the lower-cost (\$5,600/kW) case.

Figure 4.10 illustrates these results in terms of the undiscounted monetary value (in trillions of 2021\$) of an increase in global GDP in a particular year *with* fusion, relative to a deep decarbonization scenario where fusion is not available. By aggregating these benefits over time, we can calculate the potential social value of fusion as a percent increase in global GDP over the period from 2035 to 2100. Compared to a decarbonization scenario without fusion electricity, cumulative global GDP would be 0.4% higher in the base case (with fusion cost in 2050 at \$8,000/kW) and 0.9% higher in the lower-cost (\$5,600/kW) case. These results indicate that investments in developing and deploying fusion technology can create value for the global economy and support efforts to achieve decarbonization goals over the course of this century.

Figure 4.10 Potential annual global economic benefits of fusion technology in a deep decarbonization scenario



References

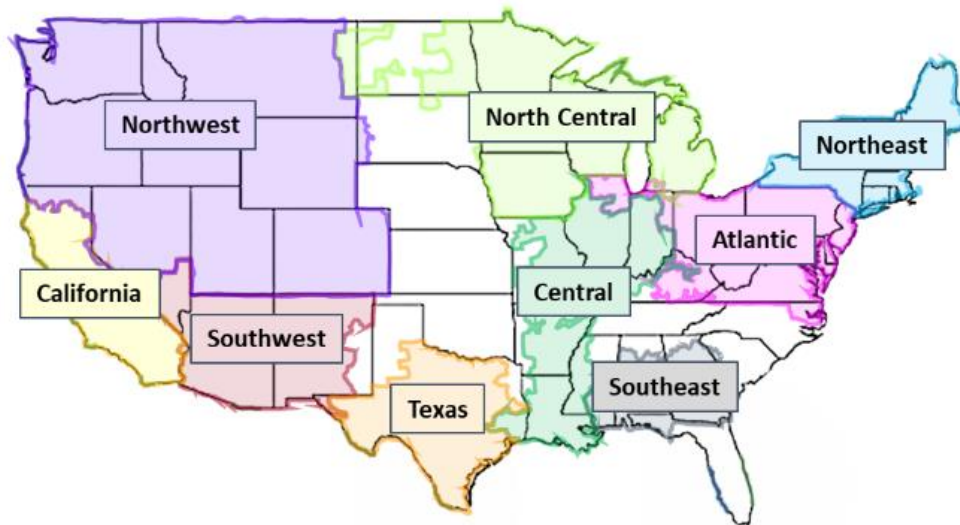
- Desport, Lucas, Angelo Gurgel, Jennifer Morris, Howard Herzog, Yen Heng Henry Chen, Sandrine Seloisse, and Sergey Paltsev. 2024. "Deploying Direct Air Capture at Scale: How Close to Reality?" *Energy Economics* 129 (January): 107244. <https://doi.org/10.1016/j.eneco.2023.107244>.
- Fajardy, Mathilde, Jennifer Morris, Angelo Gurgel, Howard Herzog, Niall Mac Dowell, and Sergey Paltsev. 2021. "The Economics of Bioenergy with Carbon Capture and Storage (BECCS) Deployment in a 1.5 °C or 2 °C World." *Global Environmental Change* 68 (March): 102262. <https://doi.org/10.1016/j.gloenvcha.2021.102262>.
- Gurgel, Angelo, Bryan K. Mignone, Jennifer Morris, Haroon Kheshgi, Matthew Mowers, Daniel Steinberg, Howard Herzog, and Sergey Paltsev. 2023. "Variable Renewable Energy Deployment in Low-Emission Scenarios: The Role of Technology Cost and Value." *Applied Energy* 344: 121119. <https://doi.org/https://doi.org/10.1016/j.apenergy.2023.121119>.
- MIT Joint Program. 2023. "Global Change Outlook." <https://globalchange.mit.edu/publications/signature/2023-global-change-outlook>.
- Morris, Jennifer F., John M. Reilly, and Y.-H. Henry Chen. 2019a. "Advanced Technologies in Energy-Economy Models for Climate Change Assessment." *Energy Economics* 80: 476–90. <https://doi.org/https://doi.org/10.1016/j.eneco.2019.01.034>.
- Morris, Jennifer, Jessica Farrell, Haroon Kheshgi, Hans Thomann, Henry Chen, Sergey Paltsev, and Howard Herzog. 2019b. "Representing the Costs of Low-Carbon Power Generation in Multi-Region Multi-Sector Energy-Economic Models." *International Journal of Greenhouse Gas Control* 87: 170–87. <https://doi.org/https://doi.org/10.1016/j.ijggc.2019.05.016>.
- United Nations Framework Convention on Climate Change. 2023. "Summary of Global Climate Action at COP 28." December 2023. https://unfccc.int/sites/default/files/resource/Summary_GCA_COP28.pdf.
- U.S. Energy Information Administration (EIA). 2023. "Annual Energy Outlook."

5. Analysis of fusion market penetration in subregions of the United States

5.1. Introduction

This chapter presents the results of two capacity expansion and dispatch modeling exercises. In the first exercise, we apply the GenX grid model to the six-state U.S. subregion known as New England. Second, we apply the Ideal Grid multi-subregional model to nine subregions spanning much of the United States. The subregions are divided along North American Electric Reliability Corporation (NERC) boundaries. [Figure 5.1](#) shows the nine subregions. The Northeast subregion includes the New England states and the state of New York.

Figure 5.1 The nine U.S. subregions modeled by the Ideal Grid



Capacity expansion and dispatch models evaluate alternative portfolios of generation and transmission capacity to serve electricity demand at the lowest system cost while also satisfying constraints such as limits on greenhouse gas emissions. These models are especially useful for capturing the complex competitive dynamics between alternative technologies. In this chapter, we use the models to understand the threshold capital cost at which a fusion power plant (FPP) becomes a cost-efficient addition to the grid, and how large a share of capacity and generation is provided by fusion at this threshold cost. We also examine how outcomes for fusion vary with different assumptions about key variables, such as the availability and cost of alternative generation technologies, the stringency of any emissions constraint, as well as the operational flexibility of FPPs.

We parameterize the GenX and Ideal Grid models to evaluate generation investments to serve load in 2050, incorporating forecasts of electricity demand and technology costs appropriate to that horizon. We survey those parameters in the next section. The structures of the two models

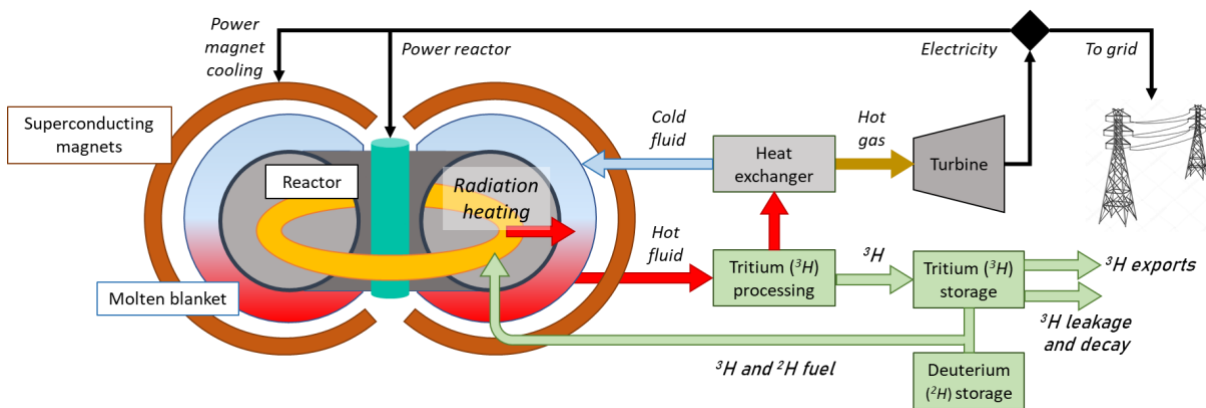
employed here are generally similar. However, the studies done with each have a slightly different focus. We use GenX to focus on the details of a single subregion, while our modeling with Ideal Grid focuses on contrasts across various subregions. Together, these two modeling exercises serve to highlight different elements of the overall competitive picture. Detailed information on the GenX and Ideal Grid models is provided in [Appendix B](#).

5.2. Modeling fusion

5.2.1. Fusion plant design and operation

For capacity expansion models like GenX and Ideal Grid, the key features of electricity generation and storage technologies include investment and operating costs, operational constraints, and emissions. For example, a key parameter for thermal power plants is the thermal efficiency with which the energy content of the fuel is converted into electrical energy. When combined with the price of fuel, this determines the gross profit margin of generation and therefore the plant's place in the dispatch merit order. Thermal power plants also have operational constraints, such as a minimum stable output, maximum ramp rate, startup time, and such, which shape a unit's duty cycle. This section describes the relevant features of an FPP as they are represented in the GenX fusion module. To construct the fusion module, we identified the key components of a generic deuterium-tritium (DT) magnetic confinement FPP, as shown in [Figure 5.2](#).

Figure 5.2 Elements of the fusion module



Energy and neutrons released by the fusion reaction heat up the molten blanket and breed tritium. The hot fluid circulates to the tritium processing system, which extracts tritium and delivers hot fluid to the heat exchanger to heat steam or gas to drive a turbine for power generation. Cold fluid from the heat exchanger is returned to the blanket tank surrounding the fusion reactor. The tritium processing system extracts tritium from the hot blanket fluid and includes tritium storage capacity. The reactor fueling system delivers tritium to the reactor along with deuterium. Excess tritium is exported from this plant site to provide initial fuel for other FPPs. Some power from the turbine is used to cool the magnets, to drive the fusion reactor, and to supply electric power for the tritium processing system and other plant operations—the remainder is sent to the grid.

Table 5.1 shows the power characteristics of our generic fusion plant and the sizes we assumed for different plant elements based on guidance from experts at the MIT Plasma Science and Fusion Center. Of course, different FPPs will have different scales and different ratios between the parameters shown in Table 5.1 based on the system design.

Table 5.1 Base case FPP size and power characteristics

Fusion power capacity (MW)	Total thermal power capacity (MW _{th})	Turbine efficiency (%)	Gross electric power capacity (MW _e)	Net electric power capacity (MW _e)
1,000	1,095	40	438	327

Note: MW_{th} = MW thermal, MW_e = MW electrical

The base case fusion power capacity of 1,000 megawatts (MW) (shown in the leftmost column) is a standard metric in the academic literature on fusion. The 327-MW_e figure shown in the rightmost column reports the base case plant's net output of electric power available to send to the grid, which is the standard metric in the electric power industry. In addition to the energy released by the fusion reactions, heat is also generated by reactions in the blanket, energy is injected into the plasma, and energy is used to pump the molten salt blanket, which brings the base case plant's total thermal power capacity to 1,095 MW_{th}. Turbine efficiency depends on the chosen power cycle. Here we assume an efficiency of 40%, in which case the plant's gross electric power capacity is 438 MW_e. The 111-MW_e difference between the plant's gross and net electric output reflects the power needed within the plant to cool the magnets, drive the fusion reactor, pump the molten blanket, and supply electric power for the tritium processing system and other plant operations. Table 5.2 shows the assumptions underlying this estimate of within-plant power requirements, which are dominated by the variable station power used to heat the plasma.

Table 5.2 Recirculating power requirements

Magnet cooling (MW _e)	Station power during operations		Recirculating power at maximum output (MW _e)
	—fixed— (MW _e)	—variable— (MW _e /MW _{th})	
10	10	0.083	111

5.2.2. Fusion plant costs

Understanding that the future costs of building and operating a fusion plant are very uncertain, we can use our grid models and knowledge of costs for other generation technologies to understand the competitive space for a fusion plant. For example, we can ask, "At what cost is

a FPP an efficient investment, and how much fusion capacity should be built?” We can then analyze how various factors shape that competitive space. To that end, we describe a potential cost structure for FPPs and parameterize this cost structure, without suggesting that these default values are a forecast of the future cost of FPPs.

We break the cost of a FPP into three components:

- The fusion plant, including long-lived components such as the reactor, heat exchangers, and tritium handling;
- Replaceable components, the lifetime of which depends on the utilization of the reactor; and
- The power block, including the turbine.

Whereas much of the reactor plant has a target 40-year life, certain components must be replaced more frequently depending on how the reactor is operated. For example, certain DT magnetic confinement designs include a vacuum vessel that has a one- to two-year nameplate lifetime, but the vacuum vessel can be replaced less frequently if the fusion plant operates below its nameplate capacity.¹³ When operated at lower power, the vacuum vessel is subject to less intense neutron damage and other stresses, extending its life. Other designs, too, may have replaceable components, including electrodes for the z-pinch fusion concept, laser beam boxes for inertial confinement devices, and solid blanket materials that serve as first-wall materials. Although these replaceable components must be designed to account for a relatively small share of the total plant’s initial cost, their short life means we must account for relatively frequent replacement. To install some types of replaceable components, the FPP must be shut down. For the base case FPP, we assume the power block is sized to the reactor’s thermal output. Later in this chapter, we examine FPP variations in which thermal storage is added to allow flexibility in electricity generation output while maintaining a higher capacity factor for the fusion reactor.

Table 5.3 shows a hypothetical capital cost breakdown for a generic FPP across the three components discussed above. The first row provides the base case cost for the 327-MW_e net power plant. The second row quotes the cost per unit of net electric capacity based on a total benchmark FPP capital cost of \$8,500/kW_e. While we use \$8,500/kW_e as an example value here, we examine the market penetration and role of FPPs for a wide range of possible capital costs, from as low as \$3,000 to as much as \$20,000 per kW_e.

¹³ By “nameplate lifetime” we mean the component’s lifetime if the fusion plant operated continuously at its full nameplate capacity.

Table 5.3 Capital cost for the base case FPP by component

Quotation convention	Fusion reactor plant		Power block	Total benchmark plant cost
	40-Year Equipment	2-Year Equipment		
(\$ million)	2,173	49	556	2,778
(\$/kW _e , net electric capacity)	6,650	150	1,700	8,500

Table 5.4 shows plant capital cost when annualized. It also shows our assumptions for operating and maintenance costs. Although the cost of replaceable components is part of the capital cost of the initial plant, in our modeling this cost is included in operating and maintenance costs because these components must be regularly replaced. In the table, component replacement costs are reported as a cost per unit of net electrical power generated based on assumptions regarding efficiency and utilization.

Table 5.4 Annualized capital cost and O&M cost for the base case plant

Real discount rate (%)	Annualized capital cost (\$/MW/yr)	Operating and maintenance cost	
		Fixed (\$/MW/yr)	Variable cost (\$/MWh)
6	565,000	85,000	12.20

We model tritium breeding, losses, and storage as linear processes. We assume that the plant produces 10% more tritium than it consumes. Some tritium is stored for later use as fuel; any excess is exported to provide fuel to start up other FPPs. Our model does not account for any revenue from exported tritium, nor does it assume any payment for the initial tritium required to start the FPP. Deuterium fuel is purchased at \$500/kg, but given very low deuterium consumption, fuel cost is negligible at roughly \$15,000/year.

5.3. Key assumptions regarding other generation technologies

Table 5.5 lists the set of generation and storage technologies available for investment in the GenX model of the New England grid. The table shows projected 2050 U.S. average capital cost for different technologies, expressed in 2021 dollars per kilowatt of capacity. Based on the assumed plant life shown for each technology and a real discount rate of 6%, upfront capital cost is translated into an annualized capital cost expressed in dollars per megawatt of capacity per year. The table also shows projected fixed and variable nonfuel operating and maintenance costs and projected average fuel cost. The last four rows of the table describe alternative scenarios for the 2050 capital cost of a FPP. For each scenario, the fixed operating and

maintenance cost is proportional to the capital cost, while the variable cost is constant across scenarios.

The rightmost two columns of [Table 5.5](#) show the assumed capacity factor and levelized cost of electricity (LCOE) for each generation option, where the LCOE is calculated using the assumed capacity factor. LCOE offers a convenient way to summarize the set of costs for each technology in a single number. However, the actual realized average capacity factor for each technology will depend on the portfolio of capacity investments made and on how technologies are dispatched to serve load throughout the hours of the year. In the GenX and Ideal Grid models, the capacity factor is an output, not an input. The LCOE is not a sufficient tool for system planning, although it is a useful metric for making rough comparisons of cost for different electricity generation options.

Table 5.5 Projected 2050 costs (U.S. average) for generation and storage technologies available for investment in the GenX model of the New England grid

	Capital cost (\$/kW)	Life (yr)	Annualized capital cost (\$/MW/yr)	Operating and maintenance cost		Mean fuel cost (\$/MWh)	Pro-forma capacity factor (%)	Pro-forma LCOE (\$/MWh)
				fixed (\$/MW/yr)	variable (\$/MWh)			
Natural gas	990	30	71,600	24,000	1.60	44.90	85	59.30
Natural gas w/ CCS ¹⁴	1,610	30	117,000	39,000	3.20	50.80	85	75.00
Utility-scale solar PV	630	30	45,900	13,000	–	–	31	21.70
Commercial rooftop PV	860	30	62,600	10,000	–	–	17	47.60
Residential rooftop PV	1,120	30	81,300	14,000	–	–	16	68.90
Onshore wind	920	30	67,100	23,000	–	–	48	21.40
Fixed offshore wind	2,310	30	168,100	71,000	–	–	53	51.50
Floating offshore wind	3,740	30	271,900	61,000	–	–	53	71.70
RoR hydro	4,070	100	244,700	18,700	–	–	66	45.60
10-hour pumped hydro	7,550	100	454,500	47,000	–	–	36	157.50
4-hour Li-ion battery	830	15	85,900	21,000	–	–	17	73.10
Fusion – \$3,000/kW	3,000	40	199,400	30,000	12.20	–	90	41.70
Fusion – \$6,000/kW	6,000	40	398,800	60,000	12.20	–	90	71.30
Fusion – \$8,500/kW	8,500	40	564,900	85,000	12.20	–	90	95.90
Fusion – \$12,000/kW	12,000	40	797,500	120,000	12.20	–	90	130.40

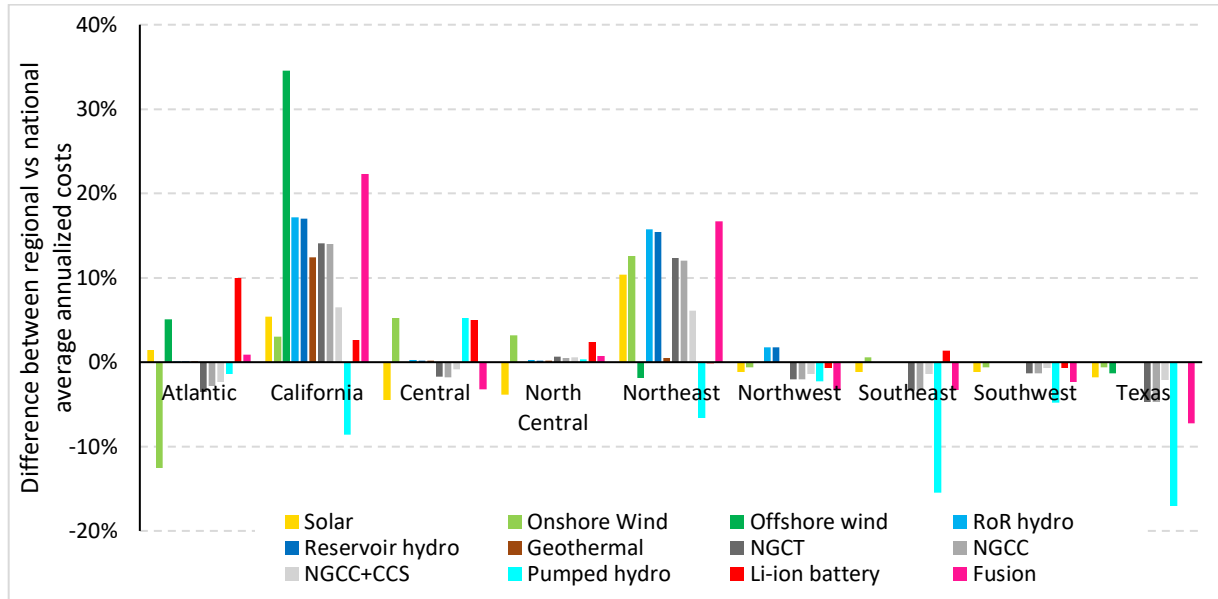
Source: Estimates of 2050 capital cost, operating and maintenance costs, fuel cost, plant lifetimes, and pro-forma capacity factors for all technologies except fusion are from the National Renewable Energy Laboratory (NREL) Annual Technology Baseline 2023 (NREL 2023). We assume a real discount rate of 6%. CCS = carbon capture and storage; Li-ion = lithium-ion; PV = photovoltaic; RoR hydro = run-of-river hydroelectric.

The Ideal Grid model incorporates a slightly different portfolio of technology options. For solar, it considers only utility-scale solar PV. For offshore wind, it considers only fixed offshore wind.

¹⁴ Natural gas combined cycle with carbon capture and storage (NGCC+CCS) assumes 95% carbon capture to yield power plant emissions of 19 gCO₂/kWh, plus an additional 19 gCO₂-equivalent emissions per kWh based on upstream emissions of methane in the natural gas supply chain. This assumption is based on an aggressive emissions mitigation program by the U.S. natural gas industry, which is projected to reduce methane emissions by about 80% between 2020 and 2050. The analysis assumes power plant efficiency corresponding to H-class NGCC with 95% capture (Schmitt et al. 2022) based on operations at steady state and near the maximum efficiency design point such that emissions per kWh of electricity generated are minimized. Thus, our NGCC+CCS emissions assumptions represent a best-case scenario for natural gas power and a worst case for FPP deployment. NGCC without CCS has emissions of 333 gCO₂/kWh (Schmitt et al. 2022) plus upstream emissions of 19 gCO₂-equivalent per kWh of net electricity output. Emissions for the natural gas combustion turbine (NGCT) option in the Ideal Grid model—at a total of 552 gCO₂/kWh—include both power plant emissions and CO₂-equivalent emissions from upstream methane emissions.

In addition to run-of-river hydroelectric power (RoR hydro), it considers potential investments in reservoir hydro. In addition to natural gas combined cycle (NGCC) plants, it includes natural gas combustion turbines (NGCT). It also includes conventional geothermal plants. Finally, it includes lithium-ion (Li-ion) batteries of three durations, as opposed to just one Li-ion battery duration represented in the GenX model. Biomass is not currently considered in either the GenX or Ideal Grid model because its role in the 2050 energy economy is still very uncertain.

Figure 5.3 Cost differences by subregion



Li-ion = lithium-ion; NGCC = natural gas combined cycle power plant; NGCC + CCS = natural gas combined cycle with carbon capture and storage; NGCT = natural gas combustion turbine; RoR hydro = run-of-river hydroelectric.

Generation and storage technology costs vary regionally across the United States. In part, this is simply because the capital cost for the same plant varies. In some cases, it is also because associated costs differ—for example, the cost of transmission investments needed to connect a wind farm to the grid. Figure 5.3 shows differences in annualized costs of the technologies across subregions in the Ideal Grid model.

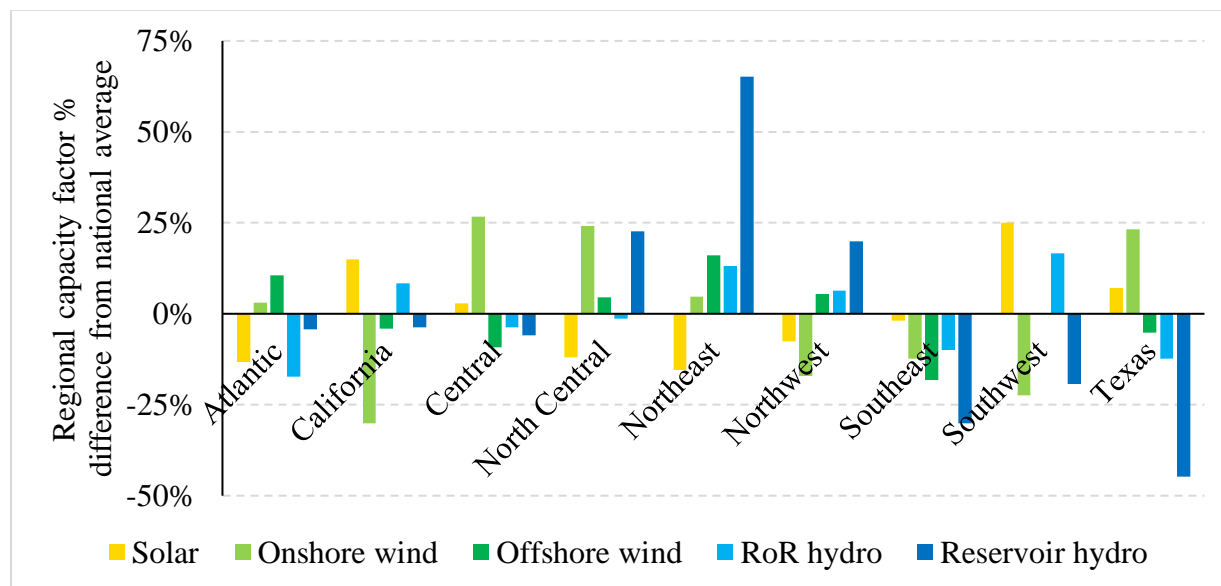
Table 5.6 Locational adjustment factors for GenX modeling of the New England grid.

	Annualized capital cost (\$/MW/yr)	New England locational adjustment	Adjusted annualized capital cost (\$/MW/yr)
Natural gas	71,600	1.16	83,000
Natural gas w/ CCS	117,000	1.04	121,700
Utility-scale solar PV	45,900	1.04	47,800
Commercial rooftop PV	62,600	1.04	65,100
Residential rooftop PV	81,300	1.04	84,500
Onshore wind	67,100	1.03	69,100
Fixed offshore wind	168,100	1.17	196,700
Floating offshore wind	271,900	1.17	318,200
RoR hydro	244,700	1.00	244,700
10-hour pumped hydro	454,500	1.00	454,500
4-hour Li-ion battery	85,900	1.16	99,600
Fusion – \$3,000/kW	199,400	1.12	223,300
Fusion – \$6,000/kW	398,800	1.12	446,600
Fusion – \$8,500/kW	564,900	1.12	632,700
Fusion – \$12,000/kW	797,500	1.12	893,200

Certain subregions are more expensive than others. For example, costs for most technologies are highest in California, while Texas has the lowest costs. In general, this makes electricity more expensive in California than in Texas. It is even more interesting to focus on the significant differences in adjustment factors between technologies within the same subregion. For example, in the Central and North Central subregions, land-based wind is more expensive than the national average, but solar is less expensive than the national average. [Table 5.6](#) lists the locational adjustment factors used by GenX to model the New England grid. At the bottom of the table, one can see that in each of our four fusion scenarios, capital costs for a plant in New England are 12% higher than the U.S. average values used to index our capital cost assumptions.

In addition to capital cost differences across subregions, there are differences in maximum annual average capacity factors for renewables based on differences in annual average insolation, wind energy, and hydropower. [Figure 5.4](#) shows differences in maximum average capacity factors across subregions in the Ideal Grid model.

Figure 5.4 Regional differences in maximum average annual variable renewable energy capacity factors

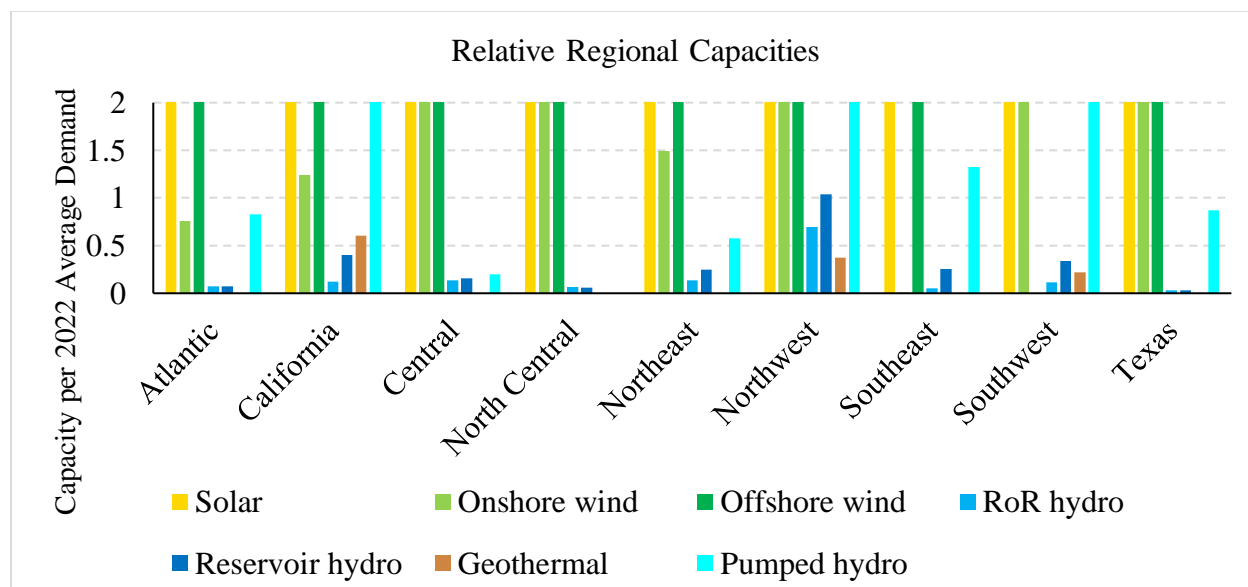


Finally, there are differences in potential renewable energy capacity across subregions depending on sites where facilities can be installed and where the resources exist. Figure 5.5 shows differences in potential renewables capacity relative to the national average across the subregions used in the Ideal Grid model. Potential solar capacity is greater than twice average demand in each subregion, and so all solar bars are truncated to this value. Potential offshore wind capacity is also not constrained in any subregion except the Southwest, which has no coastline. Lastly, potential generation from hydrothermal geothermal, reservoir hydro, and RoR hydro is severely limited in most subregions. The only subregion that is rich in hydro resources is the Northwest.

These capacity limits are defined by technical potential. They do not account for a variety of social and environmental factors that might limit the ability to exploit renewable resource potential. For example, in the New England subregion, exploiting renewables to their full technical maxima would entail converting large sections of agricultural land, woodland, and shoreline to energy generation. The sites needed to install 63 gigawatts (GW) of onshore wind would cover more than 7% of the total land mass of New England. Of course, only a fraction of this land is directly impacted—specifically, the space required for tower foundations and associated equipment. The sites needed to install 39.6 GW of solar PV capacity would cover about another one-half of 1% of this subregion’s total land mass, and that space would be fully affected. Therefore, the GenX base case analysis for New England includes a more restrictive set of capacity maxima in which no more than 4% of woodland and agricultural land can be used for new renewable generation, certain near-shore sites are not available for offshore wind farms (Mettetal et al. 2020), and growth in rooftop PV capacity is limited to the current pace of

installation (Johnson n.d.; Knight et al., 2023). The two sets of maximum constraints are shown in Table 5.7. Results in Section 5.4.2 contrasts this base case with an analysis of the New England grid that allows higher technical capacity limits for renewable generation.

Figure 5.5 Renewable energy technical maxima by subregion



All capacity values greater than twice the average demand are truncated at two.

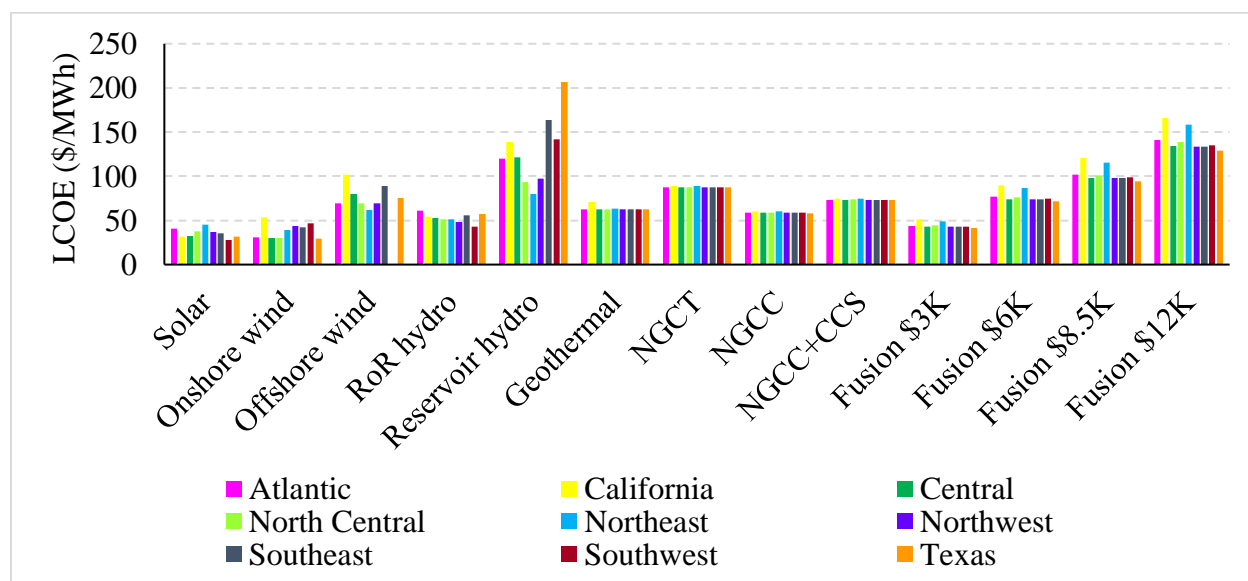
Figure 5.6 shows LCOEs for alternative technologies across the different subregions. The LCOEs are calculated using subregion-specific capital costs (from Figure 5.3), operating and maintenance costs, fuel costs, and maximum average annual capacity factors for renewables as pro-forma capacity factors (from Figure 5.4). Once again, the actual realized average capacity factor for each technology depends on the portfolio of capacity investments made and on how technologies are dispatched to serve load throughout the hours of the year. As discussed in Section 4.4 of this report, the value of variable renewable energy (VRE) technologies declines as their share of the capacity mix increases. As with the GenX model, the capacity factor is an Ideal Grid model output, not a model input.

Table 5.7 Minimum and maximum capacity limits (in MW) for renewable energy generation in the GenX model of the New England grid

Capacity constraint	Fixed offshore wind	Floating offshore wind	Onshore wind	Utility-scale solar PV	Commercial rooftop PV	Residential rooftop PV
Minimum, MW (“New England Wind Offshore Overview” 2024; Lopez et al. 2022)	5,946	–	–	–	–	–
Land-use constrained maximum, MW (Mettetal et al. 2020)	37,000	275,000	9,000	22,000	12,000	6,000
Technical maximum, MW (Cole et al., n.d.)	91,000	461,000	63,000	752,000	51,000	66,000

The minimum offshore wind values are based on procurements to date.

Figure 5.6 Levelized cost of electricity for each generation technology in each subregion at pro-forma capacity factors



The costs shown in the figure include technology-specific and subregion-specific transmission costs. LCOE estimates for fusion are based on four cost points ranging from \$3,000 to \$12,000/kW. NGCC = natural gas combined cycle power plant; NGCC + CCS = natural gas combined cycle power plant with carbon capture and storage; NGCT = natural gas combustion turbine; PV = photovoltaic; RoR hydro = run-of-river hydroelectric.

5.4. Results

Many factors shape the modeled penetration of fusion in different subregions. To analyze these results, we turn to the GenX model for New England and explore its sensitivity to key

parameters. Starting in [Section 5.4.7](#), we contrast model results for the penetration of fusion across different subregions.

All sensitivity analyses described in this chapter are outlined in [Table 5.8](#).

Table 5.8 Roadmap to modeling results for our sensitivity analyses

Section	Subregion	Assumptions	Sensitive parameters
5.4.1	New England	Renewables constrained by land-use maxima	Cost and emission cap
5.4.2	New England	Renewables constrained by technical maxima, emission cap 4 gCO ₂ /kWh	Cost
5.4.3	New England	Renewables constrained by land-use maxima, NGCC+CCS is not available	Cost and emission cap
5.4.4	New England	Renewables constrained by land-use maxima, FPPs cost \$6,000/kW	Emissions cap flexibility
5.4.5	New England	Renewables constrained by land-use maxima, FPPs cost \$6,000/kW	VRE costs, battery costs, and emission cap
5.4.6.1	New England	Renewables constrained by land-use maxima, fusion must operate as baseload	Cost and emission cap
5.4.6.2	New England	Renewables constrained by land-use maxima, fusion plant includes thermal storage	Cost and emission cap
5.4.6.3	New England	Renewables constrained by land-use maxima, FPPs cost \$6,000/kW	Nameplate lifetime, replacement downtime, and emission cap
5.4.7	Multi-subregion	Renewables constrained by technical maxima, FPPs cost \$6,000/kW	Renewables attributes, emissions cap
5.4.8	Multi-subregion	Renewables constrained by technical maxima	Cost and emission cap in all nine subregions

FPP = fusion power plant; NGCC + CCS = natural gas combined cycle power plant with carbon capture and storage; VRE = variable renewable energy.

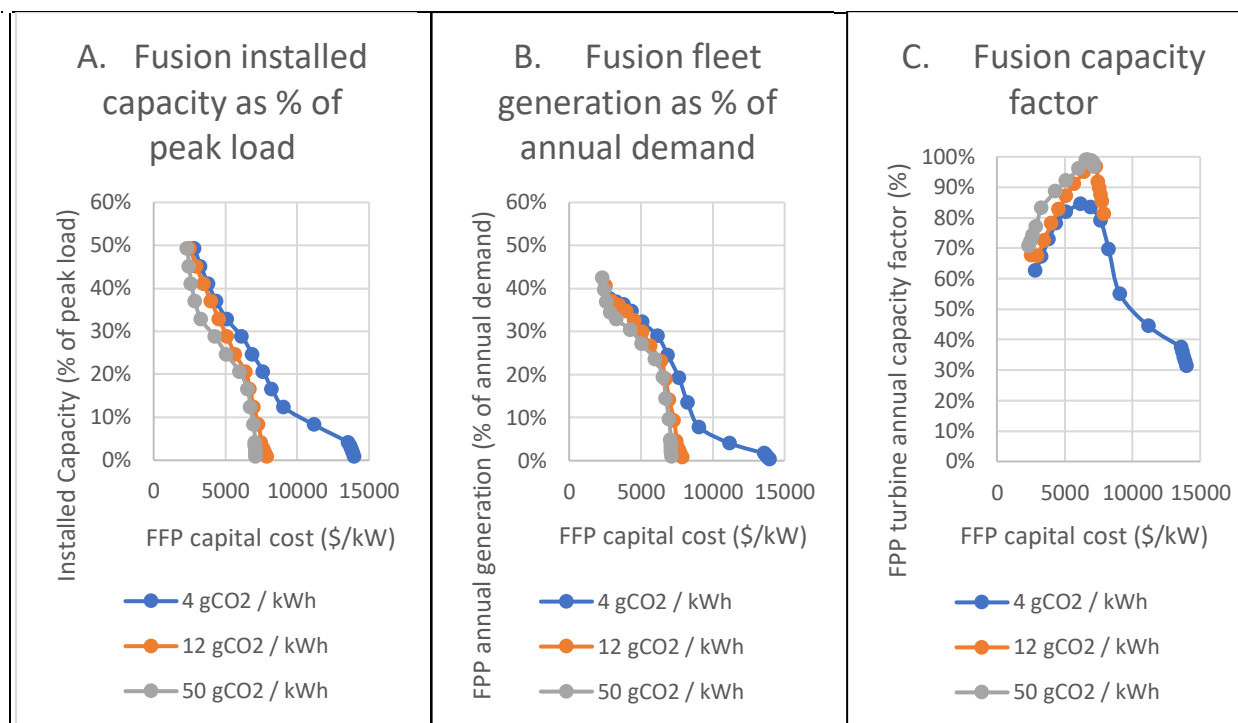
5.4.1. Sensitivity to cost and emissions cap assumptions

[Figure 5.7](#) shows how modeling results for FPP installation and operations are affected by assumptions about FPP capital cost and system-wide emissions constraints. Subfigure A shows how estimates of FPP installed capacity vary sharply with FPP capital cost. Subfigure B shows that model results for FPP share of generation depend on capital cost, while subfigure C shows how the average capacity factor for FPPs varies with capital cost. Each of the subfigures displays three lines to represent three different levels of an intensity-based CO₂ emissions cap:

- 50 gCO₂ per kWh of load, an 80% reduction relative to 1990;
- 12 gCO₂ per kWh of load, a 95% reduction relative to 1990; and
- 4 gCO₂ per kWh of load, a 98.4% reduction relative to 1990.

Whereas Figure 5.7 shows installed capacity as a percent of peak load, Table 5.9 reports the same results in megawatts at four selected levels of FPP capital cost.

Figure 5.7 GenX results for FPP installed capacity (A), generation (B), and capacity factor (C) on the New England grid depending on assumptions about FPP capital cost and system-wide emissions cap



Charts were generated under the assumption that installed VRE capacity is constrained by the land-use maxima shown in Table 5.7.

Table 5.9 Model results for installed FPP capacity (in MW) on the New England grid

Emission intensity limit (gCO ₂ /kWh)	Fusion power plant cost (\$/kW)			
	3,000	6,000	8,500	12,000
50	19,400	11,100	–	–
12	25,400	12,400	–	–
4	26,900	16,300	7,900	3,500

Table was generated assuming that renewables capacity is constrained by the land-use maxima in Table 5.7.

Figure 5.8 shows model results for installed capacity in 2050 for each of the generation technologies considered, under different assumptions about FPP capital cost and at an emissions cap of 4 gCO₂/kWh.

Figure 5.8 Installed capacity of each resource on the New England grid

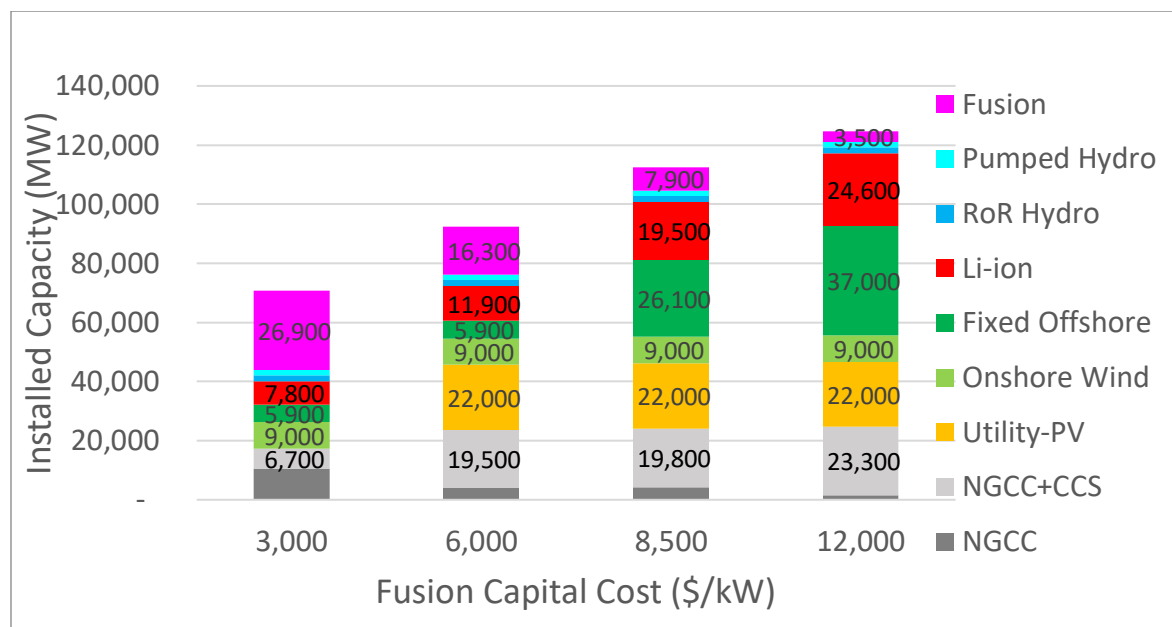


Chart was generated assuming a 4 gCO₂/kWh emissions intensity cap and assuming that VRE installed capacity is constrained by the land-use maxima in Table 5.7. Li-ion = lithium-ion; NGCC = natural gas combined cycle power plant; NGCC + CCS = natural gas combined cycle power plant with carbon capture and storage; PV = photovoltaic; RoR hydro = run-of-river hydroelectric.

We can see in Figure 5.8 that there are four cost points beyond which FPPs substitute for different competing technologies and play different roles on the grid. These cost points exist under all three emission caps but have different values depending on the stringency of the cap. Results for the 4 gCO₂/kWh emission cap may be summarized as follows:

- Above \$14,000/kW, FPPs are too expensive to play a meaningful role on the grid. Less than 500 MW of fusion capacity is installed as shown in Figure 5.7.
- At \$12,000/kW, FPPs play a limited role as a net-load follower, complementing less expensive VRE generation. Onshore wind, fixed-platform offshore wind, and utility-scale solar PV are all at their maximum allowed capacities, while natural gas combined cycle power plant with carbon capture and storage (NGCC+CCS) generation is constrained by the emissions intensity limit. Between \$12,000/kW and \$14,000/kW, FPPs displace floating platform offshore wind and rooftop solar. These are the most expensive forms of VRE, so the fact that it is less expensive to install and operate FPPs with capacity factors below 50% creates a role for FPPs in this cost range.
- At \$8,500/kW, Figure 5.8 shows that FPP capital cost makes fusion energy competitive with fixed-platform offshore wind and some NGCC+CCS. The capacity factors of fixed offshore wind and NGCC+CCS both increase, indicating that FPPs are replacing curtailed offshore wind generation and peaker NGCC+CCS units. While the FPP capacity factor rises to 55% at this cost point, the LCOE of fusion generation is still higher than that of

fixed offshore wind. However, the LCOE of VRE generation does not include the cost of any requisite supporting Li-ion battery storage and natural gas units. With FPPs on the grid, the installed capacity of these supporting resources can also be reduced, leading to overall cost savings.

- At \$6,000/kW, FPPs outcompete fixed platform offshore wind, reducing the installed capacity of this technology to the minimum allowed by the constraint in [Table 5.7](#). There is also a large commensurate reduction in installed Li-ion storage capacity. The FPP capacity factor is 80%, with FPP output falling only during periods of low grid demand or high solar and wind production. There is no further reduction in the installed capacity of NGCC+CCS, as the remaining natural gas units provide cost-effective load-following generation and remain within the emissions cap.
- At \$3,000/kW, FPPs displace all VRE resources except onshore wind, including all utility-scale solar PV. Replacing solar generation with fusion power, a clean firm form of generation, means there is much less variation in grid net load and less need for Li-ion batteries and NGCC+CCS. The NGCC capacity that remains consists of peaker units that operate when net demand exceeds FPP capacity. The capacity of NGCC units without CCS increases because zero-emission FPPs have substituted for NGCC+CCS units with low but non-zero emission levels. This creates additional space in the emissions budget that can be used by less expensive but more polluting NGCC plants without CCS. At \$3,000/kW, FPPs constitute the majority of installed capacity on the grid, and the capacity factor falls again because FPP output must be reduced during periods of low grid load (FPPs are a load-following resource).¹⁵

The same trends can be seen in our modeling results for the other two emission intensity limits, but they emerge at different cost points because more NGCC+CCS generation is allowed without violating the emissions cap.

5.4.2. Sensitivity to VRE land-use constraints

Allowing the installation of more renewable generation capacity, especially onshore wind, diminishes the role of FPPs in New England.

Our base case GenX results for New England assume that the buildout of renewable energy capacity would face land-use constraints. That assumption plays an important role in defining the competitive space for FPPs. In New England, onshore wind is a very inexpensive resource

¹⁵ FPPs are load-following at both low and high price points. At low FPP cost, there is less generation from VRE resources, so FPP output must vary in response to grid demand (i.e., the gross load). At high FPP cost, FPP generation follows net load (i.e., gross load minus VRE generation).

and relatively consistent, with an average capacity factor of 39%, and a capacity factor of at least 25% in 65% of all hours. Utility-scale solar PV is another very inexpensive resource.

If we relax the land-use constraint and imagine that renewables buildout will be constrained by technical limits only, the future New England grid is dominated by VREs and the competitive space for FPPs is sharply reduced. [Figure 5.9](#) shows grid composition as a function of fusion capital cost at the tightest emissions cap, 4 gCO₂/kWh. When the average capital cost for fusion is \$8,500/kW or more, there is no place for fusion in the cost-efficient portfolio of technologies in New England. Maximum technically feasible onshore wind capacity, at 63 GW or 103% of peak load, provides 70% of all generation. It is supplemented by almost 40 GW of utility-scale solar PV. NGCC+CCS and Li-ion batteries provide the firm generation and storage required to ensure that demand is met during periods of low wind speeds.

Figure 5.9 Installed capacity of different generation resources on the New England grid

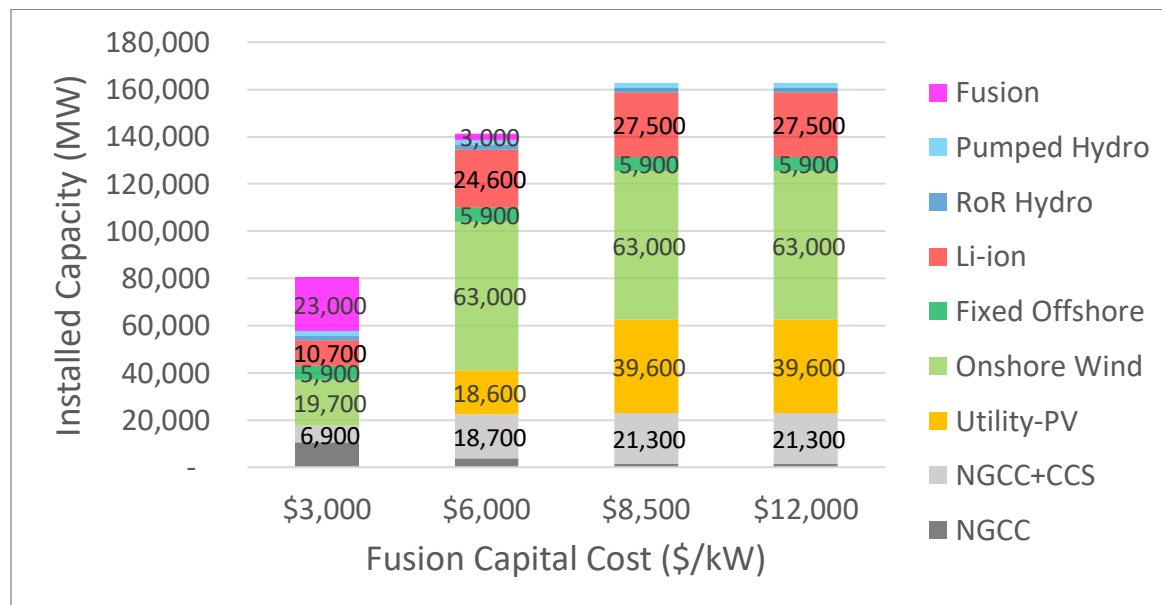


Chart was generated assuming a 4 gCO₂/kWh emissions intensity cap and assuming that installed VRE capacity is constrained by the technical maxima in Table 5.7. Note that 5,900 MW of offshore wind capacity is present in all scenarios because that amount of onshore wind has already been procured, and those assets are expected to still be operating in 2050. Li-ion = lithium-ion; NGCC = natural gas combined cycle power plant; NGCC + CCS = natural gas combined cycle power plant with carbon capture and sequestration; PV = photovoltaic; RoR hydro = run-of-river hydroelectric.

At \$6,000/kW, 3 GW of fusion substitutes for 21 GW of utility-scale solar PV, 2.5 GW of NGCC+CCS, and 3 GW of Li-ion batteries. While FPPs are more expensive than utility-scale solar PV per kW of capacity, fusion is less expensive than the required ensemble of VREs, NGCC with CCS, and battery storage. At \$3,000/kW, FPPs are less expensive than utility-scale solar PV on a LCOE basis, so an additional 20 GW of fusion replaces all remaining utility-scale solar PV and 43 GW of onshore wind capacity. Again, FPPs are still more costly than onshore wind farms at this

cost point, but savings from reduced Li-ion storage and NGCC+CCS allow FPPs to replace onshore wind. The multi-subregion analysis also shows low FPP penetration in most subregions at \$8,500/kW because solar PV is only limited by technical maxima in all regions. Land use was not a constraining factor in that analysis.

5.4.3. Sensitivity to cost of natural gas combined cycle generation with carbon capture and storage

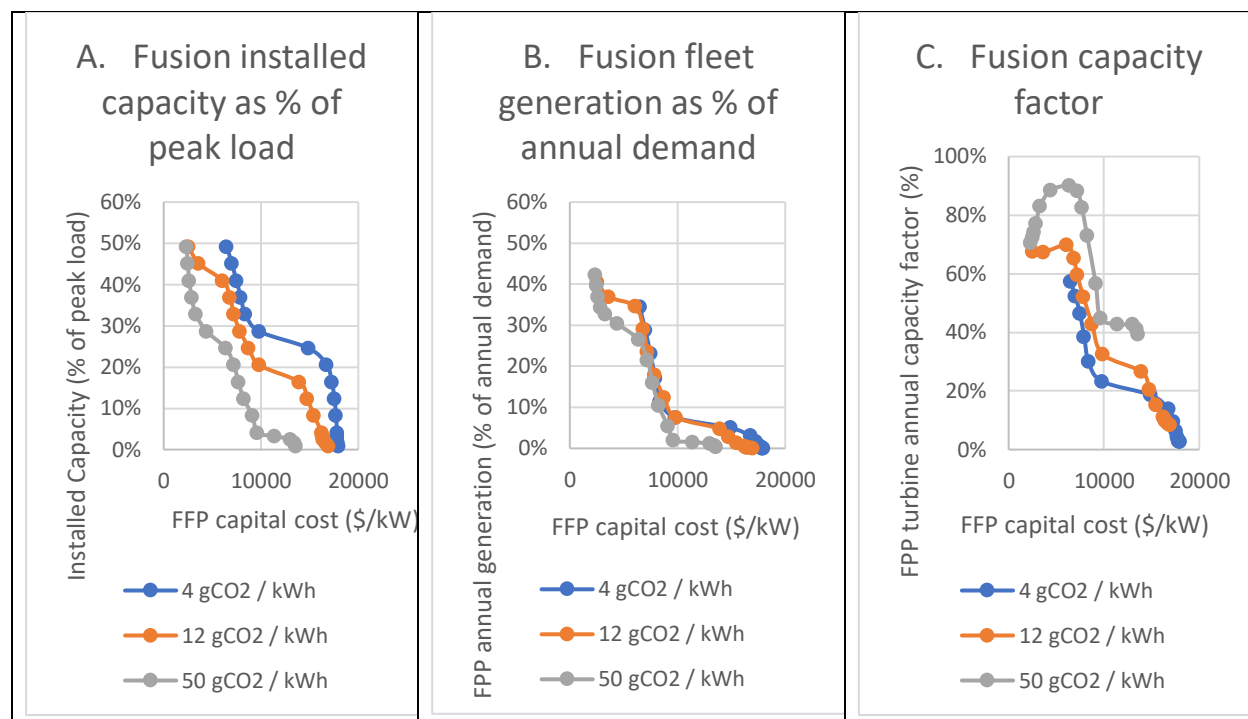
The maximum cost at which FPPs are included in the New England grid is primarily determined by the cost and availability of NGCC+CCS generation. NGCC+CCS complements and supports the inexpensive VRE resources (onshore wind, utility-scale solar PV, and fixed platform offshore wind), providing generation when grid load is high or VRE generation is low. NGCC+CCS can provide dispatchable, low-carbon generation capacity to be used when needed. However, it is not an emissions-free resource, so the assumed emissions cap constrains its use. Moving from a 50 gCO₂/kWh to a 4 gCO₂/kWh emissions intensity cap reduces NGCC+CCS generation by 75% (and reduces generation from NGCC without CCS); it also causes the FPP cost threshold to double from \$7,000/kW to \$14,000/kW. That FPP generation cost is dominated by upfront costs is not naturally advantageous for a load-following resource with a low capacity factor. However, the fact that FPPs provide zero-emission firm generation makes them an option when NGCC+CCS is limited.

Emissions for NGCC+CCS generators are challenging to model because there is relatively little data on the performance of large plants over a range of operating conditions (Sheha et al. 2024). Most emissions intensity data for NGCC+CCS come from plants that operate at steady state and near their maximum efficiency design point such that emissions per MWh of electricity generated are minimized. However, operating NGCC+CCS plants as part of a low-carbon grid with high VRE penetration will require frequent ramping of plant output with frequent startups and shutdowns. Our model does not capture the potential efficiency penalty and low CO₂ capture rate of an NGCC+CCS plant operating in dispatch mode. This means our results may underestimate emissions from NGCC+CCS plants and hence overestimate how strongly NGCC+CCS would compete with FPP.

As we do not have the data to calculate the impact of these factors directly, we instead investigate the limiting case by optimizing the New England grid without NGCC+CCS. NGCC without CCS is still allowed within the limits of the emissions cap. [Figure 5.10](#) shows the results. In the absence of NGCC+CCS, investments in fusion capacity compete against investments in additional floating platform wind and Li-ion storage to make up the difference in generation. On the margin, additional wind resources are significantly curtailed, raising their average cost. Together, these factors relax the capital cost threshold for FPP penetration. Under a 50 gCO₂/kWh emissions cap, the cost threshold is relaxed to \$13,500/kW; under a 12 gCO₂/kWh cap, the threshold is relaxed to \$17,000/kW; and under a 4 gCO₂/kWh cap, the threshold is

relaxed to \$18,000/kW. Below these cost thresholds, fusion deployment would increase sharply as FPPs substitute for expensive floating offshore wind and associated energy storage. At low FPP costs, trends in installed fusion capacity and capacity factor are largely the same as in the base case because at these cost levels, FPPs are substituting for utility-scale solar PV and onshore wind.

Figure 5.10 FPP installed capacity (A), generation (B), and capacity factor (C) in the New England grid for the scenario in which NGCC+CCS is not an option



Charts were generated using the following assumptions: 4, 12, and 50 gCO₂/kWh emissions intensity cap, constraints on installed VRE capacity based on the land-use maxima shown in Table 5.7, and no NGCC + CCS construction.

5.4.4. Interannual weather uncertainty

As detailed more fully in [Appendix B](#), the GenX model incorporates interannual uncertainty about load and about the capacity factor of renewable generators. The model has 20 different weather-year scenarios. Certain years may include winter cold snaps, where load increases sharply over the course of several days, while other years do not. The chosen portfolio of technologies must be able to serve load across all years. Certain years will have very plentiful wind, for example, while some years may have extended multi-day periods with very little wind. Thus, the chosen portfolio of technologies must be able to compensate for shortfalls in generation by a particular type of technology. When optimizing for a mix of generation technologies, the model looks at cost incurred across all weather-year scenarios and makes investments that are robust to variability across scenarios.

This interannual variability interacts with the emissions constraint. In the base case, the carbon constraint is binding in every one of the weather-year scenarios. This limits the value of investments in NGCC+CCS. In certain weather-year scenarios with plentiful wind, NGCC capacity may be severely underutilized, while in other weather-year scenarios, capacity utilization is constrained by that year’s emissions cap. An alternative policy scenario could allow flexibility in meeting the emissions cap in individual weather-year scenarios, so long as the cap is met on average across all weather-year scenarios. Allowing this flexibility would increase the value of a technology like NGCC+CCS, which competes with fusion as a dispatchable technology. As we shall see, however, the interaction between flexibility and technology choices is complicated. Unabated NGCC, as an alternative to NGCC+CCS, is also available and since it likewise benefits from flexibility in the emissions constraint it could complement non-emitting technologies, including fusion.

We ran a version of the model that allowed a specified amount of flexibility in meeting the emissions cap, ranging from a 10% exceedance of the annual cap, to 25%, 50%, and finally 75%. In all cases, strict compliance with the emissions cap is required on average across all scenarios. [Table 5.10](#) shows the results. As it happens, fusion penetration increases in some cases and decreases in others, depending on the stringency of the cap. In all cases, however, the impact of flexibility on fusion penetration is small.

Table 5.10 FPP installed capacity on the New England grid assuming an FPP cost of \$6,000/kW and flexibility in terms of emissions banking

Emission intensity limit (gCO ₂ /kWh)	Annual flexibility in emission allowances				
	Base case	10%	25%	50%	75%
50	11,100	11,300	11,300	11,300	11,300
12	12,400	12,200	12,000	12,000	12,000
4	16,300	15,900	15,300	16,000	16,000

Modeling results assume that VRE installed capacity is constrained by the technical maxima in [Table 5.7](#).

5.4.5. Sensitivity to costs for VRE and storage

Onshore wind and utility-scale solar PV are expected to be very inexpensive generation options in 2050. As demonstrated earlier, even considering the effect of curtailment, on a pure cost basis, these technologies would dominate the system. However, siting is a constraint for both options. Thus, the system turns to more expensive offshore wind to fill out its portfolio, and to storage to get the most out of installed VRE capacity. These factors define the competitive space for fusion, along with the emissions constraint and the availability of NGCC+CCS.

[Table 5.11](#) shows how the cost of VREs and storage would affect fusion penetration. We varied costs for all forms of VRE and Li-ion storage together, to between 50% and 150% of the base

case costs given in [Table 5.5](#). Lower VRE and Li-ion costs reduce installed FPP capacity on the New England grid, as shown in [Table 5.11](#). This is true at all emission intensity limits, but the effect is strongest for higher emission intensity limits. While a 25% reduction in VRE and Li-ion costs leads to a 50%–100% reduction in installed FPP capacity, a 25% increase in VRE and Li-ion storage costs increases installed FPP capacity by only 10%.

Table 5.11 Installed FPP capacity on the New England grid given an FPP cost of \$6000/kW and varying the VRE and Li-ion storage costs as a percentage of the base costs given in [Table 5.5](#)

Emission intensity limit (gCO ₂ /kWh)	Cost multiplier for VRE and Li-ion resources				
	50%	75%	Base case	125%	150%
50	–	–	11,100	12,500	13,600
12	–	2,400	12,400	14,100	15,500
4	4,200	9,000	16,300	18,000	19,600

Note that installed VRE capacity is constrained by the technical maxima in [Table 5.7](#).

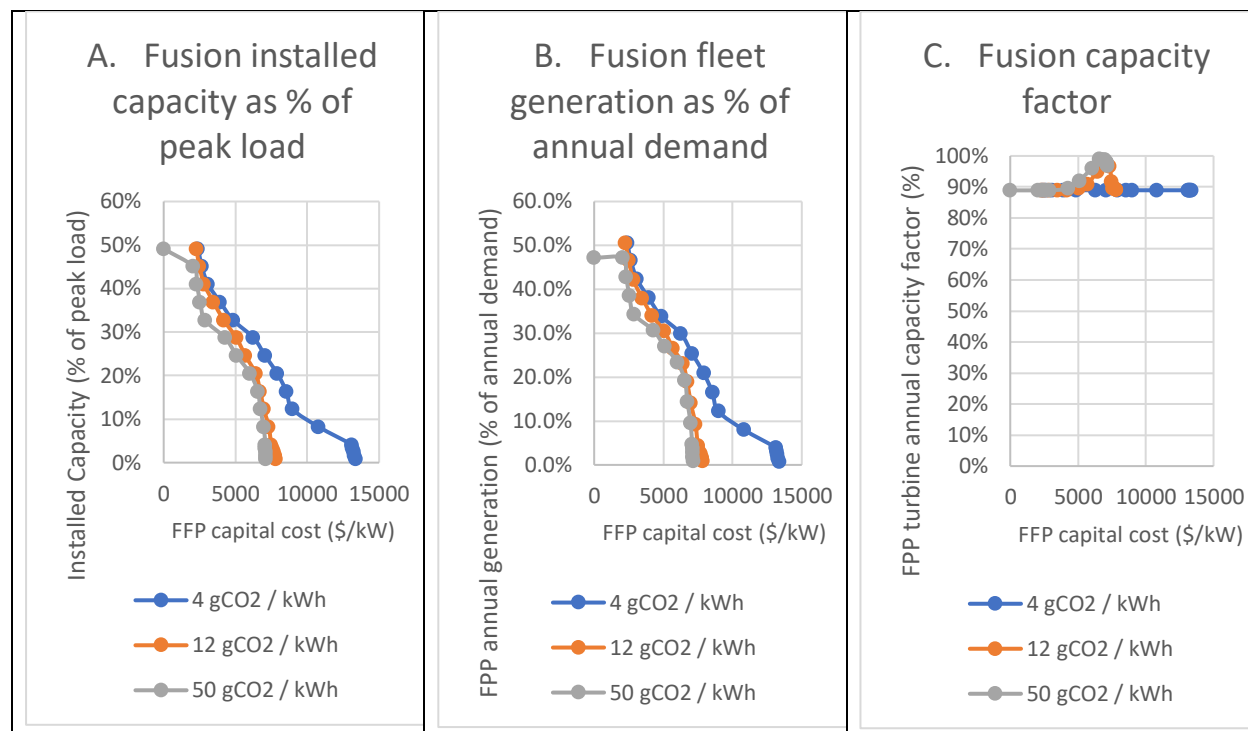
5.4.6. Sensitivity to fusion plant design and operation

5.4.6.1. Baseload operation

All our analyses to this point allowed the GenX model to optimize the dispatch of all generators. [Figure 5.11](#) shows the resulting average capacity factor for installed FPPs under alternative assumptions about capital cost and emissions caps. In many cases, the average capacity factor for fusion is well below full baseload operation. In these cases, the model projects reductions in FPP hourly generation in response to changes in hourly load or available VRE generation. Dispatching FPPs in this way is necessary to ensure the lowest average cost of electricity.

For this analysis, we examine a scenario where FPPs operate only as baseload generators. We explore how this baseload requirement would change capital cost thresholds for fusion energy and the penetration of fusion technology, as well as impacts on system costs. Constraining FPPs to operate as baseload generators slightly reduces the threshold capital cost at which fusion becomes viable on the New England grid. [Figure 5.11A](#) shows that the threshold FPP capital cost with this constraint falls from \$14,000 to \$13,500 per kW under a 4 gCO₂/kWh emissions cap and does not change under a 12 or 50 gCO₂/kWh cap. The average cost of electricity on the system increases slightly if FPPs are required to operate as baseload generators.

Figure 5.11 FPP installed capacity (A), generation (B), and capacity factor (C) on the New England grid in a scenario where FPPs must operate as baseload generators



Charts were generated assuming that the FPP capacity factor must be greater than 89% and that VRE installed capacity is constrained by the land-use maxima shown in Table 5.7.

At a FPP cost of \$3,000/kW, requiring FPPs to operate as baseload units under any emissions cap reduces installed FPP capacity. In the base case, flexible FPPs at this cost point operate alongside low-cost VRE generation and reduce their output during periods of low demand. When FPPs are required to operate as baseload, however, the cost-minimizing solution is to reduce installed FPP and VRE capacity and curtail VRE output during periods of low demand so that the FPPs can continue to operate. This raises the average cost of electricity compared to the base case with flexible FPPs.

At higher FPP costs, the installed capacity of the FPP fleet stays the same or increases compared to the base case if baseload operation is required. Under the 12 and 50 gCO₂/kWh emissions caps, installed capacity is unchanged because the capacity utilization of flexible FPPs in the base case is greater than 89%. Under the 4 gCO₂/kWh cap, the installed capacity of baseload FPPs is

greater than the installed capacity of flexible FPPs in the base case. This is surprising, as decreasing the operational flexibility of FPPs would be expected to reduce their value to the grid and cause overall installed capacity to fall. However, at these intermediate to high FPP costs, most electricity production is from VRE resources, and the requirement for FPP capacity is mostly dictated by periods of high demand and low VRE availability. Requiring FPPs to operate as baseload units means that VRE generation must be curtailed during periods of low demand and high VRE availability. For the New England grid, the least expensive option is to reduce VRE and Li-ion installed capacity and instead install more FPPs to replace the VRE generation. This raises the average cost of electricity compared to the base case with flexible FPPs. Additional natural gas with CCS cannot be installed, as the grid is operating under a stringent 4 gCO₂/kWh emissions intensity cap.

Table 5.12 Installed FPP capacity on the New England grid assuming land-use constraints on VRE capacity and FPP capacity utilization of 89% or more

Emission intensity limit (gCO ₂ /kWh)	FPP cost (\$/kW)				Change from base case (%)			
	3,000	6,000	8,500	12,000	3,000	6,000	8,500	12,000
50	17,800	11,100	–	–	–8%	0%	–	–
12	22,300	12,400	–	–	–12%	0%	–	–
4	23,500	16,600	9,200	3,500	–13%	2%	16%	0%

5.4.6.2. Thermal storage

In our base case, FPPs costing more than \$6,000/kW operate at capacity factors as low as 30%, especially under the stricter 4 gCO₂/kWh emission limit. This result is initially surprising given the high capital cost of these FPPs, but it is due to the low cost of alternative VRE generation and the valuable role that FPPs can play (and the high revenues they can earn) in providing generation during periods of low VRE availability. However, this raises the question of whether incorporating thermal energy storage (TES) into FPPs can reduce system costs further by allowing FPP reactors to operate with a high capacity factor, maximizing the use of the asset, while the FPP power block load-follows and draws heat from the TES. In this way, incorporating TES could potentially reduce the levelized cost of FPP-generated electricity.

To investigate the impact of TES on FPP threshold costs, installed capacity, and operation, we model FPPs with the option to install molten salt TES and additional power block capacity. The additional power block capacity allows the power plant to generate more electricity during scarcity periods than would be possible with FPPs that lack TES. We use the molten salt TES

costs in [Table 5.13](#). Molten salt TES systems have been deployed in commercial concentrated solar power plants (Augustine, Kesseli, and Turchi 2020; Turchi et al. 2021), but the systems are expensive. We estimated the future cost of molten salt TES systems from a review of the literature on current TES R&D efforts (Parzen, Fioriti, and Kiprakis 2023; Viswanathan et al. 2022).

At the TES costs shown in [Table 5.13](#), system optimization does not result in any appreciable installation of TES capacity over the wide range of FPP costs and emissions intensity caps we considered (\$3,000/kW–\$12,000/kW and 4–50 gCO₂/kWh, respectively). We find that FPPs with TES have the same threshold cost and that the installed capacity and capacity factor results at a given FPP cost point are within 0.1% of the equivalent base-case result.

Table 5.13 Cost assumptions used in GenX modeling of molten salt thermal energy storage (TES) integrated with a FPP

Resource	Daily heat leakage (%/day)	Energy cost (\$/kWh _e)	Charge/discharge cost (\$/kW _e)	FPP power block cost (\$/kW _e)	10-hour storage cost without power block (\$/kW _e)	10-hour storage cost with power block (\$/kW _e)
Molten salt	2%	45	375	1,270	825	2,095

Sources: Augustine et al. 2020; Parzen et al. 2023; Turchi et al. 2021; Viswanathan et al. 2022).

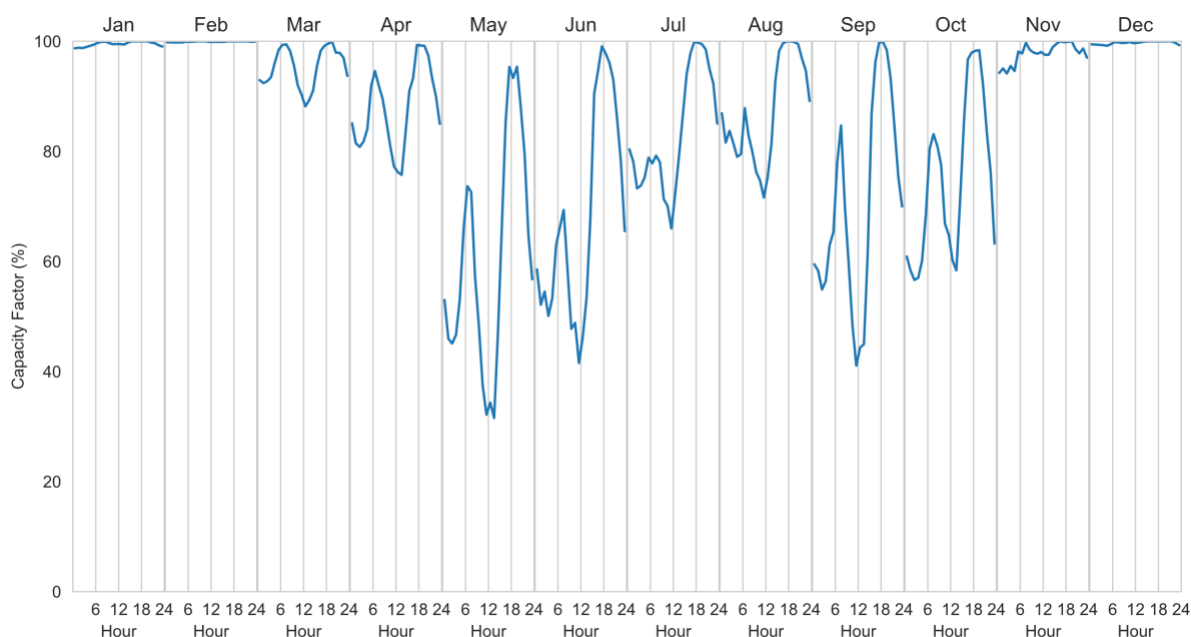
To understand why TES is not deployed, we examine how FPPs are used and when they cycled up and down. [Figure 5.12](#) shows that in New England, fusion energy is most needed in the winter months (December to February); during those months, FPPs run at nearly full capacity 24 hours per day. There is no diurnal cycling of FPPs in those months for the \$6,000/kW fusion cost case and thus there would be no value in adding TES capacity. During the summer months, FPP operation exhibits substantial diurnal cycling, but during those months FPP capacity is adequate most of the time to meet peak demand, and thus there is limited value in deploying TES to improve peaking capacity. Model results at the other FPP price points also show that demand for fusion energy is highest in the winter months and that diurnal cycling is mild, with average hourly capacity factors remaining above 90% for the \$8,500/kW case, above 80% for the \$12,000/kW case, and above 60% for the \$3,000/kW case.

The second reason that our model results do not show TES deployment with FPPs is that the costs for TES shown in [Table 5.13](#) are higher than costs for Li-ion batteries. The assumed capital cost of 4-hour Li-ion storage is \$830/kW_e. Even accounting for the shorter life of Li-ion batteries, this means that 10-hour TES is 2.5 times more costly than 4-hour Li-ion storage. TES can compete with Li-ion batteries only if the required storage duration for both is 11 hours or

more. The third reason TES is not deployed is that Li-ion batteries are more flexible than TES. Batteries can be charged using electricity from any generator, while our reference case assumption is that TES can only serve FPPs.

To explore other scenarios where TES might be included, we perform a sensitivity study over a range of lower (more stringent) emissions caps and lower thermal storage energy and power costs. We find that TES capacity is installed only in cases with low FPP costs (circa \$3,000/kW) and a very low TES cost of \$82.50/kW_e for 10-hour storage. In these cases, reactor capacity was reduced by 11% and the reactor capacity factor increased by 11%, while power block capacity remained the same. That is, total fusion electricity generation remains the same over the course of one year, but with a lower investment in reactor capacity. The cost of molten salt thermal storage with power conversion is not expected to fall as low as \$82.50/kW_e because molten salt itself is a relatively expensive material. Crushed rock thermal storage has been proposed and could be inexpensive enough (Forsberg 2023). These forms of storage could be integrated with fusion systems using an intermediate forced air loop between the power plant and the storage medium.

Figure 5.12 FPP hourly capacity factor on the New England grid, averaged over each month of one of the weather scenarios



Results shown in the figure reflect the following assumptions: FPP cost of \$6,000/kW, emissions cap of 4 gCO₂/kWh, and constraints on installed VRE capacity based on the land-use maxima in Table 5.7.

These results are consistent with findings from a recent study of FPPs with thermal storage (J. A. Schwartz et al. 2022). In that study, thermal storage was found to increase the cost threshold and capacity factor of FPPs. However, Schwartz et al. included significantly more solar

generation and allowed no emissions. Solar provides up to 50% of generation in some hours in their analysis—this creates a strong diurnal pattern that is smoothed with a combination of TES and batteries. Schwartz et al. also assume lower TES costs (\$22/kWh_{th} energy, \$0/kW_e charge and discharge, and \$750/kW_e turbine cost), but our analysis suggests that TES cost is not the determining factor.

5.4.6.3. Replaceable component lifetime and replacement downtime

Lastly, we investigate the impact of different assumptions concerning critical replacement components in a FPP, specifically in terms of component nameplate operating lifetimes and the amount of downtime required to replace components. Note that downtimes are measured in months because replacing critical components may involve removing activated materials and restarting magnets by bringing them to their required cryogenic temperatures. [Table 5.14](#) shows how varying both parameters impacts the annual availability of FPPs and their LCOE. The LCOE calculation assumes that FPP capacity factors equal the plants' annual availability.

Table 5.14 Influence of nameplate lifetime and downtime requirements for component replacement on annual availability and LCOE for a \$6,000/kW FPP

Nameplate lifetime (years)	Annual availability (%)				LCOE (\$/MWh)			
	Replacement downtime (months)				Replacement downtime (months)			
	1	2	3	6	1	2	3	6
1	92%	86%	80%	67%	78.00	82.30	86.60	99.50
2	96%	92%	89%	80%	67.00	69.20	71.30	77.80
3	97%	95%	92%	86%	63.40	64.80	66.20	70.50
4	98%	96%	94%	89%	61.60	62.60	63.70	66.90

We optimize the New England grid assuming \$6,000/kW FPPs with the component nameplate lifetimes and replacement downtimes shown in [Table 5.14](#). We find that changes in FPP installed capacity are well represented by the changes in LCOE shown in [Table 5.14](#). We find that it is very important for replaceable FPP components to have nameplate lifetimes greater than one year. Increasing nameplate lifetime from one to two years reduces the LCOE by more than \$10/MWh, making FPPs more competitive.

It is also beneficial for replaceable components to have short replacement downtimes, although this is less important than the nameplate lifetime. As shown in [Table 5.14](#), plant availability and LCOE are less affected by replacement downtimes than by component lifetimes.

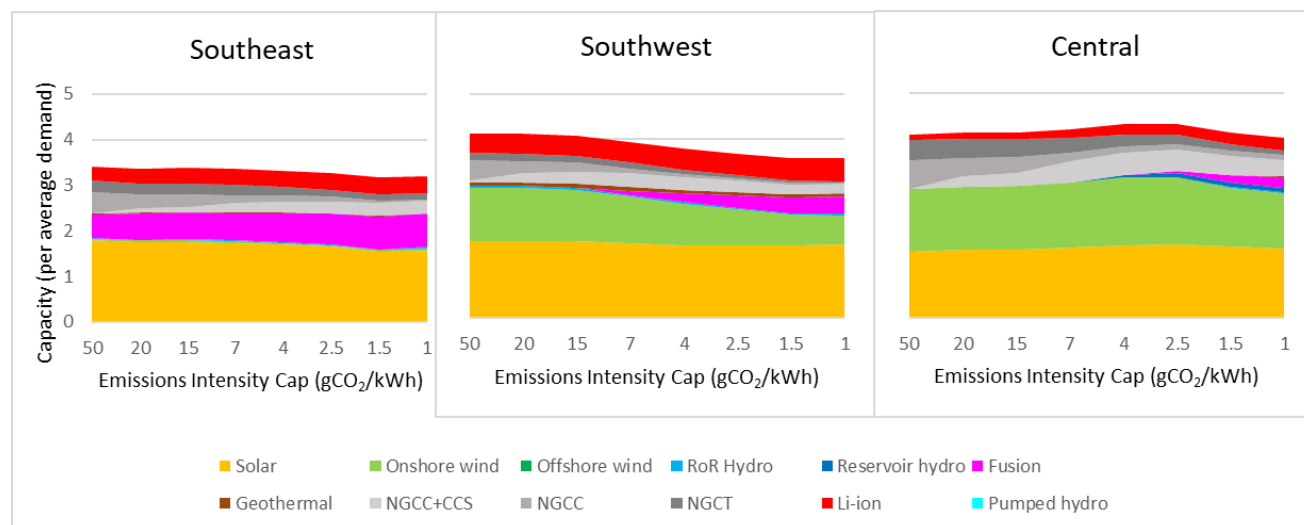
However, if replacement times add up to a large fraction of total lifetime and cause the maximum capacity factor to be less than 80%, this factor becomes an important feature to improve.

5.4.7. Differences in fusion penetration driven by subregional renewable resource attributes

This section contrasts modeled fusion penetration across different subregions of the United States.

Figure 5.13 shows that the optimal generation mix varies substantially from subregion to subregion. Fusion deployment is highest in the Southeast subregion and lowest in the Central subregion in the \$6,000/kW scenario. At this cost point, the Southeast deploys fusion even under a lenient carbon cap (50 gCO₂/kWh). Deployment in the Southwest is moderate, with FPPs entering the mix under an emissions intensity cap of about 20 gCO₂/kWh. Figure 5.14 shows the relative contribution from each generation technology for the Southeast, Southwest, and Central subregions.¹⁶

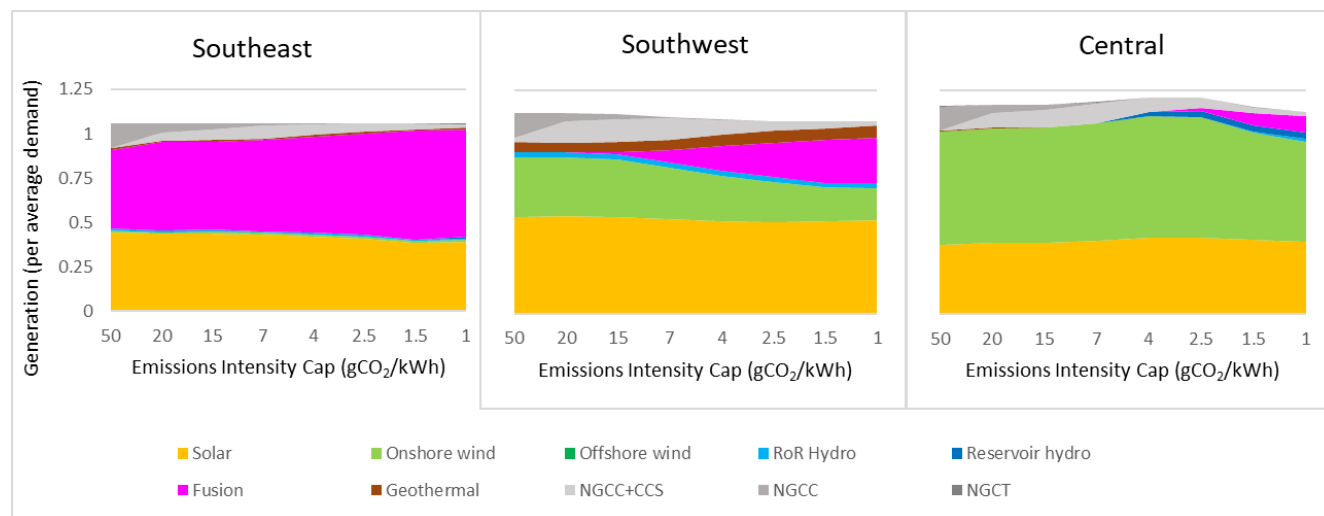
Figure 5.13 Fleet capacity required to achieve a range of emissions caps in the Southeast, Southwest, and Central subregions in 2050



Results are based on assumed U.S. average FPP capital cost of \$6,000/kW. Renewable energy capacity is constrained by the technical maxima in Figure 5.5.

¹⁶ As fusion penetration increases, total generator capacity declines because the fleet’s overall capacity factor increases. Note that in all cases, total generation is greater than 1, which is the value for which generation perfectly matches demand. Values greater than 1 indicate efficiency losses or curtailment. We consider inefficiencies in transmission, as well as in charging and discharging, and parasitic losses from energy storage operations. Fusion’s share of overall generation is larger than its share of capacity because FPPs are able to operate at a high capacity factor (CF) in comparison to most VRE generation.

Figure 5.14 Relative generation contribution from various technologies in the Southeast, Southwest, and Central subregions in 2050 for a range of emission caps



Results are based on an assumed U.S. average FPP capital cost of \$6,000/kW.

When electricity generation is constrained by carbon caps, the fleet composition and generation mix for each subregion is driven primarily by the availability of local renewable resources (solar, onshore wind, offshore wind, geothermal, RoR hydro, and reservoir hydro). Of these, hydrothermal geothermal and reservoir hydro are the only firm renewable generation options. However, these firm renewables face severe capacity limits in most subregions. The contribution from fossil fuel generation is limited by emissions caps. Diversity of renewable resources and their capacity limits, cost, quality, and capacity factors all contribute to the analysis of how much fusion is needed in each subregion. For example, in the Southeast, fusion supplies over 44% of electricity if emissions are capped at or below 50 gCO₂/kWh. This is because the only other major zero-emission generation source for the Southeast subregion is solar, which has a low annual capacity factor of 25%. This contrasts with the situation for the Central subregion, which has abundant high-quality, low-cost onshore wind; capacity factor for wind generators is also higher in the Central subregion than in any of the other eight subregions (Figure 5.1). Of all subregion attributes, renewable capacity limits were identified as the strongest differentiator in determining optimal fusion deployment.

Table 5.15 shows which renewable capacity limits are active when FPPs become a cost-efficient addition to the subregional grid for the \$6,000/kW FPP cost scenario. Note that solar is never constrained when the technical maxima in the multi-subregional analysis are applied, although if land-use maxima are imposed, as discussed in Section 5.4 for the New England subregion, solar is limited. Limits on offshore wind are only relevant in the Southwest, which has no coastline.

Table 5.15 Renewable limits that contribute to fusion deployment for the \$6,000/kW FPP cost scenario

	Atlantic	California	Central	North Central	Northeast	Northwest	Southeast	Southwest	Texas
Onshore wind	✓	✓			✓		✓		
Offshore wind								✓	
Solar									
RoR hydro	✓	✓		✓	✓	✓	✓	✓	
Reservoir hydro	✓		✓	✓	✓				
Geothermal	✓	✓	✓	✓	✓	✓	✓	✓	✓
Pumped hydro				✓					

At a fusion cost point of \$6,000/kW, we find that geothermal power output is always maximized before fusion is deployed. This is because fusion competes directly with geothermal, which is also a firm, low-carbon energy technology, and hydrothermal geothermal is less expensive. Geothermal capacity ranges from 0% to 60% of average demand across subregions, as shown in [Figure 5.5](#). Likewise, RoR hydro is maximized before fusion in all subregions except the Central and Texas subregions. Reservoir hydro also affects fusion deployment, but to a lesser extent because reservoir hydro is more expensive than other renewables and is subject to monthly availability constraints.

The two subregions that deploy the most fusion (Atlantic and Southeast) have the most stringent wind constraints. In these subregions, wind cannot produce enough electricity to satisfy one-sixth of demand, even with maximum onshore wind buildout. Thus, fusion is necessary in these subregions.

We categorize U.S. subregions based on their modeled level of fusion penetration and by how sensitive that penetration is to the stringency of emissions limits. High fusion penetration under a relatively stringent emissions cap indicates that fusion is successfully competing with renewables. High sensitivity to the emissions cap is an indication of how much additional fusion is needed to displace natural gas in providing firm power. This categorization, which also relates to the renewable resource attributes of each subregion, is shown in [Table 5.16](#). Our modeling analysis indicates that, in a decarbonized world, FPPs will have the highest penetration in locations with poor diversity, capacity, and quality of renewable resources. Onshore wind is especially important because it has the potential to provide low-cost electricity with a moderate capacity factor.

Table 5.16 Subregion categories based on renewable resources

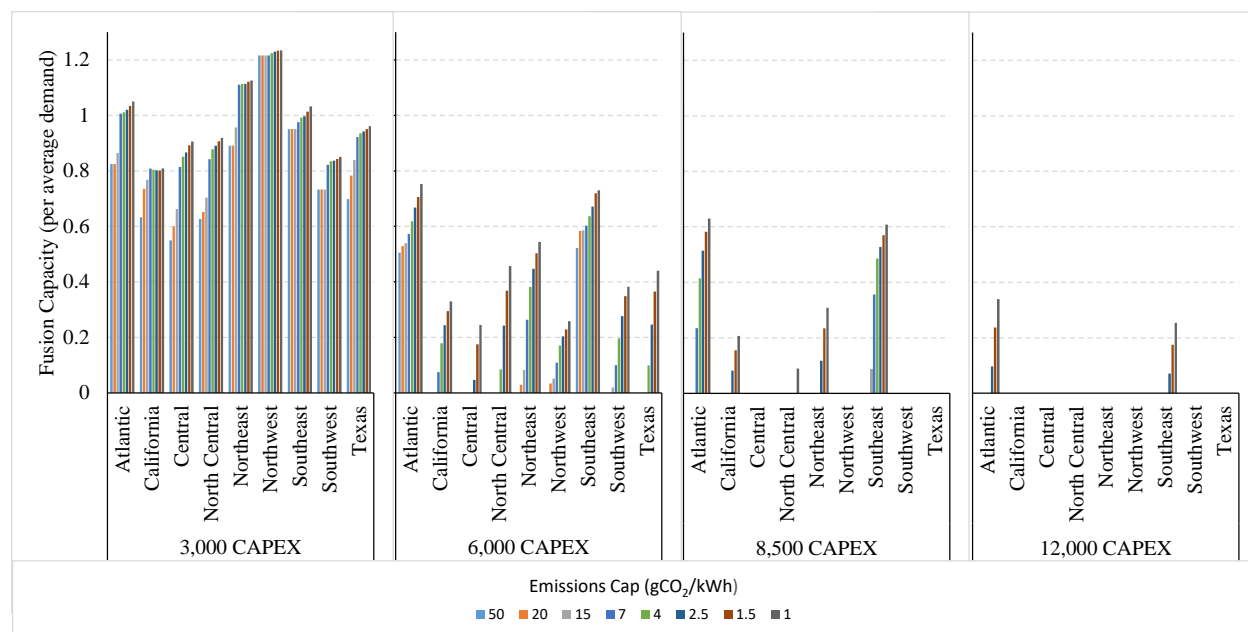
	High penetration, low sensitivity	Medium penetration, medium sensitivity	Low penetration, low sensitivity	Low penetration, high sensitivity
Subregions	Atlantic and Southeast	California, Northeast, Southwest	Northwest	Central, North Central, Texas
Renewable attributes	Poor onshore wind, hydro, and geothermal resources	Northeast has best offshore wind; California has best geothermal; Southwest has best solar; However, all three have modest onshore wind capacity or quality	Below average solar and wind resources, but excellent diversity of renewable resources, including good hydro and moderate geothermal	Abundant, high-quality, and low-cost onshore wind; limited renewables beyond onshore wind and solar
Fusion penetration at \$6,000/kW	Required at all emissions caps from 1 to 50 gCO ₂ /kWh	No penetration at 50 gCO ₂ /kWh, but reaches 33% to 55% penetration at 1 gCO ₂ /kWh	Required at all emissions caps 1 to 20 gCO ₂ /kWh, but never more than 26% penetration	Required only at 4 gCO ₂ /kWh and below, but reaches 25% to 45% penetration at 1 gCO ₂ /kWh

Model results for fusion penetration are based on a FPP cost of \$6,000/kW and assume renewable energy capacity is constrained by the technical maxima in Figure 5.5.

5.4.8. Fusion cost sensitivity analysis across U.S. subregions

Because fusion is a generation technology that is still under development, there is substantial uncertainty regarding the cost of a FPP in 2050. Figure 5.15 shows modeled fusion deployment by subregion for four cost cases, ranging from \$3,000/kW to \$12,000/kW, and nine emissions cases, with caps ranging from 1 to 50 gCO₂/kWh.

Figure 5.15 Modeled fusion buildout by subregion at varying CAPEX values and emissions caps



As detailed in [Section 5.4.7](#), fusion deployment at the \$6,000/kW cost point is largely determined by limits on renewable resource availability at the subregional level, but the competitive position for fusion changes at lower FPP capital costs (CAPEX). At lower cost points, a different subregional dynamic—driven by average solar capacity utilization—takes over. At low solar capacity factors, solar becomes more expensive and fusion becomes more competitive. At a fusion cost point of \$3,000/kW, the Northwest and Northeast see the highest levels of fusion deployment (as a share of average demand), in part due to their poor solar resources. The California and Southwest subregions, by contrast, see the lowest levels of fusion deployment because of their strong solar resources.

For the low-cost scenario where CAPEX for FPPs is \$3,000/kW, fusion deployment is less dependent on the emissions cap. At this cost point, fusion accounts for the largest share of electricity generation in all nine subregions and installed fusion capacity ranges from 55% to 124% of average demand for each subregion. In addition, the energy mix in five subregions—the Atlantic, Northeast, Northwest, Southeast, and Southwest—is independent of the emissions cap (this can be seen in [Figure 5.15](#) where the height of the bars for these subregions at \$3,000/kW fusion CAPEX is the same across different emissions caps). The simple explanation is that fusion is inexpensive enough at this cost point to win market share even absent an emissions cap. In each of these cases, the optimal generation mix has an emissions intensity of less than 50 gCO₂/kWh.

This analysis prompts the question: *At what cost point is fusion economically competitive without a carbon constraint?* The Ideal Grid model was optimized with a variety of input FPP

CAPEX values and no carbon constraint. Fusion must cost less than \$4,000/kW to compete with renewables and fossil fuel generation in all U.S. subregions absent a carbon policy.

5.5. Conclusions

The scale of fusion deployment in the electricity system will be highly dependent on the availability and cost of other low-carbon technologies, and on how tightly carbon emissions are constrained in the future. Our modeling results for nine subregions of the United States show that, in a decarbonized world, FPPs will have the highest penetration in locations with poor diversity, capacity, and quality of renewable resources such as wind, solar, hydro, and geothermal.

Fusion deployment will also be highly dependent on the degree to which social and environmental factors constrain the deployment of renewable generation options. If fusion costs are relatively high, land-use constraints for renewables can make the difference between fusion and no fusion. At medium and low cost points, land-use constraints can drive much higher levels of fusion deployment.

The role of FPPs in the electric power system is highly sensitive to costs. Based on our analysis of the New England subregion, FPPs operate as low-capacity-factor, dispatchable generators when fusion costs are high, but tend to serve mostly as a baseload resource when FPP costs are moderate and as dispatchable generators with a moderate capacity factor when FPP costs are low. These trends are directly related to fusion penetration and the relative mix of FPPs with other non-dispatchable and dispatchable resources, including energy storage.

Fusion deployment is highly sensitive to the cost of VREs and energy storage. Lower costs for VRE and energy storage reduce installed FPP capacity on the New England grid. This is true at all emissions intensity caps, but the effect is strongest for less stringent (higher) caps. While a 25% reduction in VRE and energy storage costs leads to a 50%–100% reduction in FPP installed capacity, a 25% increase in VRE and storage costs increases FPP installed capacity by only 10% in the New England case study.

The availability of firm, low-carbon natural gas power plants can have a large impact on the deployment of FPPs. Based on our analysis of the New England region, fusion deployment is strongly influenced by the availability of NGCC generators with 95% carbon capture and low upstream methane emissions. When NGCC with 95% CCS is available, the threshold cost where fusion becomes competitive is \$4,000/kW lower than in a scenario where NGCC with 95% CCS is not available.

References

- Augustine, Chad, Devon Kesseli, and Craig Turchi. 2020. "Technoeconomic Cost Analysis of NREL Concentrating Solar Power Gen3 Liquid Pathway: Preprint." www.nrel.gov/publications.
- Cole, Wesley, Maxwell Brown, Patrick Brown, Will Frazier, Matt Bower, Brian Sergi, Daniel Greer, et al. n.d. "ReEDS-2.0." [Github.Com/NREL/ReEDS-2.0](https://github.com/NREL/ReEDS-2.0).
- Forsberg, Charles. 2023. "Low-Cost Crushed-Rock Heat Storage with Oil or Salt Heat Transfer." *Applied Energy* 335 (April):120753. <https://doi.org/10.1016/j.apenergy.2023.120753>.
- Johnson, Eric. n.d. "New England Power System Outlook."
- Knight, Pat, Olivia Griot, Ellen Carlson, Jackie Litynski, Angela Zeng, Jack Smith, Shelley Kwok, Jen Stevenson Zepeda, and Sophie Kelly. 2023. "Massachusetts Technical Potential of Solar: An Analysis of Solar Potential and Siting Suitability in the Commonwealth."
- Kolbasov, B. N., V. I. Khripunov, and A. Yu Biryukov. 2016. "On Use of Beryllium in Fusion Reactors: Resources, Impurities and Necessity of Detritiation after Irradiation." *Fusion Engineering and Design* 109–111 (November):480–84. <https://doi.org/10.1016/J.FUSENGDES.2016.02.073>.
- Lopez, Anthony, Rebecca Green, Travis Williams, Eric Lantz, Grant Buster, and Billy Roberts. 2022. "Offshore Wind Energy Technical Potential for the Contiguous United States [Slides]." Golden, CO (United States). <https://doi.org/10.2172/1882929>.
- Mettetal, Elizabeth, Sharad Bharadwaj, Manohar Mogadali, Saamrat Kasina, Clea Kolster, Vignesh Venugopal, Ben Carron, Ari Gold-Parker, Robbie Shaw, Zach Ming, Amber Mahone, Arne Olson, Alex Breckel, Alex Kizer, Sam Savitz, Anne Canavati, Richard Randall, and Tomas Green. 2020. "Net-Zero New England: Ensuring Electric Reliability in a Low-Carbon Future." www.energyfuturesinitiative.org.
- "New England Wind Offshore Overview." 2024. www.newenglandforoffshorewind.org/states/overview/. 2024.
- Parzen, Maximilian, Davide Fioriti, and Aristides Kiprakis. 2023. "The Value of Competing Energy Storage in Decarbonized Power Systems," May.
- Schmitt, Tommy, Sarah Leptinsky, Marc Turner, Alexander Zoelle, Charles White, Sydney Hughes, Sally Homsy, et al. 2022. "Cost and Performance Baseline for Fossil Energy Plants Volume 1: Bituminous Coal and Natural Gas to Electricity." <https://doi.org/10.2172/1893822>.
- Schwartz, J. A., W. Ricks, E. Kolemen, and J. D. Jenkins. 2022. "The Value of Fusion Energy to a Decarbonized United States Electric Grid," September. <http://arxiv.org/abs/2209.09373>.
- Sheha, Moataz, Edward J. Graham, Emre Gençer, Dharik Mallapragada, Howard Herzog, Phillip Cross, James Custer, Adam Goff, and Ian Cormier. 2024. "Techno-Economic Analysis of a Combined Power Plant CO₂ Capture and Direct Air Capture Concept for Flexible Power Plant Operation." *Computers and Chemical Engineering* 180 (January). <https://doi.org/10.1016/j.compchemeng.2023.108472>.
- Turchi, Craig, Samuel Gage, Janna Martinek, Sameer Jape, Ken Armijo, Joe Coventry, John Pye, et al. 2021. "CSP Gen3: Liquid-Phase Pathway to SunShot." www.nrel.gov/publications.
- Viswanathan, Vilayanur, Kendall Mongird, Ryan Franks, Xiaolin Li, Vincent Sprenkle, and Richard Baxter. 2022. "2022 Grid Energy Storage Technology Cost and Performance Assessment."

6. Critical materials and supply chains for fusion power plants

6.1. Introduction

Building zero-carbon electricity generation assets, such as fusion power plants (FPPs), requires raw materials, processing capacity to refine these materials, and manufacturing capacity to produce power plant components. Supply chain considerations for raw materials include the scarcity of certain critical materials, the potential for uneven geographic distribution of resources, environmentally intensive mining processes, high rates of demand growth, and a high concentration of processing capacity for some of these materials in a few countries.

Beyond the availability of materials, development of the supply chains needed to support fusion power generation is critical to building and sustaining a large-scale fusion industry. Given the volume and number of potential future fusion power plants, it is necessary to begin scale-up activities in the various fusion subsystems, particularly where there may be bottlenecks. Understanding the dynamics of the supply chains needed to deliver components for Nth-of-a-kind fusion power plants is critical to quantifying the future role of fusion energy in the power grid. This chapter focuses on deuterium-tritium (DT) magnetic confinement devices, which are a relatively mature FPP concept. These devices, which include tokamaks, stellarators, and non-torus-based concepts, have many overlapping materials requirements.

Our review considers supply chains for four major FPP components or subsystems: high-temperature superconductors (HTS) and magnets, plasma heating, blanket materials, and alloys and composites. These four subsystems are expected to be the largest contributors to DT magnetic confinement FPP cost, other than mature technologies such as the power-generation subsystem. It is well known that most of these supply chains are not ready to support pilot-scale fusion plants, let alone widespread deployment of commercial-scale FPPs (Surrey 2019). As such, rapid scale-up of production capacity for key components is critical to the success of the fusion endeavor. A recent report from the Fusion Industry Association (Fusion Industry Association 2023) notes that there are many fusion reactor companies, but only one company, Kyoto Fusioneering, is focusing on fusion components/supply chains. Many non-fusion companies (mentioned in the same Fusion Industry Association report) have the capability to make materials and components for fusion devices, but their broad business interests may make them less responsive to fusion business opportunities and less likely to make the early investments in production capabilities needed to provide hardware for early-stage experimental systems and for supply chain scale-up. This chapter assesses each supply chain for a given DT magnetic confinement FPP subsystem component according to several criteria: whether the component is in the fundamental research phase, is manufactured on a small industrial scale, presents potential bottlenecks to large-scale fusion deployment, or is a relatively mature, stable technology ready for widespread use in fusion power plants.

HTS and plasma heating, for example, are considered to have relatively mature supply chains to support fusion applications. By contrast, the supply chain for blanket material is nascent. Supply chains for alloys and composites used in fusion reactors, particularly for first-wall materials and structural materials, require significant development before scale-up.

It is important to acknowledge, at the outset of this analysis, that multiple solutions exist for many fusion components, each presenting different trade-offs with respect to power density, regulatory burden, and reliability. While it is widely accepted that HTS will be the fundamental building block of high-field superconducting magnets, there are different options for plasma heating sources or first-wall alloy and structural materials. This chapter considers the candidate materials that are most promising based on their current state of development and potential. We begin by summarizing the state of each subsystem and describing the most promising solutions for that subsystem. We then assess the readiness of component technologies, identify associated obstacles and bottlenecks, and discuss ongoing improvements in production and performance. Finally, we identify potential pathways to scale-up for the mature industries and weaknesses that could impede scale-up in the less mature industries.

6.2. HTS and magnet assembly

Most magnetic confinement and magneto-inertial confinement FPP designs require superconducting magnets to achieve the plasma pressures required for fusion reactions. The magnets must be capable of delivering very high magnetic field strengths while minimizing associated energy requirements. The magnet system for a fusion power plant involves three primary subsystems. These integrated subsystems include the superconducting tapes that carry current with zero resistance; the structural materials that support the magnet, which must withstand the Lorentz forces that would otherwise alter the magnet's shape and integrity; and a cryostat system for cooling the magnets to the cryogenic temperatures required for superconductivity.

Two types of superconducting materials are being pursued for magnetic fusion. Fusion companies are mostly pursuing HTS magnets, whereas the ITER magnets are being built with low-temperature superconductors (LTS). Niobium-tin-based LTS have more mature supply chains, but HTS made of rare-earth barium copper oxide (REBCO) are able to carry one or two orders of magnitude more current than LTS, which is vital for achieving higher magnetic field strengths using smaller magnets. HTS magnets enable compact FPPs, with higher power density, and are expected to be less costly to build and operate (Sorbom et al. 2015).

Thus, HTS are the key enabling technology in the high-field path to a commercial fusion power plant. Since their discovery in 1986 (Bednorz and Muller 1986), these materials have progressed from individual lab-grown crystals to multi-kilometer-long, commercial high-performance tapes produced by a variety of reel-to-reel deposition methods. The fusion power generated per unit

volume in a magnetically confined plasma is proportional to the magnetic field to the fourth power, exemplifying the importance of high magnetic field and the extent to which the economics of fusion power are likely to be sensitive to superconductor performance.

Within the family of REBCO HTS tapes, performance has increased dramatically from the first-generation bismuth-strontium-calcium-copper-oxide tapes to the second-generation yttrium-barium-copper-oxide-based tapes. In particular, the yttrium-based tapes, with critical temperature¹⁷ of 93 K, are capable of carrying the high current densities appropriate for fusion magnets. Compared to LTS, which need to be operated with liquid helium at about 4 K and have low critical fields,¹⁸ yttrium-based REBCO has an extrapolated critical field of more than 100 tesla, can be operated over a wider temperature range, and can be cooled by a variety of other cryogenics in addition to helium. The target operating temperature is close to 20 K to ensure superconductivity at the required field strength and current. In addition, the specific heat capacity of the surrounding materials is proportional to temperature to the third power in this temperature range, which enables greater operational stability of the HTS magnets when at higher temperatures than LTS magnets.

Conceptual design studies of high-field devices (Sorbom et al. 2015) show that while HTS do not account for a significant fraction of total tokamak cost, the ability of superconductor manufacturers to produce and deliver the necessary amounts of high-quality HTS tape is one of the major limiting factors in the supply chain. For the HTS industry to produce enough tape to supply the large requirements of commercial magnetic confinement FPPs, one could consider the role of non-fusion applications in scale-up efforts. It is generally agreed in the industry that the cost of HTS must be less than \$50 per 1,000 amperes (kA) of current capacity per meter (m) of length (\$50/kAm) for HTS to be economically viable in other applications. The \$/kAm unit takes into account the quality of the tape per unit length. At present, HTS costs generally fall between \$100 and \$200/kAm depending on the manufacturer, making HTS cost-prohibitive for many applications. Raw materials cost for HTS is between \$2 and \$5/kAm, indicating that most of the cost of the tape is from the manufacturing process. The raw materials value also indicates that the cost of rare-earth-type HTS tape will not fall below the cost of LTS (niobium-titanium and niobium-tin LTS cost \$1–\$5/kAm). Therefore, the use of HTS instead of LTS in non-fusion applications depends on whether the additional capital cost of HTS can be justified by its benefits in terms of functionality or transformative potential, or by reduced operation costs. The operating cost justification requires calculating the difference in cooling cost for HTS

¹⁷ Critical temperature is the temperature below which superconducting materials have zero resistance to electrical current.

¹⁸ Critical field is the magnetic field strength below which superconducting materials have zero resistance to electrical current.

compared to LTS and seeing whether this reduction is enough to offset the higher capital cost of an HTS device; this is particularly important in non-fusion applications (Hartwig et al. 2012).

With increased HTS use by fusion companies, expected reductions in cost with greater cumulative production volume can be used to make projections of future HTS cost. Because HTS manufacture involves deposition processes, cost reductions for this technology may be expected to follow trends experienced with other vapor deposition processes such as those used in the manufacture of semiconductors or solar panels. The thin film solar industry, for example, experienced a learning rate of between 15% and 25%, where the learning rate is the reduction in cost with every doubling of manufactured volume of the product in question. Some potential applications that could benefit from HTS technology include transmission lines, nuclear magnetic resonance (NMR) magnets, electric motors, magnetic resonance imaging (MRI), superconducting magnetic energy storage, gyrotrons, and many more. To provide perspective on the role that fusion could play in driving HTS demand, it is worth noting that Commonwealth Fusion Systems (CFS) alone has procured a significant fraction of all HTS ever made to build SPARC.¹⁹ This suggests that while non-fusion HTS applications may be helpful in bringing down the cost of HTS tapes, fusion demand will remain the primary driver for cost reduction in the near term.

It might be reasonable to expect that a few fusion startups with traction, such as CFS, Tokamak Energy, and Type One Energy, will drive the HTS industry and that if and when other HTS suppliers emerge, they will follow the pull of these startups. Another factor that should be considered is the role of LTS in future applications. Even though the cost of niobium-titanium and niobium-tin LTS is \$1–\$5/kAm, the lower performance and stringent cryogenic requirements of LTS mean that fusion developers' preference will inevitably shift to HTS. In addition, while research devices like ITER and the Large Hadron Collider (LHC) were drivers of cost reductions for LTS, lower future demand for this technology means prices could rise as manufacturing and resources are diverted elsewhere. As discussed previously, a related factor here is the scarcity of helium, which has in fact caused a European muon collider to be built with HTS. This example also highlights the critical role of helium in providing cryogenic cooling for fusion and the advantages of using HTS, which allow for the possibility of moving to other cryogenic fluids in the future. Ultimately, we expect that demand from fusion companies will drive up production and reduce the cost of HTS. Over time, these cost reductions will increase demand for HTS in non-fusion applications, driving significant growth in HTS manufacturing.

¹⁹ SPARC is a high-field tokamak that is currently under construction. It is designed to demonstrate scientific breakeven energy (Creely et al. 2023).

While an MRI requires significantly less HTS than a tokamak, the much greater number of MRI machines in operation may mean that total HTS demand for both applications is similar.

6.2.1. Critical materials for HTS

REBCO superconducting tapes consist of multiple layers. Most of the tape is substrate metal and copper for stabilization. The REBCO layer in the superconducting tape is only 1.5–3.5 micrometers (μm) thick, which is only a few percent of the total thickness of the tape (Molodyk et al. 2021). For yttrium-based REBCO, the superconducting layer consists of about 13.3% yttrium by weight (wt%), 41.2 wt% barium, 28.6 wt% copper, and 16.8 wt% oxygen. Therefore, one tonne of REBCO tape contains only a few kilograms of yttrium. The length of REBCO tape required for a magnetic confinement fusion power plant (MC-FPP) depends on the design of the plant, but an average estimate is that 0.5 kg of yttrium is required per MW_e of generating capacity.

To put these numbers into perspective, current global annual production of yttrium oxide (Y_2O_3) is 10,000–15,000 tonnes, corresponding to 8,000–12,000 tonnes of yttrium. This is roughly 60,000 times the amount of yttrium required for the magnets of a single MC-FPP. Global reserves are estimated at over 500,000 tonnes of Y_2O_3 (enough for about 3 million MC-FPPs). Yttrium is required for various other high-value applications such as lasers, electronics, and phosphors where there are no direct substitutes for yttrium. Global markets for yttrium rely on exports from China, where most yttrium production is located. Global reserves of yttrium, by contrast, are more widely distributed. Countries with the largest yttrium reserves outside of China include Australia, Brazil, Russia, and Vietnam (U.S. Geological Survey 2024). Therefore, yttrium supply is not considered a potential materials bottleneck. Although there are multiple options for producing REBCO with other rare-earth elements, yttrium has an advantage due to its much lower probability of interaction with neutrons (Molodyk et al. 2021).

An interesting observation is that the silver layers in REBCO tape currently cost about 400 times the cost of the yttrium content in the tape. The roughly 2.5 tonnes of silver required per MC-FPP is still small relative to annual global production of silver: Specifically, each MC-FPP would use about 0.01% of global annual silver production. Other materials used to make REBCO tape, such as barium and copper, are required in quantities that are very small relative to current global production.

Demand for niobium-based superconductors could impact niobium supplies if this low-temperature superconductor were deployed at scale for FPPs, since the critical current

density²⁰ for niobium-tin is much less than for REBCO and would require more material. However, the strong advantages of REBCO (high critical temperature and high critical current density) are expected to ensure its dominance over niobium-tin as the superconducting material for commercial magnetic confinement fusion.

6.2.2. HTS manufacturer strategies

Many HTS tape manufacturers have emerged over the course of the last 20 years, each hoping to break into the array of future potential market applications for this technology. They include Faraday,²¹ SuperPower, MetOx, Theva, Fujikara, STI, and SuNam. We spoke directly with Faraday, SuperPower, and MetOx. What we learned from these conversations can be used to infer likely characteristics of the future HTS supply chain. Some of these details are summarized in Table 6.1.

Table 6.1 Key features of different HTS tape manufacturers

Company	Production capacity	Self-field critical current (at 77 K for 4 mm width)	Process	Key partnerships	Scale-up priority	Tape cost
Faraday	2,000 km annual (12 mm width)	175–200 Amp	pulsed laser deposition	CFS	power per ion beam-assisted deposition & pulsed laser deposition unit	\$100–\$150 per kAm
SuperPower	~ 100 km (12 mm width)	175–200 Amp	metal organic chemical vapor deposition (MOCVD)	Tokamak Energy	MOCVD unit improvements	N/A
MetOx	N/A	N/A	proprietary	non-fusion	N/A	N/A

The industry as a whole maintains significant restrictions on the information it shares publicly. Faraday is presently an HTS industry leader by volume—in fact, it should be noted that the partnership between CFS and Faraday was intrinsically crucial to the scale-up and growth of both companies, as demand from CFS drove Faraday’s scale-up of production capacity. The evidence that this type of partnership can drive growth gives confidence to other HTS

²⁰ Critical current is the maximum current density that can be carried by a superconductor while maintaining its superconducting performance. Self-field critical current is the critical current in the presence of the superconducting tape’s own magnetic field without any externally applied field. The self-field critical current is specific to the dimensions of the superconducting materials to account for the strength of the magnetic self-field.

²¹ Prior to 2022, Faraday Factory Japan was known as SuperOx.

manufacturers and fusion/superconductor companies that are looking to follow the same model.

Table 6.1 shows that different companies are focusing on different deposition techniques. This diversity of approaches reflects each company's history and prior experience in developing certain techniques, but it also provides an opportunity to increase throughput and drive down costs. While the two more established companies, Faraday and SuperPower, are relying on improvements to proven pulsed laser deposition and metal-organic chemical vapor deposition techniques, MetOx is looking to exploit proprietary deposition techniques that could drastically increase throughput per production line.

Following its partnership with CFS, Faraday's scale-up plans focused on increasing throughput per deposition machine, including by increasing ion-beam-assisted deposition of the buffer layer and laser power for the deposition of the superconducting layer. Faraday plans to continue increasing capacity per deposition unit, before parallelizing manufacturing lines. Improving the performance of the HTS tapes is a constant, though secondary, endeavor as Faraday tries to meet demand from CFS orders. A strong focus within Faraday is narrowing the statistical scatter of the average tape self-field critical current performance, which has a 15%–20% standard deviation at 77 K. Increasing REBCO deposition thickness is another experimental possibility, albeit one that requires careful optimization since deposition is the most expensive operation.

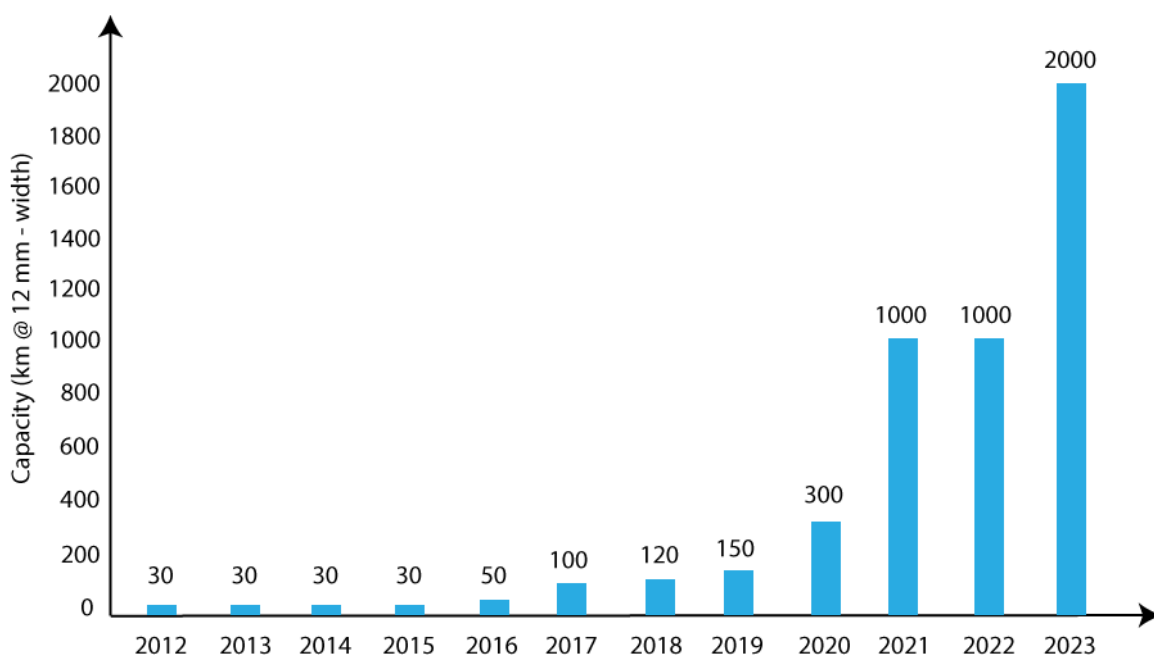
Thus far, SuperPower has not had the funding or partnerships to scale up in the same manner as Faraday. However, the company has recently taken large steps toward significantly improving its older units. The original set of pilot deposition machines at SuperPower are nearly two decades old and are not optimized for large-scale production.

SuperPower has now ordered a newly designed set of ion-beam-assisted deposition and metal organic chemical vapor deposition units, which are part of a Phase I plan to grow to large-scale commercial tape production. If the throughput of the new units is as planned, a Phase II scale-up will likely ensue. SuperPower believes its long-term advantage is in the flexibility and low cost of metal organic chemical vapor deposition as opposed to pulsed laser deposition. As described by Pinto et al. (2023), "Two main routes are used for film deposition, namely, pulsed laser deposition and metal-organic deposition. While the former technique is well established and widely used for industrial production of REBCO tapes, the latter is considered very appealing due to the inexpensive setup, basically consisting of the deposition of the precursor solution and a conversion heat treatment." An additional focus is to reduce the inefficiency of the metal-organic deposition system, which contributes significantly to the high cost of manufacturing REBCO tape.

MetOx is taking a proprietary approach to develop a high-throughput deposition technique that it believes will be superior and deliver a lower-cost HTS material than its competitors. It is difficult to speculate about the company's place in the market without further information. However, MetOx's focus seems to be on academic and industry applications of superconductors initially. The company plans to open a new production facility in 2024.

Currently, Faraday remains the industry leader by production capacity. [Figure 6.1](#) shows the exponential increase in Faraday's output since its partnership with CFS and entry into the fusion industry (Molodyk 2023). We also extrapolate from Faraday data (Molodyk 2023) to estimate that HTS cost halves for every tenfold increase in production volume.

Figure 6.1. Faraday HTS tape production



The fusion startup industry has driven exponential growth in production by Faraday, a leading HTS manufacturer (Molodyk 2023). CFS has been primarily responsible for the partnership that helped foster this growth. Most of Faraday's current production is located in Japan.

As HTS tape is produced in larger volumes, its cost should decline—and as the cost of HTS declines, demand for HTS for use in other applications will likely increase. Although fusion companies will be the initial drivers of HTS production, other industries and applications might contribute a significant portion of eventual HTS demand (Molodyk 2023); potential sources of new demand include applications in motors, energy storage devices, transmission lines, and MRI machines. When the technology is mature enough to be widely used, demand from other industries may help to drive down production costs. For example, while a motor requires significantly less HTS than a MC-FPP, motors will be produced in far larger numbers than MC-FPPs. While reducing HTS cost is important to expand markets for HTS in other applications,

HTS cost is a lesser concern for fusion deployment given the much larger costs to fabricate magnets and build a complete MC-FPP facility. Thus, ensuring sufficient HTS production capacity to supply the construction of commercial fusion power plants is key to developing a large-scale fusion industry, even as demand from both fusion and non-fusion applications drives the evolution of the HTS supply chain and reduces HTS cost.

In conclusion, recent changes in cost, performance, and production capability suggest that the competitive landscape for HTS tape manufacturing will continue to evolve rapidly over the next 5–10 years as fusion companies expand efforts to develop HTS magnets.

6.2.3. Magnet fabrication

Magnets are the most expensive part of a tokamak to fabricate—specifically, the toroidal field coils, which require the largest quantity of HTS tape by far, in addition to the poloidal field coils and the central solenoid. In stellarators, the equivalent magnet requirements are for the large, twisted superconductor coils that produce static toroidal and poloidal fields for confinement.

In tokamaks, the poloidal field and central solenoid coils require variable fields, and thus have insulated cable designs, whereas the toroidal field coils can be made using either insulated or non-insulated designs. Insulated cables require the fabrication of a twisted extruded copper matrix into which HTS tape stacks are soldered using vacuum pressure impregnation (VPI) (Hartwig et al. 2020). For non-insulated coils of this scale, HTS tape stacks must be VPI soldered into metal radial baseplates (Hartwig et al. 2024). Because SPARC is the most imminent REBCO-based magnetic confinement device, and because the SPARC toroidal field coils are to be made using a non-insulated design, we identify supply chain steps based on SPARC’s requirements. However, these supply chain steps can be expected to apply more generally to magnetic confinement fusion. Non-insulated coils have various advantages over insulated coils, including lower operating voltages and greater ability to safely survive quench. Although non-insulated designs may seem simpler than the insulated alternatives, they present various supply chain challenges. These include:

- Sourcing the baseplate metal (Nitronic®/Inconel®),
- Purifying baseplate material to remove trace high-activation metals,
- Casting or forging baseplates,
- Applying high-precision machining to cut grooves and meet tolerances, and
- Soldering the HTS tape stacks using VPI.

CFS is currently the only company that is attempting to scale magnet production to commercial levels. Some of the immediately identifiable supply chain issues CFS is encountering include the amount of metal required, costs for purification to remove impurities, managing trade-offs between cost and structural strength in forging and casting operations, and sourcing machines that can handle the tolerances required on this physical scale. Over the coming months and

years, the industry's ability to learn, project, and quantify opportunities to optimize magnet production for performance and cost may aid in reducing overall device cost.

6.3. Cryogenics

A vital subsystem in a fusion power plant is the cryostat that cools the superconducting magnets. For LTS such as niobium alloys, the only viable cryogen is liquid helium. For HTS, the candidate cryogenics are helium, hydrogen, and neon. Helium is the preferred cryogen because it provides the lowest temperature, is inert, and has excellent heat transfer properties at ultra-low temperatures, but there are questions about its availability. Overall supply *adequacy* per se is not the issue: Global reserves of helium are estimated at 48 billion cubic meters and global consumption is roughly 160 million cubic meters per year (U.S. Geological Survey 2022a; Grynia and Griffin 2017, which means that known reserves would suffice for roughly 300 years at current rates of consumption. Reserves could also expand.

However, helium has a history of heavy government involvement, price volatility, shortages, disruptions, and market failures—all of which create uncertainty about the reliability of helium supply chains. The U.S. government recently exited the helium business and prior to that had worked toward depleting its helium stockpile. Helium is produced as a byproduct of natural gas processing and natural gas liquefaction. The economic viability of producing helium depends on its concentration in natural gas, the scale of the facility, and the market price of helium. Helium recovery from natural gas processing can be economical for helium volume percentages as low as 0.3% to 0.5% (Brennan et al. 2021; Grynia and Griffin 2017). Helium recovery plants have been built at large liquefied natural gas (LNG) facilities with helium concentrations as low as 0.04% by volume (%v/v) (Rufford et al. 2014).

In response to past helium shortages, higher helium prices, and U.S. government plans to deplete its stockpile, various helium production units have been built and are coming on line. Due to the Ukraine war and other issues, the completion and commissioning of a 60-million-cubic-meter helium plant in Russia has been delayed, although the first of three trains for helium recovery at this facility is operational. As long as natural gas continues to be produced at current levels and the market price for helium is adequate to incentivize investments, the market is expected to meet medium-term helium demand, although the price of helium is expected to be higher than during periods when the U.S. government was selling off its stockpile. There are also companies, such as Helium One Global and Four Corner Helium, that are focused on finding and producing helium from helium-rich reservoirs.

Two concerns have emerged about the long-term outlook for helium:

1. **The potential for a supply decline** as the world moves toward deep decarbonization and natural gas production and consumption decline. Reduced natural gas production will reduce the potential supply of helium as a byproduct.

2. **The impact of new demand** as a result of fusion energy deployment. Each MC-FPP with helium cooling will require about 10 tonnes of helium, depending on the design, and is anticipated to have annual losses of 5% (extrapolated from Bradshaw & Hamacher, 2013). Ten thousand such FPPs could require more than 1 billion cubic meters of helium cumulatively over a period of 30 years, which would represent a 22% increase over existing helium demand. In addition, demand for helium for medical and industrial uses is also expected to rise in the decades ahead. Thus, a concern is not just access to helium supplies, but relative demands from other uses.

Our current assessment is that the long-term cost of helium can be expected to increase as demand increases and natural gas byproduct production declines. Dedicated helium reservoirs will likely be tapped to meet market demand. Companies such as Helium One Global have already had success developing methods to locate helium-rich deposits (Grynia and Griffin 2017). As a last-resort, helium could be recovered from the atmosphere (the atmospheric concentration of helium is 5.2 ppm). There is enough helium in the atmosphere to meet all projected demand, but it would be expensive to extract.

Alternatively, the cryostats for magnetic confinement FPPs could use hydrogen or neon as the cryogen. Hydrogen has no availability constraints, but it presents significant engineering challenges with respect to issues such as flammability, permeability, and metal embrittlement. Neon is an unlikely alternative, since it is scarcer and more expensive than helium. The least-expensive source for neon is as a byproduct from obsolete steelmaking plants in Russia and Ukraine.

In summary, the cryogens needed for magnetic confinement fusion will be subject to some price volatility, but there is no apparent near-term supply bottleneck. Supplies of the preferred cryogen, helium, are sufficient to meet near-term demand and additional supplies could be obtained from natural gas processing and geologic reservoirs at higher price points. Furthermore, alternative cryogens (hydrogen and neon) can be used for HTS-based magnetic confinement fusion power plants.

6.4. Plasma heating

Heating plasmas to temperatures in excess of 100 million degrees K requires high-efficiency heating technologies. Heating options include high-frequency electromagnetic waves and neutral beam injection. Many magnetic confinement experimental devices use both of these techniques. High-frequency waves in the ion cyclotron range of frequency (ICRF) are a proven technology for plasma heating and have been used in the divertor tokamaks at the Max Planck Institute, Massachusetts Institute of Technology, DIII-D National Fusion Facility, and Joint European Torus, as well as the Tore Supra tokamak (Wukitch 2019).

The components for plasma heating are relatively mature, but the needs for a commercial magnetic confinement fusion power plant are unique; the supply chain for these components needs to develop to meet requirements for voltage, frequency, and scale. In general, options for plasma heating can be divided into the older vacuum tube technology and the newer solid-state-based technology. For vacuum-tube-based technologies, tetrodes can provide ion cyclotron resonance heating, klystrons can provide lower hybrid current drive, and gyrotrons can provide electron cyclotron resonance heating.

In terms of supply chain, demand from non-fusion industries will support production of both vacuum tubes and solid-state heating technologies for the foreseeable future. For example, the U.S. military plans to invest in the continued development of tube technologies for at least the next two decades for communications and radar applications. Low-power-density applications such as ovens and microwaves have become major targets for the development of solid-state chip technology; the company Miele has already built such solid-state devices, which allow for tunable, spatially directed energy control as opposed to the old, single-frequency magnetron devices, which lead to unavoidable hot spots. However, the technical requirements for these non-fusion applications differ from the specific needs for plasma heating for fusion devices.

6.4.1. Solid-state technology

Based on advances in chip technology, solid-state heating may be able to compete with tetrodes on the lower end of the frequency spectrum. Whereas vacuum tubes operate at high voltages, chips operate at significantly lower voltages and can be utilized in parallel to deliver the same total power. An advantage of configurations that use many parallel chips to provide heating is that the system is still able to function if a few chips fail. In addition to having lower operating voltages than tubes, chips have the advantages of improved reliability and stability. It should be noted that optimizing operating chip voltage involves trade-offs between higher voltage for power capability and efficiency versus lower voltage to reduce complex electrical insulation requirements.

A downside of chip technology is that a manufacturer may no longer produce a particular component five to six years after initial production due to the generally rapid rate of technological improvement in this industry. This means that if chips need to be replaced, identical models may be difficult or impossible to source; a possible additive manufacturing solution to chip development may help alleviate this issue.

For solid-state radio-frequency devices, the key roadblock is the development of specialized chip technology. Specifically, the power capability of each chip must be increased by raising the breakdown voltage. For a given chip power level, an increase in the possible operating voltage, as dictated by the breakdown voltage, reduces the current required, ultimately reducing resistive losses. Increasing the breakdown voltage requires consideration of substrate

materials; moving from a silicon carbide (SiC) substrate to a diamond substrate may allow for this improvement by enabling a three-fold improvement in dielectric breakdown. One of the primary challenges with diamond substrates is growing industrial-sized wafers; a recent Defense Advanced Research Projects Agency (DARPA) grant has been awarded to support work in this area (Keller 2023). While it is difficult to project the pace of progress in fundamental materials research that would enable breakthroughs in diamond wafer production, development speeds for other technologies may be instructive. For example, the progression from 28-V chips to 60-V chips took about 15 years; getting to a 300-V chip might take only 10 years. A 600-V chip would allow operation of a more efficient solid-state radio-frequency heating device for fusion plasma (Wukitch 2023); this factor-of-10 increase in voltage decreases the required current and losses for a 1-MW transmitter by 90%. It is possible to build 1-MW devices for a fusion system now. However, the number of chips and associated power electronic components required imply significantly greater system complexity, and the efficiency would be low. Another consideration for solid-state chips is that reflected power levels of about 5% can cause voltage spikes that cause chip failure.

6.4.2. Vacuum tube technology

While vacuum tube technology does not offer as much flexibility as solid-state chip technology, vacuum tubes have many attractive features. For one, they can last up to tens of thousands of thermal cycles, albeit with slight performance degradation over time. The risk of significant plasma heating loss from tube failure is low, as these devices are quite robust. Screen grids are the main risk in vacuum tube devices, as excessive heating can cause failure. In addition, screen grid manufacturing is a supply chain bottleneck.

Older screen grids were made from tungsten. While the manufacturing process for these grids was simpler, this also meant there were limitations on the geometric configurations it could produce; thus, screen grid geometry could not be optimized. Current screen grids are made from pyrolytic graphite, which offers improved properties and the ability to optimize grid geometries. These grids are made via vapor deposition in a hot vacuum oven and then carefully laser cut into the desired pattern. This is a complex and difficult process that requires high levels of expertise and quality control. Additive manufacturing could be a solution for making screen grids faster and in a single process. An initial test before pursuing this approach would be to check whether the electrical and mechanical properties of printed pyrolytic graphite are comparable to those achieved from the current process. Phostec in Slovakia and MINTEQ in the United States are two companies that currently make pyrolytic graphite grids.

Overall, vacuum tube technology is mature despite the bottleneck of grid production. However, a non-military market for radio-frequency vacuum tubes has not materialized over the last few years and some fusion companies are looking more toward solid-state solutions instead. To create a supply chain to provide vacuum tubes that meet the technical and scale requirements

for fusion power plants would require funding and a compelling indication of future demand. As a part of this program, enhancement to current screen grid production techniques as well as novel methods for grid production should be pursued.

While these examples do not cover the entirety of heating technology requirements, it is apparent that improved efficiency and high production of MW-level heating sources will be an essential requirement for the deployment of magnetic fusion.

6.5. Blanket materials

In DT-fueled fusion power plants, the blanket serves three vital functions: breeding tritium, shielding neutrons, and capturing heat. Technology for blanket materials is considered more nascent than the technology for other fusion subsystems.

The fission industry offers some limited insights on potential blanket materials. Traditional fission reactors use light or heavy water as the primary coolant. Whereas molten salts were once explored as potential coolants, they were abandoned due to their corrosivity and high operating temperatures. More recently, the benefits of molten salts have prompted a reconsideration of their potential as reactor coolants, led by companies such as TerraPower and Kairos. Materion is currently the only commercial supplier of the beryllium-fluoride component in the molten salts under consideration.

A fusion blanket can be either solid or liquid. The most studied breeder choices are lithium-based ceramics, followed by liquid metals (lead-lithium or lithium), and molten fluoride salts (e.g., $2\text{LiF}-\text{BeF}_2$, known as “FLiBe”; $\text{LiF}-\text{NaF}-\text{KF}$, known as “FLiNaK”; and $\text{LiF}-\text{NaF}-\text{BeF}_2$, known as “FLiNaBe”). Relative to solid blanket systems, liquid blankets are significantly less complex, particularly for maintenance and servicing. This section discusses the main liquid blanket solutions being considered; we reference associated supply issues as an example analysis. A supply chain assessment of all blanket designs is beyond the scope of this study.

Among the three molten salts, each has distinct advantages. FLiBe in general has the most promise due to its low atomic number, which makes it a better neutron moderator. FLiNaK’s advantages lie in its slightly larger temperature operating range ($454^\circ\text{C}-1570^\circ\text{C}$) compared to FLiBe ($459^\circ\text{C}-1430^\circ\text{C}$) and the absence of toxic beryllium; however, FLiNaK has lower heat capacity than FLiBe ($c_p(\text{FLiNaK})/c_p(\text{FLiBe}) = \sim 0.75$) (Rudenko et al. 2022) (Lichtenstein et al. 2022). FLiNaBe is preferred by Japanese fusion developers due to its lower melting point of

305°C. Because of their lower lithium content compared to FLiBe, however, both FLiNaBe and FLiNaK must be enriched²² to increase their tritium breeding ratio (TBR).

Lithium, fluorine, and beryllium are all designated as critical materials by the U.S. Geological Survey (USGS). It is expected that lithium demand will increase in coming years, as it is also an important material for renewable electricity generation and storage, as well as for electric vehicle batteries (MIT Energy Initiative 2022). Therefore, we expect increased lithium demand will contribute to supply chain risk that could affect the FPP industry. However, FPP deployment will not be the primary driver of future lithium demand in comparison to other industries. A single FPP requires roughly 1% of the lithium produced globally in 2022; meanwhile, overall lithium demand is expected grow tenfold by 2050 (Wang et al. 2023).

Two of the molten salts under consideration contain beryllium, which raises significant supply chain questions. According to work by Pearson (2020), known reserves of beryllium and a scale-up in production would not be sufficient to meet the projected needs of large-scale fusion deployment. However, estimates of known reserves today are low primarily because there is currently very little demand for beryllium. If a beryllium-based molten salt blanket is found to be the most viable solution, thereby establishing higher demand for beryllium, the expectation is that additional reserves will be found. Nevertheless, the speed at which mines and processing capacity can be expanded is a concern. For this reason, non-beryllium-based molten salt and molten metals should be pursued in parallel.

Several fusion companies are pursuing a molten metal lead-lithium (LiPb) option. LiPb does not raise the beryllium supply and cost questions encountered with FLiBe (it also avoids the toxicity issues associated with beryllium, which add safety and handling burdens to plant operation). Lead, like beryllium, has neutron multiplication benefits. There are three main issues with LiPb: (1) the mass density of the fluid that must be supported by the surrounding structure; (2) lead activation; and (3) the magnetohydrodynamic (MHD) issues associated with a molten metal. The fact that LiPb contains only 0.68 wt% lithium, whereas FLiBe contains 14 wt% lithium, has consequences for tritium breeding and for the amount of lithium required per FPP. Known

²² Natural lithium is composed of 92% Li-7 and 8% Li-6. Li-7 has a high probability of interacting with high-energy (~12–14 million electron volts [MeV]) neutrons to form tritium, but no probability for interacting with neutrons at lower energies; Li-6 can produce tritium at all neutron energies encountered in the blanket (14 MeV neutrons from the fusion plasma core will moderate to lower energies as they move through the blanket). Neutronics studies at the MIT Plasma Science and Fusion Center (PSFC) indicate that the need for enrichment depends on the design of the MC-FPP. “Enriching” lithium means artificially increasing the proportion of Li-6 in order to obtain sufficient tritium breeding capabilities. In some designs that use FLiBe as the liquid blanket, no enrichment is required. However, it is commonly asserted in the fusion research community that Li-6 enrichment is a must. This requirement adds to the cost of the blanket.

reserves and current production of lead, as documented by Pearson (2020), indicate that no supply chain issues are anticipated for lead on the path to large-scale fusion deployment.

A common requirement for all the liquid blanket options is high purity, because impurities significantly increase corrosivity and can generate undesirable elements in the blanket via transmutation reactions from the neutrons. Purity requirements mean that the supply chains for producing blanket salts and alloys will have to be well developed, with rigorous quality control and purity specifications. For example, beryllium produced from mines in Utah, Kazakhstan, and Russia contains uranium in concentrations of parts per million. High-energy neutrons from the fusion reactor transmute the uranium to plutonium, creating potential challenges for waste management (Kolbasov, Khripunov, and Biryukov 2016), although the concentrations are small. There are various options for purifying beryllium to reduce its uranium content, but each of these adds processing costs and cannot completely remove the uranium (Patel 2022; Forsberg et al. 2020).

Much of the concern about relying on beryllium-based blankets centers on the adequacy of beryllium supplies to support large-scale fusion deployment. However, it is also important to assess the scale-up potential of the beryllium supply chain. Materion currently mines 80% of the world's beryllium from a single mine in Utah, which is calculated to have approximately 18,000 tonnes of remaining beryllium. Other known deposits in Colorado, Texas, and the Yukon have not yet been exploited. Remaining beryllium production at present is by the company Ulba, which is based in Kazakhstan.

Materion believes it will be able to handle demand from beryllium-based products through the 2030s at least. Most of the beryllium processed today is used in copper-based alloys for bushings, bearings, fault components, oil and gas exploration, and conventional strip products. A smaller proportion (~20%) of beryllium is used in microreactors and small modular reactors such as those made by Kairos. Without considering these non-fusion uses, the Utah mine would be able to supply beryllium for about 200 MC-FPP reactors. Not only is a scale-up and expansion of mining operations needed to support a large-scale fusion economy, also needed is the infrastructure to transport, handle, and process beryllium ores.

Materion has developed various models to assess how potential growth in the fusion industry would impact its own growth. The company believes that a public-private partnership will be crucial to help scale beryllium mining and processing capacity for fusion applications.

In conclusion, material supplies for the different liquid blanket concepts being considered present no immediate concerns. For a variety of performance reasons, fusion applications will require additional purification capabilities that are currently at relatively low technical maturity. Generally, liquid blankets are a lifetime component in a fusion power plant since the absolute

level of mass conversion in plant operation is very small (20–200 kg/year).²³ Longer term, markets and mining companies will need to respond to increased demand for materials like beryllium that are currently used on a smaller scale.

6.6. Alloys and composites

This section addresses roadblocks and potential solutions to developing alloys for use in DT-fueled magnetic confinement power plants. It provides an overview of potential materials, their maturity and suitability for fusion applications, and relevant supply chain considerations. For a magnetic confinement FPP, alloys are needed for the first wall, which experiences the highest neutron fluxes and temperatures, and for structural support in all other areas. Although manufacturers and suppliers of some candidate materials exist, alloys and composites required to meet the stringent demands for service in a FPP need extensive development. The development efforts include fundamental research on materials, accelerated testing techniques, and improved manufacturing processes.

Requirements for alloys and composites in FPPs include:

- Strength at elevated temperatures
- Ductility
- High thermal conductivity
- Radiation resistance
- Low activation
- High melting temperature
- Corrosion resistance
- Manufacturability

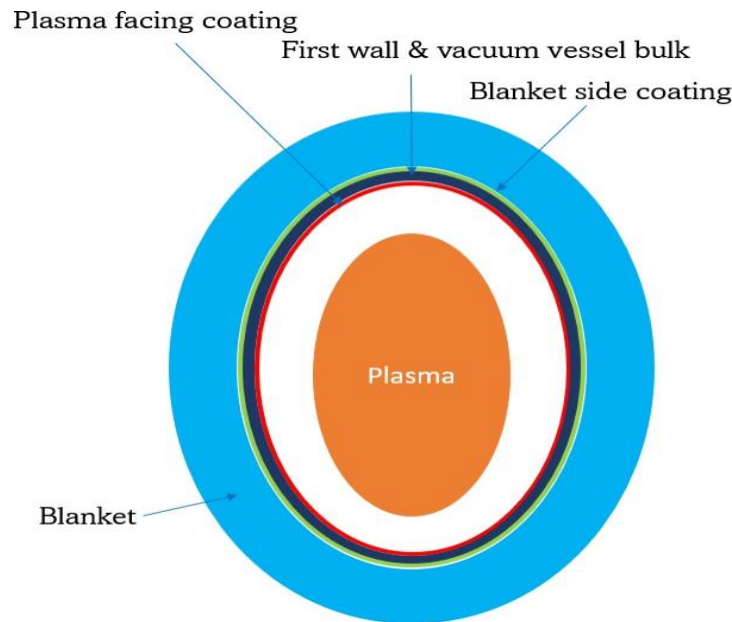
6.6.1. Vanadium alloys as a first-wall solution

Some fusion developers are currently focused on vanadium alloys for the first wall and martensitic steels for other areas internal to the magnetic confinement system that see high neutron fluxes but are not exposed to temperatures as high as the first wall. For magnetic confinement designs in which the vacuum vessel is in front of the blanket, the first wall can generally be considered as a three-layered structure: plasma-facing material, bulk material (structural), and blanket-facing material (Figure 6.2). This is a complex assembly of materials

²³ Although the liquid blanket is considered a lifetime component, some MC-FPP concepts will require ongoing redox control and replenishment of breeding materials. Redox control for a FLiBe blanket requires metal beryllium at the rate of a few kilograms per year. For blanket designs that are sensitive to Li-6 enrichment, a few kilograms per year of enriched lithium fluoride may be needed to maintain required tritium breeding performance (Vergari et al. 2023).

that must tolerate a wide variety of different conditions and be optimized for different functions.

Figure 6.2 Cross-section of core plasma, blanket, and the three layers of the first wall for designs in which the vacuum vessel is in front of the blanket



There are many good arguments for using vanadium alloys for the bulk first-wall material, including heat load capability, good fabricability, and compatibility with liquid blanket materials. The reference vanadium alloy composition, V-4Cr-4Ti, has low activation compared to most of the other materials under consideration. However, activation level depends on reactor size and operating conditions. This is important to ensure that robots or interactive machinery used in maintenance and servicing, including to replace the vacuum vessel, can function in irradiated environments without a long waiting period. In addition, activation has consequences for the cost of dealing with radioactive waste materials. Large cast batches of vanadium, on the order of hundreds of kilograms, have been made, so it is reasonable to assume that the large quantity of vanadium alloys needed for a fusion reactor can be supplied. Carpenter, Sandvik, and Kobe Steel are three companies that can provide cast manufacturing of these vanadium alloys.

6.6.2. Powder vs. melt processing of vanadium

Different avenues exist for tackling the embrittlement of vanadium alloys due to various solutes such as tritium or neutron-produced helium. The first is to develop a coating as a barrier between the FLiBe and the first wall (we expand on this option later in the discussion). The second is to consider powder processing of vanadium as opposed to casting. The Schuh Lab at MIT is exploring powder processing methods (Ng et al. 2024); these involve the creation of stable nanocrystal sizes, which can then be sintered into large masses. Nanocrystalline

materials have a very high-volume fraction of grain boundaries and can therefore accommodate more damage.

Radiation damage can cause solutes in a material like a vanadium alloy to move and form solute clusters, which results in embrittlement by creating localized defects. Stable nanocrystals in which solutes preferentially segregate to grain boundaries prevent embrittlement through two primary mechanisms: First, they limit solute migration that results in embrittlement, since solutes will prefer to remain where they are stabilized at grain boundaries; second, the grain boundaries themselves can act as defect “sinks” that accommodate the defects formed by neutron collisions (Ng 2023). Although a powdering process for vanadium alloys could potentially solve the problem of embrittlement, development of such processes is still at the fundamental research, laboratory experiment stage. At present, casting vanadium alloys remains the only way to make shapes large enough for a first wall.

Global annual production of vanadium was 110,000 tonnes in 2021; global vanadium reserves are estimated at 24 million tonnes (U.S. Geological Survey 2022d). Based on these figures, the vanadium required for an MC-FPP made with a vanadium-rich alloy would equal roughly 0.2% of current global production and less than 0.001% of global reserves. Therefore, supply chain risks for vanadium structural materials may exist primarily in the alloy production and component fabrication stages, not with respect to raw material supply.

Silicon carbide (SiC) and SiC/SiC²⁴ composites have been investigated as potential first-wall materials due to their lower activation (Jiang et al. 2021), fiber alignment (to handle stress in the appropriate direction), high thermal conductivity, and electrically insulating properties. Materials development for such composites is in its infancy and fundamental barriers must still be overcome, but early investigations point to significant promise. Other challenges with SiC-based materials are their ductility and manufacturability at first-wall scale and thickness, as well as the ability to retain high vacuum.

6.6.3. Blanket-facing coatings

The FLiBe/vanadium system poses many challenges that require the addition of a blanket-facing material or coating. Most importantly, vanadium acts as a sink for the tritium produced in the blanket (vanadium alloys are known to be hydrogen absorbing), which contributes to vanadium embrittlement (Snead et al. 2019; Jiang et al. 2021). This is in addition to the embedded helium produced by neutron irradiation in the vanadium alloy, which also causes embrittlement. It has been shown experimentally that beyond a certain hydrogen concentration, vanadium alloys experience a sharp transition from ductile to brittle (Yukawa et al. 2011). To reduce tritium

²⁴ SiC/SiC is a composite material consisting of silicon carbide fibers within a ceramic matrix of silicon carbide.

absorption into vanadium, tungsten and various ceramics have been considered as blanket-facing coatings. Tungsten has the advantages of strong metal-on-metal bonding and good hydrogen impermeability; its downside is its electrical conductivity, which allows for coupling between the blanket and the first wall. However, electrical conductivity is less of an issue with a molten-salt blanket than with a molten-metal blanket because the electrical conductivity of molten salts is four orders of magnitude less than lithium lead. Note that MHD coupling creates very high pumping pressure requirements due to the Lorentz force on the fluid; this effect is exacerbated if the first-wall material is electrically conductive.

Ceramic coatings such as Y_2O_3 , Er_2O_3 (Jiang et al. 2021), and Al_2O_3 offer advantages in terms of preventing MHD electrical coupling and excellent impermeability to hydrogen. A disadvantage is that ceramic-on-metal bonding requires further development. Despite radiation-induced conductivity (RIC), which means that electrical conductivity of the ceramic increases with increasing radiation dose (Chikada 2020), the predicted and measured conductivity values for a vanadium first wall/lithium-based blanket system are still well below the threshold at which MHD coupling becomes appreciable. Blanket-facing coatings also provide protection against corrosion and oxides that form at the liquid/metal interface, eventually spalling into the liquid and creating impurity and wall integrity issues.

6.6.4. Plasma-facing coatings

Plasma-facing components (PFCs) in a fusion reactor face extreme conditions such as very high heat fluxes, high temperatures, high radiation fluxes, and plasma exposures. Tungsten and tungsten-based materials are the conventional choices for PFCs in proposed FPP designs, and they are frequently used in research fusion devices due to their favorable performance under fusion-relevant irradiation at high temperatures. However, current tungsten-based materials are known to have drawbacks (e.g., embrittlement and fuzz formation) that preclude their use in commercial fusion plants, which will operate for longer and at much more intense plasma and irradiation conditions than existing research tokamaks. Modifications and alternatives that mitigate these concerns are a major area of fusion materials research.

One potential plasma-facing material is “tungsten heavy”, a composite with an approximate weight composition of 97W-2Fe-1Ni. This composite is analogous to a brick-and-mortar-like structure: Tungsten “bricks” approximately 50 μm thick are held together by an iron-nickel (Fe-Ni) “mortar” alloy. Tungsten has low sputtering, which is important for reducing impurity particles in the plasma, and a high heat load capability. Cracks in the tungsten bricks can be prevented from propagating by the ductile Fe-Ni alloy. Although this material shows promise, alternatives to nickel may be needed since nickel is known to have high activation and void swelling.

The amount of tungsten required per MC-FPP is estimated to be less than 0.01% of annual tungsten production (U.S. Geological Survey 2022c).

6.6.5. In-vessel structural materials

Martensitic steels are the reference/benchmark in-vessel structural components of future MC-FPPs; they are intended to be used for areas that see high neutron flux but lower temperatures than the first wall. Two types of martensitic steels are under consideration: conventional martensitic steels and reduced activation ferritic martensitic (RAFM) steels. Conventional martensitic steels include HT9 and the 400 series of stainless steels. An example of a RAFM steel is Eurofer 97. The next-generation class of steels that would satisfy in-vessel structural requirements are the oxide dispersion steels. Examples of these steels include 14YWT or 12YWT alloys, which contain 2- to 3-nanometer (nm) yttrium-titanium-oxygen nano-oxides.

In general, the performance of oxide dispersion steels exceeds that of the tempered martensites (Raj and Vijayalakshmi 2012; Ukai et al. 2020). Compared to an operating temperature range of 350°C–650°C for tempered martensites, the oxide dispersion steels with strength levels appropriate to MC-FPPs have an extra 100°C of operating range on the high and low end. In addition, the nano-oxides in oxide dispersion steels trap the helium produced by neutrons and thus reduce embrittlement. Finally, oxide dispersion steels offer a 30%–40% improvement in void swelling due to helium and a 10%–15% improvement in creep strength compared to tempered martensites. Despite the advantages of oxide dispersion steels, however, tempered martensites have advantages when it comes to production and workability. Tempered martensites can be made in mass quantities via a melt process or additive manufacturing and are weldable. Crucible is one manufacturer of tempered martensites, which are sold to companies such as Veridiam and TerraPower. Oxide dispersion steels must be made in small quantities via mechanical ball milling and they are very difficult to process or weld. One company that makes these materials is Zoz in Germany.

6.6.6. Shield material

Shielding materials in a MC-FPP are used to protect magnets and other components from neutron damage, which degrades their performance, and, in the case of HTS magnets, can render them non-superconducting. Good shielding materials are composed of elements with high cross-sections for neutron absorption and/or moderation (lower-energy neutrons have a shorter range). Only a few classes of materials have these properties—namely, cemented carbides, tungsten carbide, cemented borides, and titanium hydride. It is important to note that titanium hydride is not typically used as a shield material due to its flammable and explosive nature. Tungsten and titanium are on the USGS and EU lists of critical materials and are considered to have relatively high economic importance.

A primary shielding material being considered for MC-FPPs is titanium hydride (TiH₂) (Sorborn et al. 2015). The amount of titanium estimated to be required for a single MC-FPP is less than 0.1% of global titanium sponge production capacity, and a far lower percentage of total titanium production capacity if production for pigments is included (U.S. Geological Survey 2022b). Therefore, we do not anticipate supply chain risks for TiH₂ at the raw-materials stage.

6.6.7. Other materials

Other materials needed for MC-FPPs that require supply chain development include high-strength copper alloys, ceramics, and concrete for long-term use in the presence of high irradiation doses. Experience from fission reactors has shown that a less than 1-displacements-per-atom (dpa) dose of irradiation over a long period of time can cause concrete to degrade (Remec et al. 2018). In addition, ceramics able to withstand neutron fluxes are needed for several fusion subsystems and components, including fiber optics, glass, radio-frequency windows, and windows used in plasma diagnostics.

6.7. Conclusions

Four general conclusions emerge from our focused assessment of materials and supply chain requirements for DT-fueled HTS magnetic confinement fusion power plants.

1. Different fusion technologies are at varying stages of maturity. Identifiable issues include component bottlenecks, low production throughput, further fundamental research needs, and limited current market demand.
2. Fusion components can be separated into two categories:
 - Niche components that operate under harsh conditions, such that market opportunities for the same or similar technology in other applications are small
 - Multiple use components (HTS, radio-frequency devices) with potential for current commercial use in other fields
3. There are no raw materials showstoppers: The elements required for DT fusion power plants are generally abundant on Earth. Beryllium is potentially the most problematic, but mostly due to low present demand, rather than fundamental scarcity.
4. Whether fusion can scale to meet demand for firm low-carbon electricity generation will depend on how quickly the supply chain for key components can keep up. The main supply chain challenges for fusion center on component assembly and quality, rather than access to raw materials.

These conclusions are not surprising, since they arise from two facts: The high power density of a FPP means that overall materials requirements per unit of energy are lower than other type of electricity generators, and consumable fuels for DT fusion power plants are sufficiently abundant on Earth so there is no limit to the potential of this energy source. However, the technologies required to make fusion happen are varied and complex.

References

- Bednorz, J. G., and K. A. Muller. 1986. "Possible HighTc Superconductivity in the Ba-La-Cu-O System." *Zeitschrift Für Physik B Condensed Matter* 64 (2): 189–93. <https://doi.org/10.1007/BF01303701>.
- Bradshaw, A. M., and T. Hamacher. 2013. "Nuclear Fusion and the Helium Supply Problem." In *Fusion Engineering and Design*, 88:2694–97. <https://doi.org/10.1016/j.fusengdes.2013.01.059>.
- Brennan, Sean T., Jennifer L. Rivera, Brian A. Varela, and Andy J. Park. 2021. "National Assessment of Helium Resources within Known Natural Gas Reservoirs." *USGS Scientific Investigations Report 2021–September*. <https://doi.org/10.3133/sir20215085>.
- Chikada, Takumi. 2020. "Ceramic Coatings for Fusion Reactors." In *Comprehensive Nuclear Materials*, 6:274–83. Elsevier. <https://doi.org/10.1016/B978-0-12-803581-8.11674-1>.
- Creely, A. J., D. Brunner, R. T. Mumgaard, M. L. Reinke, M. Segal, B. N. Sorbom, and M. J. Greenwald. 2023. "SPARC as a Platform to Advance Tokamak Science." *Physics of Plasmas* 30 (9): 90601. <https://doi.org/10.1063/5.0162457/2909870/SPARC-AS-A-PLATFORM-TO-ADVANCE-TOKAMAK-SCIENCE>.
- Daniel Ng, Malik Wagih, Tianjiao Lei, and Christopher Schuh. 2024. "Design of Vanadium Alloys for Fusion Applications." In *TMS 2024 Annual Meeting and Exhibition*. Pittsburgh, PA.
- Forsberg, Charles, Guiqiu Zheng, Ronald G Ballinger, and Stephen T Lam. 2020. "Fusion Blankets and Fluoride-Salt-Cooled High-Temperature Reactors with Flibe Salt Coolant: Common Challenges, Tritium Control, and Opportunities for Synergistic Development Strategies Between Fission, Fusion, and Solar Salt Technologies." *Nuclear Technology* 206 (11): 1778–1801. <https://doi.org/10.1080/00295450.2019.1691400>.
- Fusion Industry Association. 2023. "The Fusion Industry Supply Chain: Opportunities and Challenges." https://www.fusionindustryassociation.org/wp-content/uploads/2023/05/FIA-Supply-Chain-Report_05-2023.pdf.
- Grynja, Eugene, and Peter J. Griffin. 2017. "Helium in Natural Gas - Occurrence and Production." *Journal of Natural Gas Engineering* 1 (2): 163–215. <https://doi.org/10.7569/jnge.2016.692506>.
- Hartwig, Zachary S., Rui F. Vieira, Darby Dunn, Theodore Golfinopoulos, Brian LaBombard, Christopher J. Lammi, Philip C. Michael, et al. 2024. "The SPARC Toroidal Field Model Coil Program." *IEEE Transactions on Applied Superconductivity* 34 (2): 1–16. <https://doi.org/10.1109/TASC.2023.3332613>.
- Hartwig, Zachary S., Rui F. Vieira, Brandon N. Sorbom, Rodney A. Badcock, Marta Bajko, William K. Beck, Bernardo Castaldo, et al. 2020. "VIPER: An Industrially Scalable High-Current High-Temperature Superconductor Cable." *Superconductor Science and Technology* 33 (11): 11LT01. <https://doi.org/10.1088/1361-6668/abb8c0>.
- Hartwig, Z. S., C. B. Haakonsen, R. T. Mumgaard, and L. Bromberg. 2012. "An Initial Study of Demountable High-Temperature Superconducting Toroidal Field Magnets for the Vulcan Tokamak Conceptual Design." *Fusion Engineering and Design* 87 (3): 201–14. <https://doi.org/10.1016/J.FUSENGDES.2011.10.002>.
- Jiang, Shao-Ning, Fu-Jie Zhou, Gao-Wei Zhang, Xiao-Ou Yi, Chang-Wang Yu, Xiu-Jie Wang, and Wei-Feng Rao. 2021. "Recent Progress of Vanadium-Based Alloys for Fusion Application." *Tungsten* 3 (4): 382–92. <https://doi.org/10.1007/s42864-021-00107-4>.
- Keller, John. 2023. "Wanted: Diamond Semiconductors for RF, Microwave, and Power Electronics to Operate in Harsh Environments." March 30, 2023.
- Kolbasov, B. N., V. I. Khripunov, and A. Yu Biryukov. 2016. "On Use of Beryllium in Fusion Reactors: Resources, Impurities and Necessity of Detritiation after Irradiation." *Fusion Engineering and Design* 109–111 (November):480–84. <https://doi.org/10.1016/J.FUSENGDES.2016.02.073>.
- Lichtenstein, T., M. Rose, J. Krueger, E. Wu, and M. Williamson. 2022. "Thermochemical Property Measurements of FLiNaK and FLiBe in FY 2020." Argonne, IL (United States). <https://doi.org/10.2172/1845459>.
- MIT Energy Initiative. 2022. "The Future of Energy Storage." *MIT Energy Initiative*.
- Molodyk, A. 2023. "Personal Communication."

- Molodyk, A., S. Samoilenkov, A. Markelov, P. Degtyarenko, S. Lee, V. Petrykin, M. Gaifullin, et al. 2021. "Development and Large Volume Production of Extremely High Current Density YBa₂Cu₃O₇ Superconducting Wires for Fusion." *Scientific Reports* 11 (1). <https://doi.org/10.1038/s41598-021-81559-z>.
- Ng, Daniel. 2023. "Discussion with Daniel Ng, Schuh Lab, MIT."
- Patel, Sonal. 2022. "Kairos Commissions Molten Salt Coolant Production Plant for High-Temperature Nuclear Reactors." 2022. <https://www.powermag.com/kairos-commissions-molten-salt-coolant-production-plant-for-high-temperature-nuclear-reactors/>.
- Pearson, Richard J. 2020. "Towards Commercial Fusion: Innovation, Technology Roadmapping for Start-Ups, and Critical Natural Resource Availability", PhD Thesis, . The Open University (United Kingdom).
- Pinto, Valentina, Angelo Vannozzi, Giuseppe Celentano, Massimo Tomellini, Alexander Meledin, and Silvia Orlanducci. 2023. "Nanodiamond Influence on the Nucleation and Growth of YBCO Superconducting Film Deposited by Metal–Organic Decomposition." *Crystal Growth & Design* 23 (8): 6086–99. <https://doi.org/10.1021/acs.cgd.3c00607>.
- Raj, B., and M. Vijayalakshmi. 2012. "Ferritic Steels and Advanced Ferritic–Martensitic Steels." In *Comprehensive Nuclear Materials*, 97–121. Elsevier. <https://doi.org/10.1016/B978-0-08-056033-5.00066-5>.
- Remec, Igor, Thomas M. Rosseel, Kevin G. Field, and Yann Le Pape. 2018. "Radiation-Induced Degradation of Concrete in NPPs." *ASTM Special Technical Publication STP 1608* (November): 201–11. <https://doi.org/10.1520/STP160820170059>.
- Rudenko, Alexey, Alexander Redkin, Evgeniya Il'ina, Svetlana Pershina, Peter Mushnikov, Yuriy Zaikov, Sergey Kumkov, Yalan Liu, and Weiqun Shi. 2022. "Thermal Conductivity of FLiNaK in a Molten State." *Materials* 15 (16): 5603. <https://doi.org/10.3390/ma15165603>.
- Rufford, Thomas E., K. Ida Chan, Stanley H. Huang, and Eric F. May. 2014. "A Review of Conventional and Emerging Process Technologies for the Recovery of Helium from Natural Gas." *Adsorption Science & Technology*.
- Snead, Lance L., David T. Hoelzer, Michael Rieth, and Andre A.N. Nemith. 2019. "Refractory Alloys: Vanadium, Niobium, Molybdenum, Tungsten." In *Structural Alloys for Nuclear Energy Applications*, 585–640. Elsevier. <https://doi.org/10.1016/B978-0-12-397046-6.00013-7>.
- Sorbom, B. N., J. Ball, T. R. Palmer, F. J. Mangiarotti, J. M. Sierchio, P. Bonoli, C. Kasten, et al. 2015. "ARC: A Compact, High-Field, Fusion Nuclear Science Facility and Demonstration Power Plant with Demountable Magnets." *Fusion Engineering and Design* 100: 378–405. <https://doi.org/10.1016/j.fusengdes.2015.07.008>.
- Surrey, E. 2019. "Engineering Challenges for Accelerated Fusion Demonstrators." *Philosophical Transactions of the Royal Society A: Mathematical, Physical and Engineering Sciences* 377 (2141): 20170442. <https://doi.org/10.1098/rsta.2017.0442>.
- Ukai, Shigeharu, Naoko Oono-Hori, and Satoshi Ohtsuka. 2020. "Oxide Dispersion Strengthened Steels." In *Comprehensive Nuclear Materials*, 255–92. Elsevier. <https://doi.org/10.1016/B978-0-12-803581-8.11718-7>.
- U.S. Geological Survey. 2022a. "Mineral Commodity Summaries - Helium." *U.S. Geological Survey*. <https://doi.org/10.3133/sir20215085>.
- . 2022b. "Mineral Commodity Summaries - Titanium." *U.S. Geological Surveys*.
- . 2022c. "Mineral Commodity Summaries - Tungsten." *U.S. Geological Survey*.
- . 2022d. "Mineral Commodity Summaries - Vanadium." *U.S. Geological Survey*.
- . 2022e. "Mineral Commodity Summaries - Yttrium." *U.S. Geological Survey*. <https://pubs.usgs.gov/periodicals/mcs2022/mcs2022-yttrium.pdf>.
- Vergari, Lorenzo, Raluca O. Scarlat, Ryan D. Hayes, and Massimiliano Fratoni. 2023. "The Corrosion Effects of Neutron Activation of 2LiF-BeF₂ (FLiBe)." *Nuclear Materials and Energy* 34 (March): 101289. <https://doi.org/10.1016/J.NME.2022.101289>.

Wukitch, Stephen. 2019. "Personal Communication." Massachusetts Institute of Technology.

———. 2023. "Personal Communication." Massachusetts Institute of Technology.

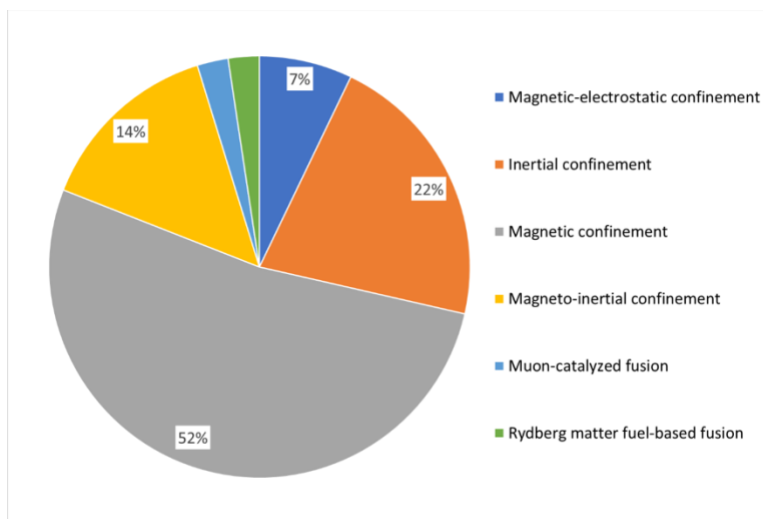
Yukawa, H., T. Nambu, and Y. Matsumoto. 2011. "V–W Alloy Membranes for Hydrogen Purification." *Journal of Alloys and Compounds* 509 (September): S881–84. <https://doi.org/10.1016/j.jallcom.2010.09.161>.

7. Techno-economic analysis of fusion power plants

7.1. Introduction

The techno-economic analysis described in this chapter was designed to provide insights into fusion energy cost drivers and the potential impact of regulation on cost. Given the current maturity of fusion concepts, we outline only relative costs. [Figure 7.1](#), which uses data from the Fusion Industry Association, shows that fusion companies are taking a variety of approaches. Roughly half (52%) are pursuing magnetic confinement designs, 14% are pursuing magneto-inertial designs, and 22% are pursuing inertial confinement. Overall, 88% of the fusion industry is currently pursuing one of these three approaches (Fusion Industry Association 2023b). Accordingly, our independent, bottom-up cost assessment focused on deuterium-tritium (DT) magnetic confinement reactors. As the most researched fusion design, published data on DT magnetic confinement is more extensive than for other fusion approaches. We also undertook a top-down estimation of costs for magneto-inertial and inertial confinement concepts.

Figure 7.1 Proportion of fusion companies pursuing different fusion approaches



Source: Fusion Industry Association 2023b.

Despite numerous published studies on proposed fusion power plant (FPP) configurations, the lack of a demonstration FPP and a commercial supply chain for essential components means that substantial uncertainty remains around current cost estimates. In deference to this uncertainty, our techno-economic analysis focuses on long-term cost potential once supply chains have been established and designs have improved. We do not generate cost estimates for first-of-a-kind (FOAK) experimental fusion reactors such as the ongoing ITER project or proposed demonstration fusion power plants such as EU DEMO. Additionally, we leverage existing studies of FPPs, fission power plants (Stewart and Shirvan 2022), and renewable energy sources to understand the relative costs of various FPP concepts. FPPs are likely to operate with

reduced radioactive materials-at-risk compared to fission, which merits less stringent regulatory oversight, as recently confirmed by regulatory bodies in the United Kingdom (UK Department for Business 2022) and the United States (Clark 2023). However, ITER underwent a licensing process similar to that for a fission nuclear reactor in France. Thus, our analysis also considers how more versus less stringent regulatory oversight affects cost. Finally, we normalize all of our cost estimates to further acknowledge the large uncertainties that apply at this stage of fusion development.

7.2. Concepts and assumptions

A FPP is made up of a fusion reactor, supporting equipment, and the facilities that house the reactor and equipment. [Table 7.1](#) summarizes key parameters for this analysis. We scale cost estimates from the literature to the parameters shown in [Table 7.1](#) by applying scaling laws, as discussed in [Appendix C](#). Many of the FPP features assumed for this analysis are based on the industry’s leading candidate materials as self-reported by fusion companies in the annual Fusion Industry Association report (Fusion Industry Association 2023c). As already noted, we acknowledge a high degree of uncertainty in cost estimates for any fusion concept at this early stage of development and highlight the need for technology advances to further develop economically critical features.

Table 7.1 General FPP parameters used for scaling in this study

Parameters	Base case values
Thermal power	1,000 MW _{th}
Electricity generation	450 MW _e
Net electric output	350 MW _e
Assumed capacity factor	0.85

Noteworthy features of our techno-economic analysis include the following:

- We used publicly available data to estimate materials costs for FPP construction and operation.
- Our analysis does not reflect the business plans of any particular fusion company.
- The economic feasibility of fusion deployment depends on the development of significant novel technologies, materials, and concepts. This analysis does not attempt to predict the success rate of research endeavors to advance needed technologies.
- Cost estimates for all civil, mechanical, and electrical work are based on non-nuclear thermal power plants using the parameters listed in [Table 7.1](#).

- We include upper- and lower-bound cost estimates. The main difference between these estimates is level of assumed regulatory oversight. The lower bound assumes no nuclear safety oversight, whereas the upper bound assumes regulatory oversight of FPP construction, fabrication, and equipment installation based on a postulated “better experience” scenario for advanced fission.²⁵
- Given the significant uncertainty around fusion-specific technology, assumptions about materials requirements were based on experimental fusion concepts and information from the Fusion Industry Association (Fusion Industry Association 2023b). All costs were escalated to 2021 dollars using the U.S. consumer price index (U.S. Bureau of Labor Statistics n.d.).
- We assume that DT FPPs have tritium-breeding capabilities that enable them to remain self-sufficient without needing to rely on external sources of tritium.

For our bottom-up cost analysis of a magnetic confinement FPP (MC-FPP), we assumed a compact high-field tokamak concept as described by Sorbom et al. in a 2015 paper that describes a tokamak design based on the use of high-temperature superconductors and estimates associated material requirements and fabrication costs (Sorbom et al. 2015). The MC-FPP configuration in our analysis is derived from this compact high-field design with a number of modifications regarding materials and scale. As an example, we assume that vanadium is used instead of nickel-based alloys for first-wall components, based in part on a recent industry study of the fusion supply chain (Fusion Industry Association 2023a). Given that MC concepts have been researched for decades, there is an extensive literature describing different designs of this type. The ARIES Studies (Farrokh Najmabadi et al. 2006) present results from several capital cost studies for various MC concepts, including the spherical torus and compact stellarator. We compare reported costs for these concepts against costs for an MC-FPP.

For a magneto-inertial FPP (MI-FPP), we utilized drawings for this general fusion concept (Friedman 2021) to support our top-down estimate. We assume that a MI-FPP is made up of four 90-MW_e reactor modules for consistency with a single 350-MW_e MC-FPP. We compare our independent cost assessment against a 2017 bottom-up estimate of cost for a generic magneto-inertial confinement FPP developed by Bechtel (Woodruff et al. 2017). We find the Bechtel study to be more in line with fusion industry trends than a subsequent 2021 analysis by the Advanced Research Projects Agency-Energy (ARPA-E) study (Hsu, Woodruff, and Nehl 2020).

²⁵ The concept of “better experience” and “median experience” was established in the Energy Economic Data Base Program, which was originally developed from empirical nuclear power plant cost data and has been expanded to address advanced nuclear power plants. “Better experience” means that the costs are at the low end of the cost range based on lowest achievable cost as judged by analysts of the database’s cost data.

To develop cost estimates for an inertial confinement FPP (IC-FPP), we used information about the First Light concept (World Nuclear News 2022) and Sandia’s Z-Machine (Sandia 2024). Unfortunately, there are no detailed, independent cost analyses in the literature for inertial confinement, so we do not attempt to compare our IC-FPP cost estimates with estimates from other sources.

7.3. Results and discussion

7.3.1. Capital costs

The economic viability of fusion energy is paramount to its successful commercial deployment. Aside from ongoing technical and engineering challenges, the main critiques of fusion deployment pertain to its cost. However, the field of fusion economics remains largely unexplored, particularly considering recent technology developments. Given that a FPP has never been constructed, no empirical data exist to help validate fusion-specific cost estimates. Thus, we use a high-level, bottom-up methodology to examine the relative economics of different FPP concepts. We do not attempt to project absolute values for the cost of any of these fusion concepts.

Figure 7.2 shows the breakdown of capital costs in our independent bottom-up estimate compared to selected results from the literature. It shows that the breakdown of capital costs in our upper- and lower-bound estimates for MC-FPPs is in line with earlier studies. In our lower-bound estimate, the combination of indirect costs plus owner’s cost and contingency is a substantially smaller portion of overall cost, reflecting an optimistic view relative to the literature. Indirect cost is typically driven by the amount of engineering and project management that needs to take place. Fission power plant indirect costs are substantially higher than fossil fuel thermal power plant indirect costs because of regulatory oversight. Our lower-bound cost estimate assumes indirect costs and contingency similar to an Nth-of-a-kind (NOAK) natural gas power plant, whereas our upper-bound cost estimate assumes indirect costs and contingency similar to the “better experience” nuclear fission plant.²⁶

In the FPP cases we examine, direct cost constitutes most of the capital cost, as shown in Figure 7.2.

²⁶ In reality, a nuclear fission plant in the U.S. experiences significantly higher indirect cost and requires higher contingency than the “better experience” nuclear fission plant. The increase in nuclear regulation oversight has substantially increased the indirect cost and assumed contingency for a nuclear fission plant beyond the “better experience” estimate that is rooted from the pre-Three Mile Island accident era.

Figure 7.2 High-level breakdown of capital costs comparing results from the literature to our lower- and upper-bound estimates for a magnetic confinement fusion plant

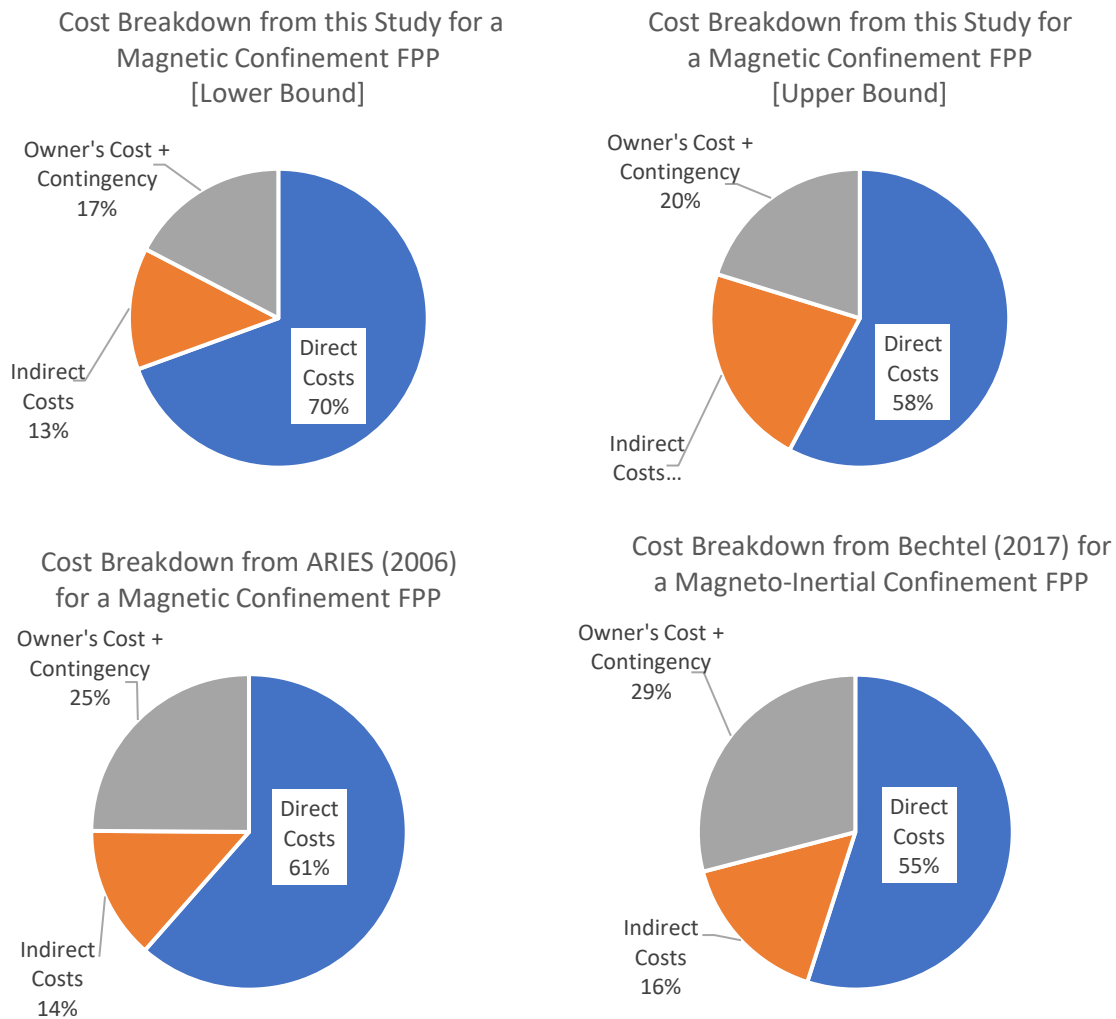


Table 7.2 summarizes the relative total direct cost for different concepts scaled for similar power ratings. Figure 7.3 shows the relative breakdown of this direct cost. Table 7.2 suggests that magneto-inertial confinement is a more cost-effective approach than magnetic confinement, whereas inertial confinement is the least cost-effective approach. Table 7.2 also includes the scientific energy gain that has been achieved for the different confinement methods as a metric for measuring progress achieved toward viable energy production from the point of view of physics and operations. For instance, the scientific energy gain (Q) achieved by magneto-inertial devices to date, albeit with smaller total investments, is approximately 30 times less than that achieved by magnetic confinement and 75 times less than inertial confinement (Wurzel and Hsu 2022). Thus, it is fair to state that the science risk associated with developing magneto-inertial confinement is much greater. On the other hand, as advocates for

this concept point out, magneto-inertial confinement holds promise for simpler reactor assemblies and projected cost savings.

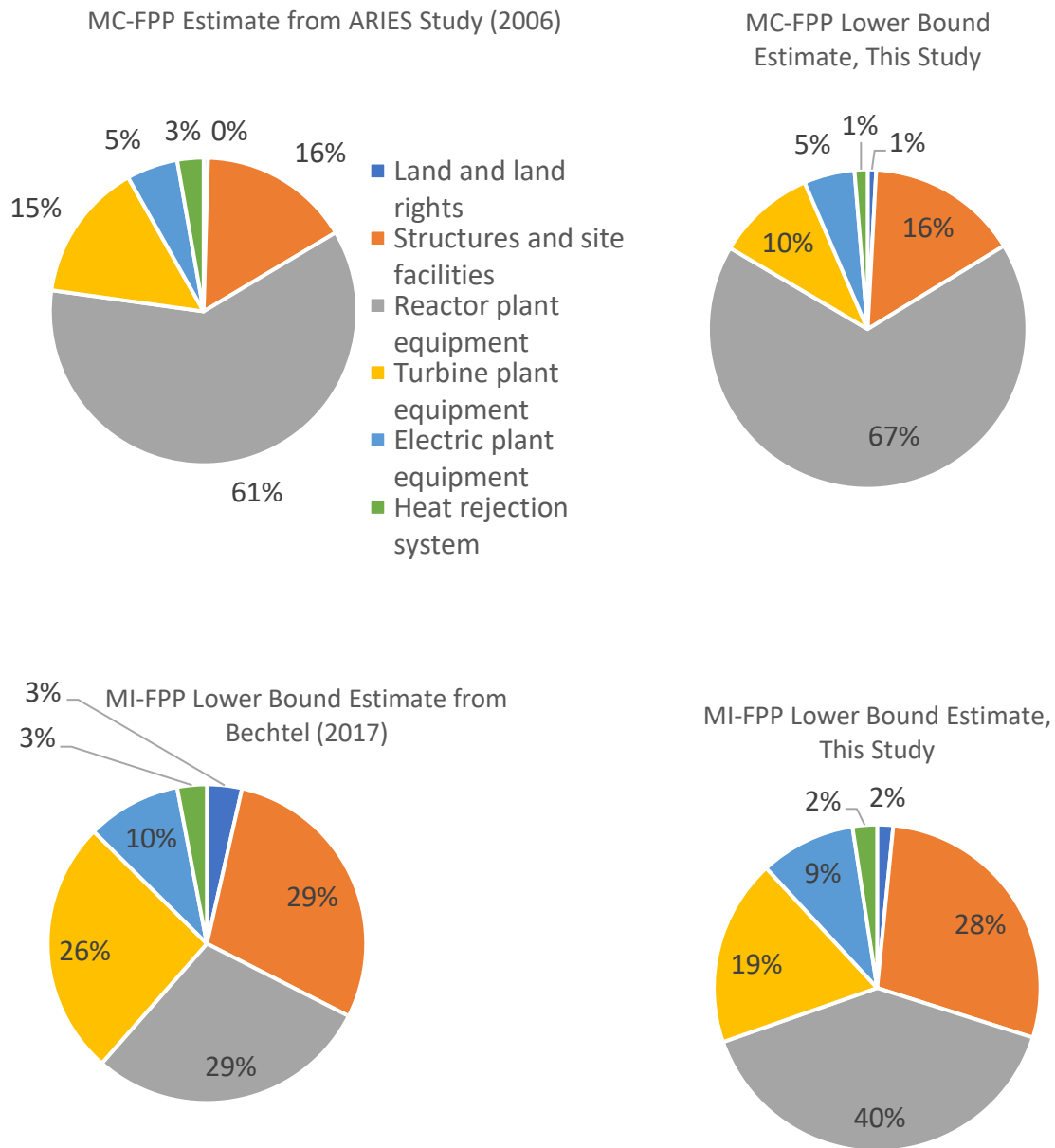
Table 7.2. Comparison of FPP direct costs and scientific energy gain

FPP concept	Source for cost data	Relative cost per MW	Scientific energy gain
Magnetic confinement	ARIES spherical torus	1.0	0.0003 (MAST)
	ARIES compact stellarator	0.8	0.007 (W7-X)
	This study	0.8 to 2.0	0.64 (JET)
Magneto-inertial	Bechtel	0.3 to 0.8	0.02 (MagLIF)
	This study	0.5 to 0.7	0.02 (MagLIF)
Inertial confinement	This study	1.7	1.54 (NIF)

Sources: For the ARIES Studies, see Najmabadi et al. (2006); for the Bechtel study, see Woodruff et al. (2017). Values for scientific energy gain values are from Wurzel and Hsu (2022) and Messinger (2022). They are derived from the UK’s Mega Amp Spherical Tokamak (MAST), Germany’s Wendelstein 7-X stellarator (W7-X), the Joint European Torus (JET), Magnetic Liner Inertial Fusion (MagLIF) experiments at Sandia National Laboratory, and the United States’ National Ignition Facility (NIF).

Our lower-bound estimates of direct cost for magnetic confinement and magneto-inertial FPPs are in line with values found in the literature. This consistency is expected, since our lower-bound analysis and the cost analyses in the literature both assume conventional manufacturing costs per kilogram of material input. However, most prior fusion cost studies do not include costs for equipment transportation, installation, and taxes. Our upper-bound cost analysis for a magneto-inertial FPP is in line with results from the Bechtel (2017) study, though not for the same reason. In the Bechtel study, both the low- and high-end estimates have the same ratio of indirect cost to total overnight cost, whereas this study escalates indirect cost percentage of total overnight cost for the upper-bound case. As already noted in connection with [Figure 7.2](#), our overall breakdown of direct cost for magnetic confinement and magneto-inertial plants is also in line with results from the literature.

Figure 7.3 Breakdown of direct costs for magnetic confinement (MC) concepts (top) and magneto-inertial (MI) concepts (bottom)



Whereas our upper-bound cost estimate for a magneto-inertial FPP is 1.4 times our lower-bound cost estimate for this technology, our upper-bound estimate for a magnetic confinement FPP is 2.5 times the lower-bound estimate. This reflects large uncertainties about the direct cost of reactor components for a magnetic confinement design, including especially costs for magnets, which will be driven by fabrication costs. In the 2015 compact high-field tokamak concept paper, fabrication costs were estimated to be a factor of 20 times greater than raw

material costs, at roughly \$1,000/kg (Sorbom et al. 2015). Our cost estimate for MC-FPPs assumes a lower-bound cost of \$150/kg for fabrication, which represents costs associated with conventional forging and welding techniques, inclusive of labor, factory equipment costs, quality assurance, and qualification (Holcomb, Peretz, and Qualls 2011; Ganda, Taiwo, and Kim 2018). Also, applying Wright's law and using a learning rate of 20%, if fabrication costs start at \$1,000/kg, they should drop to roughly \$150/kg by the 300th unit, or at the point when about 100 GW_e of MC-FPP generating capacity has been added to the grid. An additional tenfold increase in deployment could further reduce fabrication costs to roughly \$75/kg.

To understand the potential to achieve MC-FPP cost reductions by driving down fabrication costs, we asked how low fabrication costs could ultimately fall. It is reasonable to assume that these costs (in \$/kg) cannot be less than the cost to fabricate solar photovoltaic panels or common mass-produced goods such as cars, which is about \$15/kg. If fabrication costs for reactor components can be reduced by a factor of 10 from \$150/kg to \$15/kg, this would reduce total direct costs for a MC-FPP by a factor of 1.6 relative to our lower-bound estimate.

R&D investments, learning rates, and the production path for reactor equipment will determine the cost of future fusion power plants. However, there are limits to Wright's law and fusion developers and investors will need to be cautious applying it to relevant components. For instance, it would be incorrect to apply Wright's law to the total cost for a fusion power plant, since the total cost includes mature components, such as the steam turbo-generator set, that already have an established NOAK supply chain.

In line with these findings, fabrication is a cost driver across the different FPP concepts being investigated. Fabrication costs for the targets used in the inertial confinement National Ignition Facility (NIF), for example, are roughly \$2,500 per target. This cost would have to fall to less than \$1 per target for inertial confinement fusion energy to be economically viable (Goodin et al. 2004). There has been less research on inertial confinement fusion than on magnetic confinement fusion; thus, there is very little publicly available cost data for IC-FPPs. However, existing studies suggest that developments in manufacturing are critical to the development and deployment of this technology (Goodin et al. 2004). In contrast to magnetic and inertial confinement fusion designs, which face a common cost driver in terms of the cost to fabricate major reactor components, magneto-inertial designs have less demanding equipment requirements and are less sensitive to fabrication costs. This may allow MI-FPPs to start with lower costs, which could lead to faster market penetration. However, all of these findings need to be put into perspective: No FPP concept to date has been built or realized engineering net-energy gain; moreover, the technologies involved, as noted at multiple points in this report, are at widely different levels of maturity. For the less mature inertial confinement and magneto-inertial technologies, uncertainty about the underlying physics will have a greater impact on commercial viability than potential economic advantages.

In general, for all deuterium-tritium FPP concepts, upper-bound cost uncertainty is driven by regulatory factors. However, even in our upper-bound estimates, the cost impact of regulations is smaller for a fusion power plant than for a nuclear power plant (NPP). As such, our upper-bound estimate should not be interpreted as a bounding case for the relative cost of a NOAK FPP. Likewise, the future cost for deuterium-tritium FPP may become less than our lower-bound estimate. One could postulate that if fusion grows to play a large role in the global energy mix, cost declines for the fabrication of reactor components would be comparable to those seen in solar panels and lithium-ion batteries. Such assumptions would reduce direct costs for a FPP by a factor of 1.6 relative to our lower-bound estimate.

7.3.2. Operations and maintenance costs

Since DT fusion power plants are designed to breed their tritium fuel, fuel costs are negligible. Therefore, capital cost and operations and maintenance (O&M) cost will drive the cost of FPP-produced electricity. In FPPs, reactor components are subject to material damage from neutrons (particularly for DT and deuterium-deuterium fueled fusion), corrosion, and high-temperature operation, all of which shorten component lifetimes, particularly for first-wall components. Proposed lifetimes for the first wall range from 1.5 to 4 years at full power. Replacing these components results in downtime for the power plant. Different fusion concepts use different first-wall strategies. Most have blanket materials in front of the vacuum vessel, whereas others have the vacuum vessel in front of the blanket. Other concepts use a liquid first wall. The components most exposed to neutron damage vary with these design choices, as does the frequency of component replacement, which also depends on the neutron flux and the materials of construction. [Appendix C](#) explains the method we used to calculate a range of potential O&M costs for MC-FPPs. Most of the existing literature, including the ARIES Studies, quote O&M costs in the range of \$20–\$30 per MWh (escalated to 2021 dollars). This is close to our lower-bound cost estimate for an MC-FPP operating at 85% capacity factor and in line with current O&M costs for nuclear fission plants. Our upper-bound estimate of O&M costs is appreciably higher, driven by the higher capital cost of replacing reactor components in that scenario.

7.3.3. Learning curve and capacity factor considerations

Several fusion concepts, particularly magneto-inertial and inertial confinement concepts, operate in pulse mode, which will likely reduce the capacity factor of these types of FPPs and increase the levelized cost of electricity they generate. Regardless, achieving high capacity factors for the first several years of operation will be challenging for any new technology with high capital costs, as demonstrated by experience with fission power plants and fossil fuel power plants with carbon capture, as well as many solar thermal power plants and offshore wind. Slower deployment rates for these technologies led to a slower decline from FOAK costs to NOAK costs. Wind turbines, photovoltaic (PV) cells, and lithium-ion batteries, by contrast,

realized very steep learning rates because these technologies lend themselves to rapid prototyping, R&D, and manufacturing at reasonable investment. Some fusion concepts are more modular and more easily prototyped. These include most magneto-inertial concepts, which require small-scale reactor equipment with simplified auxiliaries. Benefits from this modularity may be offset by the fact that magneto-inertial concepts operate in pulse mode and thus may be limited to low-capacity factors.

7.3.4. Non-DT fusion concepts

Interest in alternatives to DT-fueled fusion is motivated by the hope that eliminating neutrons from the primary fusion reaction and thereby limiting neutron activation of reactor materials would allow for more economical systems. Neutrons produce transmutations in all materials they collide within the reactor and surrounding blanket system; transmutation commonly lead to the presence of radioactivity. In contrast to fission reactions, where most of the energy is carried by large fission products, in DT fusion reactions, 80% of the energy is carried off by neutrons. Fusion-generated neutrons are about 10 times higher in energy than neutrons generated by fission. This causes more rapid transmutation of reactor components and shortens the lifetime of reactor equipment. The resulting radioactive materials require more costly handling, monitoring, and disposal. Thus, neutronic fusion requires careful materials selection and design to mitigate these costs.

To be more competitive with fission and also reduce regulatory requirements that effectively prohibit fission energy development in several parts of the world, companies have pursued aneutronic fusion reactions using deuterium-helium-3 (DHe3) and proton-boron (pB11) fuels, as described in [Chapter 2](#). These reactions generate high-energy charged helium nuclei (often called alpha particles) that can be harnessed for power generation and contained more easily to prevent health risks and damage to reactor components. The charged alpha particles provide an opportunity for direct energy conversion to produce electricity, potentially increasing efficiency and reducing cost. However, aneutronic fusion comes with several challenges (Veil 2022; Clark 2023):

1. Neutron-generating side reactions mean that some activation of materials still occurs, albeit to a lesser extent than with DT fusion. (DHe3 fusion generates neutrons from deuterium-deuterium side reactions and pB11 fusion generates neutrons from the reaction of alpha particles with B11.)
2. Non-DT fusion reactions are orders of magnitude less likely to occur, increasing the uncertainty of achieving net-energy gain.
3. Some of the fusion companies pursuing non-DT fusion have proposed pulse-mode operation, which could translate to more expensive equipment and/or low capacity factors.

4. The helium-3 (He3) fuel needed for DHe3 fusion is more costly to generate than deuterium and tritium.

In conclusion, some non-DT fusion concepts could provide capital cost savings, both by (1) leveraging simplified reactor equipment and (2) realizing faster learning gains because related R&D can be conducted with lower capital investments. However, there is significant uncertainty about whether these concepts will achieve net-energy gain. Companies such as Helion, which is pursuing DHe3 fusion, and TAE, which is pursuing pB11 fusion, are working to overcome these challenges.

7.3.5. Cost impacts of regulation

As noted in [Section 7.3.1](#), the difference between our lower- and upper-bound cost estimates mainly reflects different assumptions about the level of regulatory oversight applied to FPP construction and installation. Significant regulatory costs can motivate fusion companies to reduce their nuclear footprint as much as possible. In general, fusion energy systems do not pose the same risks as fission energy systems because fusion does not require fissile materials and fusion fuel cannot undergo a chain reaction. Thus, major portions of the regulatory framework that exists for fission energy are not germane to fusion.

In April 2023, the U.S. Nuclear Regulatory Commission (NRC) approved an NRC staff proposal to regulate fusion technology under 10CFR part 30, “Rules of General Applicability to Domestic Licensing of Byproduct Material,” which focuses on material that may pose a hazard (Clark 2023). The fusion industry has been supportive of this NRC decision. Note that the NRC will still have to develop a new volume of “Consolidated Guidance About Materials Licenses” dedicated to fusion energy systems; in addition, new, fusion-specific regulations may still be required if the “anticipated fusion design presents hazards sufficiently beyond those of near-term fusion technologies” (Clark 2023). The Advisory Committee on Reactor Safeguards (ACRS), an independent group that advises NRC on its regulatory decision-making, also recommends revisiting fusion regulation, when commercial-relevant hazards are considered. The current rule-making is based on tritium inventory of “less than 100 grams, with 0.1 gram or less in the vacuum chamber” (Veil 2022). As FPP systems are designed, built, tested, and operated at scale, fusion energy’s radioactive footprint will increase, potentially necessitating additional regulation of hazardous materials as outlined by the NRC (Clark 2023).

Both DT and non-DT designs can benefit from a reduced regulatory burden as compared to fission. The recent NRC ruling changed past thinking that only non-DT fusion could qualify for lighter regulatory burdens. As long as a very low radioactive footprint can be maintained by relying on low-activation materials in the construction of DT FPPs, there is potential to regulate DT fusion under the same framework as non-DT fusion. This reduced scope is expected to result in significantly lower costs—by a factor of two or more—for fusion-related equipment and civil

structures, as demonstrated by the sensitivity of our lower- and upper-bound cost estimates for MC-FPPs. Thus, the fusion industry will need to strike a balance between economies of scale, fusion fuel type, and regulatory oversight in charting a path to commercially viable fusion technology.

7.3.6. Summary

Several high-level points emerge from the techno-economic analysis conducted for this study:

- Relative to the literature, our independent and somewhat different approach to estimating fusion costs reached similar conclusions with respect to the expected breakdown of direct and indirect costs for constructing a fusion power plant. In our study, as in the literature, the cost of reactor equipment is the main driver of both capital and O&M costs for FPPs.
- Magnetic confinement fusion requires capital-intensive equipment and is subject to high uncertainty with respect to fabrication cost and performance (including lifetime).
- Magneto-inertial fusion requires less capital-intensive equipment than magnetic confinement fusion and its equipment costs are easier to estimate. However, there is much larger uncertainty about achieving net-energy gain with magneto-inertial designs given lack of experience with this approach.
- R&D to improve performance by achieving higher operating power and temperature with similar structures, systems, and components could significantly reduce the cost of magnetic confinement fusion. Estimating the potential for performance improvements is difficult, however, and subject to large uncertainties given the current status of fusion technology.
- O&M costs can be significant for a FPP system, therefore concepts that reduce O&M costs while achieving reasonable capacity factors of 70% or more would have a significant edge in delivering a commercially viable product.
- Fusion energy systems do not pose the same risks as fission energy systems because fusion does not require fissile materials and fusion fuel cannot undergo a chain reaction. Thus, major portions of the existing regulatory framework for fission energy are not germane to fusion. To the extent that fusion does need to be regulated, however, the impact of regulations on FPP cost can be significant. Our analysis specifically propagated the impact of regulatory costs in a bottom-up manner. Even modest assumptions about the extent of future regulation, based on applying “better experience” factors from fission to the structures and systems needed to address tritium safety and containment of radioactive hazards within the FPP site boundary, increased direct costs by at least 40% and indirect costs by 100% relative to a no-regulation case.

Given that a FPP has never been built and that more than 85% of fusion companies anticipate deployment of their first FPP after 2030, there is great uncertainty in any cost estimate for a

future NOAK FPP. Our analysis for this study embraces uncertainty and identifies existing costs and technologies that allow for a better understanding of the differences and similarities between a fusion power plant and a conventional thermal power plant, while highlighting key areas for further R&D to improve performance and reduce costs.

References

- Clark, Brooke. 2023. "Staff Requirements – SECY-23-0001 – Options for Licensing and Regulating Fusion Energy Systems." Washington D.C. <https://www.nrc.gov/docs/ML2310/ML23103A449.pdf>.
- Friedman, Gabriel. 2021. "'The Last Energy Source We'll Ever Tame': B.C. Startup's \$400M U.K. Plant Aims to Harness Nuclear Fusion Technology." Financial Post. June 23, 2021.
- Fusion Industry Association. 2023a. "The Fusion Industry Supply Chain: Opportunities and Challenges." https://www.fusionindustryassociation.org/wp-content/uploads/2023/05/FIA-Supply-Chain-Report_05-2023.pdf
- . 2023b. "The Global Fusion Industry in 2023 Fusion Companies Survey by the Fusion Industry Association." <https://www.fusionindustryassociation.org/membership/>.
- Ganda, F., T. Taiwo, and T. Kim. 2018. "Report on the Update of Fuel Cycle Cost Algorithms," Argonne National Laboratories NTRD-FCO-2018-00439. <https://publications.anl.gov/anlpubs/2018/07/144923.pdf>
- Goodin, D. T., N. B. Alexander, L. C. Brown, D. T. Frey, R. Gallix, C. R. Gibson, J. L. Maxwell, et al. 2004. "A Cost-Effective Target Supply for Inertial Fusion Energy." *Nuclear Fusion* 44 (12): S254. <https://doi.org/10.1088/0029-5515/44/12/S17>.
- Holcomb, D., F. Peretz, and A. Qualls. 2011. "Advanced High Temperature Reactor Systems and Economic Analysis," Oak Ridge National Laboratory. <https://info.ornl.gov/sites/publications/files/Pub32466.pdf>
- Hsu, Scott, Simon Woodruff, and Colleen Nehl. 2020. "Revisit of the 2017 Costing for Four ARPA-E ALPHA Concepts." <https://doi.org/10.2172/1820946>.
- Messinger, Jonah. 2022. "Fusion Breakeven Is a Science Breakthrough." The Breakthrough Institute. December 13, 2022. <https://thebreakthrough.org/issues/energy/fusion-breakeven-is-a-science-breakthrough>.
- MIT Energy Initiative. 2018. "The Future of Nuclear Energy in a Carbon-Constrained World." Cambridge, MA: MIT Energy Initiative. <https://energy.mit.edu/research/future-nuclear-energy-carbon-constrained-world/>
- Najmabadi, Farrokh, A. Abdou, L. Bromberg, T. Brown, V. C. Chan, M. C. Chu, F. Dahlgren, et al. 2006. "The ARIES-AT Advanced Tokamak, Advanced Technology Fusion Power Plant." *Fusion Engineering and Design* 80 (1–4): 3–23. <https://doi.org/10.1016/j.fusengdes.2005.11.003>.
- Sandia, LLC. 2024. Z Pulsed Power Facility [website]. <https://www.sandia.gov/z-machine/>
- Sorbom, B. N., J. Ball, T. R. Palmer, F. J. Mangiarotti, J. M. Sierchio, P. Bonoli, C. Kasten, et al. 2015. "ARC: A Compact, High-Field, Fusion Nuclear Science Facility and Demonstration Power Plant with Demountable Magnets." *Fusion Engineering and Design* 100 (November): 378–405. <https://doi.org/10.1016/j.fusengdes.2015.07.008>.
- Stewart, W. R., and K. Shirvan. 2022. "Capital Cost Estimation for Advanced Nuclear Power Plants." *Renewable and Sustainable Energy Reviews* 155 (March): 111880. <https://doi.org/10.1016/J.RSER.2021.111880>.
- UK Department for Business, Energy & Industrial Strategy. 2022. "Towards Fusion Energy." <https://assets.publishing.service.gov.uk/media/62b1f78a8fa8f53571e130c7/towards-fusion-energy-uk-government-response.pdf>.
- U.S. Bureau of Labor Statistics. n.d. "CPI Inflation Calculator." Accessed March 16, 2024. https://www.bls.gov/data/inflation_calculator.htm.

- Veil, Andrea D. 2022. "Response to the Advisory Committee on Reactor Safeguards, 'Draft Secy White Paper on Licensing and Regulatory Fusion Energy Systems.'" Washington, D.C. .
<https://www.nrc.gov/docs/ML2230/ML22306A260.pdf>.
- Woodruff, Simon, Ronald Miller, Desmond Chan, Steve Routh, Sakti Basu, and Shankar Rao. 2017. "Conceptual Cost Study for a Fusion Power Plant Based on Four Technologies from the DOE ARPA-E ALPHA Program." Washington, D.C.
- World Nuclear News. "First Light Teams up with CNL on Tritium Production." 2022. World Nuclear Association.
- Wurzel, Samuel E., and Scott C. Hsu. 2022. "Progress toward Fusion Energy Breakeven and Gain as Measured against the Lawson Criterion." *Physics of Plasmas* 29 (6): 66. <https://doi.org/10.1063/5.0083990>.

Appendix A. Global analysis methodology

This appendix describes the global model used to examine the potential role for fusion energy across all regions of the world under a deep decarbonization 1.5°C stabilization pathway.

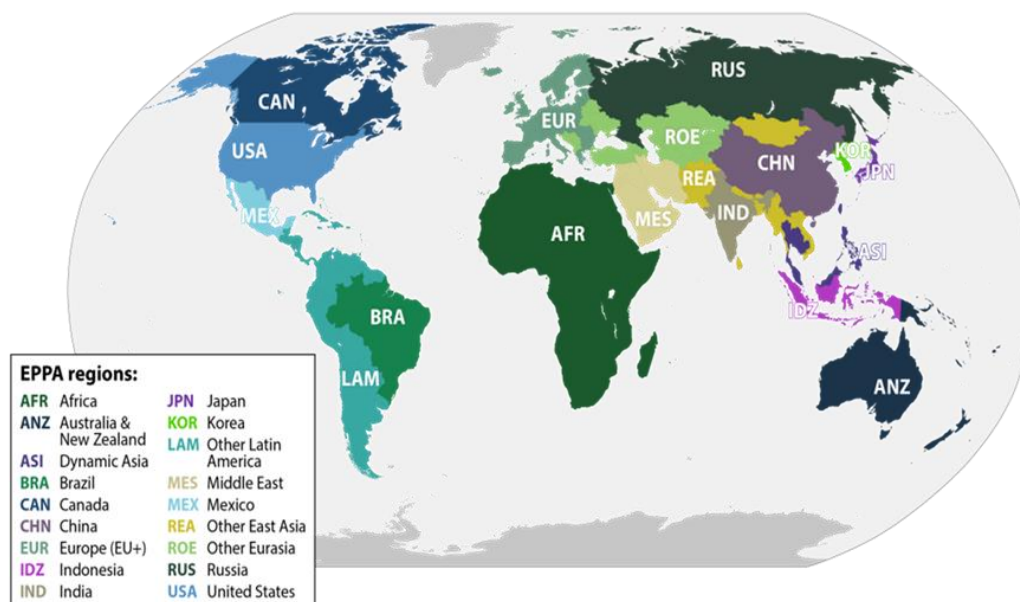
A.1. Economic Projection and Policy Analysis (EPPA) model

To assess the conditions for fusion technology to become a substantial contributor to global decarbonization in the 21st century, we use our global model, the enhanced version of MIT's Economic Projection and Policy Analysis (EPPA) model (<https://globalchange.mit.edu/research/research-tools/human-system-model>). The EPPA model is a multi-region, multi-sector, economy-wide tool for scenario analysis up to 2100. The EPPA model is designed to develop projections of economic growth, energy transitions, and anthropogenic emissions of greenhouse gases (GHG) and air pollutants. The model projects economic variables (GDP, energy use, sectoral output, consumption, etc.) and emissions of greenhouse gases (CO₂, CH₄, N₂O, HFCs, PFCs, and SF₆) and other air pollutants (CO, VOC, NO_x, SO₂, NH₃, black carbon, and organic carbon) from the combustion of carbon-based fuels, industrial processes, waste handling, agricultural activities, and land-use change.

As illustrated in [Figure A.1](#), the EPPA model explicitly represents 18 regions of the world, including the United States, China, India, Europe, Japan, Canada, Brazil, and others (for regional and sectoral details of the base version of the EPPA model, see <https://globalchange.mit.edu/research/research-tools/eppa>). In each region of the model, a representative agent seeks an optimal consumption bundle subject to a budget constraint and a set of endogenously determined prices of goods and services. The model also simulates production in each region at a sectoral level and explicitly represents interactions among sectors (through inter-industry inputs) and regions (via bilateral international trade flows).

The base year of the model is 2014. For the base year data, the model uses the Global Trade Analysis Project (GTAP) dataset (Aguiar et al. 2019). For historic periods up to 2020, the model is calibrated to economic and energy data from the International Monetary Fund (IMF) (2023) and International Energy Agency (IEA) (2023). It is solved recursively in 5-year time steps from 2020 to 2100. The model is designed for projecting long-term trends, so it does not capture business cycles or short-term shocks, such as those that often occur in, for example, commodity markets that play out over periods of less than the 5-year time step of the model.

Figure A.1 Regions of the EPPA model



Different versions of the model have been formulated for targeted studies, such as detailed exploration of decarbonization of light-duty vehicles, bioenergy with carbon capture and storage, use of natural gas and oil as feedstocks, options for emission reduction in the hard-to-abate industrial sectors, scenarios for carbon capture and storage (CCS) deployment, and others. See Chen et al. (2022) for a discussion of different versions of the EPPA model.

A.2. Accelerated Actions scenario

For global and regional GHG emission profiles, we use the Accelerated Actions scenario from the MIT Global Change Outlook (MIT Joint Program 2023). In this scenario, countries impose more aggressive emission targets than those submitted in their current Nationally Determined Contributions (NDCs) for the Paris Agreement process. We assume that advanced economies (USA, Europe, Canada, Japan, Korea, Australia, and New Zealand) reduce their greenhouse gas emissions in 2050 by about 70%–80% relative to 2015 levels. China reduces its emissions by about 70%. India reduces its CO₂ emissions by 50%, but because of growth in agriculture-related methane and nitrous oxide emissions, India's GHG emissions decline only by 13% in 2050 relative to 2015. Most other countries reduce their 2050 GHG emissions by 50%–75% with respect to 2015 levels, except for Africa (45%) and Russia (85%). These efforts by different countries result in global GHG and CO₂ emissions reductions in 2050 of about 65% and 75%, respectively, relative to their 2015 levels.

While several countries have ambitious mid-century goals, many of the targets considered here do not represent actual policies in place or in planning. In addition, many developing economies call for technology transfers and financial assistance that are not forthcoming at the levels needed. We explore this scenario simply to illustrate the potential impacts of accelerated

mitigation actions. In terms of climate impacts, this scenario is consistent with capping global warming at 1.5°C.

A.3. Levelized cost of electricity

For calculating the levelized cost of electricity (LCOE) from fusion-based generation, we use an approach developed in Morris, Reilly, and Chen (2019). LCOE calculates a single price of electricity per kilowatt-hour that should be sustained over the project economic life for the owner to recover all expenses, including capital, operating, and maintenance costs, as well as interest charges and returns on equity. Sometimes the LCOE is referred to as the “break-even” electricity price. The project economic life²⁷ is the number of years over which the plant will be amortized. Note that most plants actually operate longer than the project economic life.

The costs for the LCOE calculation can be divided into three main categories: capital costs, operating and maintenance (O&M) costs, and fuel costs. Capital costs, which we refer to as the “Total Capital Requirement,” consist of the overnight capital costs plus the interest and escalation during construction. The overnight cost is the cost of building the power plant as if the developer pays the entire cost upfront (i.e., “overnight”). It includes equipment, supporting facilities, and labor (the bare erected costs), costs for engineering services and contingencies, and owner’s costs, including feasibility studies, surveys, land, insurance, permitting, and financial transaction costs, among others.

We start with an assumption about the overnight cost. As guidance for an initial value, we use \$11,000/kW for a plant constructed in 2035. Since there is very limited information about the overnight cost for fusion power, we use the initial value as a base case and vary it in a sensitivity analysis. O&M costs are those required to run the plant on a daily basis. They are divided into fixed and variable costs depending on whether they are independent from or dependent on the quantity of energy produced. Fuel cost is the cost of purchasing the fuel used to operate the plant. In addition to cost data, the LCOE calculation requires additional inputs, including a capacity factor, project economic life, heat rate, and return rate on capital. We discuss these inputs below.

The capacity factor is the ratio of the actual output of a plant over a period of time to its output had it operated at full capacity over that time. It is expressed as a percent and is highly dependent on the type of power plant. The capacity factor is used to determine the total number of operating hours in a year, which is calculated by multiplying the number of hours in a year (8,760 hours) by the capacity factor. Heat rate is a measure of the plant’s thermal efficiency. It is the ratio of the heat content of the fuels fed into the plant expressed in megajoules (MJ or one million joules) divided by the net electricity output expressed in

²⁷ Sometimes “project economic life” is referred to as “project financial life.”

kilowatt-hours (kWh). The fuel cost in \$/kWh is equal to the fuel cost given in \$/GJ multiplied by the heat rate and divided by 1,000.

There are several rates²⁸ related to a rate of return on capital. There is a risk-free rate of return (also sometimes called an interest rate or discount rate), which is a rate for a zero-risk investment. In practice, the risk-free rate does not exist because any investment has some risk. The interest rate on the U.S. Treasury bills is often used as the risk-free rate indicator. The project cost is a combination of debt (borrowing) and equity (investment) used to finance a plant. The weighted cost of capital is a weighted average of the interest rate on the debt and the rate of return on the equity. The project economic life and the weighted cost of capital are used to calculate the capital recovery charge (CRC) rate. The CRC is the rate that gives the constant capital recovery necessary each year over the life of the plant in order to recover capital costs. The CRC is calculated as follows:

$$CRC = \frac{r}{1 - (1 + r)^{-n}} \quad (1)$$

where r is the weighted cost of capital and n is the number of years of the project economic life. The resulting formula to calculate the LCOE in \$/kWh is:

$$LCOE = \frac{TCR * CRC}{OH} + \frac{FOM}{OH} + VOM + FC \quad (2)$$

where:

TCR is total capital requirement (\$/kW),

CRC is capital recovery charge (%/year),

OH is operating hours (hours/year),

FOM is fixed O&M (\$/kW/year),

VOM is variable O&M (\$/kWh), and

FC is fuel cost (\$/kWh).

²⁸ Different terms for interest rates are used in literature. We categorize three different rates as a discount rate (or risk-free rate), a project interest rate (or cost of capital), and a capital recovery charge rate.

References

- Aguiar, Angel, Maksym Chepeliev, Erwin L. Corong, Robert McDougall, and Dominique van der Mensbrugghe. 2019. "The GTAP Data Base: Version 10." *Journal of Global Economic Analysis* 4 (1): 1–27. <https://doi.org/10.21642/JGEA.040101AF>.
- Chen, Yen-Heng Henry, Sergey Paltsev, Angelo Gurgel, John M. Reilly, and Jennifer Morris. 2022. "A Multisectoral Dynamic Model for Energy, Economic, and Climate Scenario Analysis." *Low Carbon Economy* 13 (02): 70–111. <https://doi.org/10.4236/lce.2022.132005>.
- International Energy Agency (IEA). 2023. "World Energy Outlook 2023." Paris. <https://www.iea.org/reports/world-energy-outlook-2023>.
- International Monetary Fund. 2023. "World Economic Outlook: Navigating Global Divergences." Washington, DC. <https://www.imf.org/en/Publications/WEO/Issues/2023/10/10/world-economic-outlook-october-2023>.
- MIT Joint Program. 2023. "Global Change Outlook." <https://globalchange.mit.edu/publications/signature/2023-global-change-outlook>.
- Morris, Jennifer F., John M. Reilly, and Y.-H. Henry Chen. 2019. "Advanced Technologies in Energy-Economy Models for Climate Change Assessment." *Energy Economics* 80: 476–90. <https://doi.org/https://doi.org/10.1016/j.eneco.2019.01.034>.

Appendix B. Methodology for grid and multi-subregional analysis

Chapter 5 of this report discusses results from two modeling exercises, using the capacity expansion models GenX and Ideal Grid, to explore the potential contribution of fusion energy to electricity supply within subregions of the United States in 2050. Specifically, we used these models to examine the penetration and role of fusion power plants (FPPs) under a range of scenarios in terms of cost, emissions caps, availability of renewables, and other factors. This appendix describes the GenX and Ideal Grid models, key model assumptions, and input parameters.

B.1. Overview of the GenX model

GenX is a highly configurable, open-source software that optimizes electricity grid investments and operational decisions to meet electricity demand as inexpensively as possible over a representative period (MIT Energy Initiative and Princeton University ZERO lab 2024). GenX gives insight into how new technologies and policies will impact the cost of electricity, grid resilience, and other important electricity system planning questions. The GenX model includes generation, storage, transmission, demand response, and many other resources. GenX can consider public policies when optimizing grid investments, including emission limits, portfolio requirements, and capacity reserve margins. GenX is capable of optimizing grid operations over representative periods of several years at hourly resolution, giving insight into the utilization of variable renewable generation and storage over a range of weather conditions and electricity demand.

To perform these calculations, GenX formulates the grid topology, public policies, and available technologies into a linear or mixed-integer linear constrained optimization problem, which is solved by a separate mathematical optimization tool. GenX is freely available to download and use (<https://github.com/GenXProject/GenX>) and comes packaged with the open-source HiGHS solver (Huangfu and Hall 2018). GenX is written in Julia (Bezanson et al. 2017) and relies extensively on the JuMP library (Lubin et al. 2023), which allows models created in Julia to be transferred to a wide range of mathematical solvers. Modeling for this study used the v0.3.3 release of GenX (Chakrabarti et al. 2022).

B.1.1. GenX fusion technology module

While GenX is already capable of representing a wide range of electricity sources, FPPs have a unique combination of capabilities and technical constraints that required us to develop a new fusion technology module in GenX. This FPP module is designed to be flexible enough to model a range of FPP types and designs but was focused, for purposes of this analysis, on a deuterium-tritium (DT)-fueled magnetic confinement fusion power plant. Our module enables us to accurately model the time-varying thermal and net electrical output of the FPP, the significant recirculating power fraction, tritium breeding and fuel management, and the scheduled

replacement of some components based on degree of use. We did not stipulate that FPPs must operate as baseload generation or as a load-following resource—instead, we allowed GenX to select the optimal pattern of operation given the economic costs and technical constraints of FPPs.

The GenX FPP module has four main components:

1. The plant, including the FPP reactor and cryogenically cooled superconducting magnets
2. An intermediate salt loop, which can have one or two loops and includes thermal storage
3. The power block, including the turbine and generator
4. Tritium processing and fuel management

This section describes how each component is represented in GenX before explaining how FPP costs were calculated. Input data for the model are discussed in [Section 5.2](#).

B.1.1.1. Plant

The plant comprises most of the FPP, including the fusion reactor, which generates most of the energy of the FPP. The FPP's total thermal power includes the energy released by fusion and then captured by the molten blanket around the reactor, as well as secondary reactions in the blanket. Calculating the additional energy produced in these reactions is complicated and very dependent on the design and operation of individual reactors. As this level of detail cannot be captured in our model, we assume the secondary reactions provide 15% additional power, based on discussions with experts at the MIT Plasma Science and Fusion Center (PSFC).

During normal operation, the reactor produces thermal power in pulses. According to fusion technology experts at the PSFC, a typical pulse will last 10 to 20 minutes with 1 minute of dwell time between pulses. This is much shorter than GenX's hourly resolution, so we model only hourly average power. Based on the same conversations, the power output of each pulse is not constrained by that of previous pulses, so we do not apply a ramping rate constraint to the thermal output of the FPP. This means thermal output can take any value in each hour, up to the reactor capacity. We assume the FPP uses 20-minute pulses followed by 1 minute of dwell time so the ultimate thermal power capacity of the reactor is 9.5% greater than the fusion power capacity, accounting for the pulsing and secondary reactions.

As with most power generators, an FPP reactor requires electricity to operate. This is called the station load or recirculated power. However, it is expected that FPPs will require more recirculated power than most other power generation technologies because of the large amount of energy required to sustain the fusion reaction and cryogenically cool the superconducting magnets while also serving other electricity-intensive components. Depending on FPP design and operation, 20%–35% of the gross electric power output must be recirculated.

For comparison, 4%–5% of the gross electric power output of a large fission power plant in the United States will be recirculated (IAEA 2024).

We include recirculated power in our FPP module given how significant this requirement will be to FPP operation. Our model considers only hourly averaged recirculating power requirements, rather than pulsed power, for the same reasons discussed in connection with thermal output. The recirculating power requirement for a FPP is made up of four components: magnet cooling, fixed plant power, variable plant power, and salt heating. The first component is the energy required to operate the FPP’s cryogenic magnets. The middle two components include the electricity required to operate all other parts of the FPP, including the reactor, salt pumps, tritium processing, etc. The energy required to initiate each pulse is very small and likely to be trickle-charged, so we consider it to be part of the variable plant power. The salt heating component refers to the electricity needed to ensure that the intermediate salt loop is kept molten during periods where the FPP is offline or not producing sufficient thermal energy to keep the salt molten.

B.1.1.2. Intermediate salt loop and thermal storage

The intermediate salt loop captures the thermal power of the reactor and delivers it to the turbine, smoothing the pulsed output of the plant in the process. Our model treats one- or two-stage salt loops the same and allows for the installation of additional thermal storage. The intermediate loop has two constraints: a thermal energy balance and a requirement that the average temperature of the salt remains the same. The thermal energy balance includes the thermal power from the reactor, the thermal power sent to the power block, a fixed loss term, and electric heating. The electric salt heating is assumed to be 95% efficient.

The ability to add thermal storage to a FPP creates two new investment decisions: the thermal storage capacity of the storage and the power capacity of the storage. The latter describes the heat exchangers, pumps, and other infrastructure required to transfer thermal energy into and out of the storage.

We constrain thermal storage capacity using a second thermal power balance. This power balance includes the net energy discharged from storage and a loss term. We assume that 2% of stored thermal energy leaks each day, based on descriptions of similar storage (Kelsall, Buznitsky, and Henry 2021).

B.1.1.3. Power block

The power block component converts the thermal energy delivered by the intermediate loop (including energy from thermal storage) into electrical energy. The nameplate capacity of the power block is a variable in our FPP module. In most cases, we require GenX to install FPP

reactors and power blocks with matching capacities, but these capacities can be different in the thermal energy storage case.

We calculate the gross electrical output of the power block for each hour and then subtract the recirculating power requirement for that hour to calculate net electric output. We assume that gross output can be 0%–100% of the nameplate capacity of the power block and that it has constant 40% thermal efficiency over this range. We could have added a minimum output requirement, but we did not use this option as we wished to keep the FPP model as linear as possible to make the results more easily interpretable.

B.1.1.4. Fuel management

Given the scarcity of tritium, we assume that each reactor must produce and manage its own tritium supply after startup. Our FPP module assumes that tritium processing capacity is tied to reactor capacity and therefore is not a variable, whereas the tritium and deuterium storage capacities are both investment variables.

The module includes mass balances for both fuels, tritium and deuterium, in each hour. The tritium balance includes fuel consumption and breeding by the reactor, radioactive decay of stored tritium, loss of stored material, and net transfers into tritium storage. We assume the reactor consumes 6.912 milligrams (mg) of tritium per MWh of thermal energy and breeds 7.601 mg per MWh. We assume that 0.1% of stored tritium is lost to containment materials each hour (Meschini et al. 2023). The tritium decay rate is 0.0006% per hour. The deuterium mass balance is the same, except there is no decay term and deuterium can be imported for \$500/kg.

B.1.2. FPP costs

Our FPP module includes the following investment decisions:

- Plant capacity, MW
- Power block capacity, MW
- Thermal storage energy capacity, MWh
- Thermal storage charge/discharge capacity, MW
- Tritium storage capacity, kg
- Deuterium storage capacity, kg

The direct costs of the FPP fleet are the sum of these investment variables multiplied by their annuitized capital costs. In addition, we account for four operational costs:

- Plant fixed O&M, \$/MW per year
- Plant variable O&M, \$/MWh per year
- Deuterium imports, \$/kg

- Costs for replaceable plant components

The first three operational costs are straightforward to calculate. Fixed O&M costs per MW are multiplied by plant capacity; variable O&M costs per MWh are multiplied by gross electric output; and costs per kg of deuterium imports are multiplied by the mass of deuterium required. Estimating replaceable component costs is more complex and requires us to develop a new approach to modeling this type of component.

Replaceable component costs appear to be a major determinant of whether FPPs will be installed (Schwartz et al. 2023). These components must be replaced after a certain amount of use. A replaceable component that lasts 2 years at full power operation is said to have a nameplate lifetime of 2 years. Its actual lifetime will be longer if the FPP operates at less than full capacity. Given the cost of these components and the greater variation in electricity prices over time due to variable renewable generation, it will often make sense to be judicious about when to operate a FPP to get the most value out of each replaceable component.

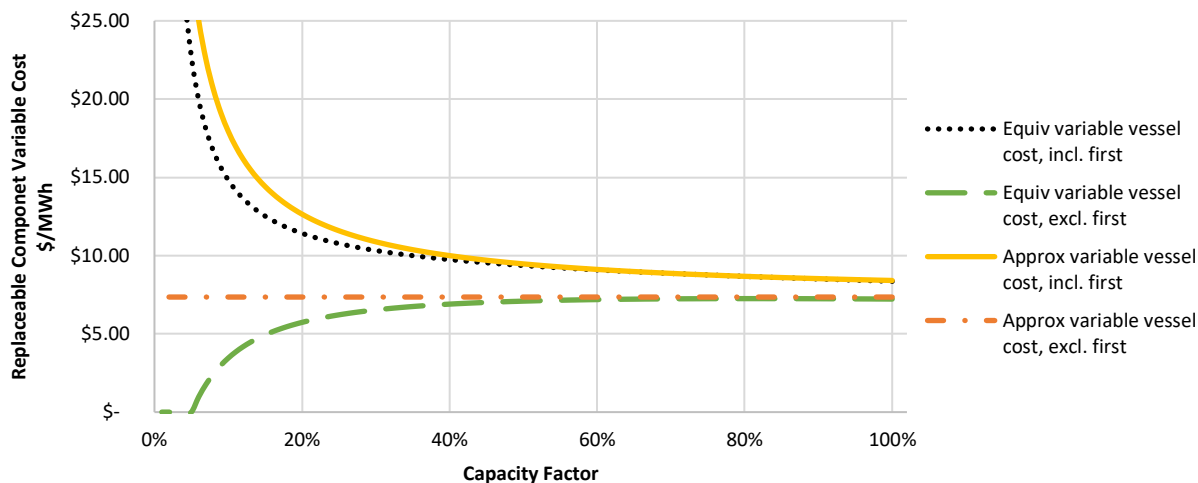
We calculate the annuitized investment cost for replaceable components as:

$$\frac{\$_{rep}r}{1 - (1 + r)^{\frac{L_{v,name}}{\mu} + L_r}}$$

where $\$_{rep}$ is the overnight cost of the replaceable component, r is the discount rate, $L_{v,name}$ is the nameplate lifetime of the component, L_r is the downtime required to replace the component, and μ is the capacity factor of the FPP.

FPP capacity factor is an output of the GenX model and represents the sum of several operational decision variables in the model. This is a non-linear function and cannot be directly included in the GenX formulation. However, we found that taking a first-order Taylor expansion of the equation around a reasonable estimate of the capacity factor gives sufficiently accurate results. The resulting approximation has a fixed component, which is the cost of the first set of replaceable components, and a capacity-factor-dependent component, which is the cost of the subsequent replaceable components. [Figure B.1](#) compares true and approximate annual annuities using the Taylor expansion approach.

Figure B.1 Comparison of approximate and actual costs for FPP replaceable components



Although this technique allows us to calculate the cost of use-dependent replaceable components, an outstanding challenge remains. Replacing components can be expected to take several months, so accounting for this replacement schedule is an important factor when optimizing the grid and deciding how many FPPs to install. The total lifetime of the replaceable components in each reactor, including their replacement time, is dependent on the capacity factor of the FPP and is not known *a priori*. These dynamics are challenging to model with a capacity expansion model such as GenX because grid operations and resource investments are optimized over a predetermined, representative period. Without knowing the lifetime of a component, the best solution currently is to optimize a representative period that is several years long so that it is likely that the full lifetime of the replaceable component will fit into the representative period.

This is computationally challenging, and we have limited data from which to generate scenarios for the stochastic optimization. Increasing the length of the representative period would reduce the number of scenarios we could consider, reducing the impact of interannual variation on the results. The results in [Chapter 3](#) show that not considering sufficient interannual variation will lead GenX to undervalue clean firm generation such as FPPs.

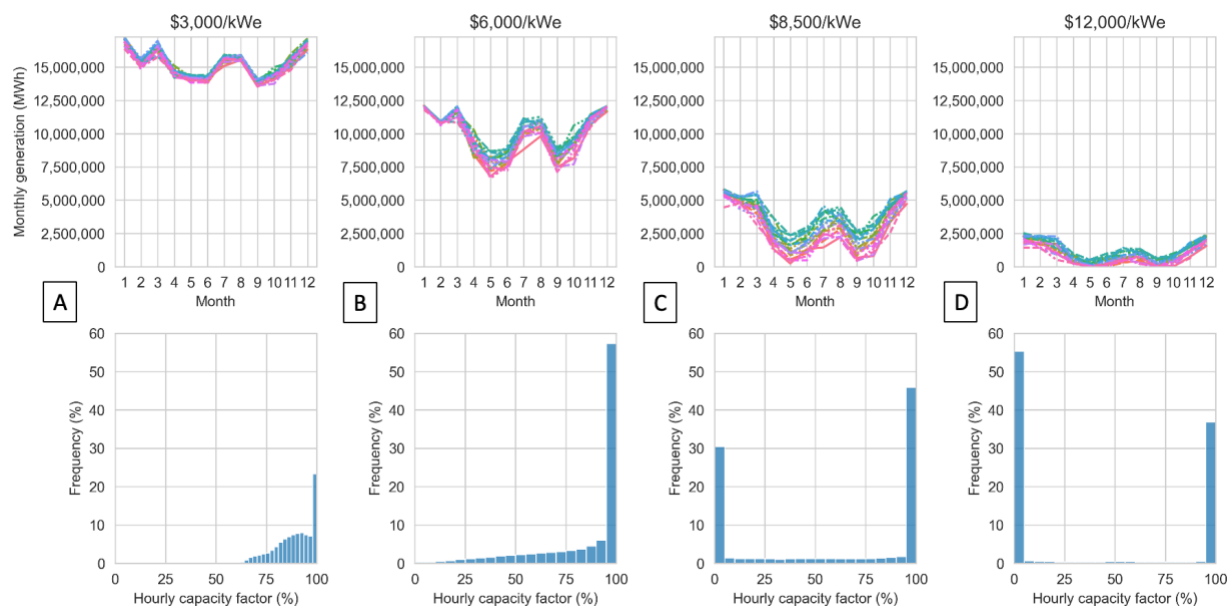
Our solution was to compare two sets of optimizations with the two limiting maintenance requirements. In the base case, the FPP fleet requires no maintenance, and in the alternative case, the entire FPP fleet must undergo maintenance. In reality, only part of the fleet will require maintenance in any given year. Reflecting this reality within GenX is a subject of ongoing work. However, we found that the cases that included a maintenance requirement produced largely the same installed capacity of FPPs as the base case, except when FPPs cost \$6,000/kW, in which case the installed capacity is lower.

Figure B.2 illustrates the reason for this outcome. The top row shows that generation is lowest in the spring and autumn months. These would be good periods to shutter some FPPs and perform maintenance. This is feasible for the \$8,500/kW and \$12,000/kW FPPs, as they are load following and all operate either at full capacity or not at all. This is shown in the lower row of Figure B.2C and B.2D. Both the \$8,500/kW and \$12,000/kW scenarios have several long periods in the spring and autumn during which some or all FPPs could undergo three months of maintenance.

Maintenance is also not an issue for FPPs that cost \$3,000/kW. In this case, shown in Figure B.2A, FPP output follows gross load so that FPP fleet output falls when demand is lower. The fleet produces full power during only 20% of hours. There are 80 FPPs on the grid, so it is possible to arrange the maintenance of individual reactors on a rotating schedule throughout the year.

Figure B.2B shows that if FPPs cost \$6,000/kW, they will operate at full power most of the time. This makes scheduling maintenance difficult. Additional generating capacity would be required to make up for lost FPP production during maintenance periods. In this case, maintenance downtime makes FPPs less competitive with fixed platform offshore wind and lithium-ion (Li-ion) battery storage, resulting in lower installed FPP capacity at this cost point.

Figure B.2 FPP generation and hourly capacity factor at four FPP cost points



Panels A–D (top) show monthly FPP generation over the twenty scenarios we considered for four representative FPP capital costs: (A) \$3,000/kWe, (B) \$6,000/kWe, (C) \$8,500/kWe, and (D) \$12,000/kWe. Panels A–D (bottom) show a histogram of the FPP hourly capacity factor over the twenty scenarios for the four FPP cost points. All cases assume an emissions intensity cap of 4 gCO₂/kWh.

B.2. Overview of the Ideal Grid model

Ideal Grid, like GenX and most capacity expansion models, optimizes the system by minimizing total system cost. Optimal capacity for each type of renewable generation is limited by available renewable resources within each subregion. These capacity limits, in combination with costs and resource characteristics within each subregion, result in a different optimal mix of generation assets in each subregion. Operational optimization is based on parameters and constraints with technology-specific characteristics. More details concerning these technology-specific characteristics are provided in the following sections. The optimization determines the capacity buildout for each technology and operation of those assets that meet demand at the lowest cost while limiting emissions to a specified cap. The Ideal Grid model post-process results provide estimates of technology curtailment, fractional energy losses due to transmission and distribution, and other valuable metrics. Lastly, the economic dispatch data are provided at an hourly resolution to show how the energy mix changes throughout the day and throughout the year.

B.2.1. System assumptions

Ideal Grid operates under a series of simplistic assumptions. Each subregion is analyzed as a single-node system with an assumed uniform transmission and distribution (TD) efficiency loss of 4.7%, tax of 6.35%, and transmission costs that are specific for each generation technology and each subregion. The model identifies the optimal mix of generation assets, assuming that there are no legacy assets. It is deterministic and operates under an assumption of perfect foresight regarding electricity demand and weather.

Ideal Grid includes 13 technologies: three types of Li-ion batteries (of 2-, 4-, and 8-hour duration); utility-scale, single-crystal silicon solar panels with an inverter loading ratio of 1.3; 2.8-MW nameplate-rated, land-based wind turbines with 90.2 meters hub height; fixed-bottom offshore wind; run-of-river hydro; reservoir hydro; pumped hydro storage; natural gas combustion turbine plants (NGCT); natural gas combined cycle plants (NGCC); natural gas combined cycle plants with 95% carbon capture and storage (95% CCS); hydrothermal geothermal; and fusion power plants. A transportation and storage fee of \$20 per tonne of captured CO₂ is assumed for all regions.

B.2.2. Data sources

Demand profiles were sourced from the National Renewable Energy Laboratory's (NREL's) 2022 *Cambium* data set (Gagnon, Cowiostoll, and Schwarz 2022). NREL provides hourly demand data within North American Electric Reliability Corporation (NERC) boundaries. All three types of hydro resources (reservoir, run-of-river, and pumped hydro storage) are subject to capacity limits in each subregion. Reservoir hydro is limited based on estimates from three sources: *Electric Power Annual*, *Hydropower Vision*, and *An Assessment of Energy Potential at Non-*

Powered Dams in the United States (Zayas 2016; Hadjerioua, Wei, and Kao 2012; “Electric Power Annual 2012” 2013). Capacity limits for run-of-river hydro are sourced from the *New Stream Reach Development* (Kao et al. 2014). Capacity limits for pumped hydro storage are obtained from NREL’s *Closed-Loop Pumped Storage Hydropower Resource 32 Assessment for the United States* (Rosenlieb, Heimiller, and Cohen 2022).

Hourly availabilities for wind and solar power are compiled from data pulled from the Zero-emissions Electricity system Planning with Hourly operational Resolution (ZEPHYR) model (Brown and Botterud 2021). For each region, hourly availability vectors are sourced for 169 equidistant sites within the boundary, each 30 miles apart. These 169 capacity factor (CF) curves are then aggregated to create a profile that is representative of the region. Wind CF values are calculated based on NREL’s Wind Integration National Dataset (WIND) Toolkit, assuming a 100-meter hub height (Draxl et al. 2015). Solar availability values are calculated based on NREL’s National Solar Radiation Database (NSRDB), assuming single-crystalline modules with single-axis tracking systems and 1.3 DC-to-AC inverter ratios (“NSRDB: National Solar Radiation Database” 2022).

Hourly availabilities for run-of-river hydro are calculated based on U.S. Geological Survey (USGS) daily flow rate data. This source provides flow rate data on over 1.9 million water resources within the United States. River resources were sorted into their appropriate regions based on latitude and longitude coordinates. These data are only available at a daily timestep, so the corresponding availability values are assumed for all 24 hours of the day. Also, reservoir hydropower availability values are constrained at monthly checkpoints to account for reservoir volume limitations. Within each month, the hourly capacity factor value is allowed to ramp without restriction.

For wind and solar resources, a collection of representative availability factor curves was manually sourced for each region, over a range of years (2007–2013) and at a variety of geographical coordinates distributed within each region. Regarding weather data, the user can select the year of weather data, the number of generation curves to be aggregated to represent overall regional VRE power output, and the distance between selected sites. In all selection options, the collection of aggregated CF curves forms an equidistant grid.

B.3. Shared grid modeling assumptions

We used the same modeling inputs in our GenX and Ideal Grid analyses where possible. In particular, we used the same cost and technical assumptions—drawn from the *2023 Annual Technology Baseline* (National Renewable Energy Laboratory [NREL] 2023)—for all generation and storage resources (Table B.1). Table B.2 and Table B.3 list the technologies included and their costs. All technical parameters for the technologies are those given in Table B.4 and Table B.5.

Table B.1 Resource descriptions taken from the 2023 NREL Annual Technology Baseline (ATB) for the Ideal Grid and GenX models

Resource	Type	Technology forecast	Financial case	Notes
Natural gas combined cycle	NG combined cycle (H-frame)	Moderate	R&D	
NGCC+CCS	NG combined cycle (H-frame) 95% CCS	Moderate	R&D	
Utility solar PV	Utility PV – Class 9	Moderate	R&D	
Commercial rooftop PV	Commercial PV – Class 9	Moderate	R&D	
Residential rooftop PV	Residential PV – Class 9	Moderate	R&D	
Onshore wind	Land-based wind – Class 7 – Technology 1	Moderate	R&D	
Fixed offshore wind	Offshore wind – Class 1	Moderate	R&D	
Floating offshore wind	Offshore wind – Class 11	Moderate	R&D	
Li-ion battery	Utility-scale battery storage – 4Hr	Moderate	R&D	GenX model not limited to 4-hour energy/power
Run-of-River hydro	Hydropower – NSD 2	Moderate	R&D	Class estimated from existing resources
Pumped hydro storage	Pumped storage hydropower – National class 13	Moderate	R&D	Class not important as no investments allowed
Quebec hydro	Hydropower – NPD 5	Moderate	R&D	Class chosen to match CEEPR Hydro study

Table B.2 Cost assumptions for the generating technologies in the Ideal Grid and GenX models

Resource	Overnight cost (\$/kW)	CAPEX (\$/kW)	Capital recovery period (years)	Discount rate (%/year)	Annualized cost (\$/MW/yr)	Fixed cost (\$/MW/yr)	Variable cost (\$/MWh/yr)	Mean fuel cost (\$/MWh)	Pro-forma capacity factor (%)	LCOE (\$/MWh)	LCOE – OPEX only (\$/MWh)
Natural gas combined cycle	880	990	30	6.0	72,000	24,000	1.60	44.90	85	59.30	49.80
NGCC+CCS	1,440	1,610	30	6.0	117,000	39,000	3.20	50.80	85	75.00	59.30
Utility solar PV	610	630	30	6.0	46,000	13,000	—	—	15	46.60	10.30
Commercial rooftop PV	830	860	30	6.0	63,000	10,000	—	—	10	100.20	13.80
Residential rooftop PV	1,120	1,120	30	6.0	81,000	14,000	—	—	10	143.10	21.00
Onshore wind	870	920	30	6.0	67,000	23,000	—	—	40	26.50	6.80
Fixed offshore wind	1,530	2,310	30	6.0	168,000	71,000	—	—	50	56.60	16.80
Floating offshore wind	2,520	3,740	30	6.0	272,000	61,000	—	—	50	78.70	14.40
Li-ion battery	830	830	15	6.0	86,000	21,000	—	—	15	73.10	14.40
Run-of-river hydro	3,810	4,070	100	6.0	245,000	19,000	—	—	65	45.60	3.20
Pumped hydro storage	7,080	7,550	100	6.0	455,000	47,000	—	—	35	157.50	14.80
Reservoir hydro	4,990	5,320	100	6.0	320,000	31,000	—	—	55	71.50	6.30

Table B.3 Cost assumptions for the storage technologies in the Ideal Grid and GenX models

Resource	Storage duration (hours)	Power CAPEX (\$/kW)	Energy CAPEX (\$/kWh)	Power annualized cost (\$/MW/yr)	Energy annualized cost (\$/MWh/yr)	Annualized cost (\$/MW/yr)	Power fixed cost (\$/MW/yr)	Energy fixed cost (\$/MWh/yr)	Total fixed cost (\$/MW/yr)
Li-ion battery	4	250	150	25,700	15,000	85,900	7,000	3,500	21,000
Pumped hydro storage	10	7,550	—	454,500	—	454,500	470,000	—	470,000

Power and energy costs are broken out for Li-ion batteries as they were allowed to be constructed with more than 4 hours of storage in some cases.

Table B.4 Technical parameters for thermal generators in the Ideal Grid and GenX models

Resource	Heat rate (MMBtu/MWh)	Thermal efficiency (%)	Max hourly ramp rate (%/hour)	Minimum plant load (%)	Tailpipe emissions intensity (tonne CO ₂ /MWh)	Upstream emissions intensity (tonne CO ₂ /MWh)	Total emissions intensity (tonne CO ₂ /MWh)
Natural gas combined cycle	6.196	55%	100%	50%	333	19	352
NGCC+CCS	7.007	49%	100%	50%	19	19	38

Table B.5 Technical parameters for storage technologies in the Ideal Grid and GenX models

Resource	Max hourly ramp rate (%/hour)	Minimum plant load (%)	Charging efficiency (%)	Discharging efficiency (%)	Round-trip efficiency (%)
Li-ion battery	100%	0%	92%	92%	85%
Pumped hydro storage	100%	0%	90%	90%	81%

References

- Bezanson, Jeff, Alan Edelman, Stefan Karpinski, and Viral B. Shah. 2017. "Julia: A Fresh Approach to Numerical Computing." *SIAM Review* 59 (1): 65–98. <https://doi.org/10.1137/141000671>.
- Brown, Patrick R., and Audun Botterud. 2021. "The Value of Inter-Regional Coordination and Transmission in Decarbonizing the US Electricity System." *Joule* 5 (1): 115–34. <https://doi.org/10.1016/j.joule.2020.11.013>.
- Chakrabarti, Sambuddha, Neha Patankar, Jesse Jenkins, Jacob Schwartz, Ruaridh Macdonald, Qingyu Xu, and Dharik Mallapragada. 2022. "GenX v0.3.3." [Github.Com/GenXProject/GenX/Releases/Tag/v0.3.3](https://github.com/GenXProject/GenX/Releases/tag/v0.3.3). 2022.
- Draxl, Caroline, Andrew Clifton, Bri Mathias Hodge, and Jim McCaa. 2015. "The Wind Integration National Dataset (WIND) Toolkit." *Applied Energy* 151 (August): 355–66. <https://doi.org/10.1016/j.apenergy.2015.03.121>.
- "Electric Power Annual 2012." 2013. U.S. Energy Information Agency (EIA). 2013. <https://www.eia.gov/electricity/annual/>.
- Gagnon, Pieter, Brady Cowiestoll, and Marty Schwarz. 2022. "Cambium 2022 Scenario Descriptions and Documentation." www.nrel.gov/publications.
- Hadjerioua, Boualem, Yaxing Wei, and Shih-Chieh Kao. 2012. "An Assessment of Energy Potential at Non-Powered Dams in the United States." <http://www.osti.gov/contact.html>.
- Huangfu, Q., and J. A. J. Hall. 2018. "Parallelizing the Dual Revised Simplex Method." *Mathematical Programming Computation* 10 (1): 119–42. <https://doi.org/10.1007/s12532-017-0130-5>.

- IAEA. 2024. "PRIS Database." <https://pris.iaea.org/pris/>.2024.
- Kao, Shih-Chieh, Ryan A. Mcmanamay, Kevin M. Stewart, Nicole M. Samu, Boualem Hadjerioua, Scott T. Deneale, Dilruba Yeasmin, M. Fayzul K. Pasha, Abdoul A. Oubeidillah, and Brennan T. Smith. 2014. "New Stream-Reach Development: A Comprehensive Assessment of Hydropower Energy Potential in the United States." Oak Ridge, TN (United States). <https://doi.org/10.2172/1130425>.
- Kelsall, Colin C., Kyle Buznitsky, and Asegun Henry. 2021. "Technoeconomic Analysis of Thermal Energy Grid Storage Using Graphite and Tin," June.
- Lubin, Miles, Oscar Dowson, Joaquim Dias Garcia, Joey Huchette, Benoît Legat, and Juan Pablo Vielma. 2023. "JuMP 1.0: Recent Improvements to a Modeling Language for Mathematical Optimization." *Mathematical Programming Computation* 15 (3): 581–89. <https://doi.org/10.1007/s12532-023-00239-3>.
- Meschini, Samuele, Sara E. Ferry, Rémi Delaporte-Mathurin, and Dennis G. Whyte. 2023. "Modeling and Analysis of the Tritium Fuel Cycle for ARC- and STEP-Class D-T Fusion Power Plants." *Nuclear Fusion* 63 (12): 126005. <https://doi.org/10.1088/1741-4326/acf3fc>.
- MIT Energy Initiative, and Princeton University ZERO lab. 2024. "GenX: A Configurable Power System Capacity Expansion Model for Studying Low-Carbon Energy Futures." *Github.Com/GenXProject/GenX*.
- NREL (National Renewable Energy Laboratory). 2023. "2023 Annual Technology Baseline." Golden, CO.
- "NSRDB: National Solar Radiation Database." 2022. NREL. 2022. <https://nsrdb.nrel.gov/>.
- Rosenlieb, Evan, Donna Heimiller, and Stuart Cohen. 2022. "Closed-Loop Pumped Storage Hydropower Resource Assessment for the United States."
- Schwartz, Jacob A., Wilson Ricks, Egemen Kolemen, and Jesse D. Jenkins. 2023. "The Value of Fusion Energy to a Decarbonized United States Electric Grid." *Joule*, April. <https://doi.org/10.1016/j.joule.2023.02.006>.
- Zayas, Jose. 2016. "Hydropower Vision Report." US Department of Energy. 2016. <https://www.energy.gov/eere/water/downloads/hydropower-vision-report-full-report>.

Appendix C. Techno-economic analysis methodology

To analyze the capital costs associated with a fusion power plant (FPP), one can evaluate the direct and indirect costs to understand where the largest costs reside. A bottom-up estimate for deuterium-tritium (DT) magnetic confinement concepts was conducted, whereas a top-down assessment was conducted for magneto-inertial and inertial confinement approaches.

C.1. Code of Accounts and scaling

A cost accounting system used in fission nuclear power plant (referred to as “NPP”) cost estimates is the uniform Code of Accounts (COA) system from the U.S. Department of Energy (DOE) Economic Data Base (EEDB). The COA system has been accepted by the International Atomic Energy Agency and formalized by the Generation IV International Forum Economic Modeling Working Group (Economic Modeling Working Group of the Generation International Forum 2007). A widely used cost accounting methodology facilitates uniformity and consistency when comparing the capital costs of NPPs across designs over time. The flexibility of the COA system allows for applications across nearly all nuclear power designs, which simplifies comparisons between NPP technologies. This flexibility explains why it has been used in many studies to estimate the costs of new power plants and compare costs across different nuclear and conventional power plant designs. However, despite its flexibility and usage for comparisons across conventional power-generating facilities, the COA system itself was not designed for fusion reactors. As a result, the COA was modified to accommodate the differences between a FPP and NPP. All the capital costs for this techno-economic analysis (TEA) fall into capitalized direct costs and capitalized indirect costs.

The direct capital costs (shown in [Table C.1](#)) were determined through a variety of methods, including bottom-up and top-down assessments, as well as referenced accounts. Although bottom-up assessments provide a robust estimate by considering fabrication, material inputs, and site labor, top-down assessments were employed when assessing bottom-up quantities was challenging. Thus, a simplified bottom-up capital cost estimate is conducted for a DT magnetic confinement plant given its great availability of data, and top-down assessments are used to determine the costs associated with inertial confinement plants and the savings associated with magneto-inertial plants. The bottom-up estimate employs a combination of methods to compute a range of capital costs, and the Nuclear Cost Estimation Tool (NCET) is referenced because it provides a bottom-up cost estimation tool for fission nuclear power plants.

Within this analysis, the Nuclear Cost Estimation Tool (NCET) developed at MIT was utilized and modified to gauge the costs associated with a fusion power plant. NCET has been used to model ~300–500 MWe fission modular power plants from first-of-a-kind (FOAK) to Nth-of-a-kind (NOAK). Similar to fission, fusion demonstrates a high initial capital cost with specialized

equipment while benefiting from low fuel costs because of the high energy density of the nuclear forces (Stewart and Shirvan 2022). The cost estimate tool within NCET utilizes power law scaling to adjust direct costs from the EEDB. The power law exponent used was 0.6.

In EEDB, there are several baseline costs for different NPPs. The lowest cost known as the “Better Experience Plant” (BE) was used for this NOAK fusion cost analysis. As it will be seen, the “Better Experience Plant” cost estimates for the non-nuclear part of the NPP are similar to the costs for NOAK thermal power plants constructed today, justifying its utilization. Given that a FPP has never been constructed, no historical data exist with which to validate the fusion-specific cost numbers. Thus, we use this methodology to examine the relative economics of different fusion power plant concepts. We do not attempt to project absolute values for the cost of any of these fusion concepts. The EEDB lists a component-by-component cost breakdown of a 1,200 MWe Westinghouse pressurized water reactor Better Experience Plant (PWR12-BE). The costs include factory costs, site labor hours, and material cost and quantity. The COA was organized into direct and indirect costs. The top-level direct accounts are structures and improvements (representing the civil works), reactor plant equipment (will be replaced with FPP-specific equipment), turbine generator equipment (assumes a steam Rankine cycle similar to a FPP), electrical plant equipment, miscellaneous equipment, and the main heat rejection system. The top-level indirect costs are construction services, engineering and home office services, and field supervision and offsite services. The direct costs are comprised of six top-level accounts and 23 subaccounts, and the indirect costs are comprised of six top-level accounts.

Table C.1 Direct costs

Account name	Account description
Land & land rights	
Structures & site facilities	
Reactor plant equipment	Vacuum vessel, blanket, magnet, fuel handling system, tritium extraction and removal, auxiliary cooling systems, cryostat, other reactor plant equipment (e.g., diverter), instrumentation and control
Turbine generator equipment	Rankine cycle assumed: turbine generator, condensing systems, feed heating system, other turbine plant equipment
Electric plant equipment	Switchgear, power and control wiring, switchboards, station service equipment, electrical structures and wiring containers, electrical lighting
Heat transfer equipment	Heat exchangers and steam generators for steam production; pumps, piping, valves required for heat removal

C.2. Buildings and structures

Through a combination of scaling methods from NCET and looking at the facility layout of ITER, relevant buildings needed for the design of magnetic confinement (MC) concepts were identified and scaled (IAEA 2000). “Structures & site facilities” is the second-greatest cost driver in the analysis. A significant cost faced by fission structures and sites is related to safety requirements induced by regulation. ITER is being built in France and was licensed similarly to a French fission power plant. However, since fusion power plants do not use fissile materials and fusion fuels cannot have chain reactions, the U.S. government plans to regulate fusion energy based on the radioactive material hazards. This provides an opportunity to reduce the cost of a fusion power plant and to quantify the impact of regulations on the cost. Generally, fission regulatory requirements increase the cost of buildings by a factor of 2.2 (Stewart and Shirvan 2022). Thus, for the “lower bound” of the capital cost, this analysis divides the reactor building costs in EEDB by a factor of 2.2 to eliminate the regulatory premium. As discussed in [Section 7.3.5](#), regulatory requirements can drive the costs of fusion power plants, so throughout this analysis, there will be brief discussions of how regulation that has impacted nuclear fission can impact nuclear fusion. Based on the NCET, the PWR12-BE was used as a basis to estimate the costs of the MC reactor containment buildings.

Detailed descriptions of the containment buildings were taken from design documents from the ITER design layout, as it represents the most detailed architecture in the open literature of buildings for a DT magnetic confinement system. A key distinction between the assumptions in this analysis and the ITER site layout is the size of the reactor building, including cryogenic cooling facilities. The ITER reactor is large because it has been designed to use low-temperature superconductors. The low magnetic field strength requires a larger reactor to achieve net positive energy. Magnetic confinement reactors designed to use high-temperature superconductors are physically smaller. Given the smaller size of the reactors for MC-FPP, ARIES spherical torus, and ARIES compact stellarator, the ITER Tokamak Hall was scaled down accordingly to represent these compact reactors. The cryogenic cooling facilities were also scaled accordingly.

After reviewing the buildings needed in a FPP, the total volume and surface area of walls, floors, and roofs were calculated for sections of the buildings, and relative quantities of materials—including concrete, reinforcement steel, structural steel, form-work, etc.—were found using the rates from the EEDB reactor building. The quantity of each material was categorized into superstructure or substructure and exterior or interior, since the costs of these sections vary. From these quantities, labor rates and the cost of materials from the PWR12-BE reactor building were used to generate bottom-up estimates. This method was also used to estimate the costs of the control room building and radioactive waste process building. The

turbine generators for FPPs are assumed to be functionally equivalent to those used by the EEDB and conventional power-generating systems.

C.3. Conventional equipment assumptions

When beginning a bottom-up estimate, it is important to distinguish NOAK assumptions relevant to existing technology and processes that have available cost data. Thus, several assumptions in this analysis rely on cost data for conventional thermal plants. The costs used in this analysis are shown and compared to a coal plant for reference in [Table C.2](#).

A coal plant with a superheated steam cycle has some components and costs that are applicable within a fusion power plant. The relevant components and costs are shown in [Table C.2](#). The sum of component costs in [Table C.2](#) represents roughly 23% of the total coal plant cost (Schmitt et al. 2022a). The turbine generator equipment and building costs within the coal plant represent NOAK systems; therefore, we compared these costs with our independent TEA analysis of the equivalent systems. [Table C.2](#) shows that our cost breakdown and total cost for a thermal plant is in line with literature values.

The data in [Table C.2](#) are also useful in estimating the savings that can be achieved through brownfield siting. By pursuing brownfield siting, existing facilities can be used, and therefore will not need to be repurchased or reconstructed, so the sum of the components mentioned in [Table C.2](#) gives a rough approximation of how much can be saved by not having to repurchase those components.

Table C.2 Relevant conventional thermal plant costs: Comparison between fusion cost assumptions and coal thermal plant costs

Direct cost accounts of FPP TEA	Lower bound (\$/kW)	Upper bound (\$/kW)	Supercritical coal thermal plant cost accounts	\$/kW
Heat rejection system	70	88	Cooling water system	182
Turbine generator equipment	535	550	Steam turbine & accessories	581
Electric plant equipment	274	402	Accessory electric plant	144
Total	879	1,040	Total	907

C.4. Reactor plant equipment

Fusion companies benefit from decades' worth of research to evaluate candidate materials for their conceptual designs. In the MC-FPP concept, vanadium alloys are assumed for the vacuum vessel (VV), including the inner VV wall, outer VV wall, VV ribbing, and VV posts. Vanadium alloys have also been assumed in the selected ARIES concept (Najmabadi et al. 2006). Thus, the base case cost analysis is based on a Vanadium alloy, "V-4CR-4Ti" (Chung et al. n.d.). Previous ARC studies that have estimated vacuum vessel lifetime were focused on Inconel 718 as the material of construction. In one such study, the lifetime of the VV is estimated to be 2 years (Segantin, Testoni, and Zucchetti 2019; Bocci et al. 2020). However, Inconel 718 has been ruled out as the best long-term choice for vacuum vessel material because the nickel content would result in long-life activated materials. Vanadium has much lower activation than nickel, but it has its own set of challenges, as described in [Chapter 6](#). Lifetime analysis for vanadium alloy vacuum vessels is required, and the absence of this information represents another area of uncertainty.

For specialized, fusion-specific equipment such as the cryostat, we utilized internal quotes. For other equipment where fission and other technology-specific examples could be found, such as tritium handling equipment and salt-to-steam heat exchangers, appropriate scaling and engineering judgment were applied. If fission cost is used, only NOAK with minimal regulatory escalation factors were assumed. From the cost of magnets, different learning rates and factors were applied to reduce the costs noted in the ARC design paper (Sorbon et al. 2015), as we believe the original ARC reference magnet cost numbers are more representative of FOAK fabrication. For the lower bound, we assumed conventional manufacturing, whereas for the upper bound, we escalated this cost to respect the specific manufacturing complexity of high-field magnets. The specific costs are outlined in [Section 7.3.1](#).

For MI-FPP equipment cost, the capacitors that drive the pistons are the cost driver, and they were estimated to cost between \$0.50 and \$1.00/Joule. The significant savings for MI-FPP are driven by the elimination of the cryo-system and magnets. The replacement costs of replaceable key components as well as the higher uncertainty of achieving net-fusion gain for MI-FPP concepts are not reflected.

For IC-FPP, the top-down approach looked at the cost of the driving force behind the "gun system" by scaling the recent refurbishment cost of the Z-Machine at Sandia (Sandia 2024) to likely energetics needed for a 1,000 MW_{th} output. We also applied the same learning rate as we assumed for the MC-FPP lower bound case. This would roughly represent the replacement for the magnet system of MC-FPP. Since IC-FPP is inherently a pulsed system, the comparison of overnight cost is not meaningful. A discussion on this front, including consideration of non-DT fusion systems, is in [Sections 7.3.3](#) and [7.3.4](#).

C.5. Indirect costs

Indirect costs were estimated as a percentage of direct costs. The percentages given based on Generation IV fission data sets that approximated indirect costs reflect the experience of the design and construction techniques (Holcomb, Peretz, and Qualls 2011). The indirect cost will depend on ranges for direct cost, learning rate, modularization (percent of work onsite vs offsite) and standardization of design. The indirect costs have significant potential to be a cost driver within the analysis. In many FPP cost studies noted in literature, indirect costs are in line with direct costs (Najmabadi 2003). For fission power plants, indirect cost as a percentage of total cost can be as high as ~80% (Eash-Gates et al. 2020), whereas for natural gas plants they are about 20% of the total cost (NREL n.d.). In the EEDB database, the Better Experience Plant realizes indirect cost of about 40% of total cost. In this work, we assumed the natural gas plant indirect cost percentage as reflected in [Table C.3](#), recognizing that such an assumption may be optimistic given FPPs will likely realize indirect costs in the range between those of a natural gas plant and an advanced fission power plant.

Table C.3 Indirect cost formulas

Indirect costs	Formula used
Design services at home office	$.14 \times \text{direct costs}$
Project & construction management at home office	$.1 \times \text{direct costs}$
Field construction management at plant site	$.1 \times \text{direct costs}$
Field construction supervision at plant site	$.5 \times \text{direct costs}$
Field indirect costs	$.16 \times \text{direct costs}$
Plant commissioning service	$.1 \times \text{direct costs}$

C.6. Operation and maintenance (O&M) costs and fuel costs

C.6.1. Operation and maintenance

Throughout fusion research, several candidate maintenance approaches and strategies have been considered. Because different reactor concepts use different materials coupled with different designs, there is not a “one-size-fits-all” approach and it is not within the scope of the TEA to create an optimized maintenance schedule; instead, several overall concepts and features of an optimal maintenance scheme were evaluated. A MC-FPP should be designed to be able to be disassembled and reassembled in order to maximize maintenance efficiency. Given that the reactor equipment design and installation greatly impact the maintenance, it is

necessary to understand where R&D needs to be concentrated to achieve the developments necessary to maintain a high availability and ultimately, a high-capacity factor.

To provide a standard functional maintenance scheme, the replaceable components should have nearly identical lifetimes to maintain plant availability (Wang et al. n.d.). Having a non-optimized maintenance schedule would result in more frequent plant shutdowns (Waganer et al. 2006). To complete the maintenance tasks in a timely manner, which also ensures worker health and safety, remote maintenance strategies on reactor components are being explored and have been a focus in the fusion industry for decades across several concepts (JET, ITER, DEMO, ARIES). While the plant is nonoperational, the level of neutron-induced radioactivity from the hot cell still exceeds levels that permit hands-on maintenance; hence, the need for remote maintenance.

Different reactor designs necessitate different maintenance approaches, horizontal and vertical maintenance strategies being prominent contenders. Within the reactor building, the bottom-up estimate assumes a vertical maintenance approach in which the reactor vessel would be lifted by a crane to perform certain maintenance tasks. The reactor building layout allows for remote O&M operations through a combination of vertical and port-based maintenance. An optimized maintenance schedule would comprise planned and unplanned maintenance timeframes for reactor and Balance-of-Plant elements. Again, given the amount of uncertainty in the maintenance schemes and material lifetimes, it is difficult to estimate an annual O&M cost. Thus, for this analysis, O&M costs are based on a percentage of the costs of the reactor plant equipment, turbine generator equipment, and electrical plant equipment. The modularity of replaceable components is critical to efficient maintenance.

The O&M costs consist of three categories:

- Fixed O&M
- Annual variable O&M
- Replaceable component costs for fusion reactor

Fixed O&M costs pertain to the number of full-time employees (FTE) expected to be at a NOAK FPP. To estimate the number of FTEs at a NOAK FPP, numbers from other industries were utilized. For instance, a thermal solar plant, where the power production system closely resembles DT-fusion energy systems (molten salt storage with superheated power cycle) currently employs 85 FTEs at a site in the United States. (“Solana Concentrating Solar Power Plant, Arizona” 2024). An advanced nuclear fission plant has been noted to potentially require 200 FTEs, half of them dedicated to security forces (Shirvan 2022). Ninety-five FTEs are assumed for the MC-FPP upper bound in recognition of the added complexity of operating a fusion power plant compared to a solar thermal. As the lower bound, about half that number is assumed based on a scenario in which multiple reactors are installed at the same site to enable

the staff to more efficiently support multiple plants. All of these assumptions are outlined in [Table C.4](#).

Annual variable O&M represents the sum of the annual equipment maintenance and the costs of the replaceable components. [Table C.4](#) details these assumptions.

Annual equipment maintenance consists of roughly 3% of the costs associated with reactor plant equipment (not including replaceable fusion reactor components), turbine generator equipment, and electric plant equipment without including transportation and installation costs.

Replaceable component costs and frequency of replacement will depend on the specific design of the FPP. Choices such as fusion fuel, containment method, material of construction, and neutron flux for each component are key differences. DT-fueled compact FPP concepts will have more frequent first wall component replacement rates than aneutronic FPP concepts. In the ARIES advanced technology, the vacuum vessel (ferritic steel) is among the components that are designed to last the lifetime of the plant, but the components that need to be replaced are the inboard first wall/blanket, outboard first wall/blanket, and the divertor. Unlike a traditional tokamak, the spherical torus has a center post. The ARIES spherical torus has a large center post that will likely need to be replaced every 2 to 3 full-power years. Unlike a MC-FPP, the vacuum vessel for ARIES spherical torus was assumed to have the lifetime of the plant.

Table C.4 O&M cost assumptions

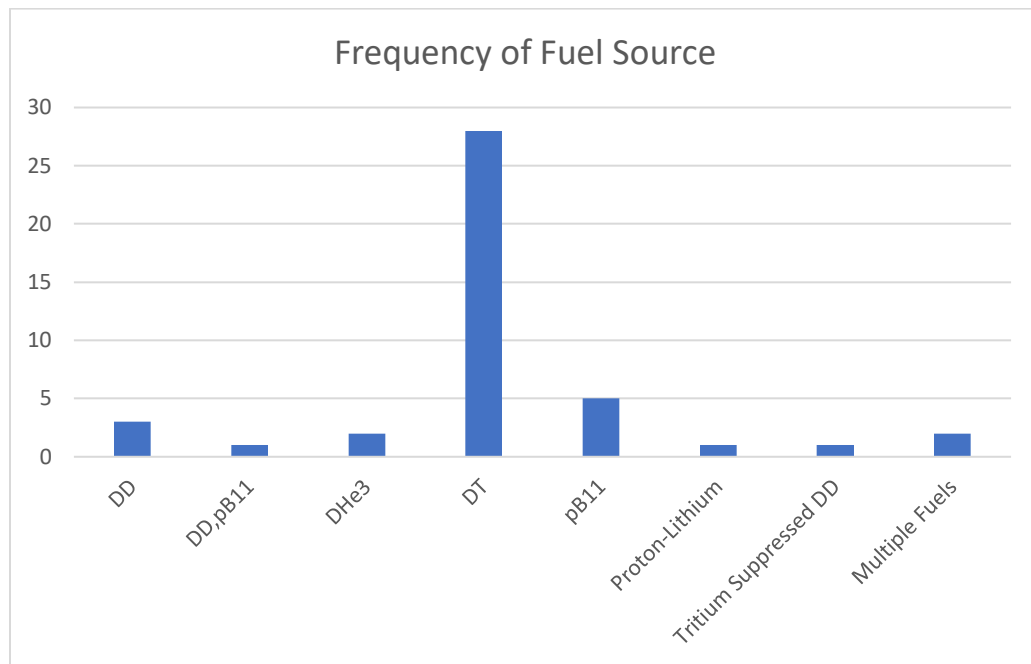
Category	Lower bound	Upper bound
Fixed O&M: FTE costs (average fully loaded cost per employee: \$200,000)	50 employees	95 employees
Annual variable O&M	Annual equipment maintenance + Reactor replaceable components	
Annual equipment maintenance (without replaceable components)	3% × [Reactor plant equipment ^a + Turbine generator equipment + Electric plant equipment] ^a Not including replaceable components	
Annual reactor replaceable components (including transport and installation)	$\left(\frac{\text{Cost of replaceable components}}{\text{Frequency of replacement}} \right)$ × (Transportation + Installation)	

Sources: “Solana Concentrating Solar Power Plant, Arizona” 2024; Stewart and Shirvan 2022.

C.6.2. Fuel costs

The fuel costs discussed in this analysis pertain to a DT fuel cycle. As shown in [Figure C.1](#), the Fusion Industry Report shows that the DT fuel cycle is the most commonly adopted fuel approach among fusion companies (Fusion Industry Association 2023).

Figure C.1 Frequency of fuel source among fusion companies



Data derived from Fusion Industry Association 2023.

For DT FPPs, the blanket needs to have tritium-breeding capabilities that allow it to achieve self-sufficiency and not reliance on external sources of tritium (Meschini et al. 2023). Annual fuel costs pertain to the DT cycle. Research regarding tritium-breeding optimization suggests that the type of structural material and blanket's Li-6 enrichment greatly impact tritium-breeding ratio outcomes. Ongoing research regarding the fuel cycle is focused on evaluating to what degree Li-6 enrichment is needed. Replenishing Li-6 might be necessary in those designs where the Li-6 enrichment must remain relatively constant to avoid a significant reduction in tritium breeding as the operations progress. However, the amount of Li-6 to be replenished is negligible compared to the total mass of the blanket and is not a significant recurring cost (Segantin et al. 2020). The cost of start-up tritium is not part of this analysis; but, in general, a kilogram may be the upper limit of tritium that can be stored on site given its radiological hazard profile. The annual cost of deuterium is so minute that we consider those costs to be negligible.

The FPP site must have enough tritium storage capacity to ensure that if power plant operations are paused, the tritium fuel can be stored until the power plant restarts. Also, if the fuel recycling, tritium extraction system, or other components in the fuel handling system have a temporary performance problem such that the tritium supply is less than the feed rate, tritium reserves from storage can be tapped. Furthermore, FPPs will be designed and operated to generate excess tritium to be used in starting up additional, new FPPs. Tritium storage

systems will hold that tritium and will periodically be used to transport the excess tritium to a new FPP.

C.7. Decommissioning and owner's cost

Decommissioning costs were computed by assuming 3% of the total capital costs. It should be noted that the amount of solid waste created by the disposal of replaceable components is an important topic in terms of both worker and public health and safety (Di Pace et al. 2012). Decommissioning of FPPs is an area that has not been significantly researched, but lessons can be taken from the fission industry.

Owner's costs are bundled with typical contingency costs and computed by multiplying the direct cost lower bound by 25%, and thus, the owner's cost represents roughly 17% of the capital costs. This amount is similar to a typical thermal power plant assumption. For NPP, this value is closer to 45% (National Renewable Energy Laboratory (NREL) 2012).

References

- Bocci, B., Z. Hartwig, S. Segantin, R. Testoni, D. Whyte, and M. Zucchetti. 2020. "ARC Reactor Materials: Activation Analysis and Optimization." *Fusion Engineering and Design* 154 (May): 111539. <https://doi.org/10.1016/J.FUSENGDES.2020.111539>.
- Chung, H. M., B. A. Loomis, D. L. Smith, and A. Loomis. n.d. "Properties of V-4CR-4Ti for Application as Fusion Reactor Structural Components."
- Di Pace, Luigi, Laila El-Guebaly, Boris Kolbasov, Vincent Massaut, and Massimo Zucchetti. 2012. "Radioactive Waste Management of Fusion Power Plants." In *Radioactive Waste*. InTech. <https://doi.org/10.5772/35045>.
- Eash-Gates, Philip, Magdalena M. Klemun, Goksin Kavlak, James McNerney, Jacopo Buongiorno, and Jessika E. Trancik. 2020. "Sources of Cost Overrun in Nuclear Power Plant Construction Call for a New Approach to Engineering Design." *Joule* 4 (11): 2348–73. <https://doi.org/10.1016/j.joule.2020.10.001>.
- Economic Modeling Working Group of the Generation International Forum, The IV. 2007. "GIF/EMWG/2007/004 Cost Estimating Guidelines for Generation IV Nuclear Energy Systems Revision 4.2."
- Fusion Industry Association. 2023. "The Global Fusion Industry in 2023 Fusion Companies Survey by the Fusion Industry Association." <https://www.fusionindustryassociation.org/membership/>.
- Holcomb, D. E., F. J. Peretz, and A. L. Qualls. 2011. "Advanced High Temperature Reactor Systems and Economic Analysis." <http://www.osti.gov/contact.html>.
- IAEA. 2000. "Technical Basis for the ITER-FEAT Outline Design" 19.
- Meschini, Samuele, Sara E. Ferry, Rémi Delaporte-Mathurin, and Dennis G. Whyte. 2023. "Modeling and Analysis of the Tritium Fuel Cycle for ARC- and STEP-Class D-T Fusion Power Plants." *Nuclear Fusion* 63 (12): 126005. <https://doi.org/10.1088/1741-4326/acf3fc>.
- Najmabadi, F. 2003. "Spherical Torus Concept as Power Plants—the ARIES-ST Study." *Fusion Engineering and Design* 65 (2): 143–64. [https://doi.org/10.1016/S0920-3796\(02\)00302-2](https://doi.org/10.1016/S0920-3796(02)00302-2).
- Najmabadi, Farrokh, A. Abdou, L. Bromberg, T. Brown, V. C. Chan, M. C. Chu, F. Dahlgren, et al. 2006. "The ARIES-AT Advanced Tokamak, Advanced Technology Fusion Power Plant." *Fusion Engineering and Design* 80 (1–4): 3–23. <https://doi.org/10.1016/j.fusengdes.2005.11.003>.
- National Renewable Energy Laboratory (NREL). n.d. "Annual Technology Baseline." <https://atb.nrel.gov/archive>

- National Renewable Energy Laboratory (NREL). 2012. "Cost Report: Cost and Performance Data for Power Generation Technologies. NCSEA Exhibit 3."
- Sandia, LLC. 2024. *Z Pulsed Power Facility*. <https://www.sandia.gov/z-machine/>.
- Schmitt, Tommy, Sarah Leptinsky, Marc Turner, Alexander Zoelle, Charles White, Sydney Hughes, Sally Homsy, et al. 2022. "Cost and Performance Baseline for Fossil Energy Plants Volume 1: Bituminous Coal and Natural Gas to Electricity." <https://doi.org/10.2172/1893822>.
- Segantin, Stefano, Raffaella Testoni, Zachary Hartwig, Dennis Whyte, and Massimo Zucchetti. 2020. "Optimization of Tritium Breeding Ratio in ARC Reactor." *Fusion Engineering and Design* 154 (May): 111531. <https://doi.org/10.1016/j.fusengdes.2020.111531>.
- Segantin, Stefano, Raffaella Testoni, and Massimo Zucchetti. 2019. "The Lifetime Determination of ARC Reactor as a Load-Following Plant in the Energy Framework." *Energy Policy* 126 (March): 66–75. <https://doi.org/10.1016/j.enpol.2018.11.010>.
- Shirvan, Koroush, and John C. Hardwick. 2022. "Overnight Capital Cost of the next AP1000." Cambridge, MA: Center for Advanced Nuclear Energy Systems (CANES) at MIT.
- "Solana Concentrating Solar Power Plant, Arizona." 2024. Verdict Media Limited. 2024.
- Sorbom, B. N., J. Ball, T. R. Palmer, F. J. Mangiarotti, J. M. Sierchio, P. Bonoli, C. Kasten, et al. 2015. "ARC: A Compact, High-Field, Fusion Nuclear Science Facility and Demonstration Power Plant with Demountable Magnets." *Fusion Engineering and Design* 100 (November): 378–405. <https://doi.org/10.1016/j.fusengdes.2015.07.008>.
- Stewart, W. R., and K. Shirvan. 2022. "Capital Cost Estimation for Advanced Nuclear Power Plants." *Renewable and Sustainable Energy Reviews* 155 (March): 111880. <https://doi.org/10.1016/J.RSER.2021.111880>.
- Wagner, Lester M., Farrokh Najmabadi, Mark Tillack, Xueren Wang, and Laila El-Guebaly. 2006. "Design Approach of the ARIES-AT Power Core and Vacuum Vessel Cost Assessment." *Fusion Engineering and Design* 80 (1–4): 181–200. <https://doi.org/10.1016/j.fusengdes.2005.06.353>.
- Wang, X. R., S. Malang, A. R. Raffray, and ARIES Team. 2005. "Maintenance Approaches for ARIES-CS Compact Stellarator Power Core." *Fusion Science and Technology* 47 (4): 1074–8. <https://doi.org/10.13182/FST05-A829>

List of figures

Figure ES.1 Dependence of global fusion penetration in the electricity system on the cost of FPP for a 1.5°C stabilization pathway scenario..... 5

Figure ES.2 Fusion electricity generation in major world regions under different cost assumptions and under a 1.5°C climate stabilization pathway. 6

Figure ES.3 Fusion penetration in U.S. subregions with different endowments of other low-carbon electricity resources for a range of emission intensity caps in a scenario with FPP capital costs of \$6,000/kW in 2050. 7

Figure ES.4 FPP installed capacity (A), generation (B), and capacity factor (C) in the New England grid, assuming that VRE installed capacity is constrained by land use. ... 9

Figure ES.5 Fusion installed capacity in the New England region of the U.S. in 2050. 10

Figure 3.1 Lorenz curve of hourly energy market revenue earned by a fusion power plant..... 35

Figure 4.1 Global annual emissions of greenhouse gases (GHG) and carbon dioxide (CO₂) in the Accelerated Actions scenario. 38

Figure 4.2 Evolution of overnight capital costs of fusion power generation (2021\$/kW). ... 40

Figure 4.3 Evolution of the global electricity generation mix in the base case where overnight costs for a fusion power plant in the U.S. reach about \$8,000/kW in 2050 and about \$4,300/kW in 2100. 42

Figure 4.4 (a) Fusion share of global electricity generation for different cost cases; (b) global electricity generation from fusion technology for different cost cases. 43

Figure 4.5 Evolution of the global electricity generation mix in different cost cases. 44

Figure 4.6 Electricity generation from fusion technology in major world regions (United States, Europe, China, India, Brazil, Canada, Higher-Income Asia, Japan, Russia) over the 2035–2055 period. 45

Figure 4.7 Electricity generation from fusion technology in EPPA regions in the 21st century. 46

Figure 4.8 Electricity generation mix in major world regions: (a) United States, (b) Europe, (c) China, (d) India, and (e) Africa. 47

Figure 4.9 Fusion electricity generation in major world regions under different cost assumptions. 48

Figure 4.10 Potential annual global economic benefits of fusion technology in a deep decarbonization scenario..... 49

Figure 5.1 The nine U.S. subregions modeled by the Ideal Grid. 51

Figure 5.2 Elements of the fusion module..... 52

Figure 5.3 Cost differences by subregion. 58

Figure 5.4 Regional differences in maximum average annual variable renewable energy capacity factors. 60

Figure 5.5	Renewable energy technical maxima by subregion.	61
Figure 5.6	Levelized cost of electricity for each generation technology in each subregion at pro-forma capacity factors	62
Figure 5.7	GenX results for FPP installed capacity (A), generation (B), and capacity factor (C) on the New England grid depending on assumptions about FPP capital cost and system-wide emissions cap.....	64
Figure 5.8	Installed capacity of each resource on the New England grid.....	65
Figure 5.9	Installed capacity of different generation resources on the New England grid... ..	67
Figure 5.10	FPP installed capacity (A), generation (B), and capacity factor (C) in the New England grid.	69
Figure 5.11	FPP installed capacity (A), generation (B), and capacity factor (C) on the New England grid in a scenario where FPPs must operate as baseload generators.	72
Figure 5.12	FPP hourly capacity factor on the New England grid, averaged over each month of one of the weather scenarios.	75
Figure 5.13	Fleet capacity required to achieve a range of emissions caps in the Southeast, Southwest, and Central subregions in 2050.	77
Figure 5.14	Relative generation contribution from various technologies in the Southeast, Southwest, and Central subregions in 2050 for a range of emission caps.....	78
Figure 5.15	Modeled fusion buildout by subregion at varying CAPEX values and emission caps.	81
Figure 6.1	Faraday HTS tape production.	91
Figure 6.2	Cross-section of core plasma, blanket, and the three layers of the first wall for designs in which the vacuum vessel is in front of the blanket.	101
Figure 7.1	Proportion of fusion companies pursuing different fusion approaches.	109
Figure 7.2	High-level breakdown of capital costs comparing results from the literature to our lower and upper bound estimates for a magnetic confinement fusion plant.	113
Figure 7.3	Breakdown of direct costs for magnetic confinement (MC) concepts (top) and magneto-inertial (MI) concepts (bottom).	115
Figure A.1	Regions of the EPPA model.....	124
Figure B.1	Comparison of approximate and actual costs for FPP replaceable components.	133
Figure B.2	FPP generation and hourly capacity factor at four FPP cost points.	134
Figure C.1	Frequency of fuel source among fusion companies.	150

List of tables

Table ES.1	Renewable resource attributes of different U.S. subregions	8
Table 2.1	Categorization of fusion companies by fuel and confinement method	19
Table 2.2	Performance metrics achieved to date by fusion confinement method	24
Table 4.1	Overnight capital costs in 2021 for non-fusion power-generating technologies (2021\$/kW)	41
Table 5.1	Base case FPP size and power characteristics	53
Table 5.2	Recirculating power requirements	53
Table 5.3	Capital cost for the base case FPP by component	55
Table 5.4	Annualized capital cost and O&M cost for the base case plant	55
Table 5.5	Projected 2050 costs (U.S. average) for generation and storage technologies available for investment in the GenX model of the New England grid	57
Table 5.6	Locational adjustment factors for GenX modeling of the New England grid	59
Table 5.7	Minimum and maximum capacity limits (in MW) for renewable energy generation in the GenX model of the New England grid	62
Table 5.8	Roadmap to modeling results for our sensitivity analyses	63
Table 5.9	Model results for installed FPP capacity (in MW) on the New England grid	64
Table 5.10	FPP installed capacity on the New England grid assuming an FPP cost of \$6,000/kW and flexibility in terms of emissions banking	70
Table 5.11	Installed FPP capacity on the New England grid given an FPP cost of \$6000/kW and varying the VRE and Li-ion storage costs as a percentage of the base costs given in Table 5.5.	71
Table 5.12	Installed FPP capacity on the New England grid assuming land-use constraints on VRE capacity and FPP capacity utilization of 89% or more	73
Table 5.13	Cost assumptions used in GenX modeling of molten salt thermal energy storage (TES) integrated with a FPP	74
Table 5.14	Influence of nameplate lifetime and downtime requirements for component replacement on annual availability and LCOE for a \$6,000/kW FPP	76
Table 5.15	Renewable limits that contribute to fusion deployment for the \$6,000/kW FPP cost scenario	79
Table 5.16	Subregion categories based on renewable resources	80
Table 6.1	Key features of different HTS tape manufacturers	89
Table 7.1	General FPP parameters used for scaling in this study	110
Table 7.2	Comparison of FPP direct costs and scientific energy gain.	114
Table B.1	Resource descriptions taken from the 2023 NREL Annual Technology Baseline (ATB) for the Ideal Grid and GenX models	137

Table B.2	Cost assumptions for the generating technologies in the Ideal Grid and GenX models.....	138
Table B.3	Cost assumptions for the storage technologies in the Ideal Grid and GenX models.....	138
Table B.4	Technical parameters for thermal generators in the Ideal Grid and GenX models.....	139
Table B.5	Technical parameters for storage technologies in the Ideal Grid and GenX models.....	139
Table C.1	Direct costs.....	142
Table C.2	Relevant conventional thermal plant costs: Comparison between fusion cost assumptions and coal thermal plant costs	144
Table C.3	Indirect cost formulas	146
Table C.4	O&M cost assumptions.....	149

Glossary and acronyms

Activation	The process of inducing radioactivity of a material by creating an isotope that is unstable. Usually occurs by neutron irradiation.
ARC	A high-field compact tokamak design developed by MIT that is being commercialized by Commonwealth Fusion Systems (CFS)
ARIES	The Advanced Reactor Innovation and Evaluation Study, a U.S. research program of advanced integrated design studies for fusion power plants
B11	Boron 11, a naturally occurring isotope of boron
Blanket	The blanket surrounds the reactor of a deuterium-tritium fusion power plant and serves three functions: 1) capture neutrons, 2) absorb energy, and 3) breed tritium fuel. The blanket can be liquid or solid.
Capacity factor	The ratio of electricity generated to the generating capacity
CAPEX	Upfront capital cost to build a power plant or other asset
CCS	Carbon capture and storage
Confinement	Physical methods used to bring fusion fuels into close proximity with each other and away from other matter
Critical current	The maximum current density that can be carried by a superconductor while maintaining its superconducting performance
Critical field	The magnetic field strength below which superconducting materials have zero resistance to electrical current
Critical temperature	The temperature below which superconducting materials have zero resistance to electrical current
Cryogen	The working fluid used to cool to very low temperatures
Cryostat	The system used to maintain the magnets at the very low temperatures required to ensure superconductivity
DD	Deuterium-deuterium fusion fuel

Deuterium	An isotope of hydrogen that has one neutron instead of none as in the most abundant hydrogen isotope. Deuterium is often referred to as D.
DHe3	Deuterium-helium3 fusion fuel
DIII-D	A tokamak experiment located at the DIII-D National Fusion Facility in California, U.S.
DT	Deuterium-tritium fusion fuel
EEDB	U.S. Department of Energy (DOE) Economic Data Base of historical U.S. Nuclear Power Plant costs
Embrittlement	The decrease in a material's ductility. In a DT fusion reactor, embrittlement is primarily due to neutron bombardment.
EPPA	MIT's Economic Projection and Policy Analysis model is a multi-region, multi-sector, economy-wide tool for scenario analysis up to the year 2100. For this study, EPPA was applied to all regions of the world.
EU DEMO	Proposed fusion power plants based on the ITER experimental reactor
Excimer laser	A type of high-efficiency laser that produces ultraviolet light
Field-reversed configuration	A magnetic confinement method that uses a toroidal electric current to create a poloidal magnetic field to confine the plasma
Firm power	Generation technologies that can be relied on to provide electricity to meet demand when needed throughout the year
Fissile	A material that can undergo fission when its nucleus is struck by a low-energy neutron. Only materials with atomic number 90 or greater are fissile. Fusion fuels are not fissile.
FLiBe	A candidate molten salt blanket with the chemical formula $2\text{LiF}-\text{BeF}_2$
FLiNaBe	A candidate molten salt blanket with the chemical formula $\text{LiF}-\text{NaF}-\text{BeF}_2$
FLiNaK	A candidate molten salt blanket with the chemical formula $\text{LiF}-\text{NaF}-\text{KF}$

FOAK	First-of-a-kind. This term is used in examining costs and reflects that the first construction of a new technology will cost more than subsequent builds of the same design.
FPP	Fusion power plant
Fuzz	A porous structure that forms on plasma-facing tungsten due to helium bombardment
gCO ₂ -equivalent	The grams of CO ₂ that have the same climate warming impact as some other greenhouse gas emissions such as methane emissions
GenX	Software that optimizes electricity grid investments and operational decisions to meet electricity demand as inexpensively as possible. For this study, GenX was applied to the six New England states within the United States.
Helium-3	An isotope of helium that has only one neutron instead of the usual two
HTS	High-temperature superconductor. These are materials that have zero resistance to electrical current at temperatures above 77 K.
Hydrothermal	A type of geothermal resource that has a natural supply of water
IC-FPP	Inertial confinement fusion power plant
ICRF	Electromagnetic waves on the ion-cyclotron range of frequency. These are one method for heating plasmas.
Ideal Grid	A capacity expansion model which optimizes the system by minimizing total system cost. For this study, it was applied to nine subregions of the United States.
Initial confinement	Use of inertial forces to compress and heat fusion fuels to achieve high density and temperatures of the fuels
IRA	U.S. Inflation Reduction Act. This is U.S. legislation that expanded the scale of production tax credits available for investments in designated low-carbon generation technologies.
IRP	Integrated resource planning

ITER	An international collaboration to build the world's largest tokamak to run experiments to demonstrate that fusion energy output can exceed energy input. ITER is under construction in France.
JET	Joint European Torus project located in the United Kingdom
LCOE	Levelized cost of electricity. A method of calculating the average cost of electricity over the life of the generating assets by accounting for the capital costs, operating and maintenance costs, fuel costs, and the capacity factor of the generator.
Li-6 and Li-7	Lithium has two naturally occurring isotopes with atomic numbers 6 and 7, respectively. Both isotopes can be used to produce tritium, but Li-6 is easier to convert to tritium.
Li-ion	Lithium-ion. Often used in rechargeable batteries.
LiPb	A candidate molten-metal blanket made of lead and lithium
Load-following	Able to adjust electricity generation output to match changing demand
LTS	Low-temperature superconductors are materials that have zero resistance to electrical current at temperatures below 30 K
Magnetic confinement	Use of magnetic fields to confine a plasma of fusion fuels
Magneto-inertial confinement	Combines features of magnetic confinement and inertial confinement
MC-FPP	Magnetic confinement fusion power plant
MHD	Magnetohydrodynamics is the study of the dynamics of electrically conducting fluids. This topic is of great importance in the design of a magnetic-confinement fusion power plant and applies to both the plasma and the liquid blanket.
MI-FPP	Magneto-inertial confinement fusion power plant
MRI	Magnetic resonance imaging. A medical imaging technique that uses superconducting materials to generate strong magnet fields.

NGCC	Natural gas combined cycle power plant. This is a high-efficiency power plant that includes gas turbines and steam turbines to maximize power generation from natural gas.
NGCC+CCS	Natural gas combined cycle power plant with carbon capture technology to separate carbon dioxide from the flue gas
NGCT	Natural gas combustion turbine power plant. These power plants are relatively low cost and low efficiency and are used primarily as peaker power plants.
NIF	National Ignition Facility located in the United States
NOAK	Nth-of-a-kind. This term is used in describing costs for mature technology.
NRC	U.S. Nuclear Regulatory Commission. An agency of the U.S. government responsible for protecting public health and safety related to nuclear energy.
O&M	Operating and maintenance costs
Overnight costs	Cost of a construction project if we assume there are no financing costs to cover the duration of the construction
PB11	Proton-boron ¹¹ fusion fuel
PFC	Plasma-facing components
Poloidal field	Field lines that follow the radial contour of a torus
PV	Solar photovoltaic electricity generation
RAFM	Reduced activation ferritic martensitic steels. Developed for fission and fusion applications and can have a range of compositions to give them desired performance, including resistance to activation.
REBCO	Rare-earth barium copper oxide high-temperature superconductors
RIC	Radiation-induced corrosion
RoR hydro	Run-of-river hydroelectric generation that harnesses river flow energy without needing a large dam or reservoir

Scientific gain Q	The ratio of fusion power produced to power absorbed by the plasma to sustain plasma conditions
SiC	Silicon carbide is a ceramic and potential material for a FPP
SPARC	A high-field compact tokamak being built by Commonwealth Fusion Systems (CFS) to run experiments to demonstrate that fusion energy output can exceed energy input. SPARC is under construction in the United States.
Stellarator	A type of magnetic confinement fusion reactor that uses magnets to create a twisted magnetic field to maintain a more stable plasma
TEA	Techno-economic analysis. Examines the costs and performance of a given technology and compares it with other technologies.
TES	Thermal energy storage
Tesla	Units of measure for magnetic field strength
TFTR	Tokamak Fusion Test Reactor located in the United States
Tokamak	A type of magnetic confinement fusion reactor that is shaped like a symmetrical donut
Toroidal field	Field lines that follow the horizontal ring contour of a torus
Torus	Donut shaped
Tritium	An isotope of hydrogen that has two neutrons instead of one as in the most abundant hydrogen isotope. Tritium is often referred to as T.
USGS	U.S. Geologic Survey is a U.S. agency that tracks production, reserves, resources, demand, and price for various minerals
VRE	Variable renewable energy, including solar and wind